

Dissertation zur Erlangung des Doktorgrades
der Fakultät für Chemie
der Ludwig-Maximilians Universität München

Phosphorus, Sulfur and Pyridine

a Unique Combination to a Great Structural Diversity

von
Stefanie Schönberger
aus München

2013

Erklärung

Diese Dissertation wurde im Sinne von §7 der Promotionsordnung vom 28. November 2011 von Herrn Prof. Dr. Konstantin Karaghiosoff betreut.

Eidesstattliche Erklärung

Diese Dissertation wurde eigenständig und ohne unerlaubte Hilfe erarbeitet.

München, den

(Stefanie Schönberger)

Dissertation eingereicht am

19.11.2013

1. Gutachter:

Prof. Dr. Konstantin Karaghiosoff

2. Gutachter:

Prof. Dr. Thomas M. Klapötke

Mündliche Prüfung:

18.12.2013

Bother me tomorrow, today, I'll buy no sorrows.

Doo, doo, doo, lookin' out my back door.

John Fogerty

Danksagung

*Niemals wird dir ein Wunsch gegeben, ohne dass dir auch die Kraft verliehen wurde,
ihn zu verwirklichen.*

(Richard Bach)

Für diese Kraft möchte ich mich im Folgenden **ganz herzlich bedanken** bei...

meinem Doktorvater *Prof. Dr. Konstantin Karaghiosoff* für die großartige Möglichkeit in seinem Arbeitskreis promovieren zu dürfen und für seine leichte Begeisterungsfähigkeit, mit der auch das kleinste Signal im NMR-Spektrum zu einem Erlebnis geworden ist,

Herrn *Prof. Dr. Thomas M. Klapötke* für die freundliche Aufnahme in seinen Arbeitskreis, seine Mühen mit quantenchemischen Berechnungen und die großartige Unterstützung vor allem zum Ende dieser Arbeit hin,

Herrn *Akad. ORat Dr. Burkhard Krumm* und Herrn *Akad. Rat Dr. Jörg Stierstorfer* für die freundliche Zusammenarbeit,

Frau *Irene S. Scheckenbach* für ihre unermüdliche Unterstützung, ohne die ich wohl oft sehr hilflos gewesen wäre,

meinen Praktikanten *Christoph Jagdhuber, Franziska Gold, Irina Bart, Simone Schmidt, Amra Blume, Laura Ascherl, Rebekka Erdmann, Marthe Ketels, Stefy Schedlbauer* und *Sinah Krönauer* ohne die diese Arbeit in der Form nicht existieren würde,

meinen Laborkollegen *Andreas Eckart, Andreas Preimesser, Dr. Susanne Scheutzow, Carolin Pflüger* und *Stefan Huber* für die angenehme Atmosphäre und Hilfsbereitschaft im Laboralltag,

Richard Moll danke ich einfach dafür, dass es ihn gibt so wie er ist und vor allem, dass ich seine verpasste musikalische Früherziehung immer wieder mit einem neuen "Lied des Tages" nachholen durfte,

den Dres. *Alexander Dippold* und *Anian Nieder* für das unermüdliche Korrekturlesen dieser Arbeit und gesonderter Dank an *Anian* auch für viele hilfreichen chemische Gesprächen und unzählige Antworten auf Fragen, die nie gestellt wurden,

Dr. Christiane Maxien und *Dr. Oliver Schön* für ihre grandiose Vorarbeit, ohne die diese Arbeit in ihrer Form wahrscheinlich nicht entstanden wäre,

den Polymerschwestern *Dr. Franziska Betzler* und *Vera Hartdegen*, die mir in der Zeit während meiner Promotion mehr als nur gute Freunde geworden sind,

auch der übrigen Teerunde *Caro Pflüger* und *Camilla Evangelisti* (ihr besonderer Dank auch für die Berechnungen),

dem gesamten Arbeitskreis *Karaghiosoff* und *Klapötke* für drei tolle, ereignisreiche und, mit Sicherheit, unvergessliche Jahre.

Mein Dank gilt auch *Felix Popp*, *Christopher Müller* und *Christoph Jagdhuber*, die mich tapfer durch das ganze Studium begleitet haben.

Besonderer Dank gilt vor allem meiner Familie, meinen Eltern *Anita* und *Robert*, meinen Geschwistern *Sebastian* und *Silvia* und meinen Großeltern *Gertrud* und *Michael*, die zwar nie verstanden haben was ich tue, mich darin aber immer bestmöglich unterstützt haben.

Table of Contents

Introduction	15
---------------------	-----------

Research Topics	23
------------------------	-----------

PART I – Anionic Phosphorus Sulfur Compounds

1. New Salts of the Cyclic Thiophosphate Anions $P_2S_8^{2-}$, $P_3S_8^{3-}$ and $P_4S_8^{4-}$	27
--	-----------

Introduction	28
Results and Discussion	31
Molecular and Crystal Structure of $[2,6\text{-Me}_2\text{C}_5\text{H}_6\text{N}]_2[P_2S_8]$	31
Molecular and Crystal Structure of $[\text{pyH}]_3[P_3S_8] \cdot 2.5 \text{ py}$	33
Molecular and Crystal Structure of $[\text{pyH}]_4[P_4S_8] \cdot \text{py}$	36
Conclusion	38
Experimental Section	39

2. The Truth about the Trithiometaphosphate PS_3^-	45
--	-----------

Introduction	46
Results and Discussion	49
Molecular and Crystal Structures of $[\text{Ph}_4\text{P}]_2[P_2S_6] \cdot \text{py}$ and $[n\text{Bu}_4\text{N}]_2[P_2S_6] \cdot \text{THF}$	49
^{31}P NMR Spectroscopic Investigation	52
Molecular and Crystal Structure of $[\text{pyH}][\text{pyPS}_3]$, $[n\text{Bu}_4\text{N}][(\text{CH}_3)_2\text{NC}_5\text{H}_4\text{NPS}_3] \cdot \text{EtCN}$ and $[(N\text{-MeIm})_2\text{H}][N\text{-MeImPS}_3]$	54
Temperature Dependent ^{31}P NMR Spectroscopy	58
Conclusion	61
Experimental Section	62

3. Synthesis and Crystal Structure of a New Salt of the Water Stable Hexathiohypodiphosphate anion: [py₂Li]₄[P₂S₆] · py	69
Introduction	70
Results and Discussion	71
Conclusion	75
Experimental Section	76

PART II – Structures of Unusual Phosphate Derivatives

1. Synthesis and Crystal Structure of the Bis(ethoxo)-tetrathio-μ-disulfido-diphosphate Salt: [pyH]₂[P₂S₆(OEt)₂]	81
Introduction	82
Results and Discussion	83
Synthesis	83
Molecular and Crystal Structure of [pyH] ₂ [P ₂ S ₆ (OEt) ₂]	84
Quantum chemical Calculations of [pyH] ₂ [P ₂ S ₆ (OEt) ₂]	88
Conclusion	89
Experimental Section	90
2. Formation and Crystal Structure of 4,4'-Oxybis(2,6-bis-(dimethylamino)-4H-1,3,5,4-thiadiazaphosphinine-4-oxide)	95
Introduction	96
Results and Discussion	97
Conclusion	104
Experimental Section	105

3. A Mixed Oxophosphate 109

Introduction	110
Results and Discussion	112
Conclusion	117
Experimental Section	117

4. On the Structural Chemistry of the $\text{H}_2\text{PO}_3\text{S}^-$ Anion 121

Introduction	122
Results and Discussion	124
Molecular and Crystal Structure of $(\text{pyH})(\text{H}_2\text{PO}_3\text{S})$	124
Molecular and Crystal Structure of $(4,4'\text{-bipyH})(4,4'\text{-bipyH}_2)\text{H}(\text{HPO}_3\text{S})_2$	128
Conclusion	132
Experimental Section	133

PART III – Pyridine-Stabilized Metal Complexes of P,S,O Anions

1. Pyridine-Stabilized Mn(II) Thio- and Oxophosphate Complexes 141

Introduction	142
Results and Discussion	143
Molecular and Crystal Structure of $[\text{py}_2\text{MnPS}_4]_2[\text{pyH}]_2 \cdot 4\text{py}$	143
Molecular and Crystal structure of $\text{py}_4\text{NaMnPS}_4$	147
Molecular and Crystal Structure of $\text{py}_4\text{Mn}(\text{H}_2\text{PO}_4)_2$	150
Conclusion	155
Experimental Section	156

2. $\text{py}_4\text{Mn}[(\text{EtO}(\text{S})\text{P}(\text{O})\text{S})_2\text{S}] \cdot \text{py}$: A New Coordination Polymer 163

Introduction	164
Results and Discussion	165
Conclusion	168
Experimental Section	168

3. On the Synthesis and Structural Characterization of Pyridine-Stabilized Tin(II) Thiophosphates 173

Introduction	174
Results and Discussion	176
Molecular and Crystal Structure of $\text{py}_2\text{Sn}(\text{pyPS}_3)_2 \cdot \text{py}$	176
Molecular and Crystal Structure of $[\text{SnPS}_4][\text{py}_2\text{H}] \cdot \text{py}$	181
Conclusion	185
Experimental Section	186

PART IV – Acyclic Phosphorus Sulfides

1. $\text{py}_2\text{P}_2\text{S}_7$: A Bis(pyridine)adduct-Stabilized Phosphorus Sulfide 193

2. New Acyclic Neutral Phosphorus Sulfides and Sulfide Oxides 201

Introduction	202
Results and Discussion	203
The Pyridine Adduct $\text{py}_2\text{P}_2\text{S}_5$	203
Molecular Structure of $\text{py}_2\text{P}_2\text{S}_5 \cdot 0.5 \text{ py}$	204
Crystal Structure of $\text{py}_2\text{P}_2\text{S}_{4.34}\text{O}_{0.66}$	206
The Pyridine Adduct $\text{py}_2\text{P}_2\text{S}_4\text{O}$	209
Quantum Chemical Calculations	209

Thermal Analyses	213
Conclusion	216
Experimental Section	216

PART V – ^{31}P NMR Investigation of Polyphosphides

Motivation	223
Introduction	224
Polyphosphorus Hydrides – Historical Notes	225
Chemical Properties of Polyphosphides	226
Results and Discussion	228
Reaction of P_4 with Sodium	229
Reaction of P_4 with Lithium	231
Conclusion	234
Experimental Section	235

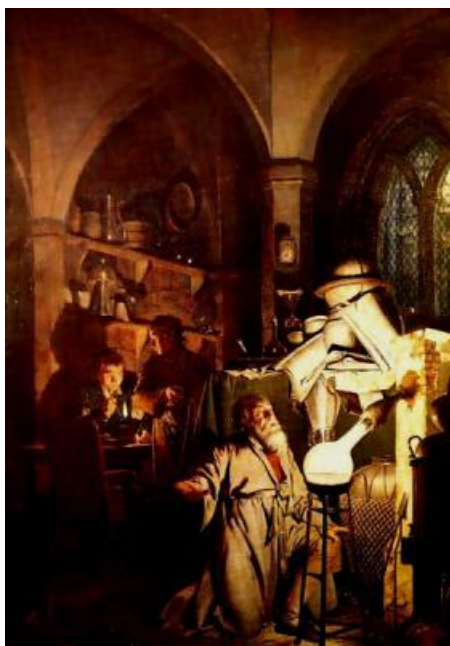
Summary 239

Introduction

The mysterious white phosphorus has most likely been discovered many times over the centuries, but in the last 350 years the knowledge has been lost over and over again. The author John Emsley writes in his book *The sordid tale of Murder, Fire, and Phosphorus – the 13th element*^[1]:

Phosphorus was discovered by the alchemists, researched by the early chemists, exploited by the industrialists of the nineteenth century and abused by the combatants of the twentieth. Its capacity for evil cursed all who tried to exploit it, from the would-be murderer to the worldwide manufacturer. But set against this tale of woe are a few remarkable benefits that phosphorus brought and it is an important ingredient in many of the things we use in our everyday lives.

It was one night in 1669 in Hamburg when *Herr Doktor* Henning Brandt accidentally discovered white phosphorus during one of his many failing attempts to synthesise the Sorcerer's Stone.



The Alchemist in Search of the Philosopher's Stone discovers Phosphorus. 1771. Oil on canvas, 50 x 40 in. Derby Museum and Art Gallery. Image copyright the Derby Museum.

Since that day, this element has made a great impression on the world. It became very popular during the industrialisation in the 19th century as the main ingredient in matches, the so called “Lucifers” and served as a horrible substance during the wartime of the 20th century.

It is to be said that mankind itself brought this devastating element to the world, nature never planned on being this cruel, it provides phosphorus only in the form of its oxides, the phosphates. These binary phosphorus oxygen anions are essential for all life on Earth, as it is part of the DNA and ATP.

This class of compounds has been investigated thoroughly over the last 200 years, but it was not until the first half of the 19th century when one of the most famous chemists started to take a closer look at the reactivity of phosphorus towards the heavier homologue of the oxygen, the sulfur. The swede *Jöns Jacob Berzelius* can be regarded as one of the founding fathers of modern chemistry along with John Dalton, Antoine Lavoisier and Robert Boyle. He invented the chemical formula notation alongside with the discovery of many new elements like selenium or silicon and others.



Jöns Jacob Berzelius (1779 – 1848)

When Berzelius heated white phosphorus in the presence of sulfur over 100 °C he lay the foundation of phosphorus sulfur chemistry by synthesising P_2S_5 in a literally explosive reaction. Until this moment it was not known if these two elements could engage in chemical interactions at all, rather than just being melt together.

In 1843 he published his results for the first time with the article *Ueber die Verbindungen des Phosphors mit dem Schwefel* in the journal *Annalen der Physik*. Berzelius began his work by apparently random melting together of the two elements until he started using stoichiometric amounts and produced various neutral binary phosphorus sulfides which became an indispensable part in inorganic chemistry. Of all the compounds he described only the P_2S_5 , which today is known to exist in its dimeric form, P_4S_{10} , could be verified. This neutral compound adopts an adamantane like structure (Figure 2). The crystal structure was first described by Vos and co-workers in 1956.^[3]

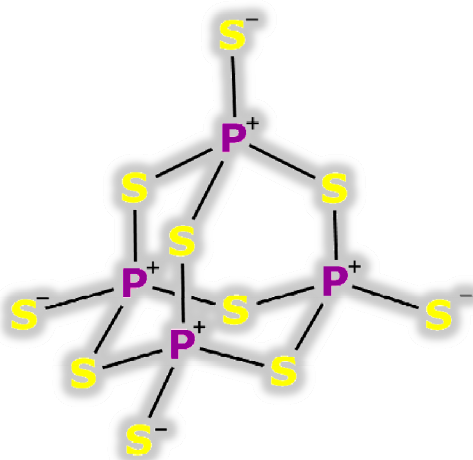


Figure 2. Molecular structure of phosphorus(V) sulfide.

The discovery that the phosphorus(V) pentasulfide inherits a dimeric structure was made by Stock and co-workers in 1905.^[4] From that point on until 1913 there was a real rush on this molecule.^[5] Then Stock patented its preparation alongside with the statement that *there are probably only three compds. of P and S, P_4S_7 and P_4S_{10} .*^[6] That there are far more than those three compounds, however, shows an excerpt of the great variety of different phosphorus sulfides (Figure 3).

The latest phosphorus sulfide which could be described, is the δ - P_4S_7 . It was described by the group of *Blachnik* in 2007.^[7] This contemporary discovery shows that there are yet more modifications of binary neutral phosphorus sulfides to be found.

But what should be acknowledged, is that all of the above mentioned compounds inherit a polycyclic, cage-like structure.

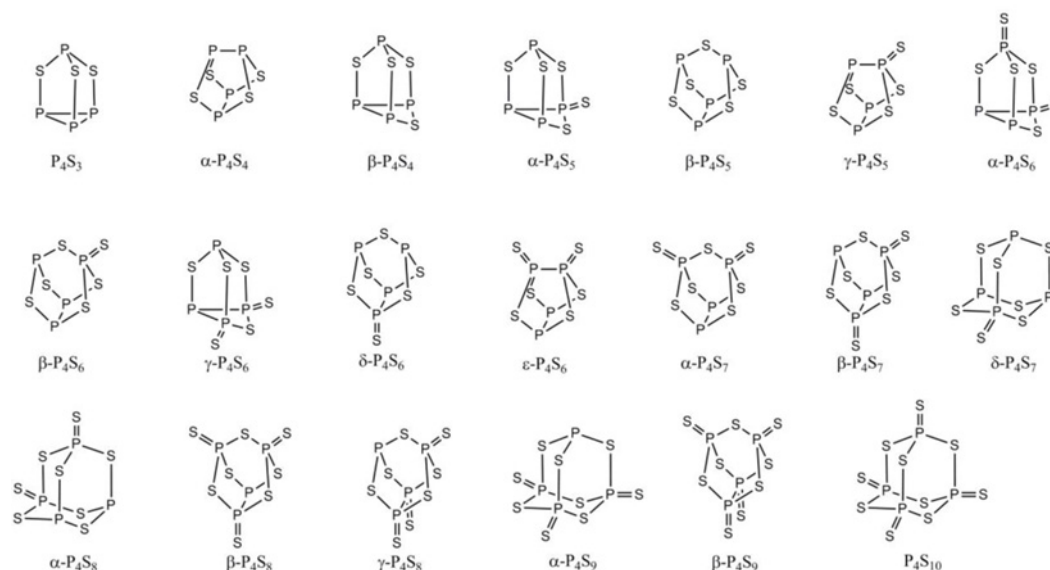


Figure 3. Examples of known phosphorus sulfides.

All these phosphorus sulfides can be regarded as anhydrides of thiophosphoric acids, which *per se* are rather unstable and therefore rather appear as their anions, the thiophosphates.^[8]

Until now a great variety of phosphates $P_xO_y^{z-}$ has been described in the literature and constitutes an integral part in all fields of chemistry. In contrast to oxophosphates, anions of phosphorus and the heavier chalcogens are less thoroughly investigated. Comparing the bond energies of oxo- and thiophosphates, the P–P, P–S and S–S bonds are rather similar, while the P–O bond is much stronger (Table 1). This means that in oxophosphates, P–O connectivity is predominant while in thiophosphates a far greater structural diversity can be expected. Thiophosphates can build up not only acyclic but also mono and even polycyclic anions because of the element independent possible connectivity.

Thiophosphates are extremely moisture and air sensitive, which presents great difficulties for their syntheses. Therefore, the list of known P,S anions is rather manageable and leaves great potential for developing new synthetic routes to unusual thiophosphate structures, and for exploring their coordination chemistry, acting as soft multidentate ligands.

Table 1. Electronegativity and bond energies in P,S and P,O compounds

X	P	S	O
EN	2.06	2.44	3.50
$\Delta\text{EN}(\text{P},\text{X})$	-	0.38	1.44
$\text{BE}(\text{P}-\text{X})$	215	230	335
$\text{BE}(\text{P}=\text{X})$	-	335	544
$\text{BE}(\text{X}-\text{X})$	215	213	139

EN = electronegativity (Allred-Rochow).

BE = bond energy in kJ/mol.^[9]

Based on the great sensitivity towards air, most synthetic routes to thiophosphates, and in general thiophosphate containing compounds, are reactions at high temperatures, starting from the elements. Metal containing anions in particular are still nearly exclusively a field of solid state chemistry. For example compounds like $\text{M}_2\text{P}_2\text{S}_6$ ($\text{M} = \text{Mg}, \text{Ca}, \text{V}, \text{Mn}, \text{Fe}, \text{Co}, \text{Ni}, \text{Pd}, \text{Zn}, \text{Cd}, \text{Hg}, \text{Sn}, \text{Pb}$) are synthesised in temperature ranges between 450°C and 800°C, respectively.^[10] Syntheses proceeding in the solution are a rarity, an example is the preparation of K_3PS_4 from H_2S , P_4S_{10} and KOH .^[11]

This reaction also shows the importance of P_4S_{10} as starting material for the preparation of thiophosphates in solution under mild conditions and at low temperature.

A new field in inorganic phosphorus sulfur chemistry is the adduct formation for stabilization of unsaturated anions in the unusual bonding situation $\sigma^3\lambda^5$. Such species oligomerize or, in the more interesting case, have to be stabilized by coordination with a base, like pyridine. The most famous representative of this class of compounds is the pyridine stabilized trithiometaphosphate anion PS_3^- , which is described in the literature with many conflicting specifications.^[12]

Pyridine plays an unusual role in the case of stabilizing unsaturated phosphorus species and is of great importance in P,S chemistry in solution, especially with regard to the ever-growing field of organic inorganic hybrid open frameworks, which combine the advantages of both organic and inorganic chemistry to give rise to new materials with fascinating properties.^[13] In these framework structures, the amine plays multiple roles, as it can act as space filler in the framework, as structure directing, templating factor and as hydrogen donor in its protonated form.

In the following work we focus on the chemistry of phosphorus in combination with sulfur, and pyridine, in its role as either cation or stabilizing factor.

- [1] J. Emsley, *The Sordid Tale of Murder, Fire and Phosphorus - The 13th Element*, John Wiley & Sons, New York, **2000**.
- [2] J. Berzelius, *Liebigs Ann. Chem.* **1843**, 46, 129.
- [3] A. Vos, E. H. Wiebenga, Koninkl. Ned. Akad. Wetenschap. **1954**, Proc. 57B, 497-499.
- [4] A. Stock, K. Thiel, *Ber. Dtsch. Chem. Ges.* **1905**, 38, 2719-2730.
- [5] a) J. Mai, *Ber. Dtsch. Chem. Ges.* **1911**, 44, 1725-1727; b) J. Mai, *Ber. Dtsch. Chem. Ges.* **1911**, 44, 1229-1233; c) V. Paul, *Application: GB GB*, **1910**; d) A. Stock, Hochschule, Breslau. *Ber.* **1910**, 43, 1223-1228; e) A. Stock, W. Scharfenburg, *Ber. Dtsch. Chem. Ges.* **1908**, 41, 558-564; f) A. Stock, K. Thiel, *Ber.* **1905**, 38, 2719-2730.
- [6] A. Stock, R. Friederici, *Angew. Chem.* **1913**, 25, 2201-2203.
- [7] H. Nowotnick, R. Blachnik, *Z. Anorg. Allg. Chem.* **2000**, 626, 611-612.
- [8] A. F. Holleman, E. Wiberg, N. Wiberg, *Lehrbuch der anorganischen Chemie*, Walter de Gruyter Verlag, Berlin, **2007**.
- [9] a) S. B. Hartley, W. S. Holmes, J. K. Jacques, M. F. Mole, J. C. McCoubrey, *Quart. Rev.* (London) **1963**, 17, 204-223; b) L. Pauling, *The Chemical Bond, Vol. 3*, Cornell University Press, Ithaca, **1967**.
- [10] W. Klingen, R. Ott, H. Hahn, *Z. Anorg. Allg. Chem.* **1973**, 396, 271-278.
- [11] H. Schaefer, G. Schaefer, A. Weiss, *Z. Naturforsch.* **1965**, 20b, 811.
- [12] a) R. Becker, W. Brockner, *Z. Naturforsch., Teil A* **1984**, 39A, 1120-1121; b) W. Brockner, R. Becker, B. Eisenmann, H. Schaefer, *Z. Anorg. Allg. Chem.* **1985**, 520, 51-58; c) M. Gjikaj, A. Adam, M. Duewel, W. Brockner, *Z. Kristallogr. - New Cryst. Struct.* **2005**, 220, 67-68; d) M. Gjikaj, W. Brockner, *Vibr. Spectrosc.* **2005**, 39, 262-265; e) M. Gjikaj, W. Brockner, A. Adam, *Z. Anorg. Allg. Chem.* **2006**, 632, 279-283; f) M. Gjikaj, C. Ehrhardt, W. Brockner, *Z. Naturforsch., B* **2006**, 61, 1049-1053; g) F. Menzel, W. Brockner, M. Ystenes, *J. Mol. Struct.* **1993**, 294, 53-56; h) F. Menzel, W. Brockner, M. Ystenes, *Vibr. Spectrosc.* **1997**, 14, 59-70; i) L. Ohse, W. Brockner, *Z. Naturforsch., A* **1988**, 43, 494-496; j) M. Ystenes, W. Brockner, F. Menzel, *Z. Naturforsch., A* **1992**, 47, 614-618; k) M. Ystenes, W. Brockner, F. Menzel, *Vibr. Spectrosc.* **1992**, 3, 285-290; l) A. Dimitrov, I. Hartwich, B. Ziemer, D. Heidemann, M. Meisel, *Z. Anorg. Allg. Chem.* **2005**, 631, 2439-2444.
- [13] a) A. K. Cheetham, G. Ferey, T. Loiseau, *Angew. Chem., Int. Ed.* **1999**, 38, 3268-3292; b) G. Ferey, *J. Solid State Chem.* **2000**, 152, 37-48.

Research Topics

The synthesis of distinct neutral or anionic P,S compounds in solution provides a great challenge for chemists. Due to the similarity in the energies of the P–P, P–S and S–S bonds nearly solely a mixture of compounds with different composition and charge is obtained. Our interest focuses on the system consisting of phosphorus, sulfur and pyridine, with the aim of a greater selectivity of P,S compounds in solution. The combination of these three components offers the opportunity of stabilizing unusual P,S compounds as pyridine adducts or pyridinium salts, integration of main group and transition metals (formation of metal-thiophosphates) and the investigation of many more reactions of this class of compounds in a basic environment.

In this work, our attention is drawn to the following five parts in particular:

I. Anionic Phosphorus Sulfur Compounds

The aim is to synthesise novel salts of thiophosphates, especially with nitrogen-containing aromatic bases as organic cations under mild conditions in solution. Furthermore, more light should be shed on the trithiometaphosphate anion. Is it really only possible to stabilize this anion by coordination with pyridine or are there other possible adducts?

II. Structures of Unusual Phosphate Derivatives

Especially the partial substitution of sulfur with oxygen in neutral and anionic P,S derivatives is to be investigated, as it increases the possibility of different intra- and intermolecular interaction, and thus gives rise to more complex build-ups in the crystal. Such compounds could be of great interest as intermediates to organic inorganic hybrid open framework materials.

III. Pyridine Stabilized Metal Complexes of P,S,O Anions

Is it possible to use oxo- and thiophosphates as ligands in metal-containing coordination complexes? What is the influence of pyridine on the composition and structures of the complexes? Furthermore, the overall structural build-up is important with regard to frameworks, as pointed out in the previous part. The synthesis in solution might lead to new stable coordination polymers, different from those accessible by solid state chemistry. The information from this study might provide the basis for a systematic study on thiophosphate metal frameworks from solution.

IV. Acyclic Phosphorus Sulfides

P_4S_{10} and many other neutral phosphorus sulfides are well known and have been described in the literature several times. As all these compounds show cage-like cyclic structures, the question arises whether it is also possible to synthesise acyclic phosphorus sulfides. The possible stabilization of such species by coordination with suitable nitrogen-containing bases at the phosphorus represents an important point of interest. Such adducts are expected to be useful precursors for the generation of reactive neutral P,S species.

V. Polyphosphides

The synthesis of phosphorus rich binary P,S anions still represents a great challenge for chemists. One possible route can be the oxidation of polyphosphides with elemental sulfur. An aim of the present thesis was to develop a synthetic route to specific polyphosphides and to investigate their reaction behaviour towards S_8 .

Motivation, concept, and accomplishment are discussed specifically in each chapter

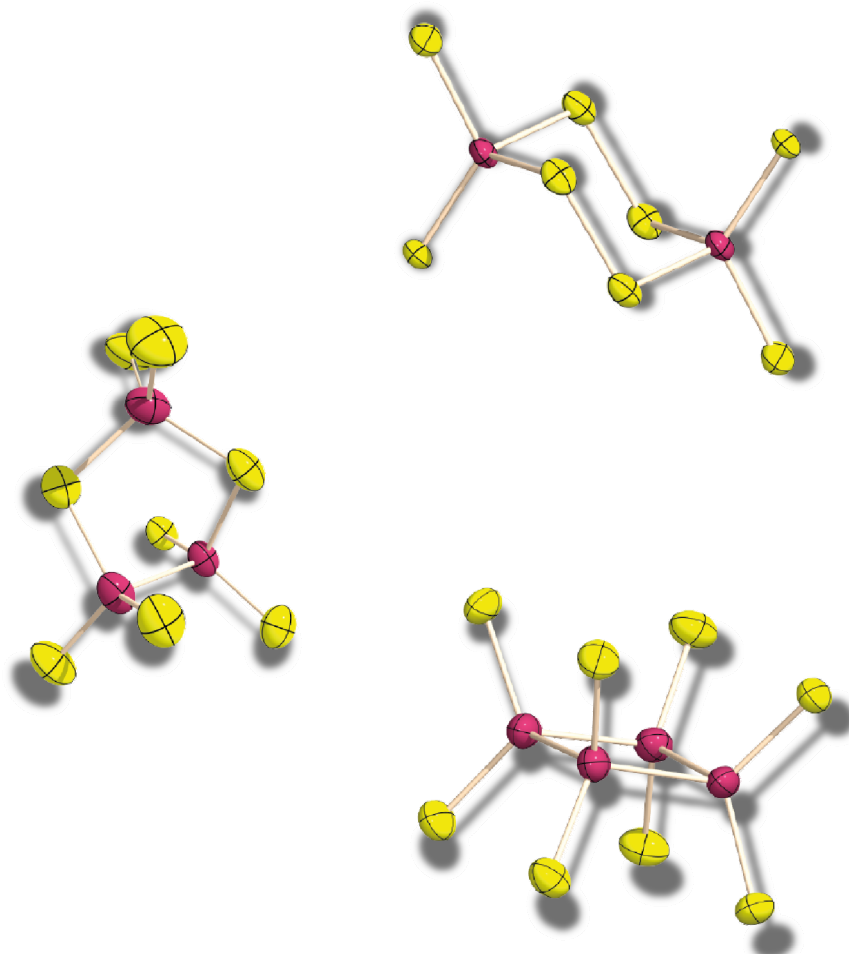
PART I

Anionic Phosphorus Sulfur Compounds

New Salts of the Cyclic Thiophosphates



As to be submitted to *Phosphorus, Sulfur Silicon Relat. Elem.*



Taking a look at the number of cyclic thiophosphate anions containing eight sulfur atoms, the three different anions $\text{P}_2\text{S}_8^{2-}$ (**I**), $\text{P}_3\text{S}_8^{3-}$ (**II**) and $\text{P}_4\text{S}_8^{4-}$ (**III**) can be found in the literature. To the best of our knowledge, so far only the Et_3NH^+ salt of **II** could be synthesized and characterized using single crystal X-ray diffraction. Syntheses of new salts of these three anions are presented and their molecular and crystal structures are discussed in the following. Each of them could be isolated with a protonated nitrogen containing aromatic base as counter ion.

Introduction

Comparing the number of known oxo- and thiophosphates, a rather great variety can be found for the P,S anions in contrast to the oxygen containing ones. This can be explained with the similar energies of the P–P, P–S and S–S single bonds (215, 230 and 213 kJ/mol, respectively)^[1], which leads to the formation of not only acyclic but also mono- and even polycyclic phosphorus sulfur anions. This however results in the disadvantage of unselective syntheses. In most cases the reaction solutions contain a mixture of different binary P,S anions with phosphorus in different oxidation states.^[2] The composition depends strongly on the amount of polysulfidic sulfur and the phosphorus source used.

On the contrary, oxophosphate anions show a strong preference of structures with exclusively P–O bonds because of the P–O bond energy being 335 kJ/mol.^[1]

Only a few salts of the eight sulfur atoms containing cyclic thiophosphates $P_2S_8^{2-}$ (**I**), $P_3S_8^{3-}$ (**II**) and $P_4S_8^{4-}$ (**III**) (Figure 1) have been described in the literature so far.^[2–12] The anion $P_2S_8^{2-}$ displays two S–S bridges between the phosphorus atoms, whereas **Ib** contains a S_1 and a S_3 bridge.^[2–4]

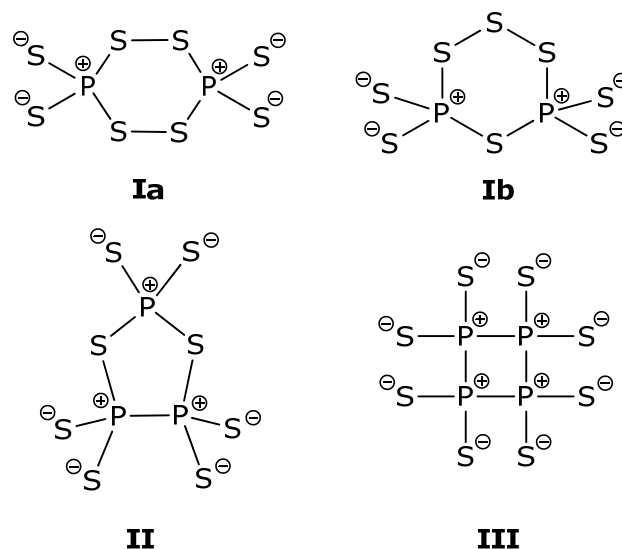


Figure 1. The three different P,S anions $P_2S_8^{2-}$ (**I**), $P_3S_8^{3-}$ (**II**) and $P_4S_8^{4-}$ (**III**).

In 1978 Minshall *et al.* were the first to describe the crystal structure of **Ia** followed by Falius in 1992.^[3] Karaghiosoff *et al.* investigated its behaviour via ^{31}P EXSY spectroscopy. They could show that this anion exists in solution in a twist and a chair

conformation (Figure 2) in the ratio 4:1. Also their ^{31}P NMR shifts could be determined with $\delta^{31}\text{P} = 119.5$ ppm (twist) and $\delta^{31}\text{P} = 55.5$ ppm (chair).^[5]

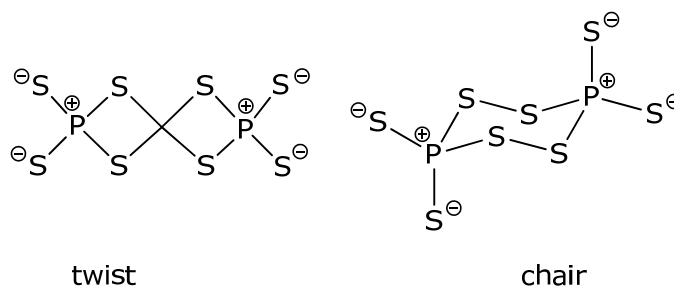
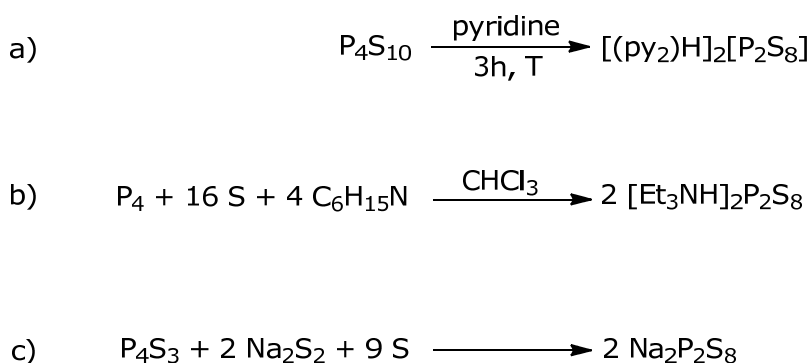


Figure 2. Two $\text{P}_2\text{S}_8^{2-}$ conformers of isomer **Ia**.

Thiophosphates in general are known to be rather moisture and air sensitive. This anion however has been proven to be stable over a long period of time when exposed to air.^[5] Also the selectivity of the synthetic routes shows the stability of $\text{P}_2\text{S}_8^{2-}$ (Scheme 1).

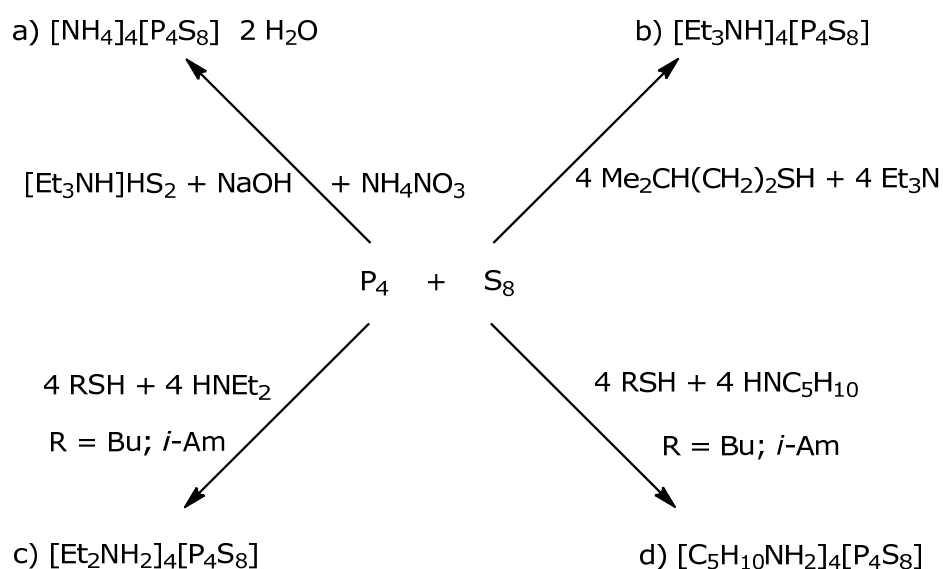


Scheme 1. Possible synthetic routes for the $\text{P}_2\text{S}_8^{2-}$ anion; a) Minshall *et al.*^[3]; b) Falius *et al.*^[2]; c) Karaghiosoff *et al.*^[5].

In 1992 the anion $\text{P}_3\text{S}_8^{3-}$ (**II**) was described by Falius for the first time. He prepared its Et_3NH^+ salt by refluxing stoichiometric amounts of white phosphorus, sulfur and triethylamine in chloroform and obtained single crystals after recrystallization from acetonitrile.^[2] A five-membered ring consisting of two sulfur and three phosphorus atoms forms the core of this anion. The remaining six sulfur atoms are bonded exocyclically to the phosphorus. $[\text{Et}_3\text{NH}][\text{P}_3\text{S}_8]$ is the only salt with the $\text{P}_3\text{S}_8^{3-}$ anion described so far. The synthesis of further salts provides an interesting challenge to explore more about the properties and chemistry of this rare anion.

The $P_4S_8^{4-}$ anion is well known and can be synthesized by the oxidation of white phosphorus by polysulfidic sulfur (Scheme 2). It has been described in the literature before.^[6–9] The first salt, which was structurally characterized using single crystal X-ray diffraction was $[NH_4]_4[P_4S_8] \cdot 2 H_2O$.^[6]

Due to previous research it is already known, that thiophosphates with a four membered ring of phosphorus atoms can be synthesized by using elemental phosphorus and alkyl polysulfides in a nonaqueous medium. The reaction proceeds fast at ambient temperature yielding a mixture of different thiophosphates.^[7] *Falius* and *Krause* proposed a reaction mechanism in which the polysulfide anions attack the P_4 tetrahedron, forming different P,S anions. In most cases however a four membered ring of phosphorus atoms can be observed. Until now it has also been reported on the crystal structures of the salts $[Et_3NH]_4[P_4S_8]$,^[8] $[Et_2NH_2]_4[P_4S_8]$ and $[C_5H_{10}NH_2]_4[P_4S_8]$ ^[9] (Scheme 2).



Scheme 2. Possible synthetic routes to the $P_4S_8^{4-}$ anion; a) *Falius et al.*^[6] b) *Badeeva et al.*^[8]; c) and d) *Gubaidullin et al.*^[9]

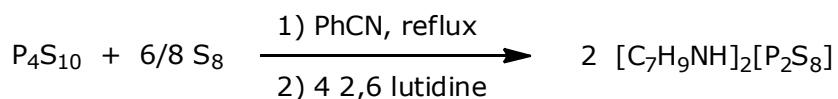
The results of *Falius* were complemented by the observations of *Badeeva et al.* in 2005.^[8] Further synthetic routes using mercaptanes, amines and copper complexes were described using quantum chemical calculations.^[9–12]

Summing up these results and observations it can be asserted that the oxidation of phosphorus by polysulfidic sulfur provides a challenging task for chemists to learn more about the complexity of cyclic thiophosphate anions.

Results and Discussion

Molecular and Crystal Structure [2,6-Me₂C₅H₃NH]₂[P₂S₈] (**1**)

The lutidinium salt **1** of the anion P₂S₈²⁻ was obtained by refluxing a solution of P₄S₁₀ and elemental sulfur in benzonitrile and subsequent addition of 2,6-lutidine.



Scheme 3. Synthesis of [2,6-Me₂C₅H₆N]₂[P₂S₈] (**1**).

Compound **1** is soluble in most common polar aprotic organic solvents like tetrahydrofuran or acetonitrile.

The lutidinium salt **1** crystallizes in the form of colourless blocks in the monoclinic space group *P*2₁/*n* with four asymmetric units in the unit cell. Figure 3 shows the molecular structure of **1**, selected atom distances and bond angles are listed.

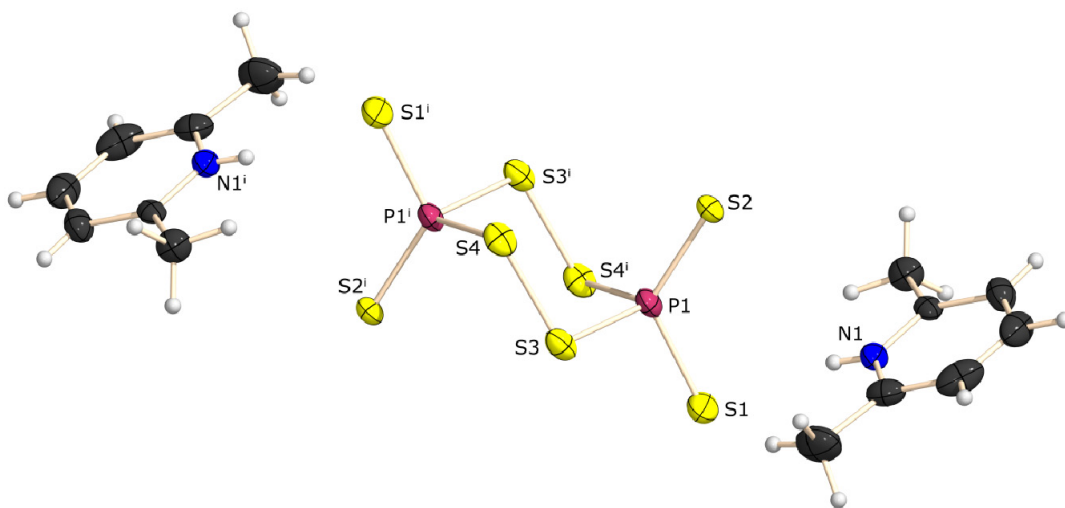


Figure 3. Molecular structure of **1**. Thermal ellipsoids are set at 50% probability level. Symmetry operation *i* = 1-*x*, 1-*y*, 2-*z*. Selected atom distances [Å] and bond angles [°]: P1-S1 1.994(2), P1-S2 1.945(2), P1-S3 2.127(2), P1-S4ⁱ 2.125(2), S3-S4 2.049(2); S1-P1-S2 122.5(1), S1-P1-S3 101.0(1), S1-P1-S4ⁱ 99.8(1), S2-P1-S3 112.7(1), S2-P1-S4ⁱ 114.4(1), S3-P1-S4ⁱ 104.0(1), P1-S3-S4 102.5(1), P1-S4ⁱ-S3ⁱ 102.0(1); P1-S3-S4-P1ⁱ 72.6(1).

In Table 1 selected average atom distances of **1**, [pyH]₂[P₂S₈] and Na₂[P₂S₈] are compared. In **1** the bond lengths of single coordinated sulfur and the phosphorus atoms (S1–P1, S2–P1) are only up to 3.9% longer than the ones found in the other two compounds. The distance between the bridging sulfur atoms and phosphorus (S3–P1, S4–P1) lies with 2.126(2) Å between the value found in the pyridinium (2.084(5) Å) and the sodium salt (2.130(4) Å). The value for the bond length between the two bridging sulfur atoms is with 2.049(2) Å in the same range as the one found in [pyH]₂[P₂S₈] (2.047(7) Å), shorter than 2.059(4) Å as found in Na₂P₂S₈ and longer than the average value of 2.031(17) Å for this type of bond as described by Allen *et al.*^[13]. Taking a look at the bond angles within the P₂S₈²⁻ entity one will find, that they differ quite strongly in all three salts. It seems that the degree of contortion in every salt is different depending on the packing in the crystal.

Figure 4 shows the unit cell of **1**. Between the counterions electrostatic interactions can be found. The sulfur atom S1 has a distance to the nitrogen atom of the lutidinium cation of 3.281(4) Å, which is below the sum of the van der Waals radii of sulfur and nitrogen (3.35 Å^[15]). The N–H distance has a value of 0.88(1) Å, a hydrogen acceptor distance of 2.41(1) Å and an N–H–S angle of 173°, which is very close to linearity.

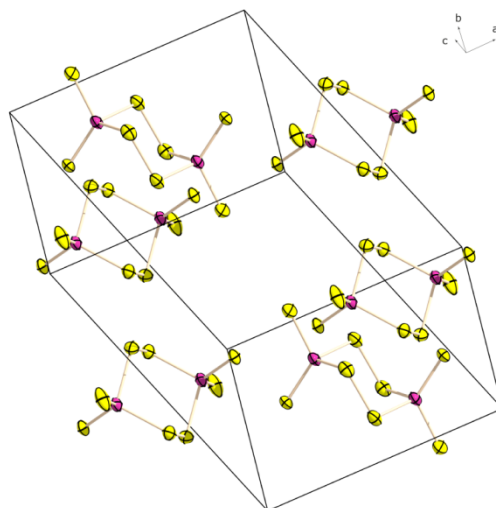


Figure 4. Unit cell of **1**. View along c axis. Thermal ellipsoids are set at 50% probability level. Hydrogen, nitrogen and carbon atoms are omitted for clarity.

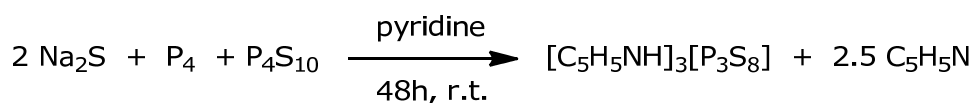
Table 1. Comparison of average atom distances and bond angles in **1**.

	1	[pyH] ₂ [P ₂ S ₈] ^[a]	Na ₂ [P ₂ S ₈] ^[b]	Ref. ^[13]
distances[Å]				
P–S ^[oc]	1.970(2)	1.962(2)	1.956(4)	
P–S ^[tc]	2.126(2)	2.084(5)	2.130(4)	
S–S	2.049(2)	2.047(7)	2.059(4)	2.031(17)
P–O				1.621(7)
angles[°]				
S ^[oc] –P–S ^[oc]	122.5(1)	118.1(1)	122.1(2)	
S ^[oc] –P–S ^[tc]	113.5(1)	116.6(1)	112.6(2)	
S ^[oc] –P–S ^[tc]	100.4(1)	109.9(1)	101.9(2)	
S ^[tc] –P–S ^[tc]	104.0(2)	102.2(2)	107.1(2)	
ΣP–S–P		334.70	336.60	
torsion angle [°]				
P–S–S–P	72.6(1)	86.37(2)	72.8	

^[a] Karaghiosoff *et al.*, ^[b] Minshall *et al.*; [oc]= onefold coordinated, [tc] = twofold coordinated.

Molecular and Crystal Structure of [pyH]₃[P₃S₈] · 2.5 py (**2**)

The salt [pyH]₃[P₃S₈] · 2.5 py (**2**) could be synthesized by stirring a suspension of P₄, Na₂S and P₄S₁₀ in pyridine at ambient temperature.



Scheme 4. Synthesis of [pyH]₃[P₃S₈] · 2.5 py (**2**).

This molecule is rather insoluble in common organic solvents and sensitive towards moisture and air. For this anion an A₂X spin system can be observed (δ_A = 134.3 ppm, δ_A = 85.0 ppm, J_{AX} = 15.1 Hz).

Compound **2** crystallizes as yellow blocks in the triclinic space group *P*–1 with two formula units in the unit cell. The structure of the anion in **2** is shown in Figure 5 and selected atom distances and bond angles are given.

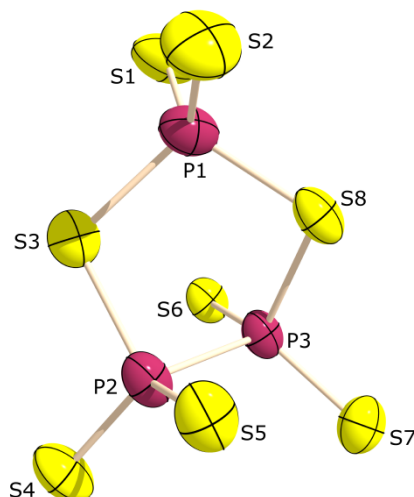


Figure 5. Structure of the anion in **2**. Pyridinium and solvent molecules are omitted for clarity. Ellipsoids are drawn at 50% probability level. Selected bond distances [\AA] and bond angles [$^\circ$]: P1-S1 1.973(3), P1-S2 1.981(3), P1-S3 2.127(3), P1-S8 2.124(3), P2-S3 2.124(3), P2-S4 1.976 (3), P2-S5 1.970(2), P2-P3 2.280(2), P3-S6 1.967(2), P3-S7 1.965(3), P3-S8 2.138(3);
S1-P1-S2 117.7(2), S4-P2-S5 118.3(2), S6-P3-S7 119.1(2), S3-P1-S8 104.4(2), S3-P2-P3 94.6(2), P2-P3-S8 94.1(2), P1-S3-P2 102.7(2), P1-S8-P3 104.3(2).

The five membered ring of $\text{P}_3\text{S}_8^{3-}$ consists of two sulfur and three phosphorus atoms. Within the ring two phosphorus atoms are connected directly while the third one is bridged by the sulfur atoms. Each phosphorus atom is further coordinated by two exocyclic sulfur atoms. The endocyclic P-S bond lengths within the ring are with an average value of $2.128(3) \text{ \AA}$ elongated compared to a single bond (2.11 \AA)^[14]. The exocyclic P-S atom distances, which have an average value of $1.972(2) \text{ \AA}$, are however closer to a P-S double bond ($1.954(5) \text{ \AA}$)^[13]. These results are in good accordance with those found by Falius.^[2] By comparing the bond angles within the ring it can be asserted that the S-P-S bond angles are larger than the P-S-P angles. Furthermore the torsion angles have an average value of $72.3(2)^\circ$, which indicates a deviation from planarity. Obviously the five membered ring is not able to form a half chair conformation as proposed by Falius^[2]. To find a compromise between the occurring strains, the anion is arranged in an envelope conformation, which allows the lowest total strain for the structure (Figure 6).

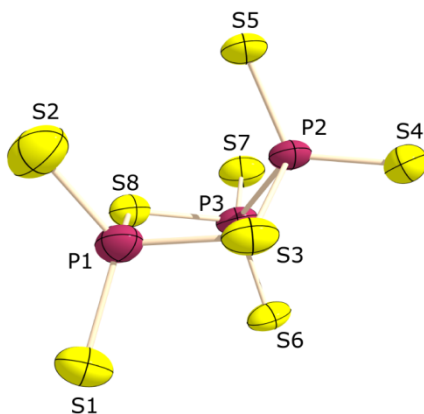


Figure 6. Envelope conformation of the anion in **2**.

The unit cell contains two formula units of the $P_3S_8^{3-}$ anion. These two entities are oriented in opposite direction and are adjacent. The emerging space is filled with pyridinium cations and pyridine molecules. In the crystal structure only weak electrostatic interactions can be found. In Figure 7 the described unit cell of **2** is shown.

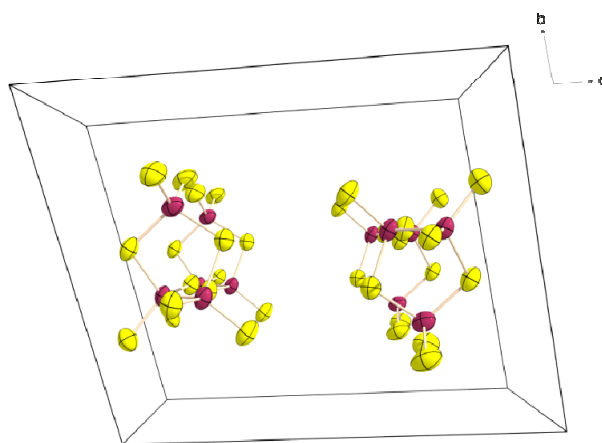
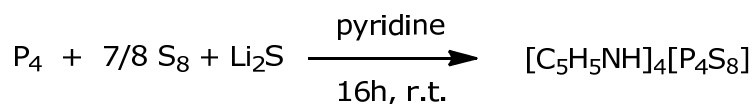


Figure 7. Four formula units and the cell edges of the unit cell of **2** with view along the *a* axis. Pyridinium cations and solvent molecules are omitted for clarity. Ellipsoids are drawn at 50% probability level.

Molecular and Crystal Structure of [pyH]₄[P₄S₈] · py (**3**)

The pyridinium salt of the P₄S₈⁴⁻ anion was obtained by suspending P₄, Li₂S and S₈ in pyridine and stirring at ambient temperature.



Scheme 5. Synthesis of [pyH]₄[P₄S₈] · py (**3**)

The salt **3** is rather insoluble in common organic solvents but not quite as sensitive towards moisture and air as **2**.

Compound **3** crystallizes as colourless plates in the monoclinic space group C2/c with four formula units in the unit cell. Due to a high disorder in the pyridinium cations and solvent molecules all structural parameters of these species are afflicted with a high standard deviation. Figure 8 shows the structure of the anion in **3** and selected atom distances and bond angles are listed.

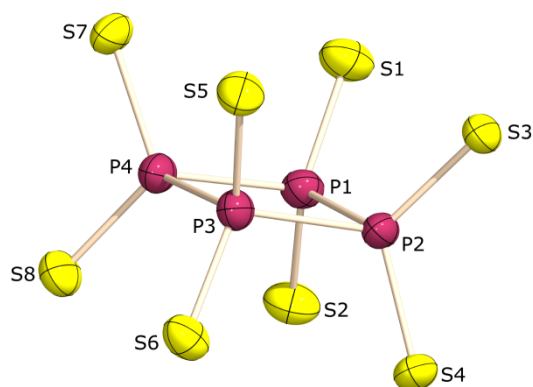


Figure 8. Structure of the anion in **3**. Pyridinium and solvent molecules are omitted for clarity. Ellipsoids are drawn at 50% probability level. Selected atom distances [Å] and bond angles [°]: P1-S1 1.983(2), P1-S2 1.976(2), P2-S3 1.979(2), P2-S4 1.997(2), P3-S5 1.982(2), P3-S6 1.980(2), P4-S7 1.986(2), P4-S8 1.976(2), P1-P2 2.279(2), P2-P3 2.275(2), P3-P4 2.293(2), P4-P1 2.283(2);
S1-P1-S2 120.4(2), S3-P2-S4 116.4(2), S5-P3-S6 120.3(2), S7-P4-S8 118.6(2), P1-P2-P3 90.2(1), P2-P3-P4 90.0(1), P3-P4-P1 90.0(1), P4-P1-P2 90.1(1).

The phosphorus atoms form a four membered ring. Each one is further coordinated by two sulfur atoms. Within the ring the four P–P angles have values between 90.0(1) and 90.2(1) °. Because of an average P–P–P torsion angle of 1.7(1) ° this motive is very close to a planar square. Furthermore the distances between the PS_3^- units have an average value of 2.283(2) Å, which is elongated compared to a single bond (2.256(5) Å)^[13]. This can be explained by repulsions between the phosphorus atoms and the occurring ring strain. For the literature-known compounds the same observations can be ascertained (Table 2). Though there are little aberrations which can be explained by the use of different counterions and therefore varying strong interactions, which influence the P–P distances as well. In Table 2, atom distances and bond angles of the four known $\text{P}_4\text{S}_8^{2-}$ salts are listed and compared with those of **3**. The eight P–S bond lengths are with an average value of 1.982(3) Å closer to a P–S double (1.954(5) Å)^[13] than a single bond (2.11 Å)^[14], which fits very well with those observed in [a-d]. The four pyridinium counterions stabilize the anion by weak interactions and due to their position the unit is electrostatically shielded from the outside forming single entities.

Table 2 Comparison of atom distances and bond angles in **3** with literature-known salts of $\text{P}_4\text{S}_8^{2-}$.

	3	$[\text{NH}_4]_4[\text{P}_4\text{S}_8] \cdot 2 \text{ H}_2\text{O}$ ^[6]	$[\text{Et}_3\text{NH}]_4[\text{P}_4\text{S}_8]$ ^[8]	$[\text{Et}_2\text{H}_2\text{N}]_4[\text{P}_4\text{S}_8]$ ^[9]	$[\text{C}_5\text{H}_{12}\text{N}]_4[\text{P}_4\text{S}_8]$ ^[9]
average distances [Å]					
P–S	1.982(2)	1.976(1)	1.983(1)	1.976(1)	1.981(1)
P–P	2.283(2)	2.284(1)	2.308(1)	2.289(1)	2.293(2)
average angles [°]					
S–P–S	118.9(2)	118.6(1)	117.2(1)	118.5(5)	118.5(4)
P–P–P	90.1(1)	90.0(1)	90.0(1)	90.4(3)	90.0(3)

Falius *et al.*^[6], Badeeva *et al.*^[8], Gubaidullin *et al.*^[9].

The $\text{P}_4\text{S}_8^{4-}$ anions form aligned chains in which the molecules have the same orientation. These entities are stacked sequentially alternated and the emerging space is filled by pyridine. In Figure 9 the unit cell of **3** is shown.

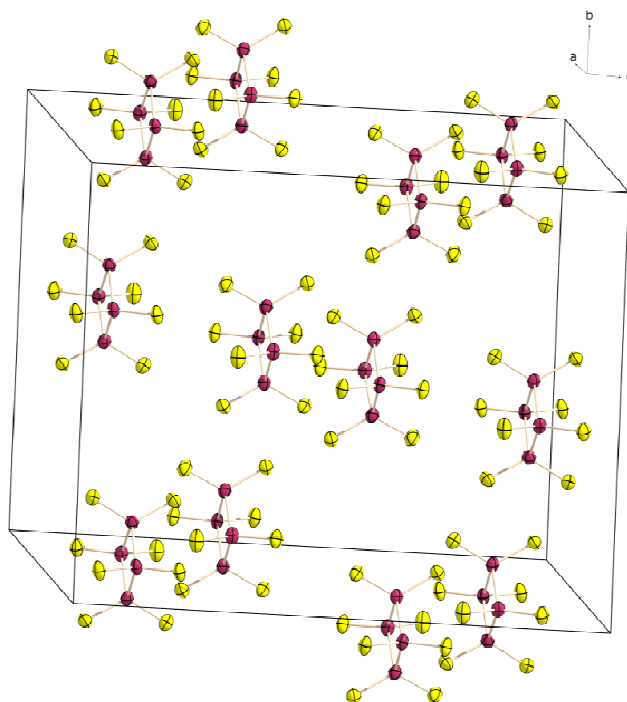
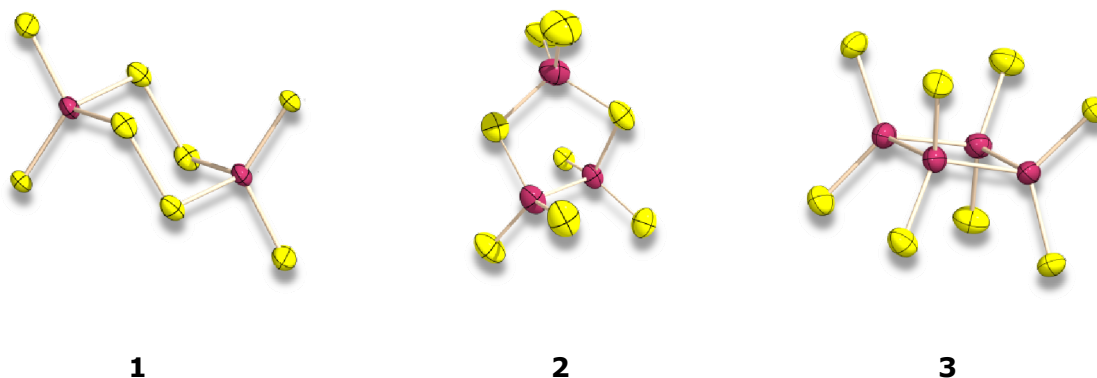


Figure 9. Unit cell of **3** with view along the *c* axis. Pyridinium and solvent molecules are omitted for clarity - Ellipsoids are drawn at 50% probability level.

Conclusion

Three new ionic compounds ($[2,6\text{-Me}_2\text{C}_5\text{H}_6\text{N}]_2[\text{P}_2\text{S}_8]$ (**1**), $[\text{pyH}]_3[\text{P}_3\text{S}_8] \cdot 2.5 \text{ py}$ (**2**) and $[\text{pyH}]_4[\text{P}_4\text{S}_8] \cdot \text{py}$ (**3**)) of the cyclic, eight sulfur atoms containing anions $\text{P}_n\text{S}_8^{n-}$ ($n = 2\text{--}4$) have been prepared and their structures elucidated by single crystal X-ray diffraction.



In the series of anions of $\text{P}_n\text{S}_8^{n-}$ ($n = 2\text{--}4$), a clear trend towards a decrease in ring size is observed with the increase of the phosphorus content.

The syntheses of **1–3** present new, straightforward, reproducible and selective routes with good yields, using convenient and easily accessible starting materials. Furthermore the reaction conditions are rather mild. These results extend our knowledge concerning previous studies on cyclic thiophosphates and provide further evidence for the variety of possible salts containing the above mentioned anions. Therefore these fundamental achievements complement the knowledge in this research area and provide the basis for a systematic investigation of the family of thiophosphates in basic solution and detailed studies of their chemistry.

Experimental Section

General. Na₂S was obtained from Sigma-Aldrich Inc., used as supplied without further purification and stored under inert gas atmosphere. P₄S₁₀ was commercially obtained (Riedel-de H  en) and was purified by extraction with CS₂ before use. P₄ was commercially obtained from ThermPhos. All solvents were dried using commonly known methods and freshly distilled before use. **³¹P NMR** chemical shifts are referred to 85% H₃PO₄ as external standard. All spectra were measured, if not mentioned otherwise, at 25 °C. The %-data correspond to the intensities in the ³¹P NMR spectra with respect to the total intensity. The difference to 100 % belongs to not assignable signals. **IR** spectra were recorded on a PerkinElmer BX FT IR spectrometer equipped with a Smiths DuraSamplIR II diamond ATR unit. Transmittance values are qualitatively described as “very strong” (vs), “strong” (s), “medium” (m), “weak” (w) and “very weak” (vw). **Raman** spectra were recorded on a Bruker RAM II spectrometer equipped with a Nd:YAG laser (200 mW) operating at 1064 nm and a reflection angle of 180 °. The intensities are reported as percentages of the most intense peak and are given in parentheses. Low resolution mass spectra were recorded on a JEOL MStation JMS-700 with 4-nitrobenzyl alcohol as matrix for FAB measurements. **Elemental analyses** (CHNS) were performed with an Elementar Vario EL instrument. Due to the formation of glassy (P₂O₅)_x(H₂O)_yC during measurement, the values deviate considerably from the calculated ones. **Melting and decomposition points** were determined by differential scanning calorimetry (Linseis DSC-PT10, calibrated with standard pure indium and zinc). Measurements were performed at a heating rate of 5 °C min⁻¹ in closed aluminum sample pans with a

0.1 mm hole in the lid for gas release to avoid an unsafe increase in pressure under a nitrogen flow of 20 mL min^{-1} with an empty identical aluminum sample pan as a reference. Melting points were checked with a Büchi Melting Point B-540 in open glass capillaries.

X-ray Crystallography. The single-crystal X-ray diffraction data were collected using an Oxford Xcalibur3 diffractometer equipped with a Spellman generator (voltage 50 kV, current 40 mA), Enhance molybdenum K_α radiation source ($\lambda = 71.073 \text{ pm}$), Oxford Cryosystems Cryostream cooling unit, four circle kappa platform and a Sapphire CCD detector. Data collection and reduction were performed with CrysAlisPro.^[16] The structures were solved with SIR97^[17], SIR2004^[18], refined with SHELXL-97^[19], and checked with PLATON^[20], all integrated into the WinGX software suite^[21]. The finalized CIF files were checked with checkCIF.^[22] All non-hydrogen atoms were refined anisotropically. The hydrogen atoms were located in difference Fourier maps and placed with a C–H distance of 0.98 \AA for C–H bonds. Intra- and intermolecular contacts were analyzed with DIAMOND (version 3.2i), thermal ellipsoids are drawn at the 50% probability level. Selected crystallographic data and refinement details for the structure determination of compound **1–3** are summarized in Table 3.

[2,6-Me₂C₅H₃NH]₂[P₂S₈] (1): P₄S₁₀ (108.8 mg, 0.24 mmol) and sulfur (31.0 mg, 0.96 mmol) were suspended in benzonitrile (1.5 mL) and refluxed until a yellow-brownish solution with yellow precipitate was observed. Afterwards 2,6-lutidine (111 mL, 4 eq) was added. The now brown solution was another time refluxed for 1 h. After two days a small amount of colourless block shaped crystals of **1** could be obtained.

³¹P{¹H} NMR (PhCN, lutidine, rt): δ [ppm] = 128.7 (s, 21%), 119.1 (**1**, s, 24%), 55.7 (**1**, s, 6%).

[pyH]₃[P₃S₈] · 2.5 py (2): Na₂S (0.42 g, 5.32 mmol) was added to a suspension of P₄ (390.0 mg, 2.65 mmol) in pyridine (15 mL). The yellow mixture was stirred for 30 min and P₄S₁₀ (1.18 g, 2.66 mmol) was added. After another 48 h of stirring at ambient temperature the orange solution was separated and dried *in vacuo* yielding yellow blocks of **2**. (Yield: 875.3 mg, 1.1 mmol, 56% with respect to P₄)

³¹P NMR (pyridine, rt): δ [ppm] = 170.1 (PS_3^- , s, br, 34%) 134.3 (**2**, d, $^1J_{\text{PP}}$ = 15.1 Hz, 39%), 85.0 (**2**, t, $^1J_{\text{PP}}$ = 15.1 Hz 18%). **Mass spectrometry** m/z (ESI+) = 743.5 ($[\text{C}_{25}\text{H}_{25}\text{N}_5\text{P}_3\text{S}_8]^+$), 742.5 ($[\text{C}_{25}\text{H}_{24}\text{N}_5\text{P}_3\text{S}_8]^+$), 586.6 ($[\text{C}_{15}\text{H}_{15}\text{N}_3\text{P}_3\text{S}_8]^+$), 585.6 ($[\text{C}_{15}\text{H}_{14}\text{N}_3\text{P}_3\text{S}_8]^+$), 506.5 ($[\text{C}_{10}\text{H}_9\text{N}_2\text{P}_3\text{S}_8]^+$), 446.9 ($[\text{H}_4\text{NP}_3\text{S}_8]^+$), 427.1 ($[\text{C}_5\text{H}_4\text{NP}_3\text{S}_8]^+$), 405.8 ($[\text{C}_3\text{H}_6\text{NP}_3\text{S}_8]^+$), 389.9 ($[\text{C}_3\text{H}_5\text{P}_3\text{S}_8]^+$), 303.1 ($[\text{C}_2\text{H}_{11}\text{NP}_2\text{S}_6]^+$), 126.7 ($[\text{PS}_3]^+$). m/z (ESI-) = 210.0 ($[\text{H}_6\text{NP}_2\text{S}_4]^-$), 206.9 ($[\text{H}_3\text{NP}_2\text{S}_4]^-$), 190.9 ($[\text{P}_2\text{S}_4]^-$). **Raman** (500 mW, rt): ν [cm^{-1}] = 3060 (100), 1590 (47), 1218 (29), 1034 (68), 999 (89), 473 (30), 362 (79). **IR** (200 mW, rt): ν [cm^{-1}] = 3075 (vw), 3034 (v), 1927 (br, v), 1869 (br, v), 1633 (v), 1609 (v), 1588 (m), 1572 (vw), 1530 (v), 1484 (m), 1453 (w), 1437 (s), 1258 (br, w), 1216 (w), 1147 (m), 1067 (m), 1031 (m), 1013 (v), 997 (m), 914 (br, m), 748 (s) 700 (vs). **DSC** (5 °C/min): T_{dec} = 103.9 °C.

[pyH]₄[P₄S₈] · py (3**):** P₄ (610.0 mg, 4.9 mmol) was suspended in pyridine (48 mL) and S₈ (1.58 g, 49.3 mmol) and Li₂S (1.33 g, 29.0 mmol) were added. The solution was stirred over night at ambient temperature. Afterwards the green precipitate was removed and the dark green solution was dried *in vacuo* yielding colourless crystals of **3**. (Yield: 3585.2 mg, 4.6 mmol, 93.9% with respect to P₄)

³¹P NMR (THF, rt): δ [ppm] = 119.4 (s, 99%). **Elemental analysis** [P₄S₈][pyH]₄·py: calcd. C 38.50, N 8.98, H 3.75, S 32.89; found: C 34.93, N 8.19, H 2.68, S 34.62. **Mass spectrometry** m/z (ESI+) = 519.0 ($[\text{C}_8\text{H}_{16}\text{N}_2\text{P}_4\text{S}_8]^+$), 509.3 ($[\text{C}_7\text{H}_{18}\text{N}_2\text{P}_4\text{S}_8]^+$), 465.3 ($[\text{C}_5\text{H}_{12}\text{NP}_4\text{S}_8]^+$), 429.1 ($[\text{C}_5\text{H}_6\text{NP}_3\text{S}_8]^+$), 427.1 ($[\text{C}_5\text{H}_4\text{NP}_3\text{S}_8]^+$), 409.3 ($[\text{H}_4\text{NP}_4\text{S}_8]^+$), 343.3 ($[\text{C}_3\text{H}_9\text{NP}_3\text{S}_6]^+$), 303.1 ($[\text{H}_6\text{P}_3\text{S}_6]^+$), 126.7 ($[\text{PS}_3]^+$). m/z (ESI-) = 287.7 ($[\text{H}_2\text{P}_3\text{S}_6]^-$), 218.8 ($[\text{H}_3\text{NP}_2\text{S}_4]^-$). **Raman** (500 mW, rt): ν [cm^{-1}] = 3062 (7), 1597 (3), 1574 (3), 1224 (3), 1032 (6), 1007 (9), 992 (7), 654 (4), 474 (59), 439 (11), 248 (13), 220 (100), 187 (8), 154 (82). **IR** (200 mW, rt): ν [cm^{-1}] = 3087 (w), 3055 (br, w), 2996 (w), 1931 (vw), 1871 (vw), 1627 (w), 1595 (s), 1580 (w), 1487 (m), 1440 (s), 1216 (m), 1148 (m), 1097 (br, m), 1068 (m), 1033 (m), 1000 (s), 940 (m), 750 (s), 698 (vs), 674 (vw). **DSC** (5 °C/min): T_{dec} = 123.1 °C.

Table 3 Structural and refinement data of compounds **1**, **2**, and **3**.

	1	2	3
formula	C ₇ H ₁₀ NPS ₄	C _{27.5} H _{29.5} N _{5.5} P ₃ S ₈	C ₅₀ H ₅₈ N ₁₀ P ₈ S ₁₆
M [g/mol]	267.37	786.46	1558.78
crystal system	monoclinic	triclinic	monoclinic
space group	<i>P</i> 2 ₁ / <i>n</i>	<i>P</i> –1	<i>C</i> 2/ <i>c</i>
colour/Habit	colourless block	yellow block	colourless plate
crystal size	0.2x0.08x0.05	0.2x0.15x0.1	0.25x0.15x0.1
<i>a</i> [Å]	9.2222(5)	8.619(5)	17.2108(10)
<i>b</i> [Å]	7.9190(4)	13.476(5)	18.6899(8)
<i>c</i> [Å]	15.9445(10)	16.177(5)	22.4809(12)
α [°]		98.313(5)	
β [°]	96.079(5)	94.653(5)	103.826(6)
γ [°]		104.000(5)	
<i>V</i> [Å ³]	1157.87(10)	1790.7(14)	7021.9(6)
<i>Z</i>	4	2	4
ρ_{calc} [g/cm ^{–3}]	1.534	1.459	1.474
μ [mm ^{–1}]	0.914	0.662	0.711
<i>F</i> (000)	552	812	3216
θ range [°]	4.12–24.98	4.31–25.35	4.13–23.50
<i>T</i> [K]	173(2)	173(2)	100(2)
Index ranges	–10 ≤ <i>h</i> ≤ 10 –9 ≤ <i>k</i> ≤ 9 –18 ≤ <i>l</i> ≤ 18	–10 ≤ <i>h</i> ≤ 10 –15 ≤ <i>k</i> ≤ 16 –19 ≤ <i>l</i> ≤ 18	–12 ≤ <i>h</i> ≤ 20 –13 ≤ <i>k</i> ≤ 22 –27 ≤ <i>l</i> ≤ 24
data collected	10202	12687	10786
data unique	2019	6444	5092
data obs.	1322	3229	2475
<i>R</i> (int)	0.0564	0.0694	0.0602
GOOF	0.915	0.998	0.965
<i>R</i> ₁ , <i>wR</i> ₂ (<i>I</i> > 2 σ <i>I</i> ₀)	0.0501, 0.1244	0.0790, 0.1483	0.0589, 0.0906
<i>R</i> ₁ , <i>wR</i> ₂ (all data)	0.0776, 0.1318	0.1660, 0.1899	0.1407, 0.1207
larg. diff peak/ hole (e/Å)	1.590 –0.357	0.796 –0.328	0.640 –0.382

Acknowledgement

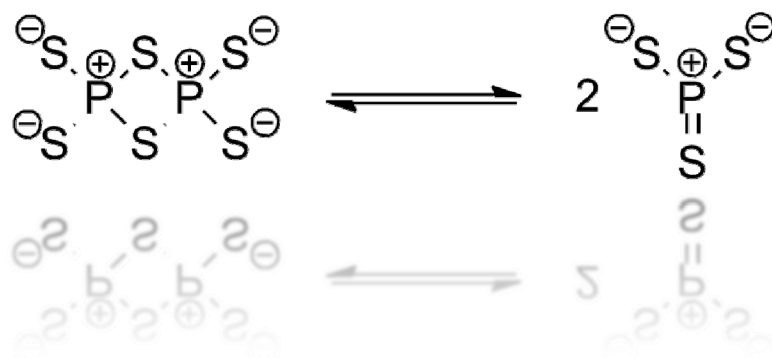
Financial support by the Department of Chemistry, Ludwig Maximilian University, is gratefully acknowledged. We thank Prof. T. M. Klapötke, Department of Chemistry, Ludwig Maximilian University, for the generous allocation of diffractometer time and for his continuous support.

-
- [1] a) L. Pauling, *The Chemical Bond*, Vol. 3, Cornell University Press, Ithaca, **1967**; b) S. B. Hartley, W. S. Holmes, J. K. Jacques, M. F. Mole, J. C. McCoubrey, *Quart. Rev. (London)* **1963**, *17*, 204-223.
 - [2] H. Falius, A. Schliephake, D. Schomburg, *Z. Anorg. Allg. Chem.* **1992**, *611*, 141-148.
 - [3] P. C. Minshall, G. M. Sheldrick, *Acta Cryst., Section B* **1978**, *34*, 1378-1380.
 - [4] H. Gruber, U. Muller, *Z. Anorg. Allg. Chem.* **1997**, *623*, 957-961.
 - [5] C. Rotter, *Dissertation* LMU München (Munich), **2009**.
 - [6] H. Falius, W. Krause, W. S. Sheldrick, *Angew. Chem.* **1981**, *93*, 121-122.
 - [7] W. Krause, H. Falius, *Z. Anorg. Allg. Chem.* **1983**, *496*, 80-93.
 - [8] E. K. Badeeva, D. B. Krivolapov, A. T. Gubaidullin, I. A. Litvinov, E. S. Batyeva, O. G. Sinyashin, *Mendeleev Commun.* **2005**, 22-23.
 - [9] A. T. Gubaidullin, E. K. Badeeva, D. B. Krivolapov, I. A. Litvinov, E. S. Batyeva, O. G. Sinyashin, *J. Struct. Chem.* **2007**, *48*, 954-959.
 - [10] E. K. Badeeva, E. V. Platova, E. S. Batyeva, L. I. Kursheva, E. E. Zvereva, A. E. Vandyukov, S. A. Katsyuba, V. I. Kovalenko, O. G. Sinyashin, *Heteroat. Chem.* **2011**, *22*, 24-30.
 - [11] O. G. Sinyashin, E. S. Batyeva, V. I. Kovalenko, E. K. Badeeva, E. V. Platova, A. E. Vandyukov, E. E. Zvereva, L. I. Kursheva, *Phosphorus, Sulfur Silicon Relat. Elem.* **2011**, *186*, 852-853.
 - [12] L. I. Kursheva, E. S. Batyeva, E. E. Zvereva, E. K. Badeeva, E. V. Platova, O. G. Sinyashin, *Phosphorus, Sulfur Silicon Relat. Elem.* **2013**, *188*, 490-492.
 - [13] F. H. Allen, O. Kennard, D. G. Watson, L. Brammer, A. G. Orpen, R. Taylor, *J. Chem. Soc., Perkin Trans. 2* **1987**, S1-S19.
 - [14] A. F. Holleman, E. Wiberg, N. Wiberg, *Lehrbuch der anorganischen Chemie*, 102 ed., Walter de Gruyter Verlag, Berlin/New York, **1995**.
 - [15] A. Bondi, *J. Phys. Chem.* **1966**, *70*, 3006-3007.
 - [16] *CrysAlisPro 1.171.36.21*, Agilent Technologies, **2012**.
 - [17] A. Altomare, G. Cascarano, C. Giacovazzo, A. Guagliardi, A. A. G. Moliterni, M. C. Burla, G. Poidori, M. Camalli, R. Spagna, **1997**, 343.
 - [18] a) M. C. Burla, R. Caliandro, M. Camalli, B. Carrozzini, G. L. Cascarano, L. De Caro, C. Giacovazzo, G. Polidori, R. Spagna, Institute of Crystallography, Bari (Italy), **2004**; b) M. C.

- Burla, R. Caliendo, M. Camalli, B. Carrozzini, G. L. Cascarano, L. De Caro, C. Giacovazzo, G. Polidori, R. Spagna, *Journal of Applied Crystallography* **2005**, 38, 381-388.
- [19] a) G. M. Sheldrick, *SHELXL-97, Program for the Refinement of Crystal Structures*. University of Göttingen, Göttingen (Germany), **1997**; b) G. M. Sheldrick, *Acta Crystallographica, Section A: Foundations of Crystallography* **2008**, A64, 112-122.
- [20] A. L. Spek, *Platon, A Multipurpose Crystallographic Tool*, Utrecht University, Utrecht, The Netherlands, **2012**.
- [21] L. J. Farrugia, *J. Appl. Crystallogr.* **1999**, 32, 837-838.
- [22] <http://journals.iucr.org/services/cif/checkcif.html>

The Truth about the Trithiometaphosphate PS_3^-

As to be submitted to *Z. Anorg. Allg. Chem.*



Two new salts containing the $\text{P}_2\text{S}_6^{2-}$ anion have been prepared as well as three new salts of the donorstabilized trithiometaphosphate PS_3^- . As educts, phosphorus sulfides (P_4S_3 , P_4S_{10}), Na_2S_2 and elemental sulfur in common organic solvents like THF or acetonitrile are used. We are able to contribute new results to the question whether and if so how, the trithiometaphosphate anion can be stabilized in the crystal. Temperature dependent ^{31}P NMR spectroscopy is performed, showing an equilibrium between the adduct stabilized and the free monomeric trithiometaphosphate anion in solution.

Introduction

Comparing the variety of known oxophosphate anions with the one of thiophosphates, a rather great diversity for the latter can be found. This occurs due to the similar energies of the P–P, P–S and S–S bonds (215, 230, 213 kJ/mol) in contrary to the P–O bond (335 kJ/mol).^[1,2] So it can be understood that even mono- and polycyclic phosphorus–sulfur anions can be formed by different combinations of the three possible linkages compared to only one possibility in the P–O anions, with a few exceptions. Despite this aspect, the formation of binary thiophosphates containing a central phosphorus atom with a low coordination number (σ^2 or σ^3) in the oxidation state III and V, respectively, is a rather unexplored area. These compounds show an electronic gap at the phosphorus atom and are therefore rather unstable. Recently we could contribute to the results on the stabilization of compounds containing such a phosphorus atom. We showed that oligomerisation can be avoided by filling the electronic gap at the phosphorus by coordination with a base like pyridine.^[3] Most of the compounds containing a $\sigma^3\lambda^5$ phosphorus atom, however, can only be synthesised and isolated as the salts of their stable oligomers (Figure 1).

For example, in the PS_2^- anion the twofold coordination of the phosphorus atom is avoided by forming the cyclic oligomers $\text{P}_4\text{S}_8^{4-}$, $\text{P}_5\text{S}_{10}^{5-}$, $\text{P}_6\text{S}_{12}^{6-}$.^[4]

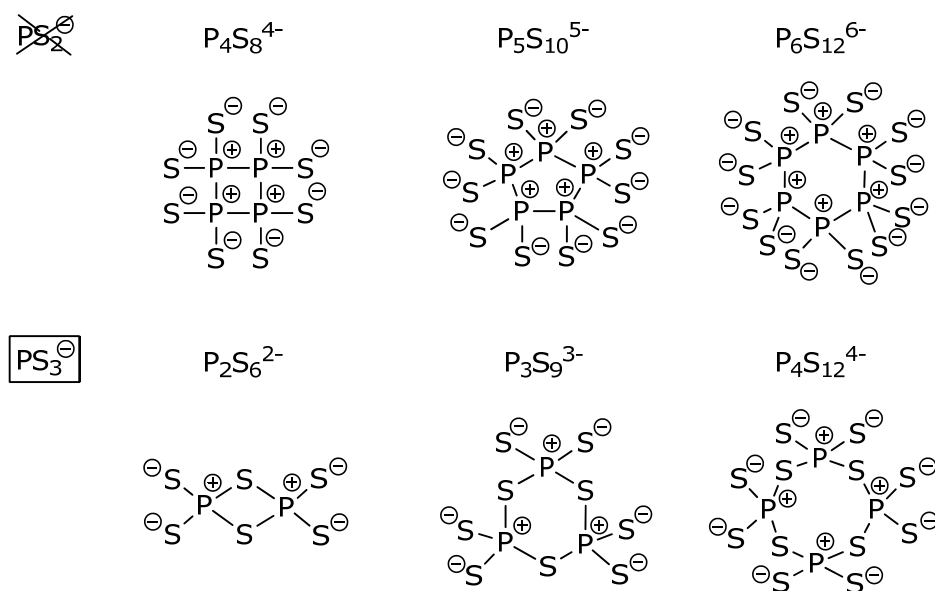


Figure 1. Binary phosphorus-sulfur anions.

According to the literature (see below), the trithiometaphosphate anion seems to be an exception. But also the corresponding cyclic oligomers $P_2S_6^{2-}$, $P_3S_9^{3-}$ and $P_4S_{12}^{4-}$ have been described in the literature.^[6]

The phosphorus atom in PS_3^- has the formal oxidation state +V, but is only threefold coordinated and has therefore an unsaturated coordination sphere. One possibility to stabilize compounds with a phosphorus atom in this situation was investigated by Yoshifuji *et al.*^[11] They could show that big bulky substituents can stabilize a $\sigma^3\lambda^5$ phosphorus atom (Figure 5).

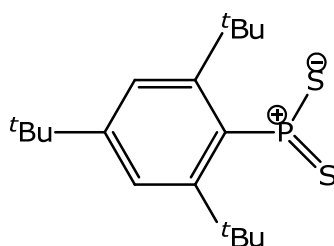
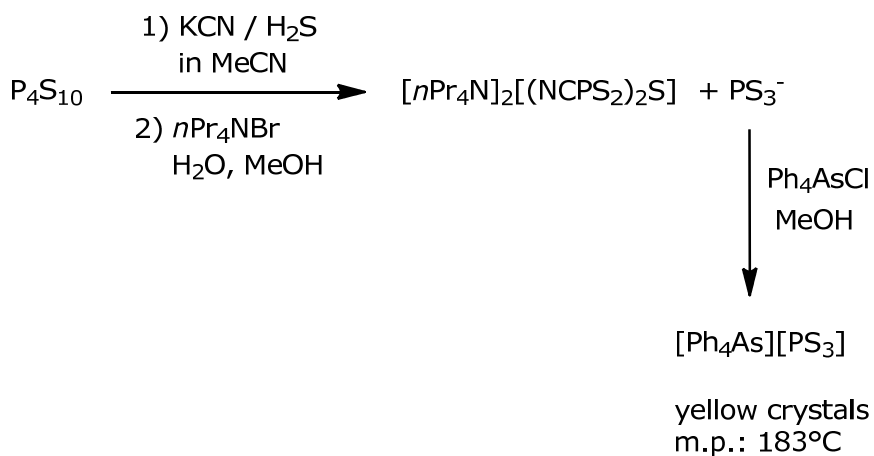


Figure 2. Example of a dithiophosphorane stabilized by the bulky substituent supermesityl.

But this sterical protection is missing in the PS_3^- anion. Due to this reason, the synthesis of the trithiometaphosphate anion PS_3^- is a very appealing preparative challenge. Obviously, Roesky and coworkers had the same idea and tried to find an answer for the problem.^[5] They investigated the nucleophilic degradation of P_4S_{10} with KCN/ H_2S in acetonitrile which resulted in the formation of the $(NCPS_2)_2S^{2-}$ anion, isolated as the nPr_4N^+ salt on addition of nPr_4NBr in $H_2O/MeOH$ (Scheme 1).



Scheme 1. Synthesis and isolation of a trithiometaphosphate salt by Roesky.

Most of the contributions to the investigation of the monomeric and dimeric trithiometaphosphate anions, the PS_3^- and $\text{P}_2\text{S}_6^{2-}$, originate from the group of Brockner.^[6d-i, 6m,n, 7] Our group showed that the selenium analogue, the PSe_3^- anion, can be obtained in the solid state by filling the electronic gap at the phosphorus by coordination with a base.^[8] We also determined the crystal structure of this anion as pyridine adduct in 2009.^[9] For the sulfur analogue our group proposed the same stabilization, as we observed a ^{31}P NMR shift of 300 ppm for the trithiometaphosphate. This anion was synthesised by the reaction of P_4S_3 , Li_2S_2 and elemental sulfur in pyridine. The stabilization of this molecule could also be shown by the X-ray characterization of the Me_2NH_2^+ , Et_2NH_2^+ and pyH^+ salt of the pyridine adduct of the PS_3^- , alongside with the discussion on the equilibrium between the mono-, di- and trimeric form of this unusual anion.^[10] Dimitrov *et al.* claimed that at least one hydrogen bond between the cationic N–H group and the sulfur atoms is crucial for the stabilization of the adduct in the crystal. They further stated that at high temperature a second ^{31}P NMR signal appears, which can be ascribed to the base free PS_3^- . ^{31}P NMR chemical shifts of 129–130 ppm for $\text{py} \rightarrow \text{PS}_3^-$ and 210–230 ppm for the pyridine free PS_3^- were reported.^[10]

Brocker *et al.* used high temperature synthesis starting from the elements phosphorus, sulfur and the alkali metals, yielding solids which are mostly insoluble in common solvents. In the case of $\text{Na}_2\text{P}_2\text{S}_6$ and $\text{K}_2\text{P}_2\text{S}_6$ they succeeded in dissolving the compounds in acetonitrile by adding the corresponding crown ether.^[6g] Their characterization relied mostly on the use of X-ray diffraction methods and Raman spectroscopy. Interestingly, the Raman spectrum of a molten alkali bromide $\text{Ti}_2\text{P}_2\text{S}_6$ mixture measured at different temperatures indicated a dissociation of the anion into the monomeric form. Brocker *et al.* were therefore the first to postulate an equilibrium between the monomeric and dimeric form.

In the following, this suggestion is confirmed by using ^{31}P , ^{31}P EXSY NMR spectroscopy to investigate a solution of new $\text{P}_2\text{S}_6^{2-}$ salts soluble in common organic solvents. During our studies, we were able to synthesise new salts of the two anions PS_3^- and $\text{P}_2\text{S}_6^{2-}$, both of which are discussed in terms of single crystal X-ray diffraction.

Results and Discussion

Molecular and Crystal Structures of $[\text{Ph}_4\text{P}]_2[\text{P}_2\text{S}_6] \cdot \text{py}$ (**1**) and $[\text{nBu}_4\text{N}]_2[\text{P}_2\text{S}_6] \cdot \text{THF}$ (**2**)

The dimeric form of the trithiometaphosphate, the $\text{P}_2\text{S}_6^{2-}$ anion, is easily accessible by mixing stoichiometric amounts of P_4S_3 , Na_2S_2 , elemental sulfur and the bromide salt of the counterion. For **1**, pyridine was used as solvent and the educts were stirred for 1 d. In the case of **2**, the solvent used was THF and the product was recrystallized from acetonitrile.

Yellow block shaped crystals of **1**, suitable for single crystal X-ray diffraction, could be isolated from the yellow reaction solution. Compound **1** crystallizes in the monoclinic space group $P 2_1/c$ with four formula units in the unit cell. In Figure 3, the molecular structure of **1** is depicted, and selected atom distances and bond angles are listed.

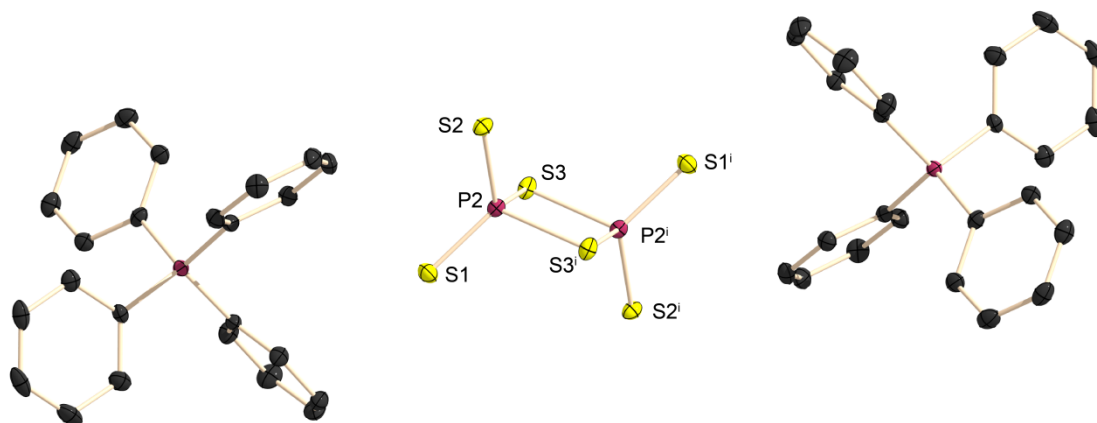


Figure 3. Molecular structure of **1** in the crystal. Thermal ellipsoids are set at 50% probability level. Hydrogen atoms are omitted for clarity. Selected atom distances [\AA] and bond angles [$^\circ$]: P2-S1/P2-S2 1.962(1)/1.964(1), P2-S3i/P2-S3 2.144(1)/2.159(1); S1-P2-S2 118.7(1), $\text{S1-P2-S3i/S1-P2-S3}$ 111.4(1)/111.3(1), $\text{S2-P2-S3i/S2-P2-S3}$ 110.7(1)/110.0(1), S3i-P2-S3 91.5(1), P2-S3-P2 88.5(1).

The $\text{P}_2\text{S}_6^{2-}$ anion lies on a crystallographic inversion centre which is located in the middle of the four-membered ring. Therefore half of the anion is generated by symmetry. The exocyclic bonded sulfur atoms are arranged nearly orthogonal to the

plane of the four-membered P_2S_2 ring. The bond lengths between the phosphorus and the exocyclic sulfur atoms are 1.982(1) Å (P2–S1) and 1.964(1) Å (P2–S2) and therefore closer to a P–S double (1.922(14) Å) than a single bond, as found in phosphorus(V) compounds.^[11] The endocyclic P–S distances correspond with 2.159(1) Å (P2–S3) and 2.143(1) Å (P2(i)–S3) to P–S single bonds. The phosphorus atom is surrounded in a distorted tetrahedral arrangement by four sulfur atoms. The endocyclic S3–P2–S3i angle is 91.5(1)°, whereas the exocyclic S–P–S angles range from 110.0° to 118.7°. The angle at the endocyclic sulfur atom P2–S3–P2(i) is 88.5(1)°.

There are no significant interactions in the structure other than the electrostatic attraction between cations and anions. The pyridine solvent molecules are located between the cations.

The compound $[nBu_4N]_2[P_2S_6] \cdot THF$ (**2**) crystallizes in the form of yellow blocks in the triclinic space group $P\bar{1}$. The unit cell contains three crystallographically independent $P_2S_6^{2-}$.

The conformation of the $P_2S_6^{2-}$ anion does not differ from the one reported for compound **1** or literature-known compounds. The anion consists of a planar four-membered ring formed by two phosphorus and two sulfur atoms. Four further sulfur atoms are bonded exocyclically to the two phosphorus atoms standing orthogonal to the ring plane. The average endocyclic P–S distance is 2.149(1) Å, while the exocyclic one is shorter with a value of 1.964(1) Å. Both phosphorus atoms are distorted tetrahedrally surrounded by four sulfur atoms. The average angles are S_{exo} –P– S_{exo} 116.6(1)°, S_{exo} –P– S_{endo} 111.6(1)°. Figure 4 shows the molecular structure of **2** and selected parameters of the anions are listed.

As in the case of **1**, in **2** no significant interaction other than the electrostatic attraction between cations and anions can be found in the crystal.

All important crystallographic and refinement data for the crystal structures are provided in Table 2.

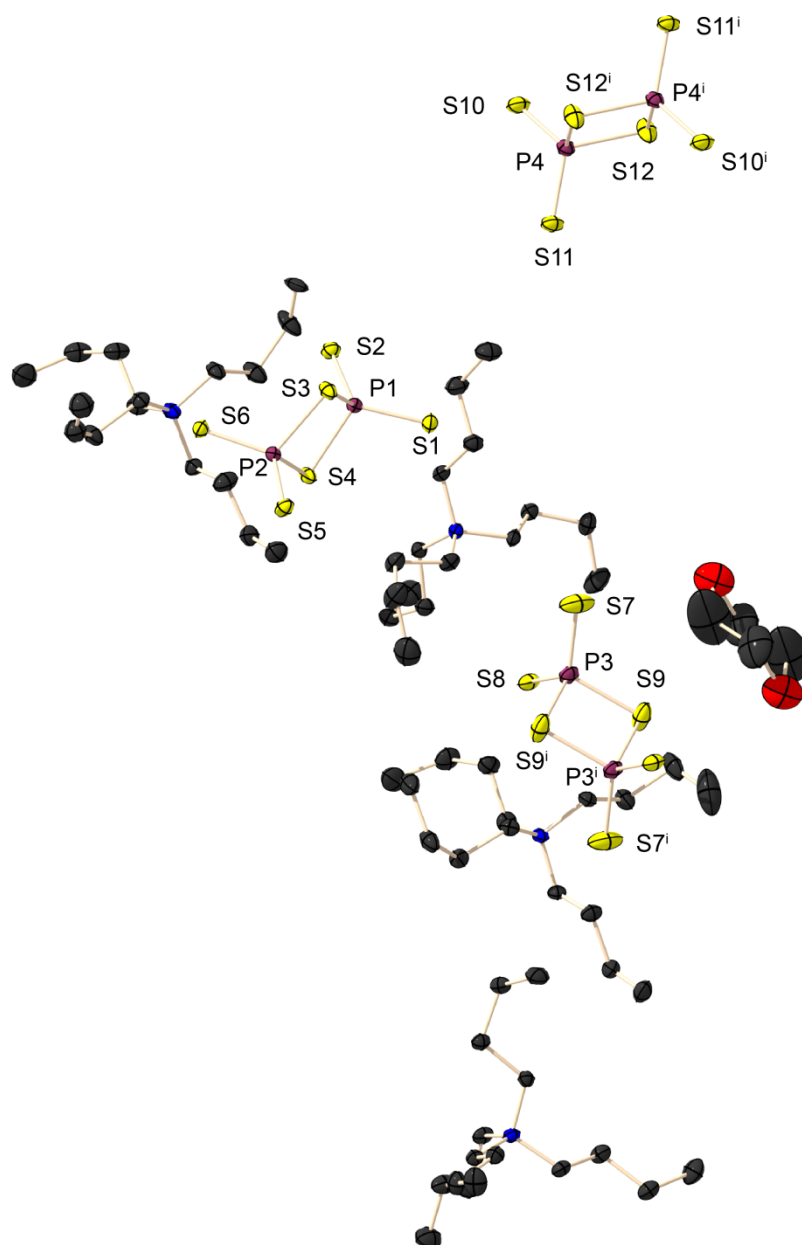


Figure 4. Molecular structure of **1** in the crystal. Thermal ellipsoids are set at 50% probability level. Hydrogen atoms are omitted for clarity. Symmetry operations: *i* = 1-*x*, 2-*y*, 1-*z*; *ii* = -*x*, 2-*y*, 2-*z*. Selected atom distances [Å] and bond angles [°]: P1-S1/P1-S2 1.972(2)/1.968(2), P1-S3/P1-S4 2.145(2)/2.149(2), P2-S3/P2-S4 2.148(2)/2.150(2), P2-S5/P2-S6 1.970(2)/ 1.967(2), P3-S7/P3-S8 1.961(2)/1.969(2), P3-S9 1.967(2), P4-S10/P4-S11 1.968(2)/ 1.967(2) , P4-S12 2.149(2); S1-P1-S2/S5-P2-S6 117.0(1)/116.4(1), S1-P1-S3/S1-P1-S4 110.9(1)/110.3(1), S2-P1-S3/S2-P1-S4 111.8(1)/113.0(1), S5-P2-S3/S5-P2-S4 111.0(1)/112.4(1), S6-P2-S3/S6-P2-S4 112.2(1)/111.2(1), S3-P1-S4/S3-P1-S4 91.1(1)/91.0(1) P1-S3-P2/P1-S4-P2 88.5(1)/88.4(1), S7-P3-S8 117.1(1), S7-P3-S9/S7-P3-S9i 112.8(1)/110.0(1), S8-P3-S9/S8-P3-S9i 111.3(1)/111.0(1), S9-P3-S9i 91.0(1), P3-S9-P3i 89.2(1), S10-P4-S11 116.3(1), S10-P4-S12/S10-P4-S12ii 112.2(1)/111.3(1), S11-P4-S12/S11-P4-S12ii 111.5(1)/111.7(1), P4-S12-P4ii 88.9(1).

^{31}P NMR Spectroscopic Investigations

As **2** is soluble in common polar solvents like pyridine, acetonitrile or propionitrile, it was now possible to determine the ^{31}P NMR chemical shift of this anion, which has not been reliably reported until now.^[2b] Surprisingly the ^{31}P NMR spectrum consists of two signals with $\delta^{31}\text{P} = 297.5$ ppm and $\delta^{31}\text{P} = 30.2$ ppm (Figure 5).

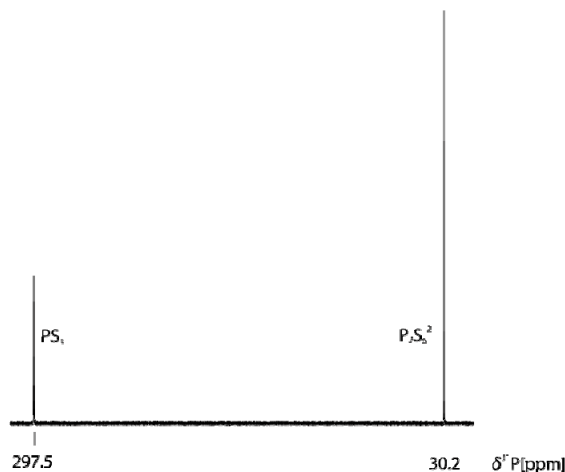
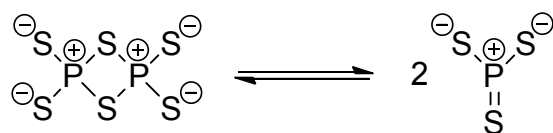


Figure 5. Observed $^{31}\text{P}\{^1\text{H}\}$ NMR spectrum of $[\text{nBu}_4\text{N}]_2[\text{P}_2\text{S}_6] \cdot \text{THF}$ dissolved in benzonitrile (0.16 m, 25 °C, 4096 scans with a PD = 0.5 s, 2 h measuring time, $\nu_0 = 161.8347$ MHz, broadband ^1H decoupling, 0.5 Hz line broadening).

The extremely unusual low field shift of 298.2 ppm for thiooxophosphoranes has been mentioned by Yoshifuji *et al.* before.^[11] Those molecules contain a central phosphorus atom in a similar bonding situation as in the trithiometaphosphate PS_3^- . Based on the assumption that the dimeric anion spontaneously dissociates into the PS_3^- , the ^{31}P NMR signal at 297.5 ppm was ascribed to the trithiometaphosphate. The ^{31}P NMR signal at 30.2 ppm was ascribed to the dimer $\text{P}_2\text{S}_6^{2-}$.



Scheme 2. Equilibrium between the monomeric trithiometaphosphate PS_3^- and the corresponding dimer $\text{P}_2\text{S}_6^{2-}$.

The ^{31}P , ^{31}P EXSY NMR spectrum (Figure 6) reveals that, because of the existence of crosspeaks between the two signals, interconversion between the trithiometaphosphate and the corresponding dimer is slow on the NMR time scale at ambient temperature (Scheme 2).

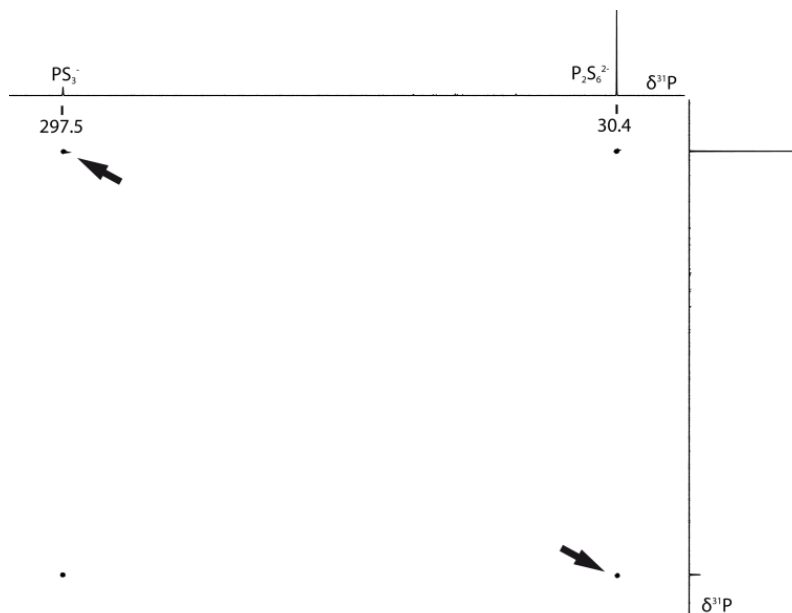


Figure 6. ^{31}P , ^{31}P EXSY NMR spectrum of the $\text{P}_2\text{S}_6^{2-}$ anion dissolved in propionitrile. Crosspeaks are marked with arrows (0.16 m, 25 °C, matrix 2048 × 2048, mixing time 0.5 sec).

To justify the assignment of the ^{31}P NMR chemical shift of the monomeric trithiometaphosphate PS_3^- quantum chemical calculations at the MPW1PW91 level of theory using an augmented polarized quadruple-zeta basis set (aug-cc-pVQZ) were performed for phosphorus. The obtained ^{31}P NMR chemical shift for PS_3^- was 299.2 ppm referring to H_3PO_4 , which corresponds very well to the experimentally observed ^{31}P NMR chemical shift of 297.5 ppm for neutral dithioxophosphoranes.^[11] So the calculations underline our assumption about the equilibrium between the mono- and dimeric form of this unusual anion in the solution.

Molecular and Crystal Structure of [pyH][pyPS₃] (**3**), [*n*Bu₄N][(*CH*₃)₂NC₅H₄NPS₃]·EtCN (**4**) and [(*N*-MeIm)₂H][*N*- MeImPS₃] (**5**)

Colourless plates of (pyH)(pyPS₃) **3** could be obtained by refluxing P₄S₁₀ in pyridine and subsequent addition of water. The compound crystallizes in the monoclinic space group *P*2₁/*c* with four formula units in the unit cell. Figure 7 shows the molecular structure and gives selected atom distances and bond angles.

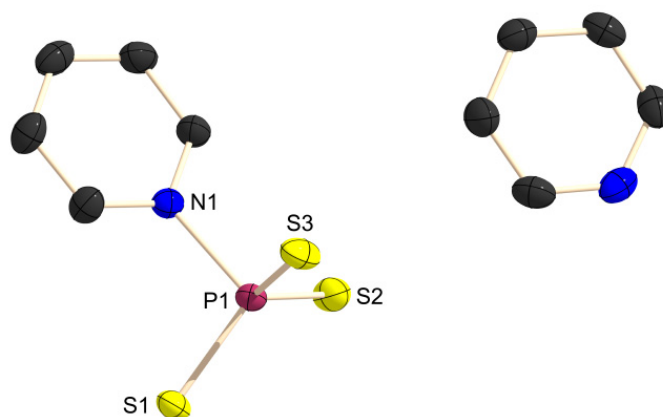


Figure 7. Molecular structure of **3** in the crystal. Thermal ellipsoids are set at 50% probability level. Hydrogen atoms are omitted for clarity. Selected atom distances [Å] and bond angles [°]: P1–S1 1.989(1), P1–S2 1.985(2), P1–S3 1.979(2), P1–N1 1.920(2), S1–P1–S2 114.6(1), S2–P1–S3 117.2(2), S3–P1–S1 115.8(2), S1–P1–N1 103.1(2), S2–P1–N1 102.4(1), S3–P1–N1 100.2(1).

After dissolving the yellow powder of [*n*Bu₄N]₂P₂S₆ (**2**) in propionitrile, the addition of 4-dimethylaminopyridine, and storing the reaction solution at –25°C, yellow block shaped crystals of [4-Me₂NC₅H₄NPS₃][*n*Bu₄N] · EtCN (**4**) were obtained. Compound **4** crystallizes in the triclinic space group *P*–1 with two formula units in the unit cell. Figure 8 shows the molecular structure of **4** and selected atom distances and bond angles are listed.

Colourless plate shaped crystals of [(*N*-MeIm)₂H][*N*-MeImPS₃] (**5**) were obtained by refluxing P₄S₁₀ in *N*-methyl imidazole. Compound **5** crystallizes in the monoclinic space group *P*2₁/*c* with four formula units in the unit cell. Figure 9 shows the molecular structure and gives selected atom distances and bond angles.

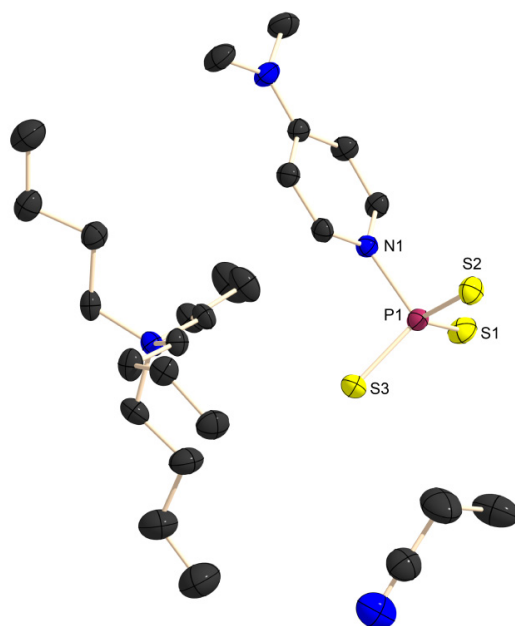


Figure 8. Molecular structure of **4** in the crystal. Thermal ellipsoids are set at 50% probability level. Hydrogen atoms are omitted for clarity. Selected atom distances [\AA] and bond angles [$^\circ$]: P1–S1 1.983(1), P1–S2 1.986(1), P1–S3 1.984(1), P1–N1 1.886(1), S1–P1–S2 116.2(1), S2–P1–S3 114.9(1), S3–P1–S1 115.9(1), S1–P1–N1 102.7(1), S2–P1–N1 101.1(1), S3–P1–N1 102.9(1).

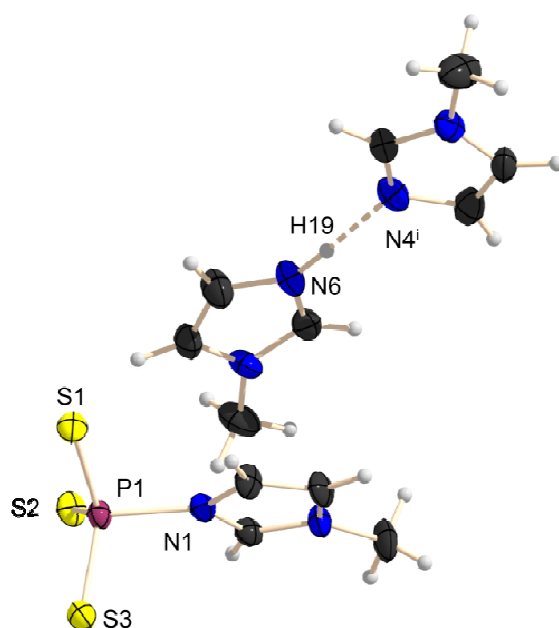


Figure 9. Molecular structure of **5**. Ellipsoids are drawn at the 50% probability level. Hydrogen atoms are omitted for clarity. Selected atom distances [\AA] and bond angles [$^\circ$]: P1–S1 1.986(2), P1–S2 1.991(2), P1–S3 1.998(3), P1–N1 1.836(3), S1–P1–S2 117.2(1), S2–P1–S3 113.8(2), S3–P1–S1 115.1(2), S1–P1–N1 101.7(2), S2–P1–N1 102.9(3), S3–P1–N1 103.3(2);

N6–H19 0.91(5), H \cdots N4ⁱ 1.76(5), N6 \cdots N4ⁱ 2.669(6); N6–H19 \cdots N4ⁱ 177(5).

In the structures **3–5** the phosphorus atom is surrounded distorted tetrahedrally by three sulfur atoms and one molecule of the coordinating aromatic nitrogen-containing base. In Table 1, the average values of the structural parameters are listed for ease of comparison. The P–S distances are with average values of 1.985(2) Å in **3**, 1.984(1) Å in **4** and 1.994(3) Å observed in **5** well within the range for values expected for the weighted mean of two P–S double and one single bond (1.922(14) Å^[12] and 2.11 Å^[13], respectively). The distance expected for a P–N single bond is 1.652(24) Å^[12]. The values found in compounds **3–5** are, however, longer with 1.920(2), 1.886(1) and 1.836(3) Å respectively, indicating only weak coordination of the pyridine molecule to the phosphorus. Strongly elongated P–N distances similar to these have also been reported for the pyridine adduct of PS_3^- (1.906(2) Å),^[10] and the compounds $\text{py}_2\text{P}_2\text{S}_5$ (1.862(6) Å and 1.865(3) Å)^[3a], the $\text{py}_2\text{P}_2\text{S}_7$ (1.869(3) Å and 1.865(3) Å)^[3b], in which an analogue bonding situation is found. The occurrence of elongated P–N bond in trichalcogenophosphate-pyridine anions has already been evaluated theoretically by Klapötke *et al.*^[14]

What attracts attention is the decrease in the P–N distance from **3** to **5**. This can be explained by the increase of the basicity of the coordinating molecule and therefore its stronger electron donating character.

Although an almost tetrahedral environment around the phosphorus atom might be expected, the sums of the S–P–S angles indicate a strong deviation towards a planar PS_3 arrangement with values of 347.6°, 347.0° and 346.1°. A similar situation is found for $\text{py}_2\text{P}_2\text{S}_5$ ^[3a], $\text{py}_2\text{P}_2\text{S}_7$ ^[3b] and the pyridine adduct of the PS_3^- ^[10] anion with values of 341.8°, 344° and 347°, respectively. This provides further evidence for a weak coordination of pyridine to phosphorus and also reflects the difference in the P–N distances of **3**, **4** and **5**. A decrease of this bond length leads to a trend of the surrounding of the phosphorus towards a tetrahedral arrangement.

Table 1. Average values of structural parameters in the anions of **3–5**.

	3	4	5
P–S	1.985(2)	1.984(1)	1.994(3)
P–N	1.920(2)	1.886(1)	1.836(3)
$\Sigma\text{S–P–S}$	347.6	347.0	346.1

Comparing the structures **3–5** with the salts of the pyridine adduct of this anion described by Dimitrov *et al.*, not only are the cell parameters different, but also the

whole build-up in the crystal. *Dimitrov* claimed that at least one hydrogen bond between the cationic N–H group and the sulfur atoms is crucial for the stabilization of the adduct in the crystal. He observed two P–S distances with similar values of 1.980(2) Å and 1.986(2) Å. However, the third one is 2.004(1) Å, which occurs due to the formation of a N–H⋯S interaction between the pyridinium cation and the PS₃[−] entity. The values are 3.271(1) and 3.396(1) Å for the N⋯S distances, which is in the range of the sum of the van der Waals radii of nitrogen and sulfur (3.37 Å)^[15] However, this interaction could not be observed in the structure of **3**. The shortest N⋯S distance found has a value of 3.693(3) Å and can therefore not be regarded as an electrostatic interaction, much less a hydrogen bond. This also explains the elongation of the P–N bond length in **3** compared to the one described by *Dimitrov* (1.906(2) Å)^[10]. Also in the structure **4**, no interaction of the sulfur atoms with the NH groups of the cations could be observed. In **5**, the shortest N⋯S distance found has a value of 3.840(4) Å, and in **4**, the value is as high as 4.382(2) Å.

This shows that the assumption of *Dimitrov* regarding the stability of the PS₃[−] adduct in the crystal cannot be confirmed, and that despite the lack of an electrostatic N–H⋯S interaction these compounds can be isolated and are stable in the solid state.

All important crystallographic and refinement data for the crystal structures are provided in Table 2.

Table 2. Details for X-ray data collection and structure refinement for **1–5**.

	1	2	3	4	5
CCDC	967693	963617	937611	967697	938880
Empirical formula	C ₂₉ H ₂₅ NP ₂ S ₃	C ₁₃₂ H ₂₆₈ N ₈ O P ₈ S ₂₄	C ₁₀ H ₁₁ N ₂ PS ₃	C ₂₆ H ₅₁ N ₄ PS ₃	C ₁₂ H ₁₉ N ₆ PS ₃
Formula mass	545.65	3000.74	286.36	546.86	374.48
T[K]	100(2)	100(2)	173(2)	200(2)	173(2)
Crystal size [mm]	0.3×0.3×0.25	0.4×0.12×0.08	0.25×0.18× 0.09	0.3×0.15×0.1	0.25×0.1×0.02
Crystal description	yellow block	yellow needle	yellow block	colourless block	colourless plate
Crystal system	monoclinic	triclinic	monoclinic	triclinic	monoclinic
space group	<i>P</i> 2 ₁ / <i>c</i>	<i>P</i> −1	<i>P</i> 2 ₁ / <i>n</i>	<i>P</i> −1	<i>P</i> 2 ₁ / <i>c</i>
<i>a</i> [Å]	9.41741(11)	11.1073(8)	7.6813(3)	10.7269(5)	7.7400(4)
<i>b</i> [Å]	12.31227(13)	15.4662(11)	21.2394(7)	10.8430(4)	9.4680(6)
<i>c</i> [Å]	23.2297(3)	27.2591(19)	8.4530(3)	14.7239(6)	25.132(2)

	1	2	3	4	5
α [°]		97.892(7)	90	98.584(3)	90
β [°]	96.0144(11)	96.433(6)	109.272(4)	102.892(4)	95.083(6)
γ [°]		106.977(8)	90	105.500(4)	90
V [Å ³]	2678.64(5)	4378.7(5)	1301.79(8)	1568.40(13)	1834.5(2)
Z	4	1	4	2	4
ρ_{calc} [g/cm ³]	1.353	1.138	1.461	1.158	1.356
μ [mm ⁻¹]	0.416	0.409	0.666	0.308	0.496
$F(000)$	1136	1628	592	596	784
θ range [°]	3.75–27.00	3.71–32.58	4.23–32.50	3.66– 27.00	4.33–25.96
Index ranges	$-12 \leq h \leq 12$	$-13 \leq h \leq 13$	$-10 \leq h \leq 10$	$-13 \leq h \leq 13$	$-9 \leq h \leq 9$
	$-15 \leq k \leq 15$	$-18 \leq k \leq 18$	$-28 \leq k \leq 28$	$-13 \leq k \leq 13$	$-11 \leq k \leq 9$
	$-29 \leq l \leq 29$	$-32 \leq l \leq 32$	$-11 \leq l \leq 11$	$-18 \leq l \leq 18$	$-31 \leq l \leq 25$
Reflns.					
collected	28478	41863	15434	17264	7462
obsd.	4832	10500	2886	4416	2189
unique	5827	15854	3219	6817	3735
R_{int}	0.0287	0.0417	0.0239	0.0345	0.0712
R_1, wR_2 [I > 2 σ]	0.0368, 0.0875	0.0406, 0.0962	0.0252, 0.0630	0.0376, 0.0873	0.0622, 0.1164
R_1, wR_2 [all data]	0.0483, 0.0950	0.0714, 0.1110	0.0297, 0.0659	0.0693, 0.0973	0.0930, 0.1234
GOOF on F^2	1.052	0.975	1.053	0.928	0.966
larg. diff	1.203	0.872,	0.300	0.550	0.372
peak/hole (e/Å)	−0.416	−0.766	−0.191	−0.285	−0.376

Temperature Dependent ³¹P NMR Spectroscopy

The behaviour of **4** dissolved in propionitrile was investigated at different temperatures using ³¹P NMR spectroscopy. The appearance of the signal for the free monomeric anion at higher temperatures at the chemical shift reported by Dimitrov *et al.* could not be confirmed by our study. The ³¹P NMR spectra of **4**, observed at different temperatures are shown in Figure 10.

The ³¹P NMR signal of the anion in **4** shifts from high field ($\delta^{31}\text{P} = 138.1$ ppm) at low temperature (−80 °C) to lower field ($\delta^{31}\text{P} = 286.6$ ppm) at high temperature (80 °C).

Interestingly, the signal converges to the one observed for the free monomeric trithiometaphosphate anion in propionitrile at 297.5 ppm. As this solvent has a boiling point at about 90 °C, it was not possible to measure ^{31}P NMR spectra above 80 °C.

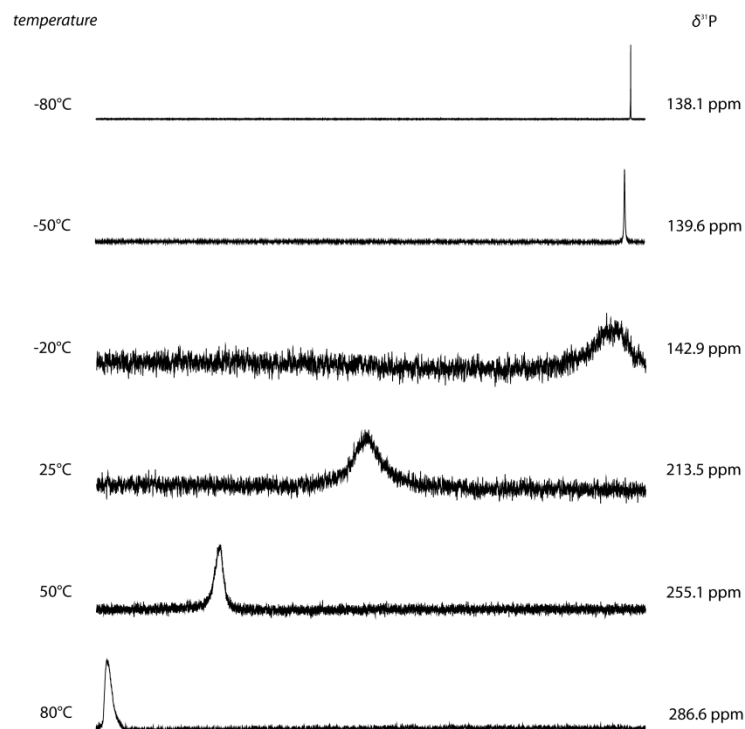
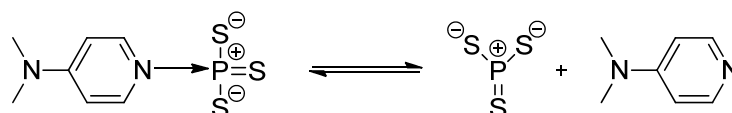


Figure 10. $^{31}\text{P}\{^1\text{H}\}$ NMR spectra of **4** dissolved in propionitrile at different temperatures (0.1 m, 1024 scans with a PD = 0.5 s, broadband ^1H decoupling).

Nevertheless the signal observed for **4** in the ^{31}P NMR spectra at different temperatures can be interpreted as an average signal between the adduct stabilized trithiometaphosphate anion and the free monomeric one. Depending on the temperature, the equilibrium between these two compounds, is either on the side of the adduct (at low temperatures), or on the side of the free anion (at high temperatures) (Scheme 3).



Scheme 3. Temperature dependent equilibrium between the adduct stabilized trithiometaphosphate anion and the free monomeric trithiometaphosphate anion.

When **5** is dissolved in propionitrile and the solution is investigated by ^{31}P NMR spectroscopy at different temperatures, the observations do not differ significantly from those discussed above (Figure 11).

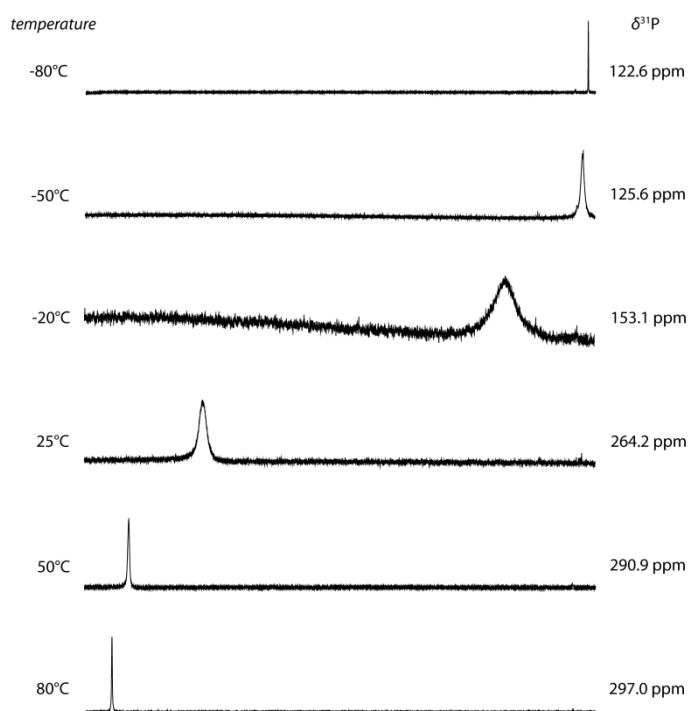


Figure 11. $^{31}\text{P}\{^1\text{H}\}$ NMR spectra of **5** dissolved in propionitrile at different temperatures (0.1 M, 1024 scans with a PD = 0.5 s, broadband ^1H decoupling).

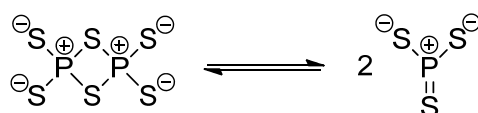
The ^{31}P NMR signal is shifted from high field ($\delta^{31}\text{P} = 122.6$) at low temperatures ($-80\text{ }^\circ\text{C}$) to low field ($\delta^{31}\text{P} = 297.0$ ppm) at $80\text{ }^\circ\text{C}$. The ^{31}P NMR chemical shift at $80\text{ }^\circ\text{C}$ corresponds to the free monomeric trithiometaphosphate anion PS_3^- as already shown before. This is conclusive evidence for the existence of a temperature dependent equilibrium between the adduct stabilized trithiometaphosphate and the free monomeric anion in solution.

In contrast, at $-80\text{ }^\circ\text{C}$ the equilibrium is almost completely on the side of the adduct stabilized trithiometaphosphate anion in both cases because the ^{31}P NMR shifts at $-50\text{ }^\circ\text{C}$ don't differ significantly to the values at $-80\text{ }^\circ\text{C}$.

Conclusion

Despite several investigations on the existence and stability of the trithiometaphosphate anion (PS_3^-) described in the literature, there is still a lot of mystery connected to this simple, but intriguing anion. Our results show clearly, that PS_3^- forms spontaneously and is stable as the monomer in solution.

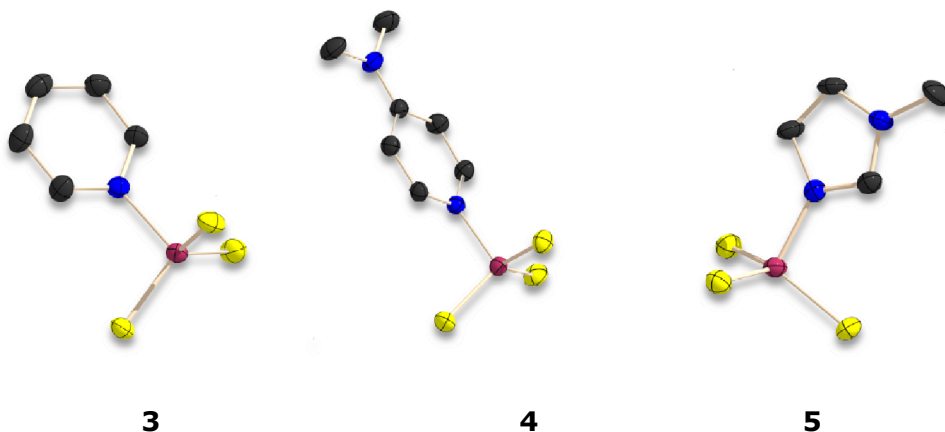
The thiophosphate anion $\text{P}_2\text{S}_6^{2-}$, formally the dimer of the PS_3^- , turns out to be an ideal precursor for the monomeric form. Salts with organic cations (Ph_4P^+ , $n\text{Bu}_4\text{N}^+$) were readily obtained from the reaction of P_4S_3 with Na_2S_2 and elemental sulfur in the presence of the bromide salts of the cations. In contrast to metal salts of this anion, (like $\text{K}_2\text{P}_2\text{S}_6$ or $\text{Na}_2\text{P}_2\text{S}_6$), they are rather soluble in common polar organic solvents like pyridine, acetonitrile or propionitrile. In solution the $\text{P}_2\text{S}_6^{2-}$ anion spontaneously dissociates and forms an equilibrium with the monomeric trithiometaphosphate



The presence of this equilibrium has been proven without any doubt by a ^{31}P , ^{31}P EXSY 2D-experiment. The ^{31}P NMR chemical shift of the PS_3^- anion ($\delta^{31}\text{P} = 297.5$ ppm) is in accordance with calculated value and also with the values observed for dithioxophosphoranes.

The spontaneous formation of the PS_3^- anion is nearly as remarkable as the low electrophilicity, which is quite unexpected for a $\sigma^3\lambda^5$ phosphorus atom. With strong nitrogen bases like pyridine (**3**), *p*-dimethylaminopyridine (Steglich's base) (**4**) and *N*-methylimidazole (**5**) only weak adducts are formed. This is clearly demonstrated by variable temperature ^{31}P NMR spectroscopy in solution and by strongly elongated P–N distances within the adducts in the solid state.

In contrast to statements in the literature, our results show that hydrogen bonding between the sulfur atoms and the cations is not required to stabilize the adducts in the solid state.



With these experimental results it becomes evident that the trithiometaphosphate anion exists as a stable species in solution. The adducts of PS_3^- provide a convenient source of this anion and open the door to a systematic investigation of its reactivity.

Experimental Section

General conditions. All reactions were carried out under inert gas atmosphere using Argon (Messer Griesheim, purity 4.6 in 50 L steel cylinder) and working with Schlenk techniques. The glass vessels used were stored in a 130 °C drying oven. Before filling they were flame dried *in vacuo* at 10^{-3} mbar. Elemental sulfur was used as received (Acros Organics). P_4S_{10} and P_4S_3 were commercially obtained (Riedel-de Hën) and purified by extraction with CS_2 before use. All other chemicals were used as obtained. The solvents were dried with commonly known methods and freshly distilled before use. **NMR Spectroscopy.** NMR spectra were recorded using a Jeol EX 400 Eclipse instrument operating at 161.997 MHz (^{31}P). Chemical shifts are referred to 85% H_3PO_4 as external standard. If not mentioned otherwise, all spectra were measured at 25 °C. The % data correspond to the intensities in the ^{31}P NMR spectra with respect to the total intensity. The difference to 100% belongs to not assignable signals. **Mass Spectrometry.** The mass spectrometry was performed with a MStation JMS 700 (Jeol). Measurements were carried out using the ionisationmethode DEI+/EI+. This method involves the problem of exposing the compounds to air, while embedding them into the matrix (p-nitroalcohol). **IR Spectroscopy.** The spectra were recorded using a PerkinElmer Spektrum one FT-IR instrument (KBr); Perkin-Elmer Spectrum BXII FT-IR instrument equipped with a Diamant-ATR Dura Sampler at 25 °C (neat). Raman spectra were recorded on a Bruker RAMII Raman instrument

($\lambda = 1064$ nm, 200 mW, 25 °C) equipped with D418-T Detector at 200 mW at 25 °C.

Melting and decomposition points were determined by differential scanning calorimetry (Linseis DSC-PT10, calibrated with standard pure indium and zinc). Measurements were performed at a heating rate of 5 °C min⁻¹ in closed aluminum sample pans with a 0.1 mm hole in the lid for gas release to avoid an unsafe increase in pressure under a nitrogen flow of 20 mL min⁻¹ with an empty identical aluminum sample pan as a reference. Melting points were checked with a Büchi Melting Point B-540 in open glass capillaries.

X-ray Crystallography. The single-crystal X-ray diffraction data were collected using an Oxford Xcalibur3 diffractometer equipped with a Spellman generator (voltage 50 kV, current 40 mA), Enhance molybdenum K α radiation source ($\lambda = 71.073$ pm), Oxford Cryosystems Cryostream cooling unit, four circle kappa platform and a Sapphire CCD detector. Data collection and reduction were performed with CrysAlisPro.^[16] The structures were solved with SIR97^[17], SIR2004^[18], refined with SHELXL-97^[19], and checked with PLATON^[20], all integrated into the WinGX software suite^[21]. The finalized CIF files were checked with checkCIF.^[22] All non-hydrogen atoms were refined anisotropically. The hydrogen atoms were located in difference Fourier maps and placed with a C–H distance of 0.98 Å for C–H bonds. Intra- and intermolecular contacts were analysed with DIAMOND (version 3.2i), thermal ellipsoids are drawn at the 50% probability level. Selected crystallographic data and refinement details for the structure determination of compounds **1–5** are summarized in Table 2. CCDC 967693, 963617, 937611, 967697, 938880 contains the supplementary crystallographic data for compounds **1–5**. These data can be obtained free of charge from The Cambridge Crystallographic Data Centre via www.ccdc.cam.ac.uk/data_request/cif.

[Ph₄P]₂[P₂S₆]·py (1): P₄S₃ (880 mg, 4 mmol), Na₂S₂ (881 mg, 8 mmol) and sulfur (641 mg, 20 mmol) in pyridine (40 mL) were stirred for 24 h at room temperature yielding a yellow solution. Ph₄PBr (6700 mg, 16 mmol) was added and the white precipitate of NaBr removed by filtration. The orange reaction solution was stored at +4 °C. After five days yellow crystals of [Ph₄P]₂[P₂S₆] · py were obtained. (Yield: 2.83 g, 5.2 mmol, 65%)

$^{31}\text{P}\{^1\text{H}\}$ NMR (THF, rt): δ [ppm] = 237.9 (pyPS_3^- , 83%), 128.8 ($\text{P}_2\text{S}_7^{2-}$, 36%).
 T_{dec} : decomposition at 173°C.

$[\text{nBu}_4\text{N}]_2[\text{P}_2\text{S}_6]\cdot\text{THF}$ (2**)**: P_4S_3 (4.4 g, 20.0 mmol), Na_2S_2 (3.2 g, 40.0 mmol) and sulfur (3.2 g, 12.5 mmol) were stirred in THF (80 mL) at room temperature. After one day, a solution of nBu_4NBr (25.8 g, 80.0 mmol) in acetonitrile (20 mL) was added. The white precipitate of NaBr was removed and the yellow solution was stored at -25°C . Within 24 h, yellow crystals of $[\text{nBu}_4\text{N}]_2[\text{P}_2\text{S}_6]\cdot\text{THF}$ formed, which were separated, washed twice with 10 mL of cold THF and dried *in vacuo*. (Yield: 15.67 g, 6.42 mmol, 32 % with respect to P_4S_3)

$^{31}\text{P}\{^1\text{H}\}$ NMR (THF, rt): δ [ppm] = 297.5 (PS_3^- , 38%), 30.2 ($\text{P}_2\text{S}_6^{2-}$, 36%). **Mass spectrometry** m/z (EI+) = 496.1 ($[\text{nBu}_4\text{NP}_2\text{S}_6]^-$), 482.4 ($[\text{M}-\text{CH}_3]^-$), 466.5 ($[\text{M}-\text{C}_2\text{H}_5]^-$), 432.5 ($[\text{M}-\text{S}_2]^-$), 336.3 ($[\text{M}-\text{PS}_4]^-$), 297.5 ($[\text{M}-\text{C}_{14}\text{H}_{32}]^-$), 280.3 ($[\text{M}-\text{C}_{15}\text{H}_{32}]^-$), 266.5 ($[\text{M}-\text{C}_{16}\text{H}_{34}]^-$), 253.5 ($[\text{P}_2\text{S}_6]^-$), 153.4 ($[\text{PS}_4]^-$). **Raman** (200 mW, rt): ν [cm^{-1}] = 2942 (43), 2921 (41), 2872 (35), 1449 (27), 1325 (11), 879 (11), 601 (21), 417 (100), 357 (27), 307 (38), 249 (29), 197 (21), 168 (16). **IR** (200 mW, rt): ν [cm^{-1}] = 2958 (ws), 2936 (s), 2872 (s), 1486 (m), 1462 (m), 1382 (w), 1262 (ww), 1152 (ww), 1107 (ww), 1068 (ww), 1024 (ww), 880 (w), 803 (ww), 736 (ww), 654 (s), 543 (ws), 520 (w). **DSC** (5 $^\circ\text{C}/\text{min}$): T_{dec} = 186°C.

$[\text{pyH}][\text{pyPS}_3]$ (3**)**: P_4S_{10} (3.00 g, 6.8 mmol) was stirred in pyridine (60 mL) over night at ambient temperature. The yellow solution was refluxed for 1 h. Subsequently water (10 mL) was added and the solution was stirred over night at ambient temperature. The precipitate was removed and the yellow solution was another time refluxed for 1 h. After two days yellow block shaped crystals of **3** could be obtained from the orange solution.

^{31}P NMR (pyridine, rt): δ [ppm] = 293.3 (PS_3^- , 68%), 30.2 ($\text{P}_2\text{S}_6^{2-}$, 12%). **Elemental analysis** $[\text{pyH}][\text{pyPS}_3]$: calcd. C 41.94, N 9.78, H 3.87, S 33.59; found: C 40.29, N 9.78, H 4.09, S 31.10. **Mass spectrometry** m/z (FAB-) = 280.2 ($[\text{M}-\text{H}]^-$), 175.21 ($[\text{C}_5\text{H}_6\text{NPS}_2]^-$), 80.1 ($[\text{C}_5\text{H}_6\text{N}]^-$), 79.0 ($\text{C}_5\text{H}_5\text{N}$). **Raman** (300 mW, rt): ν [cm^{-1}] = 3057 (56), 2990 (6), 2955 (8), 2910 (4), 1598 (7), 1583 (13), 1483 (5), 1218 (11), 1147 (5), 1031 (79), 992 (100). **IR** (200 mW, rt): ν [cm^{-1}] = 3077 (w), 3023 (w), 3000 (w), 1597 (m), 1580 (s), 1481 (m), 1436 (vs), 1216 (m), 1146 (m), 1068 (m), 1030 (s), 990 (s), 746 (s), 699 (vs). **DSC** (5 $^\circ\text{C}/\text{min}$): T_{dec} = 108°C.

[*n*Bu₄N][4-(CH₃)₂NC₅H₄NPS₃]·EtCN (4): One equivalent of [*n*Bu₄N]₂[P₂S₆]·THF (2) (500 mg, 0.64 mmol) and one equivalent of 4-(CH₃)₂NC₅H₄N (75 mg, 0.64 mmol) were dissolved in propionitrile. The yellow suspension was refluxed for one h. The resulting yellow solution was stored at -25 °C. After one week, yellow crystals of [*n*Bu₄N][4-(CH₃)₂NC₅H₄NPS₃] were obtained. The solution was dried *in vacuo* and the product recrystallized from THF, which was removed afterwards. (yield: 0.69 mmol, 378,0 mg, 54%)

³¹P{¹H} NMR (PrCN, rt): δ [ppm] = 213.5 (s, br, PS₃⁻, 69%), 128.8 (s, P₂S₇²⁻, 7%), 30.2 (s, P₂S₆²⁻, 8%).

[(*N*-MeIm)₂H][*N*-MeImPS₃] (5): P₄S₁₀ (220.0 mg, 0.5 mmol) was refluxed in *N*-methylimidazole (6 mL) to give a yellow solution, which was stored at +4 °C. After one day, a few colorless plate shaped crystals of **5** were obtained, therefore a yield could not be determined.

³¹P{¹H} NMR (THF, rt): δ [ppm] = 125.1 (s, br, 43%), 80.1 (s, PS₄³⁻, 36%), 79.3 (ss, 12%), 70.5 (s, 15%).

Acknowledgement

Financial support by the Department of Chemistry, Ludwig Maximilian University, is gratefully acknowledged. We thank Prof. T. M. Klapötke, Department of Chemistry, Ludwig Maximilian University, for the generous allocation of diffractometer time and for his continuous support.

-
- [1] L. Pauling, *The Chemical Bond*, Vol. 3, Cornell University Press, Ithaca, **1967**.
 - [2] S. B. Hartley, W. S. Holmes, J. K. Jacques, M. F. Mole, J. C. McCoubrey, *Quart. Rev.* (London) **1963**, 17, 204-223.
 - [3] a) S. Schönberger, C. Jagdhuber, L. Ascherl, C. Evangelisti, T. M. Klapötke, K. Karaghiosoff, *Z. Anorg. Allg. Chem.* **2013**, DOI: 10.1002/zaac.201300419. b) C. Rotter, C. Evangelisti, S. Schoenberger, T. M. Klapoetke, K. Karaghiosoff, *Chem. Commun.* **2010**, 46, 5024-5025.

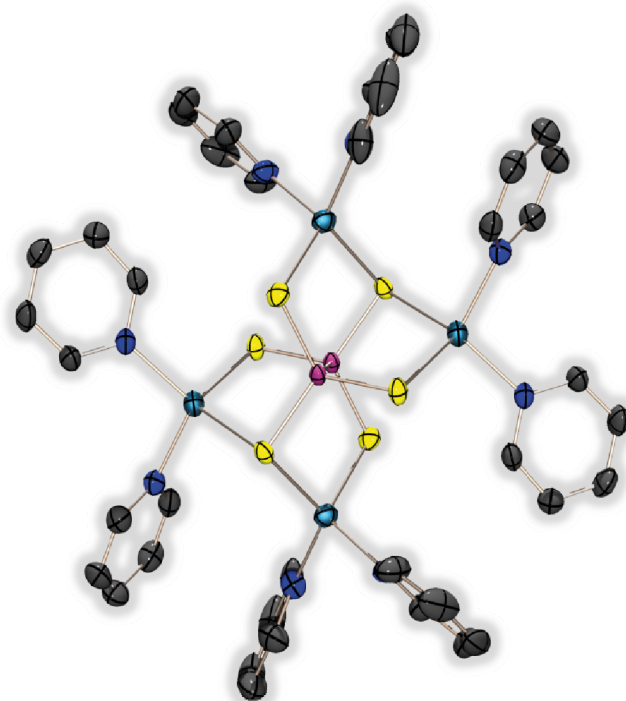
- [4] a) E. K. Badeeva, D. B. Krivolapov, A. T. Gubaidullin, I. A. Litvinov, E. S. Batyeva, O. G. Sinyashin, *Mendeleev Commun.* **2005**, 22-23; b) H. Buerger, G. Pawelke, H. Falius, *Spectrochim. Acta, Part A* **1981**, 37A, 753-755; c) H. Falius, W. Krause, W. S. Sheldrick, *Angew. Chem.* **1981**, 93, 121-122; d) H. Falius, A. Schliephake, D. Schomburg, *Z. Anorg. Allg. Chem.* **1992**, 611, 141-148; e) H. H. Falius, A. B. Schliephake, *Inorg. Synth.* **1989**, 25, 5-7; f) W. Krause, H. Falius, *Z. Anorg. Allg. Chem.* **1983**, 496, 80-93.
- [5] H. W. Roesky, R. Ahlrichs, S. Brode, *Angew. Chem.* **1986**, 98, 91-93.
- [6] a) H. Andrae, R. Blachnik, *J. Therm. Anal.* **1989**, 35, 595-607; b) H. Andrae, R. Blachnik, *J. Alloys and Compd.* **1992**, 189, 209-215; c) J. Angenault, X. Cieren, G. Wallez, M. Quarton, *J. Solid State Chem.* **2000**, 153, 55-65; d) R. Becker, W. Brockner, *Z. Naturforsch., A* **1984**, 39A, 1120-1121; e) W. Brockner, R. Becker, B. Eisenmann, H. Schaefer, *Z. Anorg. Allg. Chem.* **1985**, 520, 51-58; f) M. Gjikaj, A. Adam, M. Duewel, W. Brockner, *Z. Kristallogr. - New Cryst. Struct.* **2005**, 220, 67-68; g) M. Gjikaj, W. Brockner, *Vibr. Spec.* **2005**, 39, 262-265; h) M. Gjikaj, W. Brockner, A. Adam, *Z. Anorg. Allg. Chem.* **2006**, 632, 279-283; i) M. Gjikaj, C. Ehrhardt, W. Brockner, *Z. Naturforsch., B* **2006**, 61, 1049-1053; j) J. A. Hanko, M. G. Kanatzidis, *J. Solid State Chem.* **2000**, 151, 326-329; k) J. A. Hanko, J. Sayettat, S. Jobic, R. Brec, M. G. Kanatzidis, *Chem. Mater.* **1998**, 10, 3040-3049; l) D. Lathrop, D. Franke, R. Maxwell, T. Tepe, R. Flesher, Z. Zhang, H. Eckert, *Solid State Nucl. Magn. Reson.* **1992**, 1, 73-83; m) F. Menzel, W. Brockner, M. Ystenes, *J. Molec. Struct.* **1993**, 294, 53-56; n) L. Ohse, W. Brockner, *Z. Naturforsch., A* **1988**, 43, 494-496; o) P. S. Salmon, S. Xin, H. E. Fischer, *Phys. Rev. B Condens. Matter Mater. Phys.* **1998**, 58, 6115-6123; p) P. Toffoli, P. Khodadad, N. Rodier, *Acta Cryst., B* **1978**, B34, 3561-3564; q) Y. V. Voroshilov, M. V. Potorii, V. Y. Gebesh, *Neorg. Mater.* **1994**, 30, 479-483; r) G. U. Wolf, M. Meisel, *Z. Anorg. Allg. Chem.* **1982**, 494, 49-54.
- [7] a) F. Menzel, W. Brockner, M. Ystenes, *Vibr. Spectrosc.* **1997**, 14, 59-70; b) M. Ystenes, W. Brockner, F. Menzel, *Z. Naturforsch., A* **1992**, 47, 614-618; c) M. Ystenes, W. Brockner, F. Menzel, *Vibr. Spectrosc.* **1992**, 3, 285-290.
- [8] K. Karaghiosoff, M. Schuster, Phosphorus, *Sulfur Silicon Relat. Elem.* **2001**, 168-169, 117-122.
- [9] C. Rotter, *Dissertation* **2008**, München.
- [10] A. Dimitrov, I. Hartwich, B. Ziemer, D. Heidemann, M. Meisel, *Z. Anorg. Allg. Chem.* **2005**, 631, 2439-2444.
- [11] a) M. Yoshifuji, K. Toyota, K. Ando, N. Inamoto, *Chemistry Lett.* **1984**, 317-318. b) M. Yoshifuji, S. Sangu, K. Kamijo, K. Toyota, *Chem. Ber.* **1996**, 129, 1049-1055. b)
- [12] F. H. Allen, O. Kennard, D. G. Watson, L. Brammer, A. G. Orpen, R. Taylor, *J. Chem. Soc., Perkin Trans. 2* (1972-1999) **1987**, S1-S19.
- [13] A. F. Holleman, E. Wiberg, N. Wiberg, *Lehrbuch der anorganischen Chemie*, Walter de Gruyter Verlag, Berlin, **2007**.
- [14] E. Gokcinar, K. Karaghiosoff, T. M. Klapoetke, C. Evangelisti, C. Rotter, *Phosphorus, Sulfur Silicon Relat. Elem.* **2010**, 185, 2527-2534.
- [15] A. Bondi, *J. Phys. Chem.* **1966**, 70, 3006-3007.

- [16] *CrysAlisPro 1.171.36.21, Agilent Technologies, 2012.*
- [17] A. Altomare, G. Cascarano, C. Giacovazzo, A. Guagliardi, A. A. G. Moliterni, M. C. Burla, G. Poidori, M. Camalli, R. Spagna, **1997**, 343.
- [18] a) M. C. Burla, R. Caliendo, M. Camalli, B. Carrozzini, G. L. Cascarano, L. De Caro, C. Giacovazzo, G. Polidori, R. Spagna, Institute of Crystallography, Bari (Italy), **2004**; b) M. C. Burla, R. Caliendo, M. Camalli, B. Carrozzini, G. L. Cascarano, L. De Caro, C. Giacovazzo, G. Polidori, R. Spagna, *Journal of Applied Crystallography* **2005**, 38, 381-388.
- [19] a) G. M. Sheldrick, *SHELXL-97, Program for the Refinement of Crystal Structures. University of Göttingen, Göttingen (Germany), 1997*; b) G. M. Sheldrick, *Acta Crystallographica, Section A: Foundations of Crystallography* **2008**, A64, 112-122.
- [20] A. L. Spek, *Platon, A Multipurpose Crystallographic Tool, Utrecht University, Utrecht, The Netherlands, 2012.*
- [21] L. J. Farrugia, *J. Appl. Crystallogr.* **1999**, 32, 837-838.
- [22] <http://journals.iucr.org/services/cif/checkcif.html>

Synthesis and Crystal Structure of a New Salt of the Water Stable Hexathiohypodiphosphate



As submitted to *Heteroatom. Chem.*



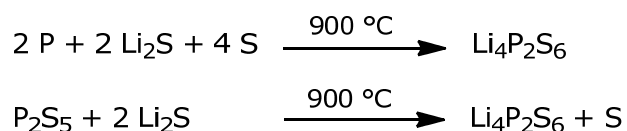
A new rare example of a synthetic route in solution to the hexathiohypodiphosphate anion $\text{P}_2\text{S}_6^{4-}$ is presented. Starting from P_4S_3 , Li_2S and elemental sulfur in pyridine this reaction yields yellow block shaped crystals of $[\text{py}_2\text{Li}]_4[\text{P}_2\text{S}_6] \cdot 2 \text{ py}$ (1). The molecular structure of this hitherto unknown compound was determined by single crystal X-ray diffraction and reveals a heteronorboman skeleton within the $\text{Li}_4\text{P}_2\text{S}_6$ entity.

Introduction

The hexathiohypodiphosphate anion $\text{P}_2\text{S}_6^{4-}$ has first been mentioned as early as 1894 by Friedel.^[1] He synthesized its Fe(II) salt starting from the elements at high temperature. Since then many more salts of this anion have been described with different metal cations. All of those compounds have been synthesised, using solid state reactions, mainly starting from red phosphorus, sulfur and the metal.

In 1968 Falius was the first, who succeeded in developing a synthesis in solution. He started from PCl_3 and Na_2S in water and obtain the sodium salt $\text{Na}_4\text{P}_2\text{S}_6 \cdot 6 \text{H}_2\text{O}$. With this, the ^{31}P NMR chemical shift of $\delta^{31}\text{P} = 110.7 \text{ ppm}$ could be determined for this anion.^[2] Salts of the hexathiohypodiphosphate anion $\text{P}_2\text{S}_6^{4-}$ are subject of continuing research due to their physical properties like semi-conductivity, ferroelectricity or luminescence (depending on the metal cation used).^[3] But also in matters of intercalation chemistry^[4], nonlinear optical material processing^[5] or the ever growing field of solid electrolytes suitable for lithium batteries^[6] this anion is of great importance. On this account it was our goal to develop a new approach to synthesize metal thiophosphates under mild conditions like reaction in solution at low temperature, ideally at room temperature. This would have a series of advantages, for example it would be less energetically demanding and thus cheaper. Also the products would be purer, as the precipitation implies a purification step. As thiophosphate compounds are mostly a domain of typical solid state chemistry, the approach of working in solution would lower the production costs and efforts tremendously.

The most important but not yet accomplished application is the use of thiophosphates as cathode or electrolyte material in modern lithium ion accumulators. So thiophosphates are especially in the focus of investigation concerning the improvement of the capacity of accumulators.^[7] Until now primarily iron containing phosphates are used. To reduce the weight of the material a replacement for the redox active material is desired. This could be accomplished by the use of compounds containing an element-element bond, as does the $\text{P}_2\text{S}_6^{4-}$ anion. A synthetic route to the lithium salt $\text{Li}_4\text{P}_2\text{S}_6$, using common solid state methods, has already been described in the literature, starting from Li_2S , phosphorus and sulfur or P_2S_5 in the melt at 900°C (Scheme 1).^[8]

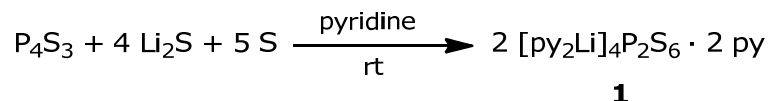


Scheme 1. Solid state syntheses of $\text{Li}_4\text{P}_2\text{S}_6$.^[8]

In the following a newly developed synthesis, fitting the criteria of mild reaction conditions, is presented. The cheap and easily accessible P_4S_3 , Li_2S and elemental sulfur are used as educts and the reaction proceeds in pyridine as reaction medium at ambient temperature.

Results and Discussion

The salt $[\text{py}_2\text{Li}]_4[\text{P}_2\text{S}_6] \cdot 2 \text{ py}$ (**1**) was obtained in excellent yield as yellow crystals from the reaction of P_4S_3 , Li_2S and elemental sulfur in pyridine (Scheme 2).



Scheme 2. Synthesis of **1**.

Compound **1** is soluble in highly polar solvents like HMPT, DMPU or water. It is remarkably stable in water over several days. In HMPT and DMPU decomposition takes place.

Compound **1** crystallizes in the monoclinic space group $P2_1/c$ with two formula units in the unit cell. Figure 3 shows the molecular structure and contains selected atom distances and bond angles.

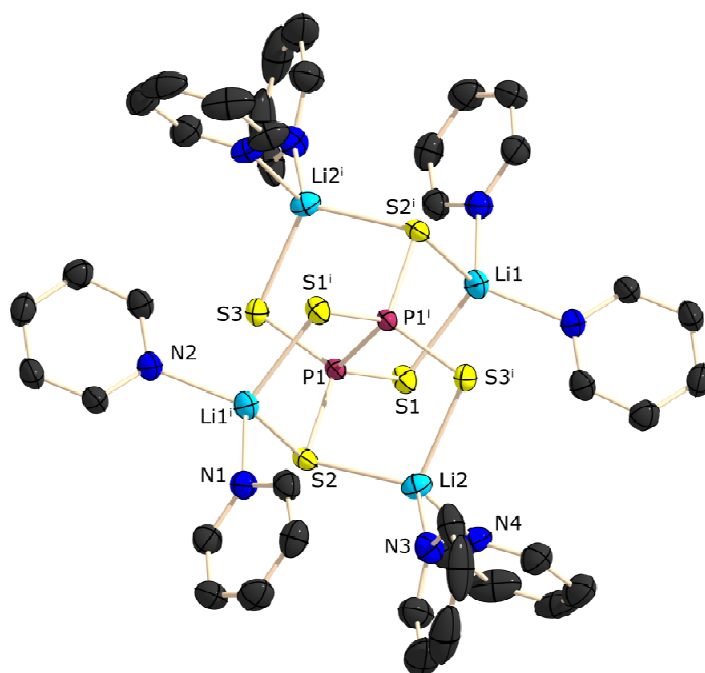


Figure 1. Molecular structure of **1**. Thermal ellipsoids are set at 50% probability level. Hydrogen atoms are omitted for clarity. Symmetry operation: $i = 1-x, -y, -z$. Selected atom distances [Å] and bond angles [°]: P1–P1ⁱ 2.251(1), P1–S1 2.013(1), P1–S2 2.039(1), P1–S3 2.015(2), Li1–S2ⁱ 2.491(3), Li1–S1 2.451(3), Li2–S2 2.490(3), Li2–S3ⁱ 2.438(3), Li1–N1 2.070(3), Li1–N2 2.086(3), Li2–N3 2.083(3), Li2–N4 2.067(3);

S1–P1–S2 112.5(1), S1–P1–S3 114.0(1), S2–P1–S3 111.4(1), Li1–S1–P1 92.5(1), Li1–S2ⁱ–P1ⁱ 92.5(2), Li2–S2–P1 93.5(1), Li2–S3ⁱ–P1ⁱ 98.0(1), Li1–S2ⁱ–Li2ⁱ 103.1(2), S2ⁱ–Li1–S1 102.9(2), S3ⁱ–Li2–S2 104.8(2), N1–Li1–N2 103.8(2), N3–Li2–N4 97.5(2).

The molecular structure of $[\text{py}_2\text{Li}]_4[\text{P}_2\text{S}_6] \cdot 2 \text{ py}$ comprises a $\text{P}_2\text{S}_6^{4-}$ anion, surrounded by four lithium cations. Each lithium cation is coordinated by two sulfur atoms bonded to the two different phosphorus atoms. The sulfur atoms S1 and S3 are connected to one phosphorus and one lithium atom, while S2 coordinates to two lithium atoms and is therefore threefold coordinated. This lead to a polycyclic arrangement of the $\text{Li}_4\text{P}_2\text{S}_6$ entity, which is built up by two hetero norbornan skeletons connected over one edge (Figure 2).

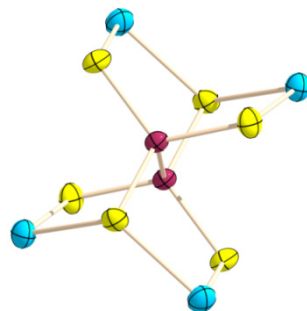


Figure 2. Two hetero norbornan skeletons connected over one edge in the $\text{Li}_4\text{P}_2\text{S}_6$ entity. Pyridine molecules are omitted for clarity.

The coordination sphere of the lithium cations is completed by two pyridine molecules, building isolated, neutral $[\text{py}_2\text{Li}]_4[\text{P}_2\text{S}_6]$ units.

The sulfur atoms of the $\text{P}_2\text{S}_6^{4-}$ anion are arranged in a staggered conformation forming an ethane like structure. The P–P bond length is with 2.251(1) Å in good accordance with the expected value of 2.256(5) Å^[9]. The distance of the threefold coordinated sulfur atom (S2) to the phosphorus is with a value of 2.039(1) Å slightly longer than the P1–S1 and P1–S3 distances with 2.013(1) and 2.015(1) Å. The average P–S bond length is with 2.022(1) Å well between a P–S single and a double bond (2.11 Å^[10] and 1.954(5) Å^[9] respectively). All these values do not differ significantly from those found in the literature for isolated hexathiohypodiphosphate anions like $\text{Na}_4\text{P}_2\text{S}_6 \cdot 4 \text{H}_2\text{O}$ ^[11] or $\text{K}_4\text{P}_2\text{S}_6 \cdot 4 \text{H}_2\text{O}$ ^[12].

The structure of $\text{Li}_4\text{P}_2\text{S}_6$, reported by Mercier *et al.*, is built up by LiS_6 octahedra, which are arranged in a stack with ABAB sequence along one axis.

In this structure the Li–S distances have a value of 2.630(2) Å, which is significantly longer than the average bond length of 2.471(3) Å found in **1**. This can be explained by a sixfold coordination in $\text{Li}_4\text{P}_2\text{S}_6$ in compared to the four fold one of the lithium in **1**.

The Li–N distances in **1** are with an average value of 2.077(3) Å in very good accordance with the ones found in the structure of $[\text{PhSLi} \cdot \text{py}_2]_n$ ^[13]. Also the N–Li–N bond angles of 100.2(3)°, observed there, fit very well with 100.7(2)°, as found in **1**.

The S–Li–S and Li–S–Li bond angles have values of 103.1(2)° and 103.9(2)° respectively.

In the crystal no interactions, other than those within one neutral $[\text{py}_2\text{Li}]_4[\text{P}_2\text{S}_6] \cdot 2 \text{ py}$ entity, can be found. Two additional uncoordinated pyridine molecules can be found completing the unit cell (Figure 3).

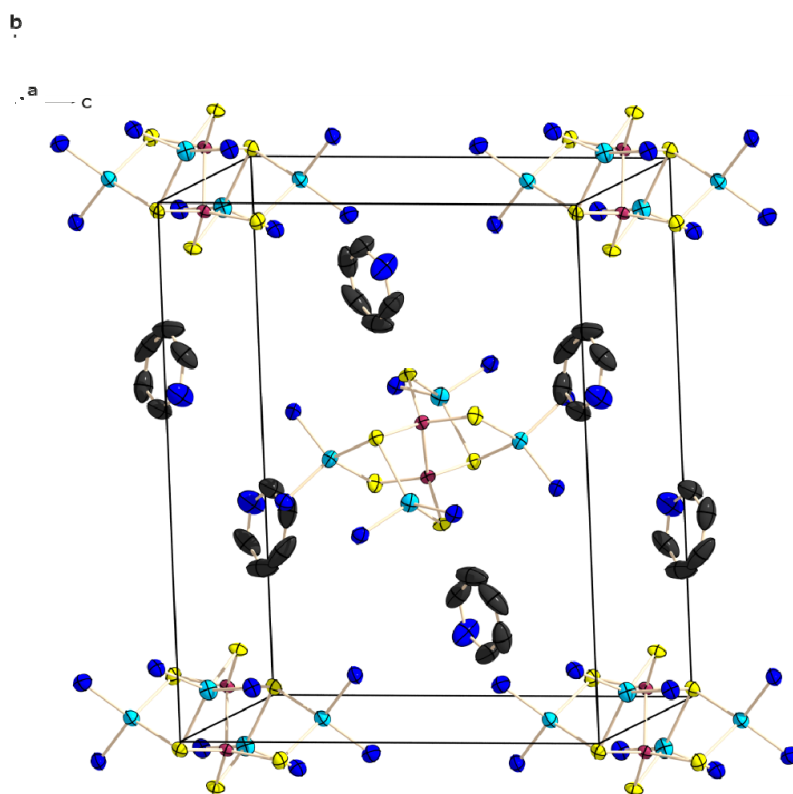
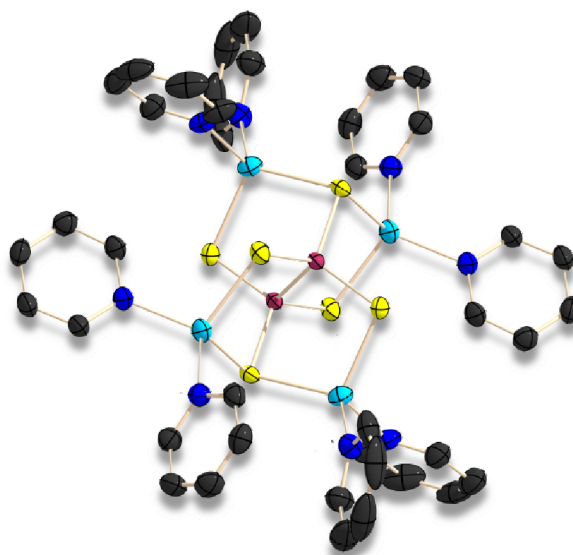


Figure 3. Unit cell of **1**. Hydrogen atoms and carbon atoms partially omitted for clarity.

Conclusion

The new lithium hexathiohypodiphosphate $[\text{py}_2\text{Li}]_4[\text{P}_2\text{S}_6] \cdot 2 \text{ py}$ (**1**) was prepared in excellent yield (99%) starting from P_4S_3 , Li_2S and elemental sulfur in pyridine. The reaction proceeds at room temperature.



The structure of **1** could be determined, using single crystal X-ray diffraction. According to these results the Li^+ ions coordinate to the staggered $\text{P}_2\text{S}_6^{4-}$ anion to form a novel $\text{Li}_4\text{P}_2\text{S}_6$ polycycle, formally consisting of two heteronornornanes. Compared to solvent free $\text{Li}_4\text{P}_2\text{S}_6$ with LiS_6 octahedra in **1** the lithium adopts its preferred tetrahedral coordination, with two pyridine molecules completing its coordination sphere. This concept is anticipated to be applicable for other metal thiophosphate systems. Remarkable is the water stability of the $\text{P}_2\text{S}_6^{4-}$ anion which is an important property for the possible use of its salts in practical applications.

The bond parameters and conformation determined for the $\text{P}_2\text{S}_6^{4-}$ anion do not deviate significantly from those found in other metal salts reported in the literature. The observed Li-S distances correspond well to those found in $[\text{PhSLi} \cdot \text{py}_2]_n$. Nevertheless it is the first time that the coordination sphere of the lithium cations is not only completed by $\text{P}_2\text{S}_6^{4-}$ molecules. This opens up the possibility to occupy the free positions with further motives and thus increase the structural diversity.

Experimental Section

General. Li_2S was obtained from Sigma-Aldrich Inc. and used as supplied without further purification. Pyridine (Aldrich) was dried using commonly known methods. P_4S_3 was commercially obtained (Riedel-de H  en), and was purified by extraction with CS_2 before use. **^{31}P NMR** Chemical shifts are referred to 85% H_3PO_4 as external standard. All spectra were measured, if not mentioned otherwise, at 25 °C. The % data correspond to the intensities in the ^{31}P NMR spectra with respect to the total intensity. The difference to 100 % belongs to not assignable signals. **Infrared spectra** were recorded on a PerkinElmer BX FT IR spectrometer equipped with a Smiths DuraSamplIR II diamond ATR unit. Transmittance values are qualitatively described as “very strong” (vs), “strong” (s), “medium” (m), “weak” (w) and “very weak” (vw). **Mass spectra** were recorded on a JEOL MStation JMS-700 with 4-nitrobenzyl alcohol as matrix for DEI measurements. **Melting and decomposition points** were determined by differential scanning calorimetry (Linseis DSC-PT10, calibrated with standard pure indium and zinc). Measurements were performed at a heating rate of 5 °C min⁻¹ in closed aluminum sample pans with a 0.1 mm hole in the lid for gas release to avoid an unsafe increase in pressure under a nitrogen flow of 20 mL min⁻¹ with an empty identical aluminum sample pan as a reference. **Melting points** were checked with a B  chi Melting Point B-540 in open glass capillaries.

X-ray Crystallography. The single-crystal X-ray diffraction data were collected using an Oxford Xcalibur3 diffractometer equipped with a Spellman generator (voltage 50 kV, current 40 mA), Enhance molybdenum K_α radiation source ($\lambda = 71.073$ pm), Oxford Cryosystems Cryostream cooling unit, four circle kappa platform and a Sapphire CCD detector. Data collection and reduction were performed with CrysAlisPro.^[14] The structures were solved with SIR97^[15], SIR2004^[16], refined with SHELXL-97^[17], and checked with PLATON^[18], all integrated into the WinGX software suite^[19]. The finalized CIF files were checked with checkCIF.^[20] All non-hydrogen atoms were refined anisotropically. The hydrogen atoms were located in difference Fourier maps and placed with a C–H distance of 0.98   for C–H bonds. Intra- and intermolecular contacts were analyzed with DIAMOND (version 3.2i), thermal ellipsoids are drawn at the 50% probability level. Selected crystallographic data and refinement details for the structure determination of compound **1** are summarized in Table 3. CCDC 968437 contains the supplementary crystallographic data for compound **1**. These data can be obtained free of charge from The Cambridge Crystallographic Data Centre via www.ccdc.cam.ac.uk/data_request/cif.

[py₂Li]₄[P₂S₆] · 2 py (1): P₄S₃ (220 mg, 1 mmol), sulfur (160 mg, 5 mmol) and Li₂S (184 mg, 4 mmol) were suspended in pyridine (10 mL). The yellow reaction solution was stirred for 2 h and precipitates as colourless block shaped crystals. The product **1** was separated from the solution and dried in *vacuo* (yield: 99% 2.1 g, 1.97 mmol, 99% with respect to P₄S₃).

³¹P{¹H} NMR (H₂O, rt): δ [ppm] = 111.1 (s, 100%). **Mass spectrometry** *m/z* (DEI+) = 281.8 (M_S = [Li₄P₂S₆]⁺), 251.8 ([M_S–Li₄]⁺), 219.9 ([M_S–Li₄S]⁺), 188.9 ([M_S–Li₄S₂]⁺), 156.9 ([M_S–Li₄PS₂]⁺), 125.0 ([M_S–Li₄PS₃]⁺), 94.0 ([M_S–Li₄PS₄]⁺), 64.0 ([Li₄PS₅]⁺). **IR** (200 mW, rt): ν [cm^{−1}] = 3057 (w), 2950 (w), 1597 (w), 1573 (ww), 1531 (ww), 1486 (w), 1442 (m), 1220 (ww), 1120 (w), 1034 (vs), 959 (m), 893 (w), 751 (w), 702 (m), 625 (vs), 469 (m), 413 (m). **DSC** (5 °C/min): T_{dec} = 162.1 °C.

Table 3. Crystallographic and refinement data for **1**.

1			
empirical formula	C ₅₀ H ₅₀ Li ₄ N ₁₀ P ₂ S ₆	<i>F</i> (000)	1116
formula mass	1073.06	Θ range [°]	4.15 – 32.36
<i>T</i> [K]	173(2)	index ranges	−25 ≤ <i>h</i> ≤ 25
crystal size [mm]	0.4 × 0.35 × 0.05		−10 ≤ <i>k</i> ≤ 11
crystal description	colourless block		−21 ≤ <i>l</i> ≤ 22
crystal system	monoclinic	reflns. collected	39951
space group	<i>P</i> 2 ₁ / <i>c</i>	reflns. obsd.	4040
<i>a</i> [Å]	10.6899(2)	reflns. unique	5038
<i>b</i> [Å]	17.9376(4)	<i>R</i> _{int}	0.0322
<i>c</i> [Å]	14.5311(3)	<i>R</i> ₁ , <i>wR</i> ₂ (2σ data)	0.0279, 0.0689
β [°]	91.524(2)	<i>R</i> ₁ , <i>wR</i> ₂ (all data)	0.0365, 0.0707
<i>V</i> [Å ³]	2785.37(10)	GOOF on <i>F</i> ²	1.015
<i>Z</i>	2	larg. diff peak/	0.286
ρ _{calcd.} [g cm ^{−3}]	1.279	hole (e/Å)	−0.274
μ [mm ^{−1}]	0.346		

Acknowledgement

Financial support by the Department of Chemistry, Ludwig Maximilian University, is gratefully acknowledged. We thank Prof. T. M. Klapötke, Department of Chemistry,

Ludwig Maximilian University, for the generous allocation of diffractometer time and for his continuous support.

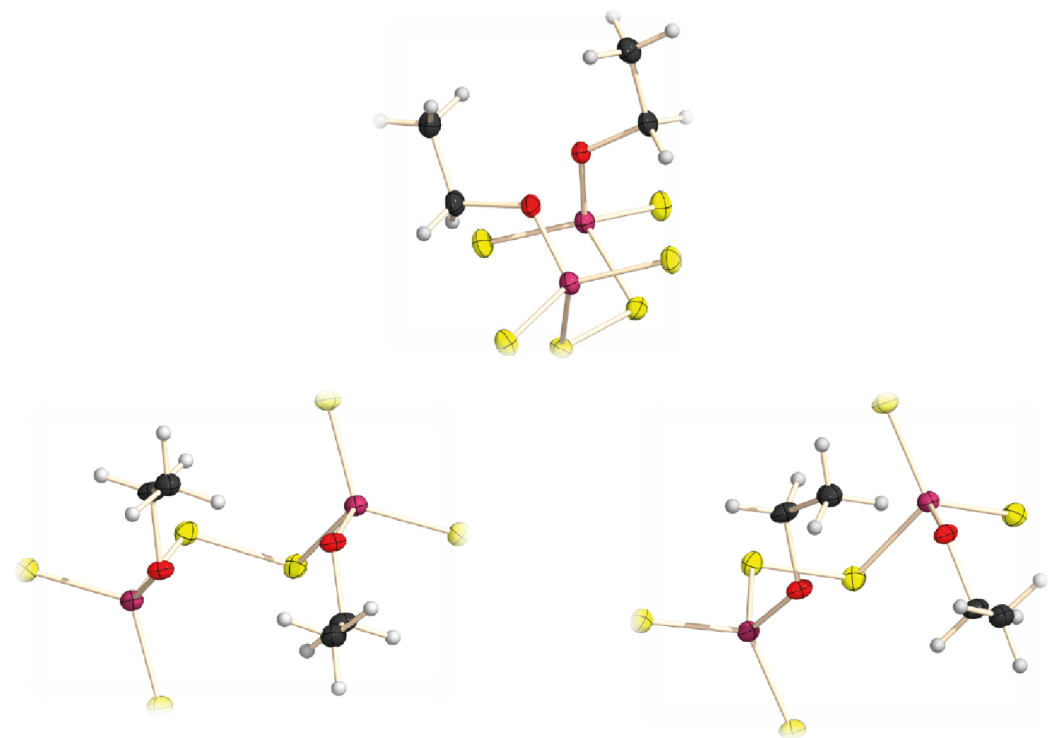
- [1] M. Friedel, *Bull. Soc. Chim. France* **1894**, 115.
- [2] H. Falius, *Z. Anorg. Allg. Chem.* **1968**, 356, 189-194.
- [3] a) O. Mys, I. Martynyuk-Lototska, A. Grabar, R. Vlokh, *J. Phys. Condens. Matter* **2009**, 21, 265401/265401-265401/265407; b) Y. Wu, W. Bensch, *Journal of Solid State Chemistry* **2009**, 182, 471-478.
- [4] A. A. El-Meligi, *Mater. Chem. Phys.* **2004**, 84, 331-340.
- [5] I. Lagadic, P. G. Lacroix, R. Clement, *Chem. Mater.* **1997**, 9, 2004-2012.
- [6] K. Takada, S. Kondo, J. Watanabe, T. Inada, A. Kajiyama, H. Sasaki, (National Institute for Research In Inorganic Materials, Japan; Toda Kogyo Corp.; Japan Storage Battery Co., Ltd.; Denki Kagaku Kogyo Co., Ltd.). Application: JP JP, **2003**, p. 5 pp.
- [7] M. Armand, J. M. Tarascon, *Nature (London, United Kingdom)* **2008**, 451, 652-657.
- [8] R. Mercier, J. P. Malugani, B. Fahys, J. Douglade, G. Robert, *J. Solid State Chem.* **1982**, 43, 151-162.
- [9] F. H. Allen, O. Kennard, D. G. Watson, L. Brammer, A. G. Orpen, R. Taylor, *J. Chem. Soc., Perkin Trans. 2* **1987**, S1-S19.
- [10] A. F. Holleman, N. Wiberg, *Lehrbuch der anorganischen Chemie*, 102 ed., Walter de Gruyter Verlag, Berlin/New York, **1995**.
- [11] T. Fincher, G. LeBret, D. A. Cleary, *J. Solid State Chem.* **1998**, 141, 274-281.
- [12] M. Gjikaj, C. Ehrhardt, *Z. Anorg. Allg. Chem.* **2007**, 633, 1048-1054.
- [13] A. J. Banister, W. Clegg, W. R. Gill, *J. Chem. Soc., Chem. Commun.* **1987**, 850-852.
- [14] *CrysAlisPro 1.171.36.21, Agilent Technologies*, **2012**.
- [15] A. Altomare, G. Cascarano, C. Giacovazzo, A. Guagliardi, A. A. G. Moliterni, M. C. Burla, G. Poidori, M. Camalli, R. Spagne, **1997**, 343.
- [16] a) M. C. Burla, R. Caliendo, M. Camalli, B. Carrozzini, G. L. Cascarano, L. De Caro, C. Giacovazzo, G. Polidori, R. Spagna, Institute of Crystallography, Bari (Italy), **2004**; b) M. C. Burla, R. Caliendo, M. Camalli, B. Carrozzini, G. L. Cascarano, L. De Caro, C. Giacovazzo, G. Polidori, R. Spagna, *Journal of Applied Crystallography* **2005**, 38, 381-388.
- [17] a) G. M. Sheldrick, *SHELXL-97, Program for the Refinement of Crystal Structures. University of Göttingen, Göttingen (Germany)*, **1997**; b) G. M. Sheldrick, *Acta Crystallographica, Section A: Foundations of Crystallography* **2008**, A64, 112-122.
- [18] A. L. Spek, *Platon, A Multipurpose Crystallographic Tool, Utrecht University, Utrecht, The Netherlands*, **2012**.
- [19] L. J. Farrugia, *J. Appl. Crystallogr.* **1999**, 32, 837-838.
- [20] <http://journals.iucr.org/services/cif/checkcif.html>

PART II

Structures of Unusual Phosphate Derivatives

Synthesis and Crystal Structure of the Bis(ethoxo)tetrathio- μ -disulfido-diphosphate Salt: $[\text{pyH}]_2[\text{P}_2\text{S}_6(\text{OEt})_2]$

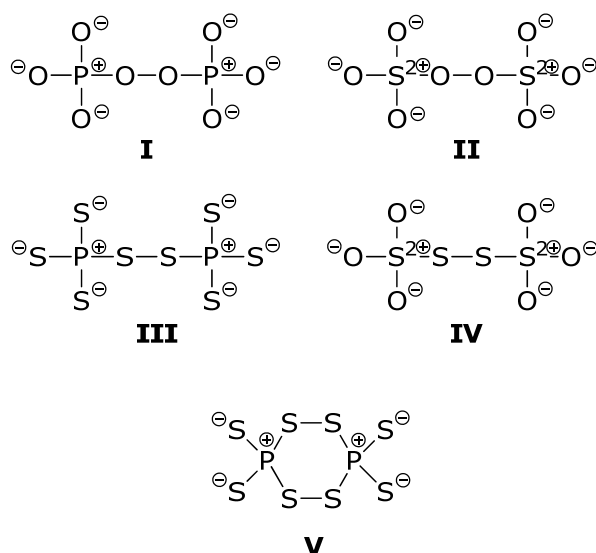
As accepted in *Z. Anorg. Allg. Chem.* (in parts).



The new dithiophosphate anion $\text{P}_2\text{S}_6(\text{OEt})_2^{2-}$ was obtained from the reaction of commercially available P_4S_{10} with Na_2S in pyridine and subsequent ethanolysis and isolated as the stable bis(pyridinium) salt (**1**). The molecular structure of **1** in the crystal was determined by single crystal X-ray diffraction and reveals a PSSP dihedral angle of $87.3(1)^\circ$ within the anion. The compound is a rare representative of a thiodiphosphate anion with a disulfide bridge between the two phosphorus atoms.

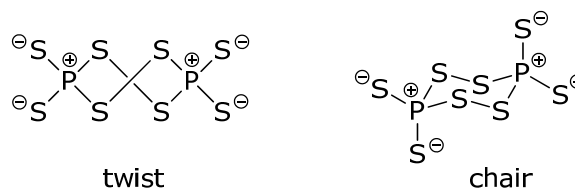
Introduction

In the family of thiopolyphosphate anions $P_nS_m^{x-}$ representatives with a polysulfide bridge between the phosphorus atoms are quite rare. An example is provided by the thiodiphosphate anion $P_2S_8^{4-}$ (**III**, Scheme 1). This species has been used as ligand in transition metal thiophosphates in the solid state, where it acts as a bridge between the metal atoms, yielding fascinating three-dimensional networks.^[1] Also for the corresponding peroxodiphosphate anion, $P_2O_8^{4-}$ (**I**), the salts of which are used for several applications, a very limited number of structures has been reported in the literature.^[2] This is in contrast to the related peroxodisulfate $S_2O_8^{2-}$ (**II**) and tetrathionate anion $S_4O_6^{2-}$ (**IV**)



Scheme 1. Diphosphates and disulfates with dichalcogenide bridges.

A cyclic version of a thiodiphosphate anion with the PSSP structural motive is provided by the $P_2S_8^{2-}$ anion (**V**)^[3]. Structural information for several salts of this anion could be obtained by single crystal X-ray diffraction.^[3b,4] Our group has shown that $P_2S_8^{2-}$ exists in solution as an equilibrium mixture between the *twist* and the *chair* conformer.^[4b]



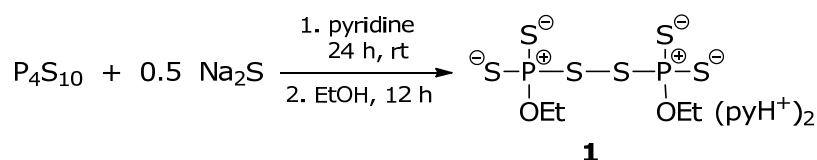
Scheme 2. The two conformers of the $\text{P}_2\text{S}_8^{2-}$ anion.

Here we report on the synthesis of a new anion – $\text{P}_2\text{S}_6(\text{OEt})_2^{2-}$ – with a disulfide bridge between the two phosphorus atoms, which has been isolated as the bis(pyridinium) salt (**1**) and characterized by single crystal X-ray diffraction.

Results and Discussion

Synthesis

The pyridinium salt of the new anion $\text{P}_2\text{S}_6(\text{OEt})_2^{2-}$ was readily obtained starting from commercially available P_4S_{10} . Reaction with 0.5 equivalents of Na_2S in pyridine in moist air yields a yellow solution, containing according to ^{31}P NMR, $\text{py}_2\text{P}_2\text{S}_5^{[5]}$, $\text{py}_2\text{P}_2\text{S}_4\text{O}^{[5]}$ and the pyridine adduct of $\text{PS}_3^{-[6]}$ as main products, together with small amounts of $\text{P}_2\text{S}_8^{2- [4b]}$ and $\text{P}_2\text{S}_7^{2- [7]}$. In addition a colourless crystalline precipitate was formed. In order to determine the identity of the precipitate it was dissolved in ethanol. Salt **1** crystallized from the ethanolic solution within 2–3 d at ambient temperature. The ^{31}P NMR spectrum of the ethanolic solution showed the presence of $(\text{EtO})_2\text{PS}_2^-$ as the main species together with smaller amounts of $\text{PS}(\text{OH})(\text{SH})\text{O}^-$ and $\text{PS}(\text{OH})_2\text{O}^-$.^[8]



Compound **1** was isolated as colourless crystalline solid, which is quite air stable and hydrolyses completely when dissolved in water. The ^{31}P NMR of the water solution indicates the presence of $(\text{EtO})_2\text{PS}_2^-$, $(\text{EtO})\text{PS}(\text{OH})\text{O}^-$, $(\text{EtO})\text{P}(\text{OH})\text{O}_2^-$ and H_2PO_4^- .^[8]

The anion in **1** represents a first example of an alcohol substituted derivative of the $\text{P}_2\text{S}_8^{4-}$ anion. Thus it belongs to the family of anions, in which two phosphorus(V) or sulfur(VI) atoms are connected by a dichalcogenide group (Scheme 1). The anion $\text{P}_2\text{S}_6(\text{OEt})_2^{2-}$ should exhibit interesting ligand properties due to the two phosphate groups being capable of coordination. In this context the molecular structure of **1** is of particular interest. In order to investigate the influence of the ethoxy groups on the molecular structure and conformation of the P,S-framework in the anion of **1** single crystal X-ray studies were performed.

Molecular and Crystal Structure of $(\text{pyH})_2[\text{P}_2\text{S}_6(\text{OEt})_2]$ (**1**)

Colourless block shaped crystals of **1** were isolated by slow evaporation of an ethanolic solution. The compound crystallizes in the monoclinic space group $C2/c$ with four formula units in the unit cell. The asymmetric unit contains half of the anion and one pyridinium cation. Figure 1 shows the molecular structure of the anion and gives selected atom distances and angles.

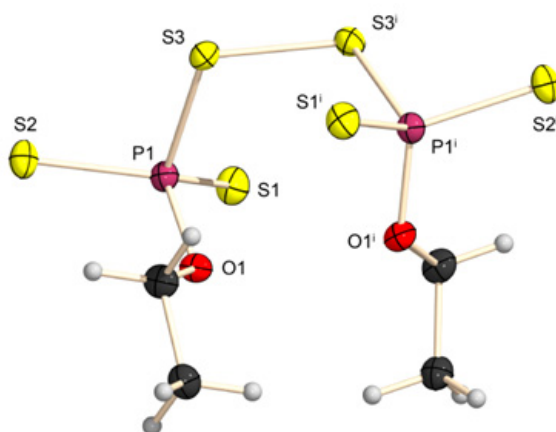


Figure 1. Molecular structure of **1** in the crystal. Thermal ellipsoids are shown at 50% probability level. Symmetry operation $i = 2-x, y, 0.5-z$. Selected atom distances and bond angles: S1–P1 1.956 (2); S2–P1 1.985(2), P1–O1 1.606(2), P1–S3 2.128(2), S3–S3ⁱ 2.047(2), O1–C 1.460(1); O1–P1–S1 106.3(1), O1–P1–S2 111.2(2), S1–P1–S2 120.1(1), O1–P1–S3 105.4(1), S1–P1–S3 113.7(2), S2–P1–S3 99.2(2), S3ⁱ–S3–P1 107.7(1), C–O1–P1 121.0(2).

In the anion $\text{P}_2\text{S}_6(\text{OEt})_2^{2-}$ the phosphorus atoms display a slightly distorted tetrahedral environment. The observed P–S distances to the terminal sulfur atoms are with 1.956(2) Å and 1.985(2) Å between those reported for P,S single (2.11 Å^[9]) and double (1.92 Å^[4a]) bonds. The distance between phosphorus and the adjacent sulfur atom of the disulfide bridge corresponds with 2.128(2) Å to a P,S single bond. The S–S distance of 2.047(2) Å compares well to the corresponding one observed in disulfides. The P–O distance of 1.606(2) Å does not deviate substantially from the expected value (1.621(7) Å^[4a]). The P–S–S–P torsion angle of 87.2(1)° lies in the same range of magnitude as the corresponding torsion angle in the $\text{P}_2\text{S}_8^{2-}$ anion (Table 1); it is however smaller than those observed in the anions $\text{P}_2\text{S}_8^{4-}$ (98.7°^[1c], 96.7°^[1a]) and $\text{S}_4\text{O}_6^{2-}$ (108.4°)^[10]. Comparing the data in Table 1 it is evident, that the opening of the sixmembered ring in $\text{P}_2\text{S}_8^{2-}$ and substitution of two sulfur atoms with ethoxy groups has little influence on the conformation of the P,S framework.

Table 1. Comparison of atom distances and angles of **1** with those found in salts of the $\text{P}_2\text{S}_8^{2-}$ anion.

	1	$[\text{PPN}]_2[\text{P}_2\text{S}_8]^{[4b]}$	$[(\text{py}_2)\text{H}]_2[\text{P}_2\text{S}_8]^{[3b]}$	Ref. ^[4a]
distances[Å]				
P–S	1.970(2)	1.962(2)	1.956(4)	
P–S3	2.128(2)	2.084(5)	2.130(4)	
S–S	2.047(2)	2.047(7)	2.059(4)	2.031(17)
P–O	1.606(2)			1.621(7)
angles[°]				
S1–P–S2	120.1(1)	118.1(1)	122.1(2)	
S1–P–S3	113.7(1)	116.6(1)	112.6(2)	
S2–P–S3	99.2(1)	109.9(1)	101.9(2)	
S3–S3 ⁱ –P	107.7(1)	104.1(1)	104.6(2)	
torsion angle [°]				
P–S–S ⁱ –P ⁱ	87.3(1)	86.4(1)	72.8(1)	

Taking a look at the intra- and intermolecular interaction one finds that in the salts of the $\text{P}_2\text{S}_8^{2-}$ anions the molecules are well defined and electrostatically shielded from the outside without any kind of interaction between each other, whereas in the product of their reaction with ethanol the situation is rather different.

Table 2 and Figure 2 give an overview of all interactions found in and around the asymmetric unit of **1**.

Table 2. Intra- and intermolecular interaction in **1** (the sum of the van der Waals radii of hydrogen and sulfur atom mounts up to 3.00 Å).

D–H...A	d(D–H) (Å)	d(H...A) (Å)	d(D ...A) (Å)	∠ D–H...A (°)
N1 ⁱⁱⁱ –H1 ⁱⁱⁱ ...S2	0.81(4)	2.50(4)	3.264(3)	157(3)
C2–H2A...S2	0.93(4)	2.88(4)	3.391(3)	116(2)
C1 ⁱⁱ –H1A ⁱⁱ ...S1	0.96(3)	2.92(4)	3.801(4)	154(3)
C3 ^{iv} –H3 ^{iv} ...S3	0.90(4)	2.87(4)	3.570(4)	137(3)

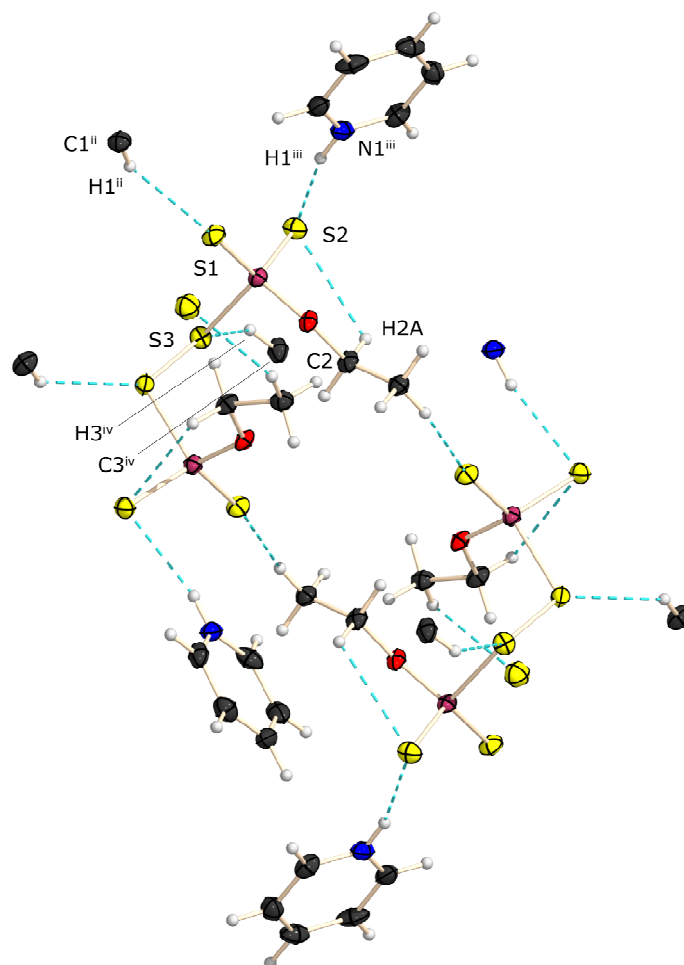


Figure 2. Intra- and intermolecular interaction in **1**.

The hydrogen at the nitrogen atom of the pyridinium cation is linked to the S2 atom of the $(\text{PS}_2\text{OEt})_2$ unit. With a D \cdots A distance of 3.264(3) Å and a D–H \cdots A bond angle of 157(3)° this can be regarded as a strong interaction, as the sum of the van der Waals radii of nitrogen and sulfur is 3.35 Å^[6]. Due to sterical reasons the N–H \cdots S angle deviates from the expected 180°. The same sulfur atom is also connected intramolecularly to one of the hydrogen atoms of the ethoxy group. This interaction is very weak with a distance of 3.391(3) Å and has therefore electrostatic character. The same is true for the attraction between one hydrogen of the other carbon of the ethoxy group and the S1 atom (C1ⁱⁱ–H1Aⁱⁱ \cdots S1) with a H \cdots A distance of 2.92(4) Å, which is just below the sum of the van der Waals radii of hydrogen and sulfur (3.00 Å).^[6]

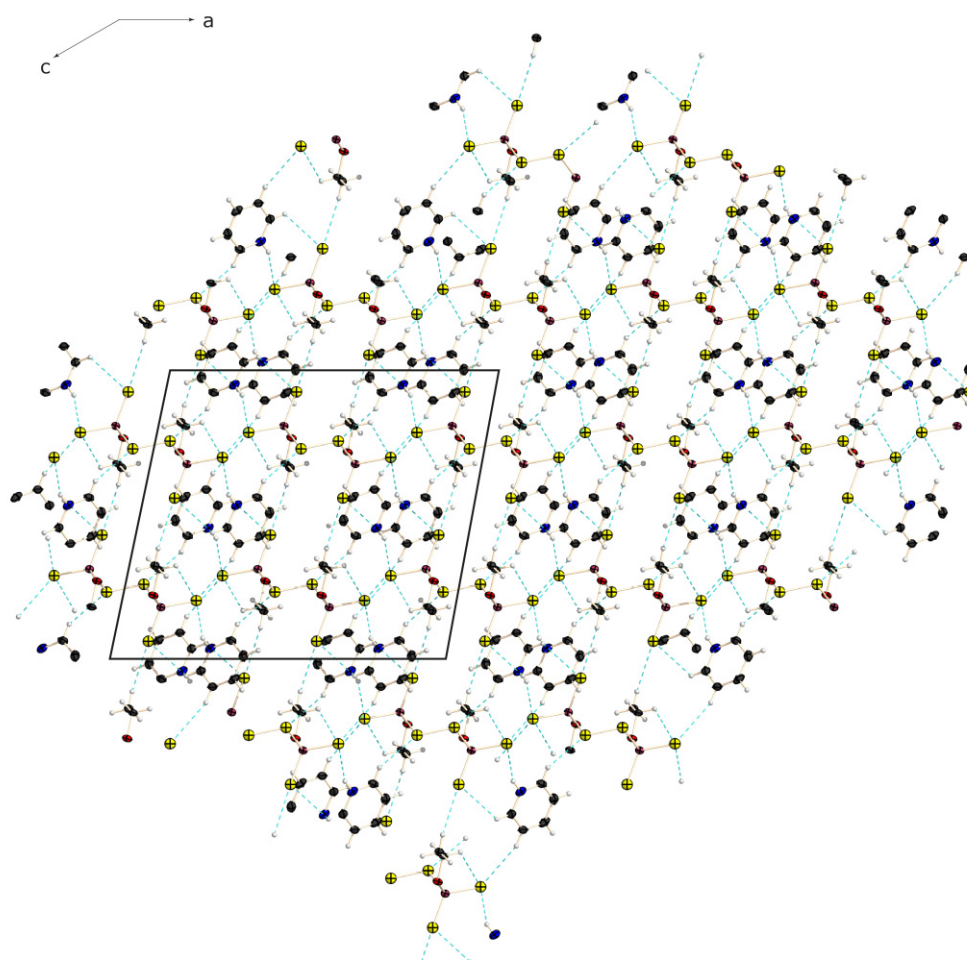


Figure 3. Network of **1**.

The bridging sulfur atom coordinates to the hydrogen atom at the C3 of the pyridinium ion with a barely shorter distance of 3.570(4) Å and an angle of 137(3)°.

This variety of intra- and intermolecular interactions leads to the formation of a vast three dimensional network as can be seen in Figure 3

Quantumchemical Calculations

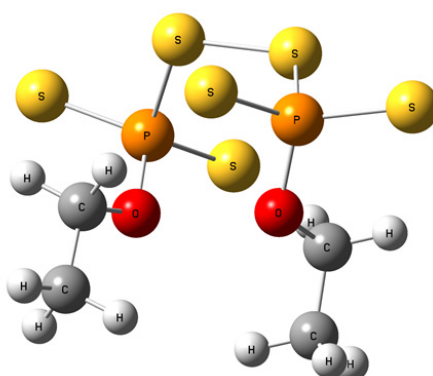


Figure 4. Computed structure of the di-anion $[P_2S_6(OEt)_2]^{2-}$ at MPW1PW91/aug-cc-pVDZ level of theory.

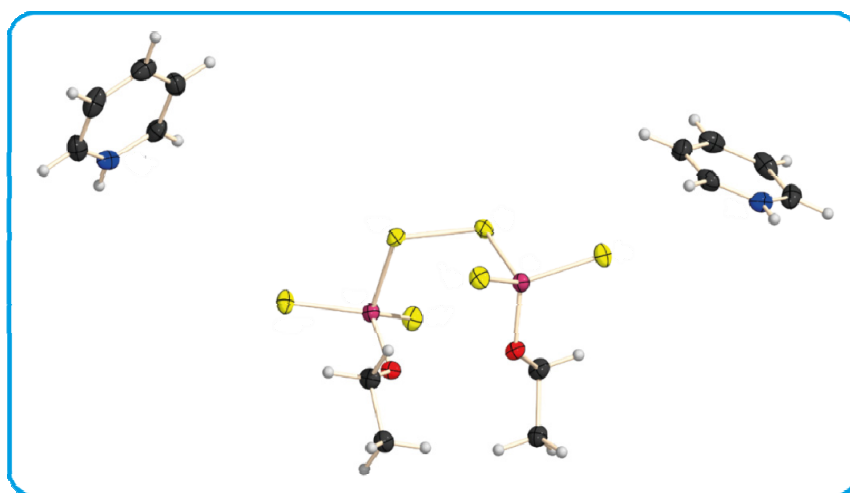
Due to the hydrolytic instability of **1** its ^{31}P NMR chemical shift could not be determined. Information about the ^{31}P NMR parameters was obtained from quantum-chemical calculations. In order to compute the ^{31}P NMR chemical shift of the dianion $[C_4H_{10}O_2P_2S_6]^{2-}$, the isotropic magnetic shieldings were computed using the GIAO (Gauge-Independent Atomic Orbital) method implemented in Gaussian 09.^[11, 12] The structure was optimized in C_2 symmetry (Figure 1) and the frequencies calculated ($NIMAG = 0$) at MPW1PW91/aug-cc-pVDZ level of theory, subsequently, the NMR shielding tensors were calculated at the same level of theory using the GIAO method and accounting for solvent (dipole) effects by placing the solute in a cavity within the solvent reaction field using the SMD method.^[11] Table 2 summarizes the computed isotropic magnetic shieldings and relative ^{31}P NMR chemical shifts (ppm) referenced to H_3PO_4 .

Table 3. Computed isotropic magnetic shieldings (GIAO method^[9, 10], MPW1PW91/aug-cc-pVDZ) and relative ^{31}P chemical shifts (ppm) referenced to H_3PO_4 .

The $\text{P}_2\text{S}_6(\text{OEt})_2^{2-}$ anion

compound	$[\text{C}_4\text{H}_{10}\text{O}_2\text{P}_2\text{S}_6]^{2-}$	H_3PO_4
$-E/$ a.u.	3381.146718	644.135802
NIMAG	0	0
p.g.	C_2	C_3
$\delta^{31}\text{P}$ / ppm, calcd. isotr. shielding	232.3	361.6
$\delta^{31}\text{P}$ / ppm, calcd. (ref. to H_3PO_4)	129.3	0.0

Conclusion



The synthesis of the new anion $\text{P}_2\text{S}_6(\text{OEt})_2^{2-}$ and its isolation as the bis(pyridinium) salt **1** provides a route to a new thiodiphosphate anion with a high sulfur content. This anion is a rare example of a compound with a disulfide bridge between the two phosphorus atoms. Its molecular structure in the crystal shows a dihedral PSSP angle of $87.3(1)^\circ$. In the crystal electrostatic $\text{N-H}\cdots\text{S}$ and $\text{C-H}\cdots\text{S}$ interactions result in the formation of a complicated three-dimensional network. The new anion $\text{P}_2\text{S}_6(\text{OEt})_2^{2-}$ is anticipated to display an interesting coordination chemistry.

Experimental Section

General. Na₂S and solvents were obtained from Sigma-Aldrich Inc. or Acros Organics (analytical grade) and were used as supplied without further purification. P₄S₁₀ was commercially obtained (Riedel-de H  en) and purified by recrystallization from CS₂. NMR spectra were recorded using a Jeol EX 400 Eclipse instrument operating at 161.997 MHz (³¹P). Chemical shifts are referred to 85% H₃PO₄ as external standard. All spectra were measured, if not mentioned otherwise, at 25 °C. Infrared (IR) spectra were recorded on a PerkinElmer BX FT IR spectrometer equipped with a Smiths DuraSamplIR II diamond ATR unit. Transmittance values are qualitatively described as “very strong” (vs), “strong” (s), “medium” (m), “weak” (w) and “very weak” (vw). Raman spectra were recorded on a Bruker RAM II spectrometer equipped with a Nd:YAG laser (200 mW) operating at 1064 nm and a reflection angle of 180°. The intensities are reported as percentages of the most intense peak and are given in parentheses. Low resolution mass spectra were recorded on a JEOL MStation JMS-700 with 4-nitrobenzyl alcohol as matrix for FAB measurements. Elemental analyses (CHNS) were performed with an Elementar Vario EL. Due to the formation of glassy (P₂O₅)_x(H₂O)_yC during measurement, the values deviate considerably from the calculated ones. Melting and decomposition points were determined by differential scanning calorimetry (Linseis DSC-PT10, calibrated with standard pure indium and zinc). Measurements were performed at a heating rate of 5 °C min⁻¹ in closed aluminum sample pans with a 0.1 mm hole in the lid for gas release to avoid an unsafe increase in pressure under a nitrogen flow of 20 mL min⁻¹ with an empty identical aluminum sample pan as a reference. Melting points were checked with a B  chi Melting Point B-540 in open glass capillaries.

X-ray Crystallography. For all compounds, an Oxford XCalibur3 diffractometer with a CCD area detector was employed for data collection using Mo-K_{  } radiation (λ = 0.71073   ). The structures were solved using direct methods (SIR2004)^[13] and refined by full-matrix least-squares on F^2 (SHELXL-97)^[14]. All non-hydrogen atoms were refined anisotropically. The hydrogen atoms were located in difference Fourier maps and placed with a C–H distance of 0.99    for CH₂ groups. ORTEP plots are shown with thermal ellipsoids at the 50% probability level. CCDC 948131 contains the supplementary crystallographic data for this paper. These data can be obtained free of charge from The Cambridge Crystallographic Data Centre via www.ccdc.cam.ac.uk/data_request/cif.

Table 3. Crystallographic and refinement data for **1**.

1			
empirical formula	$\text{C}_{14}\text{H}_{22}\text{N}_2\text{O}_2\text{P}_2\text{S}_6$	$F(000)$	1048
formula mass	504.64	Θ range [°]	4.25 – 30.03
T [K]	173(2)	index ranges	$-25 \leq h \leq 25$
crystal size [mm]	$0.4 \times 0.35 \times 0.05$		$-10 \leq k \leq 11$
crystal description	colourless plate		$-21 \leq l \leq 22$
crystal system	monoclinic	reflns. collected	11444
space group	$C2/c$	reflns. obsd.	2424
a [Å]	18.125(2)	reflns. unique	3309
b [Å]	8.131(1)	R_{int}	0.0523
c [Å]	15.680(1)	R_1, wR_2 (2σ data)	0.0401, 0.0824
β [°]	100.341(5)	R_1, wR_2 (all data)	0.0674, 0.0957
V [Å ³]	2273.3(4)	GOOF on F^2	1.049
Z	4	larg. diff peak/hole	0.405/−0.294
$\rho_{\text{calcd.}}$ [g cm ^{−3}]	1.474	(e/Å)	
μ [mm ^{−1}]	0.755		

[P₂S₆O₂C₄H₁₀][C₅H₆N]₂: P₄S₁₀ (0.182 g, 0.409 mmol) and Na₂S (0.015 g, 0.192 mmol) were stirred in pyridine (5 mL) for 24 h. White powder precipitated from the yellow reaction mixture. The reaction solution was investigated by ³¹P NMR spectroscopy and showed the signals of pyPS₃[−] ($\delta^{31}\text{P}$ = 183.1 ppm, 19%), P₂S₇^{2−} ($\delta^{31}\text{P}$ = 129.5 ppm, 3%), P₂S₈^{2−} ($\delta^{31}\text{P}$ = 120.0 ppm (twist), 56.3 ppm (chair), 4%), py₂P₂S₅ ($\delta^{31}\text{P}$ = 104.5 ppm, 58%) and py₂P₂S₄O ($\delta^{31}\text{P}$ = 97.9 ppm, 16%). The precipitate was separated from the solution, dried *in vacuo* and dissolved in 6 mL of EtOH. After 12 h stirring at ambient temperature a yellow solution was obtained, from which after 2–3 d colorless crystals of [pyH]₂[P₂S₆(OEt)₂] separated (58.7 mg, 29%). The ³¹P NMR spectrum of the mother liquor displayed signals at 113.4 ppm ((EtO)₂PS₂[−], 82%), 96.8 ppm (PS(OH)(SH)O[−], 16%) and 58.4 ppm (PS(OH)₂O[−], 2%).

Elemental analysis ([pyH]₂[P₂S₆O₂C₄H₁₀]): calcd. C 33.32, N 5.55, H 4.39, S 38.12; found C 30.45, N 4.75, H 3.95, S 36.73. **Mass spectrometry** m/z (FAB[−]) = 345.1 ([S₆P₂(OEt)₂][−]), 319.0 ([M−C₂H₅][−]), 303.1 ([M−2C₂H₅][−]), 299.0 ([M−C₂H₅O][−]), 287.1 ([M−2C₂H₅][−]), 271.0 ([M−PS₃OEt][−]), 205.1 ([M−PS₂OC₂H₅][−]), 185.2 ([M−PS₂OC₃H₈][−]), 175.0 ([M−PS₃OEt][−]), 141.1 ([M−PS₂OC₂H₅][−]), 127.0 ([M−PS₃][−]), 46 ([M−P₂S₆OC₂H₅][−]). **Raman** (200 mW, r.t.): ν [cm^{−1}] = 3068 (35),

2975 (43), 2929 (69), 2885 (47), 1629 (41), 1455 (45), 1196 (34), 1009 (72), 883 (39), 502 (45), 474 (65), 393 (56), 220 (100). **IR** (200 mW, r.t.): ν [cm^{-1}] = 3413.9 (br, vw), 3204.2 (vw), 3137.7 (vw), 3125.0 (vw), 3087.9 (w), 3057.8 (w), 2985.9 (w), 2973.0 (w), 2943.4 (w), 2885.9 (w), 2757.0 (br, w), 2132.3 (vw), 2000.3 (vw), 1893.9 (vw), 1839.4 (vw), 1630.9 (w), 1603.1 (w), 1529.3 (m), 1482.3 (m), 1441.8 (vw), 1381.8 (w), 1330.3 (vw), 1247.1 (w), 1193.6 (m), 1152.7 (w), 1084.8 (w), 1047.8 (w), 1017.0 (s), 930.3 (br, vs), 766.1 (s), 755.8 (m), 741.9 (vs), 712.0 (m), 675.8 (vs), 666.4 (vs). **M.p.**: 298.6 °C.

Acknowledgement

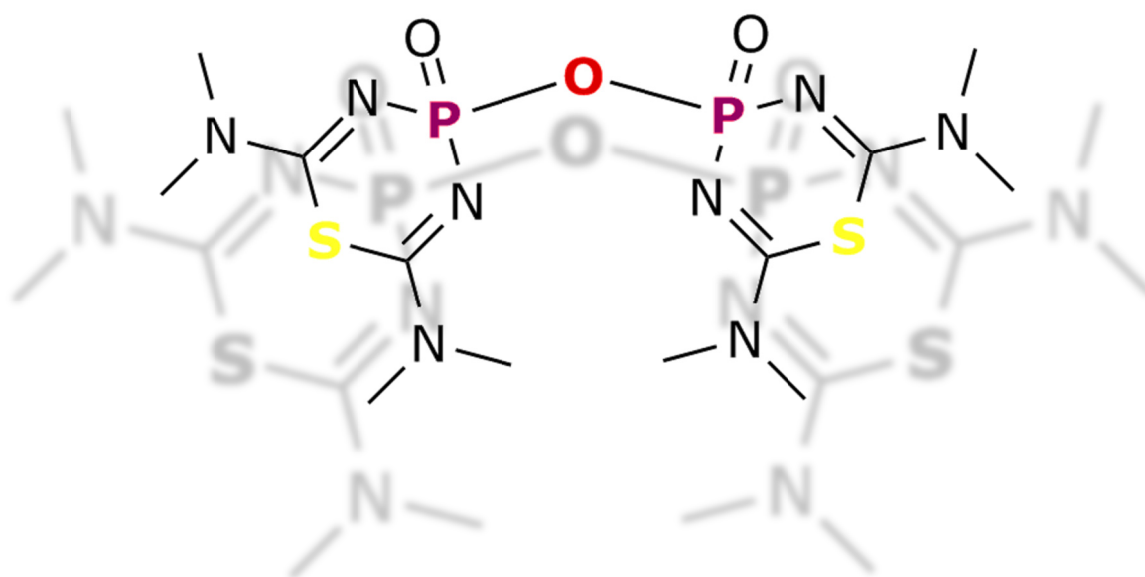
Financial support by the Department of Chemistry, University of Munich, is gratefully acknowledged. Tabea Strauss is thanked for the help with the synthesis.

-
- [1] a) R. Brec, G. Ouvrard, M. Evain, P. Grenouilleau, J. Rouxel, *J. Solid State Chem.* **1983**, 47, 174-184; b) P. Grenouilleau, R. Brec, M. Evain, J. Rouxel, *Rev. Chim. Miner.* **1983**, 20, 628-635; c) Y. Wu, W. Bensch, *Inorg. Chem.* **2007**, 46, 6170-6177.
 - [2] O. Oeckler, L. Montbrun, *Z. Anorg. Allg. Chem.* **2008**, 634, 279-287.
 - [3] a) H. Falius, A. Schliephake, D. Schomburg, *Z. Anorg. Allg. Chem.* **1992**, 611, 141-148; b) P. C. Minshall, G. M. Sheldrick, *Acta Crystallographica Section B* **1978**, 34, 1378-1380.
 - [4] a) F. H. Allen, O. Kennard, D. G. Watson, L. Brammer, A. G. Orpen, R. Taylor, *J. Chem. Soc., Perkin Trans. 2* **1987**, S1-S19; b) C. R. Dissertation, **2009**.
 - [5] S. Schönberger, C. Jagdhuber, L. Ascherl, C. Evangelisti, T. M. Klapötke, K. Karaghiosoff, *Z. Anorg. Allg. Chem.* **2013**, DOI: 10.1002/zaac.201300419.
 - [6] A. Dimitrov, I. Hartwich, B. Ziemer, D. Heidemann, M. Meisel, *Zeitschrift fuer Anorganische und Allgemeine Chemie* **2005**, 631, 2439-2444.
 - [7] H. Falius, A. Schliephake, D. Schomburg, *Zeitschrift fuer Anorganische und Allgemeine Chemie* **1992**, 611, 141-148.
 - [8] A. J. Burn, S. K. Dewan, I. Gosney, P. S. G. Tan, *Journal of the Chemical Society, Perkin Trans. 2* **1990**, 753-758.
 - [9] A. F. Holleman, E. Wiberg, N. Wiberg, *Lehrbuch der Anorganischen Chemie*, Walter de Gruyter Verlag, Berlin, **2007**.
 - [10] R. P. Sharma, A. Singh, P. Venugopalan, P. Brandao, V. Felix, *Polyhedron* **2012**, 40, 175-184.
 - [11] Gaussian 09, Revision **A.1**, M. J. Frisch, G. W. Trucks, H. B. Schlegel, G. E. Scuseria, M. A. Robb, J. R. Cheeseman, G. Scalmani, V. Barone, B. Mennucci, G. A. Petersson, H. Nakatsuji, M. Caricato, X. Li, H. P. Hratchian, A. F. Izmaylov, J. Bloino, G. Zheng, J. L. Sonnenberg, M.

- Hada, M. Ehara, K. Toyota, R. Fukuda, J. Hasegawa, M. Ishida, T. Nakajima, Y. Honda, O. Kitao, H. Nakai, T. Vreven, J. A. Montgomery, Jr., J. E. Peralta, F. Ogliaro, M. Bearpark, J. J. Heyd, E. Brothers, K. N. Kudin, V. N. Staroverov, R. Kobayashi, J. Normand, K. Raghavachari, A. Rendell, J. C. Burant, S. S. Iyengar, J. Tomasi, M. Cossi, N. Rega, J. M. Millam, M. Klene, J. E. Knox, J. B. Cross, V. Bakken, C. Adamo, J. Jaramillo, R. Gomperts, R. E. Stratmann, O. Yazyev, A. J. Austin, R. Cammi, C. Pomelli, J. W. Ochterski, R. L. Martin, K. Morokuma, V. G. Zakrzewski, G. A. Voth, P. Salvador, J. J. Dannenberg, S. Dapprich, A. D. Daniels, O. Farkas, J. B. Foresman, J. V. Ortiz, J. Cioslowski, and D. J. Fox, Gaussian, Inc., Wallingford CT, 2009.
- [12] a) Wolinski, K.; Hilton, J. F.; Pulay, P. *J. Am. Chem. Soc.* **1990**, *112*, 8251; b) Dodds, J. L.; McWeeny, R.; Sadlej, A. J. *Mol. Phys.* **1980**, *41*, 1419; c) Ditchfield, R. *Mol. Phys.* **1974**, *27*, 789; d) McWeeny, R. *Phys. Rev.* **1962**, *126*, 1028.
- [13] a) M. C. Burla, R. Caliendo, M. Camalli, B. Carrozzini, G. L. Cascarano, L. De Caro, C. Giacovazzo, G. Polidori, R. Spagna, Institute of Crystallography, Bari (Italy), **2004**; b) M. C. Burla, R. Caliendo, M. Camalli, B. Carrozzini, G. L. Cascarano, L. De Caro, C. Giacovazzo, G. Polidori, R. Spagna, *Journal of Applied Crystallography* **2005**, *38*, 381-388.
- [14] a) G. M. Sheldrick, University of Göttingen, Göttingen (Germany), **1997**; b) G. M. Sheldrick, *Acta Crystallographica, Section A: Foundations of Crystallography* **2008**, *A64*, 112-122.

Formation and Crystal Structure of 4,4'-Oxybis(2,6-bis(dimethylamino)-4H- 1,3,5,4-thiadiazaphosphinine 4-oxide)

As accepted in *Phosphorus, Sulfur Silicon Relat. Elem.*



The reaction of P_4S_{10} with dimethyl cyanamide as solvent yields a complex mixture of products, from which the new compound 4,4'-oxybis(2,6-bis(dimethylamino)-4H-1,3,5,4-thiadiazaphosphinine 4-oxide) (**1**) was isolated. In this pyrophosphate derivative the phosphorus atoms are part of the, otherwise rarely encountered, 1,3,5,4-thiadiazaphosphinine ring. The molecular structure of the new compound was elucidated by single crystal X-ray diffraction, showing an almost planar thiadiazaphosphinine ring and a cis-like arrangement of the heterocycles at the two phosphorus atoms.

Introduction

The reaction of P_4S_{10} with nitrogen containing nucleophiles represents a challenge for chemists since several years. Roesky *et al.* investigated the nucleophilic attack of different anions on P_4S_{10} already in 1970.^[1] Mainly alkali metal salts of cyanide, azide and thiocyanate were allowed to react with phosphorus(V) sulfide in acetonitrile. The reaction with $[(n-C_3H_7)_4N][(N_3)_2PS_2]$ in MeCN yielded a white precipitate, which was characterized using IR- and ^{31}P NMR spectroscopy. The ^{31}P NMR spectrum of this compound showed two triplets of equal intensity (Table 1). For its structure a P_4S_{10} motive with one endocyclic sulfur being substituted by a nitrogen atom, resulting in the $(n-C_3H_7)_4N^+$ salt of the anion $P_4S_9N^-$ (**I**) was proposed (Figure 1).

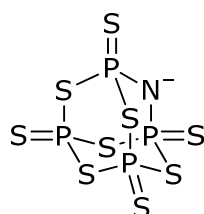


Figure 1. Structure of the $P_4S_9N^-$ anion (**I**) by Roesky^[1]

Eight years later Retuert *et al.* observed nearly identical ^{31}P NMR signals, when they investigated a suspension of P_4S_{10} in PhCN.^[2] They claimed the structure of the orange crystalline product, resulting from this reaction, to be a neutral P_4S_{10} adamantane-like cage, with two exocyclic sulfur atoms being substituted by $=N-CS-C_6H_5$ groups (Figure 2).

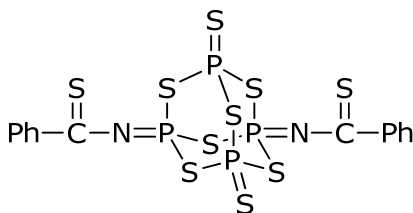


Figure 2. Structure of $P_4S_8(NC(S)C_6H_5)$ (**II**) by Retuert.

Neels and co-workers tried to answer the question, to which of the above mentioned compounds the observed ^{31}P NMR shift can be assigned.^[3] For the formation of the

product acetonitrile was used as solvent, so it is likely, that it is generally formed by reaction of P_4S_{10} with nitriles. They reproduced the synthesis of *Retuert* and isolated crystals of the 3,5-diphenyl-1,2,4-dithiazolium salt of **2** and determined the structure using single crystal X-ray diffraction.

Table 1. Comparison of ^{31}P NMR shifts and coupling constants.

Compound	$\delta P1$ [ppm]	$\delta P2$ [ppm]	$^2J_{P1P2}$ [Hz]
$P_4S_9N^-$ ^[1]	67.8	32.8	21.5
$P_4S_8(NC(S)Ph)_2$ ^[2]	67	30	21
$P_4S_{10} + 2 PhCN$ ^[3]	67.6	32.8	21.5
α - P_4S_9 ^[4]	64.6	48.8	96.3
β - P_4S_9 ^[5]	52.0	44.2	30.5
P_4S_{10} ^[4]	56.1	-	-

In the course of our investigations on the reactivity of P_4S_{10} we took a closer look at the influence of different nitrogen containing basic solvents on its reaction behaviour.

Results and Discussion

P_4S_{10} was dissolved in benzonitrile or propionitrile on prolonged heating. ^{31}P NMR spectra of the reaction solutions showed the formation of complex mixtures of products. In both cases also ^{31}P NMR signals indicating the presence of compound **2** were observed. This was also the case, when pyridine and 2,2'-bipyridine was added to the solution.

The reaction of P_4S_{10} with dimethyl cyanamide resulted in the isolation of an unexpected product. Refluxing P_4S_{10} in dimethyl cyanamide yields a brown reaction solution. Here also a complex mixture of different products could be observed in the ^{31}P NMR. From this solution a small amount of colourless crystals could be obtained. The product was identified by single crystal X-ray diffraction as the novel compound 4,4'-oxybis(2,6-bis(dimethylamino)-4*H*-1,3,5,4-thiadiazaphosphinine 4-oxide) (**1**) (Figure 3).

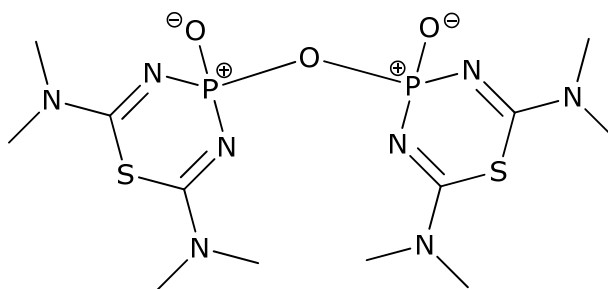
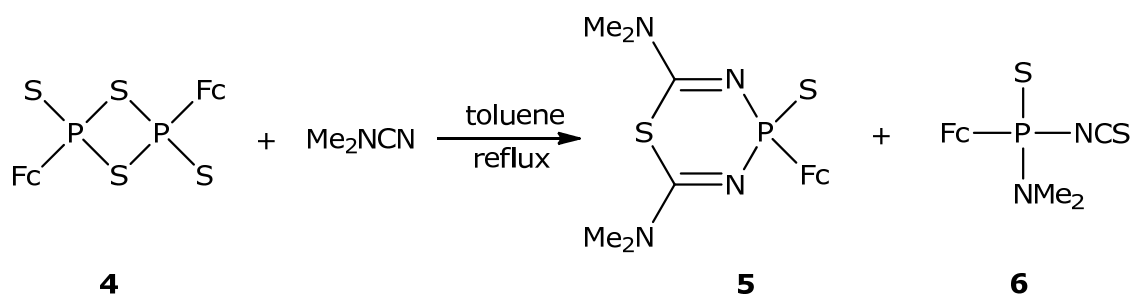


Figure 3. Chemical structure of 4,4'-oxybis(2,6-bis(dimethylamino)-4H-1,3,5,4-thiadiazaphosphinine 4-oxide) (**1**).

In the literature only one compound has been reported, containing a 1,3,5,4-thiadiazaphosphinine ring, which has been characterized in terms of single crystal X-ray diffraction. Woollins *et al.* described the formation of the *P*-ferrocenyl substituted 2,6-bis(dimethylamino)-1,3,5,4-thiadiazaphosphorine-4-sulfide (**5**) in good yield together with small amounts of the thiocyanate (**6**) from the reaction of the corresponding ferrocenyl perthiophosphonic acid anhydride (**4**) with an excess of dimethyl cyanamide.^[6]



Scheme 1. Synthesis of compound **5**.^[6]

Compound **1** crystallizes in the orthorhombic space group *Pbcn* with four formula units in the unit cell. Figure 4 shows the molecular structure and selected atom distances and bond angles are listed.

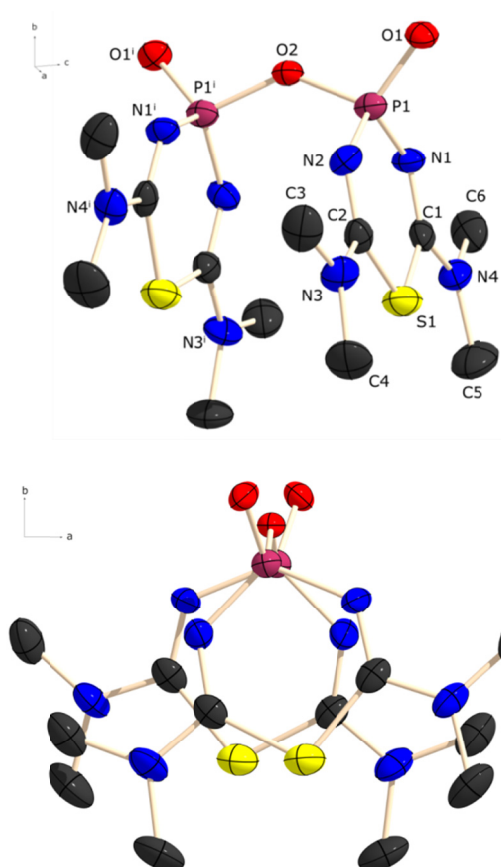


Figure 4. Molecular structure of **1** (two different viewing directions). Thermal ellipsoids are set at 50% probability level. Hydrogen atoms are omitted for clarity. Symmetry operation: $i = 1-x, y, 0.5-z$. Selected atom distances [Å] and bond angles [°]: P1–O1 1.496(2), P1–O2 1.607(2), P1–N1/P1–N2 1.626(3)/1.617(3), N1–C1/N2–C2 1.273(4)/1.295(4), S1–C1/S1–C2 1.786(3)/1.774(3), C1–N4/C2–N3 1.348(4)/1.342(4);

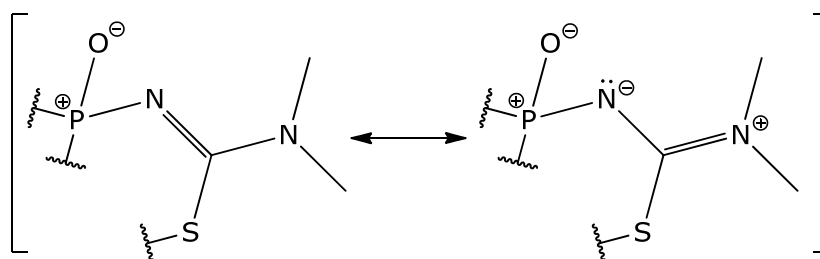
O1–P1–O2 108.0(2), P1–O2–P1*i* 134.2(2), O1–P1–N1 123.9(2), O1–P1–N2 113.6(2), O2–P1–N1 105.2(2), O2–P1–N2 104.5(2).

The terminal N–C entities of two dimethyl cyanamide molecules are connected by a phosphorus atom at the nitrogen end and by a sulfur atom at the carbon end of the former CN group, forming a 1,3,5,4-thiadiazaphosphinine ring. In contrast to the thiadiazaphosphinine ring in **5**, which adopts a distorted boat conformation^[6], the phosphinine ring in **1** deviates only slightly from planarity with values of the torsion angles within the ring between $-3.9(4)$ and $1.1(5)^\circ$. A comparison of atom distances and bond angles of the thiadiazaphosphinine ring in **1** and **5** is presented in Table 2.

Table 2. Comparison of atom distances (Å) and bond angles (°) within the thiadiazaphosphinine ring in compounds **1** and **5**^[6] and standard values compiled by Allen^[7].

	1	5	Ref. ^[7]
P–N	1.626(3)/1.617(3)	1.648(6)/1.664(4)	1.652(24)
N–C	1.273(4)/1.295(4)	1.289(6)/1.290(6)	1.279(8)
C–NMe ₂	1.348(4)/1.342(4)	1.365(6)/1.335(6)	1.419(17)
C–S	1.786(3)/1.774(3)	1.788(5)/1.771(5)	1.712(13)
N–P–N	111.7(2)	108.2(2)	
P–N–C	125.6(3)/126.4(3)	122.6(4)/121.0(4)	
N–C–S	126.8(3)/127.1(3)	125.4(5)/127.3(4)	
C–S–C	102.2(2)	101.0(2)	

What attracts attention is that the bond lengths found in **1** and **5** are all in about the same range. The P–N bond distances in **1** are in the range, expected for P–N single bonds and are slightly shorter compared to those in **5**. The C–S bond lengths in both compounds are practically equal. The endocyclic C–N bond lengths within the ring of **1** and **5** correspond to double bonds. The exocyclic C–N distances to the dimethylamino groups are clearly shortened compared to C–N single bonds. Together with the coplanarity of the methyl groups this indicates a delocalization of the nitrogen lone pair as shown in Scheme 2.

**Scheme 2.** Mesomerism in the 1,3,5,4-thiadiazaphosphinine rings of **1**.

For a discussion of the structural parameters of the diphosphate moiety the closely related pyrophosphate derivative **7**^[8] and the diphosphoric tetraamides **8**^[9-11], **9**^[12] (Figure 5) can be consulted for comparative reasons. In the bridging O–P–O–P–O entity the bond length between phosphorus and the terminal oxygen atoms (1.496(2) Å) are shorter as compared to the P–O distance to the bridging oxygen atom (1.607(2) Å) as was to be expected. Both values are in good accordance with those of 1.444–1.497 Å and 1.591–1.627 Å, respectively, reported for compounds **7–9**.^[8-12] The P–O–P angle

(134.2(2)°) is smaller compared to that observed in **7**, probably as consequence of the bulkier substituents of the latter. The value of **1**, however, fits well to those found in the tetraamides **8** and **9** (125.1–133.8°).^[9–12]

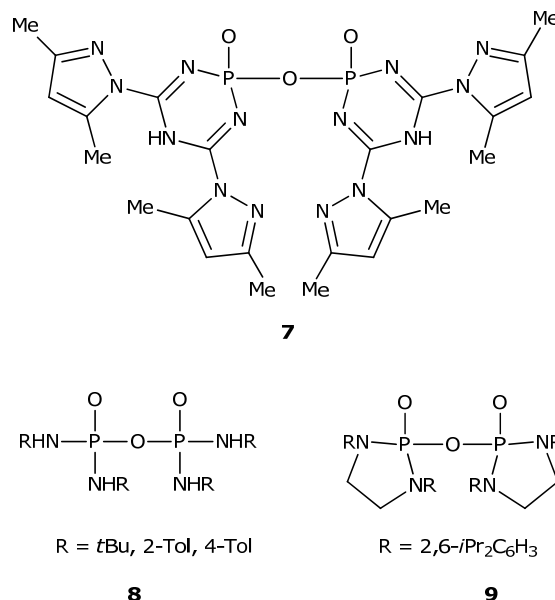


Figure 5. Structurally characterized diphenylphosphoric tetraamides.^[8–12]

The three dimensional build-up of the structure is affected by several intra- and intermolecular interactions. An overview can be found in Table 3.

Table 3. Intra- and intermolecular interaction in **1** (van der Waals radii [Å]: H: 1.20; C: 1.70; N: 1.55; O: 1.52).^[9]

D–H⋯A	d(D–H) (Å)	d(H⋯A) (Å)	d(D⋯A) (Å)	∠ D–H⋯A (°)
C3–H3A⋯N3	0.98(1)	2.37(1)	2.717(5)	99.8(3)
C6–H6A⋯N2	0.98(1)	2.47(1)	2.715(5)	93.7(3)
C3–H3C⋯N5i	0.98(1)	2.58(1)	3.492(6)	155.0(3)
C3ii–H3B ii ⋯O1	0.98(1)	2.31(1)	3.260(5)	164.6(3)

Symmetry operations: i = 1–x, y, 0.5–z, ii = 1.5–x, 0.5–y, z.

One would expect the two thiadiazaphosphinine rings in **1** to be oriented *trans* to each other as they are rather bulky. However a *cis* orientation of the two phosphinine rings is observed. A similar arrangement in the solid state is found for the triazaphosphinine rings in **7**.^[8] The observed orientation is most probably caused by three different electrostatic interactions in the molecular unit (Figure 6).

Hydrogen bonds between H3A and N3, as well as between H6A and N2 are observed within one asymmetric unit. The donor acceptor distances are with 2.717(5) and 2.715(5) Å well below the sum of the van der Waals radii of carbon and nitrogen (3.25 Å). These are rather strong interactions and have therefore a great influence on the structure, prohibiting rotation of the methyl groups. This allows the heterocycles to move closer together. The interaction between H3C and N5 connects both rings with a D...A distance of 3.492(6) Å. This electrostatic interaction is rather weak but nevertheless results in the rings being kept together.

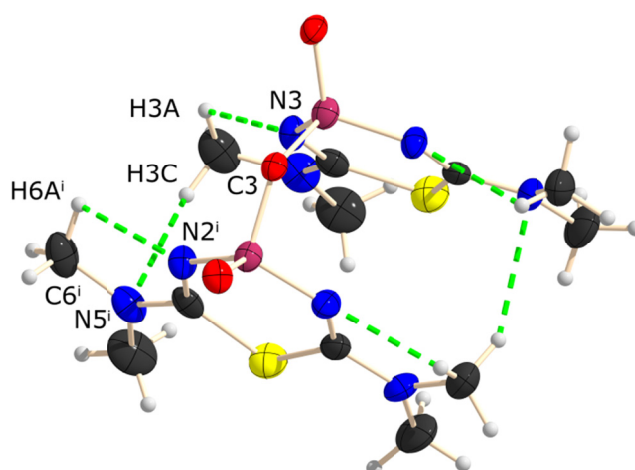


Figure 5. C-H...N interactions in **1**.

In the crystal of **1** one molecule is connected to four others *via* C3-H3B...O1 interactions (Figure 7). The contact of the carbon to the acceptor oxygen atom has a D...A distance of 3.260(5) Å and the D-H...A angle of 164.6(3)°.

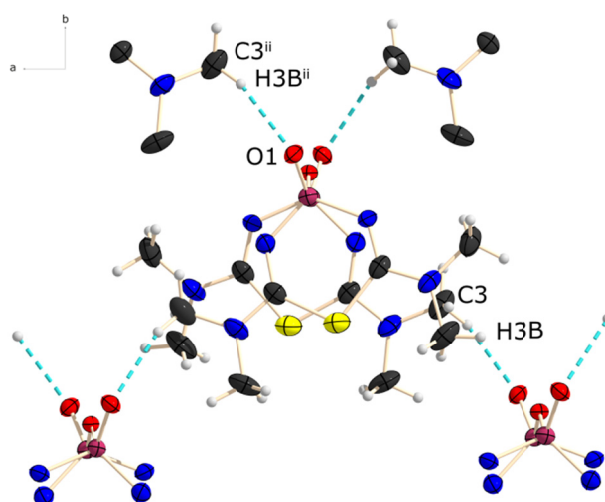


Figure 6. C-H...O interactions, connecting the molecules in **1**.

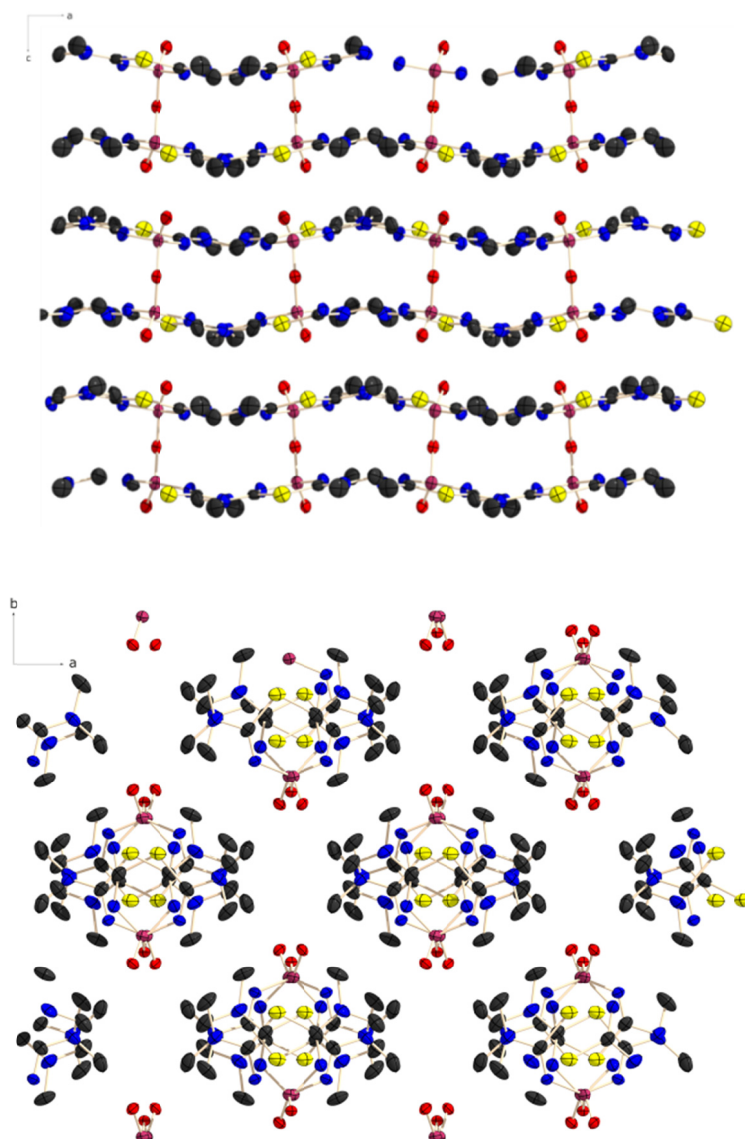
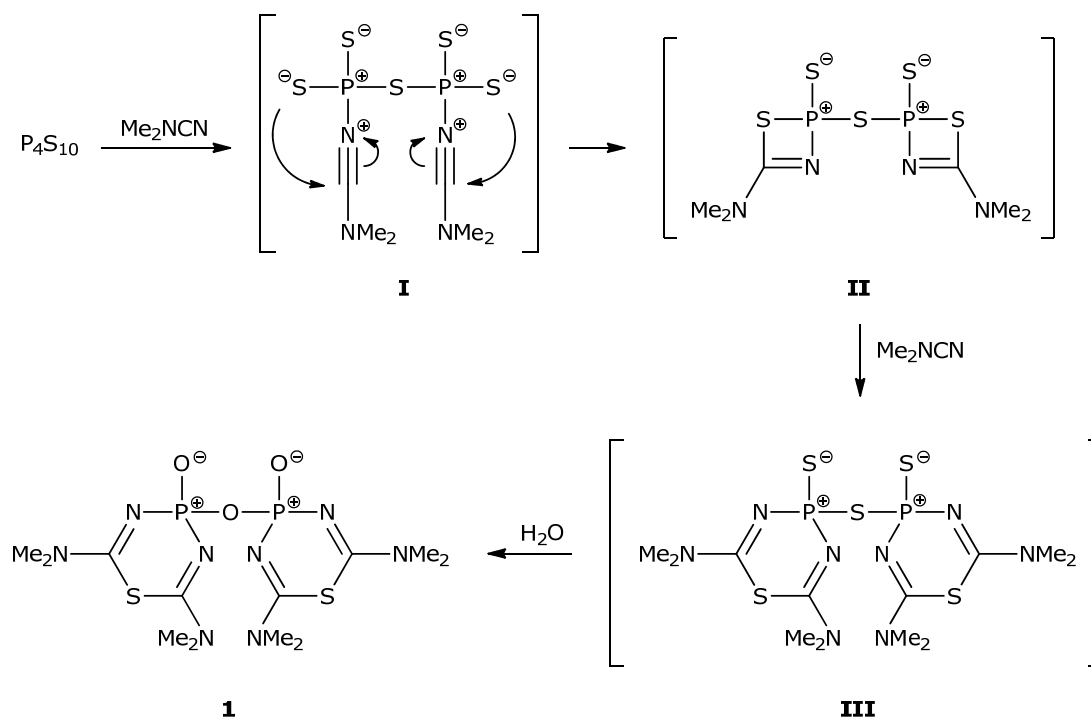


Figure 7. Layers parallel to the *ab* plane and chains along the *c* axis in **1**.

Possible Mechanism of Formation

Regarding the formation mechanism of compound **1**, we can only speculate (Scheme 3). Obviously traces of water are responsible for the presence of the oxygen atoms.

The compound may have formed from the reactive species (**I**). This species is analogous to the bis(pyridine) adduct of P_2S_5 ^[14], which is known to be stable and isolatable. In contrast **I** contains a reactive $-C\equiv N$ bond, which undergoes cyclization with one of the terminal sulfur atoms, yielding the intermediate **II**.

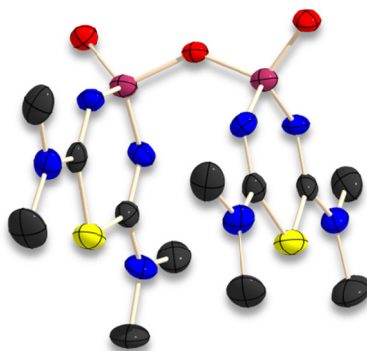


Scheme 3. Proposed mechanism for the formation of **1**.

A similar intermediate has been considered for the formation of the thiadiazaphosphinine ring in **5**.^[6] This species reacts further with more dimethyl cyanamide, which is formally inserted into the P–S bond of the four-membered ring in **II** yielding **III**. In the presence of water, **III** is converted to the isolated product **1**.

Conclusion

Herein the new pyrophosphate derivative 4,4'-oxybis(2,6-bis(dimethylamino)-4H-1,3,5,4-thiadiazaphosphinine 4-oxide) (**1**) is presented. Its unexpected formation in the course of the reaction of P_4S_{10} and dimethyl cyanamide shows the variable reactivity of P_4S_{10} depending on the nitrogen base employed. Compound **1** is the second representative with a 1,3,5,4-thiadiazaphosphinine ring, which could be characterized using single crystal X-ray diffraction.



The presence of a planar thiadiazaphosphinine ring in **1**, in contrast to the boat conformation in **5**, points to a structurally flexible ring system. The conformation of **1** is mainly influenced by electrostatic C–H \cdots N and C–H \cdots O interactions. These intra- and intermolecular hydrogen bonds lead to a layered arrangement in the crystal.

Experimental Section

General: Dimethyl cyanamide was obtained from Sigma-Aldrich Inc. and used as supplied without further purification. P₄S₁₀ was commercially obtained (Riedel-de H  en) and was purified by extraction with CS₂ before use. ³¹P NMR spectra were recorded using a Jeol EX 400 Eclipse instrument operating at 161.997 MHz. Chemical shifts are referred to 85% H₃PO₄ as external standard. All spectra were measured, if not mentioned otherwise, at 25   C. The % data correspond to the intensities in the ³¹P NMR spectra with respect to the total intensity. The difference to 100% belongs to not determinable signals.

X-ray Crystallography: An Oxford XCalibur3 diffractometer equipped with a CCD area detector was employed for data collection using Mo-K   radiation (λ = 0.71073   ). The structures were solved using direct methods (SIR2004)^[15] and refined by full-matrix least-squares on F² (SHELXL-97)^[16]. All non-hydrogen atoms were refined anisotropically. The hydrogen atoms were located in difference Fourier maps and placed with a C–H distance of 0.98    for C–H bonds. Intra- and intermolecular contacts were analyzed with DIAMOND (version 3.2i), thermal ellipsoids are drawn at the 50% probability level. Selected crystallographic data and refinement details for the structure determination of compound **1** are summarized in Table 4. CCDC 966235 contains the supplementary crystallographic data for compound **1**. These data can be obtained free of charge from The Cambridge Crystallographic Data Centre via www.ccdc.cam.ac.uk/data_request/cif.

Table 3. Crystallographic and refinement data for **1**.

1			
formula	C ₁₂ H ₂₄ N ₈ O ₃ P ₂ S ₂	$\rho_{\text{calc}}[\text{g}/\text{cm}^{-3}]$	1.497
M [g/mol]	454.45	$\mu [\text{mm}^{-1}]$	0.454
crystal system	orthorhombic	$F(000)$	952
space group	<i>Pbcn</i>	θ range [°]	4.17–26.00
color/Habit	colourless block	T [K]	173(2)
crystal size	0.2x0.25x0.020	data collected	9762
a [Å]	11.4631(8)	data unique	1978
b [Å]	12.4813(8)	data observed	903
c [Å]	14.0977(11)	R (int)	0.0920
α [°]	90	GOOF	0.725
β [°]	90	R_1, wR_2 ($I > 2\sigma I_0$)	0.0833, 0.0765
γ [°]	90	R_1, wR_2 (all data)	0.1041, 0.0415
V [Å ³]	2017.0(2)	larg. diff peak/hole	
Z	4	($e/\text{Å}$)	0.333/−0.260

Reaction of P₄S₁₀ with Benzonitrile and Propionitrile

P₄S₁₀ (0.25 mmol, 111 mg) in 1.5 mL of benzonitrile was heated to 120 °C for 3 h, when a dark yellow solution was obtained. The ³¹P NMR spectrum of the reaction solution showed the signals of an A₂X₂ spin system as main product (86%): $\delta_A = 68.9$, $\delta_X = 33.9$, $J_{AX} = 21.5$ Hz.

Similarly P₄S₁₀ (0.27 mmol, 121 mg) in propionitrile (1.5 mL) was heated to 100 °C for 4 h. After cooling to ambient temperature the remaining P₄S₁₀ was separated by filtration. The ³¹P NMR spectrum of the dark yellow filtrate showed a series of signals in the range of $\delta = 155$ –20 ppm and with a relative intensity of 38% the signals of an A₂X₂ spin system: $\delta_A = 70.2$, $\delta_X = 34.4$, $J_{AX} = 21.5$ Hz.

P₄S₁₀ (0.37 mmol, 168 mg) was refluxed for 3 h in dimethylcyanamide (1.5 mL, 1300.5 mg) yielding a brown solution. Colourless block shaped crystals of **1** were obtained in the NMR tube.

Reaction of P₄S₁₀ With Dimethyl Cyanamide

P₄S₁₀ (0.37 mmol, 168 mg) was refluxed for 3 h of dimethyl cyanamide (1.5 mL) yielding a dark yellow solution. The ³¹P NMR spectrum of the reaction solution indicated the presence of a complex mixture of products and displayed main signals at δ = 64.8, 61.1, 18.2, 16.9 and 11.6 ppm. After 7 d a small amount of colourless block shaped crystals of **1** were obtained from the solution.

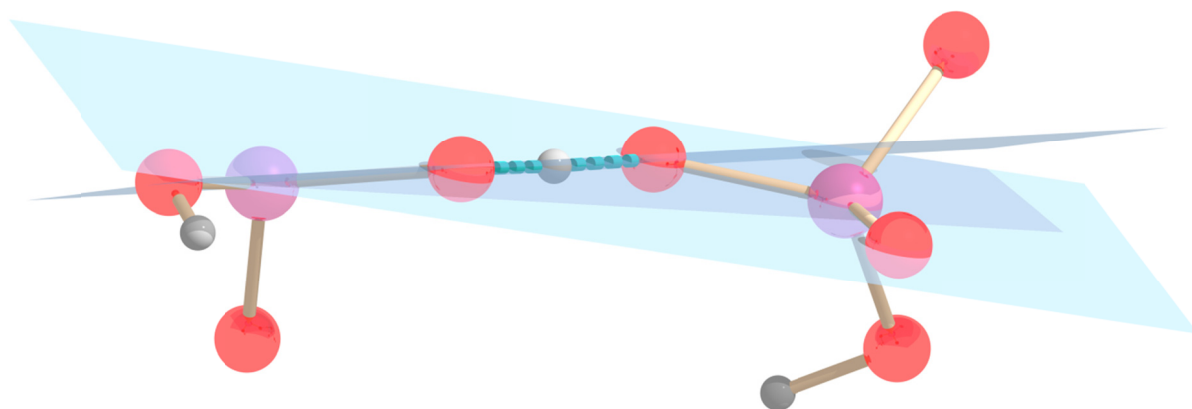
Acknowledgement

Financial support by the Department of Chemistry, Ludwig Maximilian University, is gratefully acknowledged. We thank Prof. T. M. Klapötke, Department of Chemistry, Ludwig Maximilian University, for the generous allocation of diffractometer time and for his continuous support.

-
- [1] H. W. Roesky, F. N. Tebbe, E. L. Muetterties, *Inorg. Chem.* **1970**, 9, 831-836.
 - [2] P. J. Retuert, F. Martinez, F. Horn, *Chem.-Ztg.* **1978**, 102, 68.
 - [3] J. Neels, B. Ziemer, M. Meisel, P. Z. Leibnitz, *Anorg. Allg. Chem.* **1986**, 542, 123-130.
 - [4] E. R. Andrew, W. Vennart, G. Bonnard, R. M. Croiset, M. Demarcq, E. Mathieu, *Chem. Phys. Lett.* **1976**, 43, 317-320.
 - [5] M. Meisel, H. Grunze, *Z. Anorg. Allg. Chem.* **1970**, 373, 265-278.
 - [6] M. St J. Foreman, A. M. Z. Slawin, J. D. Woollins, *J. Chem. Soc., Chem. Commun.* **1997**, 1269-1270; b) M. St J. Foreman, R. J. Mortimer, A. M. Z. Slawin, J. D. Woollins, *J. Chem. Soc., Dalton Trans.* **1999**, 3419-3430.
 - [7] F. H. Allen, O. Kennard, D. G. Watson, L. Brammer, A. G. Orpen, R. Taylor, *J. Chem. Soc., Perkin Trans. 2* **1987**, S1-S19.
 - [8] V. Chandrasekhar, V. Krishnan, R. Azhakar, T. Senapati, A. Dey, R. S. Narayanan, *Inorg. Chem.* **2011**, 50, 2568-2579.
 - [9] M. Pourayoubi, A. Tarahhomi, F. K. Ahmadabad, K. Fejfarova, A. van der Lee, M. Dusek, *Acta Crystallogr., Sect. C* **2012**, C68, o164-o169.
 - [10] M. Pourayoubi, Z. Padelkova, M. R. Chaijan, A. Ruzicka *Acta Crystallogr., Sect. E: Struct. Rep. Online* **2011**, E67, o450-o451.
 - [11] M. Pourayoubi, H. Fadaei, A. Tarahhomi, M. Parvez, *Z. Kristallogr.* **2012**, 227, 205-206.
 - [12] N. A. Giffin, A. D. Hendsbee, T. L. Roemmele, M. D. Lumsden, C. C. Pye, J. D. Masuda, *Inorg. Chem.* **2012**, 51, 11837-11850.
 - [13] A. Bondi, *J. Phys. Chem.* **1966**, 70, 3006-3007.

- [14] S. Schönberger, C. Jagdhuber, L. Ascherl, C. Evangelisti, T. M. Klapötke, K. Karaghiosoff, Z. *Anorg. Allg. Chem.* **2013**, DOI: 10.1002/zaac.201300419.
- [15] M. C. Burla, R. Caliendo, M. Camalli, B. Carrozzini, G. L. Cascarano, L. De Caro, C. Giacovazzo, G. Polidori, R. Spagna, *J. Appl. Cryst.* **2005**, 38, 381-388.
- [16] a) G. M. Sheldrick, *SHELXL-97: Program for the Refinement of Crystal Structures*, University of Göttingen, Göttingen (Germany), **1997**; b) G. M. Sheldrick, *Acta Crystallogr., Section A* **2008**, A64, 112-122.

Very Strong Hydrogen Bonds in a Mixed Oxophosphate



Strong and weak hydrogen bonds are essential in determining the structure of open frameworks. Herein it is reported on the crystal structure of the pyridinium salt of an oxophosphate. Its anionic part consists of three different anions, connected by very strong hydrogen bonds. Further weak hydrogen bonds and electrostatic interactions lead to the formation of a vast and very complex build-up in the crystal.

Introduction

It was Linus Pauling, who defined hydrogen bonds as one of the first chemists in 1940. In his book *The nature of chemical bonds and the structure of molecules and crystals*^[1] he stated that *under certain conditions an atom of hydrogen is attracted by rather strong forces to two atoms, instead of only one, so that it may be considered to be acting as a bond between them. This is called the hydrogen bond*. Further he writes that *it is formed only between the most electronegative atoms*. Hereby the hydrogen is covalently bonded to a donor atom (D) and interacts in a mostly electrostatic way with an acceptor (A), which possesses at least one pair of free electrons. D and A are mostly oxygen, nitrogen, fluorine and in some cases also chlorine. In the recent time it has also been reported on sulfur acting as the acceptor and thus forming O–H...S^[2] and N–H...S^[3] hydrogen bonds but in this case the rather dispersive nature of the H...S interaction has to be taken into consideration. C–H groups are also discussed as possible H-donors. Here mainly IR spectroscopical evidence and theoretical studies are offered.^[4]

In the book *The hydrogen bond* by Pimentel and McClellan^[5], the basic concept and additionally the properties of this bonding type are summarized. Especially intermolecular H-bonds lead to great changes in the properties of compounds, such as increase in viscosity, thermal, acoustic and electrical conductivity, dielectric properties and the dipole moment. Furthermore they lead to a higher melting and boiling point, which in present times is rather important in the field of material science as phase transition is to be prevented in a certain temperature range.^[6] Also the surface tension can be increased by the formation of these interactions.

From the early 1960s also the interest in compounds containing very strong hydrogen bonds is ever growing.^[7] Since then this type of bonding has been reviewed several times. Compounds forming strong H-bonds do not necessarily have to be anions but can also be neutral or cationic.^[3]

But what is the difference between weak and strong hydrogen bonds? In the first mentioned the interaction between the hydrogen and the acceptor is predominantly electrostatic, while in the latter the proton cannot clearly be assigned to either of the heteroatoms. In the following this system is noted X–H–Y^[3] and can be explained as a three-centre-four electron bond, the proton being partially covalently linked to both, the X and the Y. Rough criteria for a distinction of weak and strong H-bonds are that $d(D\cdots A)$ should be slightly smaller than the sum of the van der Waals radii of D and A

and the hydrogen atom is located nearer to the donor atom. In strong bonds, on the other hand, $d(X\cdots Y)$ is at least 0.3 Å shorter than the sum of the van der Waals radii of X and Y and the proton should be rather centred between both heteroatoms.¹ Thus the distance of $O\cdots O$ should be slightly smaller than 3.04 Å for a weak and less than 2.74 Å for a strong hydrogen bond. In the case of $N\cdots O$ the values are 3.07 Å and 2.77 Å respectively.^[3] Theoretical studies by *Grabowski* on that topic declare the ranges to be 2.4–2.55 Å for $O\cdots O$ and 2.5–2.6 Å for $N\cdots O$.^[4a]

This shows how fluctuating the specification of this kind of hydrogen bond is and that there are indeed no distinct rules or borderlines for a precise definition.

Desiraju states that it is a mixture of four different forces, which is responsible for the formation of very strong hydrogen bonds. These forces are electrostatic, concerning the acid-base interaction, polarization, meaning how hard or soft X and Y are, van der Waals (dispersion and repulsion) and also the covalent force, leading to charge transfer.^[9]

Keeping all the above in mind, in the following a pyridinium salt of a mixed oxophosphate shall be discussed in terms of weak and strong hydrogen bonds. The impact on the structural build-up of such compounds in the solid state is enlightened.

¹ Van der Waals radii [Å] important in this work: H: 1.20; C: 1.70; N: 1.55; O: 1.52; S: 1.80.[8] A. Bondi, *Journal of Physical Chemistry* **1966**, 70, 3006-3007.

Results and Discussion

Molecular and Crystal Structure of $[\text{pyH}]_3[\text{H}(\text{HP}_2\text{O}_7)(\text{H}(\text{HPO}_4))]\cdot 0.5 \text{ py} \text{ (1)}$

Single crystals of compound **1** were obtained from the hydrolysis of $\text{py}_2\text{P}_2\text{S}_4\text{O}_{10}$. Compound **1** crystallizes in the monoclinic space group $P-1$ with two formula units in the unit cell. Figure 1 shows the molecular structure of the asymmetric unit and selected atom distances, as well as bond angles are listed.

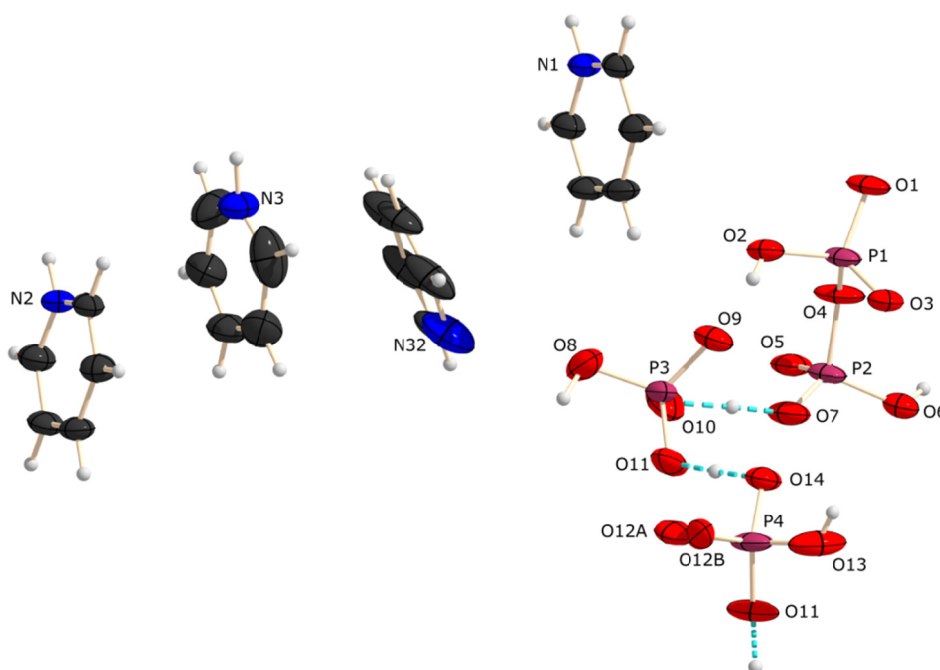


Figure 1. Molecular structure of **1**. Thermal ellipsoids are set at 50% probability. Selected atom distances [\AA] and bond angles [$^\circ$]: P1–O1 1.506(3), P1–O2 1.542(3), P1–O3 1.484(3), P1–O4 1.604(3), P2–O7 1.481(3), P2–O5 1.509(4), P2–O6 1.539(3), P2–O4 1.608(3), P3–O9 1.505(3), P3–O11 1.507(3), P3–O8 1.554(3), P3–O10 1.554(4), P4–O12A 1.45(3), P4–O15 1.522(3), P4–O14 1.553(3), P4–O13 1.552(4), P4–O12B 1.59(3);

O3–P1–O1 117.0(3), O3–P1–O2 112.8(2), O1–P1–O2 107.4(2), O3–P1–O4 109.4 (3), O1–P1–O4 103.7(2), O2–P1–O4 105.5(2), O9–P3–O11 113.3(2), O9–P3–O8 111.8(2), O11–P3–O8 109.8(2), O9–P3–O10 110.5(2), O11–P3–O10 109.5(3), O8–P3–O10 101.3(2), O7–P2–O5 116.5(2), O7–P2–O6 108.5(3), O5–P2–O6 111.5(2), O7–P2–O4 110.7(2), O5–P2–O4 103.3(2), O6–P2–O4 105.8(3), O12A–P4–O15 118.6(12), O12A–P4–O14 116.9(7), O15–P4–O14 110.2(2), O15–P4–O13 107.0(2), O14–P4–O13 105.3(3), O12A–P4–O12B 27.3(14), O15–P4–O12B 106.3(4), O14–P4–O12B 104.0(7), O13–P4–O12B 123.6(8).

Strong Hydrogen Bonding

The anionic part of this compound consists of one $\text{H}_2\text{P}_2\text{O}_7^{2-}$ and two HPO_4^{2-} entities. Each of these three is connected to two other anions by very strong hydrogen bonds (drawn in light blue). The dihydrogendiphosphate entity (A1) is connected to the monohydrogenphosphate one, containing P3 (A2), by the O7–H7–O10 interaction with X–H and H–Y distances of 1.15(1) and 1.37(1) Å respectively.

The O···O distance is rather short with a value of 2.523(6) Å and the bond is close to linearity with an angle of 178(1)°. A2 is connected to the monohydrogenphosphate anion, containing P4, (A3) *via* O11–H14–O14 interactions with X–H and H–Y distances of 1.24(1) and 1.25(8) Å and an angle of 178(7)°.

In Table 1 all intra- and intermolecular interactions found in **1** are listed.

Table 1. Intermolecular interaction in **1** (the sum of the van der Waals radii of hydrogen and sulfur atom mounts up to 3.00 Å, hydrogen and oxygen to 2.72 Å).

X–H–Y	d(X–H) (Å)	d(H–Y) (Å)	d(D···A) (Å)	∠ X–H–Y (°)
O7–H7···O10	1.15(1)	1.37(1)	2.523(6)	178(1)
O11–H14···O14	1.24(1)	1.25(8)	2.484(6)	178(7)
O15–H15···O15 ⁱ	1.23(1)	1.23(2)	2.468(5)	180(1)
D–H···A	d(D–H) (Å)	d(H···A) (Å)	d(D···A) (Å)	∠ D–H···A (°)
O6–H6···O1 ⁱⁱ	0.87(7)	1.60(7)	2.459(5)	173(6)
O13–H13···O5 ⁱⁱⁱ	0.89(1)	1.69(1)	2.558(5)	165(1)
O2–H2···O9	0.89(1)	1.62(1)	2.475(5)	163(1)
O8–H8···O12 [*]				
*O8–H8···O12A	1.03(1)	1.52(4)	2.47(5)	150(2)
O8–H8···O12B _b	1.03(1)	1.52(2)	2.47(2)	171(1)
N1 ^{iv} –H1 ^{iv} ···O3	0.96(6)	1.69(6)	2.611(5)	161(5)
N2 ^v –H4 ^v ···O5	0.97(6)	1.68(7)	2.637(6)	169(7)
N3 ^{vi} –H3 ^{vi} ···O12 ^{**}				
** N3–H3···O12B _b	1.03(6)	1.68(7)	2.68(2)	167(7)
N3–H3···O12A _a	1.03(6)	1.79(8)	2.67(2)	143(7)

Symmetry operations: i = $-x, -y+2, -z+1$; ii = $-x, -y+2, -z+1$; iii = $x, y+1, z$; iv = $-1+x, y, z$; v = $1-x, 1-y, 1-z$; vi = $-1+x, y, z$.

The dihydrogendiphosphate unit is connected to another inversion related diphosphate unit by an O6–H6···O1ⁱⁱ contact (dark blue lines in Figure 2). A short donor acceptor distance of 2.459(5) Å can be found, as well as an angle of 173(6)°, which is very close to linearity. This arrangement leads to the formation of ten-membered rings.

On the opposite side of this connection in each A1 an O2–H2···O9 (lilac line) interaction with A2 can be found. With a donor–acceptor distance of 2.475(5) Å and an angle of 163(1)° these connections lead to the formation of an eight-membered ring system, consisting of three phosphorus and five oxygen atoms.

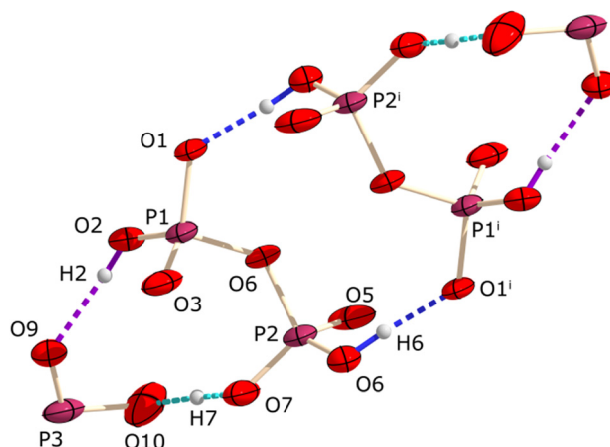


Figure 2. Hydrogen bonds between the diphosphate entities.

Every A2 unit is further bonded to two A3 anions (Figure 3). In addition to the already mentioned O11–H14–O14 bonds, O8–H8···O12 interactions (lilac line) connect every A2 to an A3 and *vice versa*. These contacts lead to twelve membered rings, built up by four alternating A2 and A3 units.

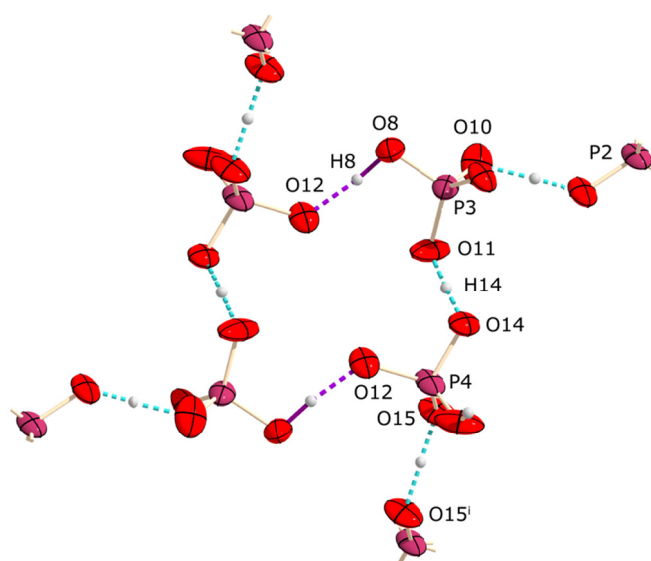


Figure 3. Interactions in the A2-A3 building block.

All the above mentioned interactions considered, the rings are arranged to form infinite chains parallel to each other (Figure 4). The three pyridinium counter ions are linked to the anionic chains by N–H···O contacts. The N···O distances are with 2.611(5) Å (N1···O3), 2.637(6) Å (N2···O5) and 2.666(6) Å (N3···O12) all in the same range. The N–H···O angles lie in the range between 157(7)° and 169(7)°.

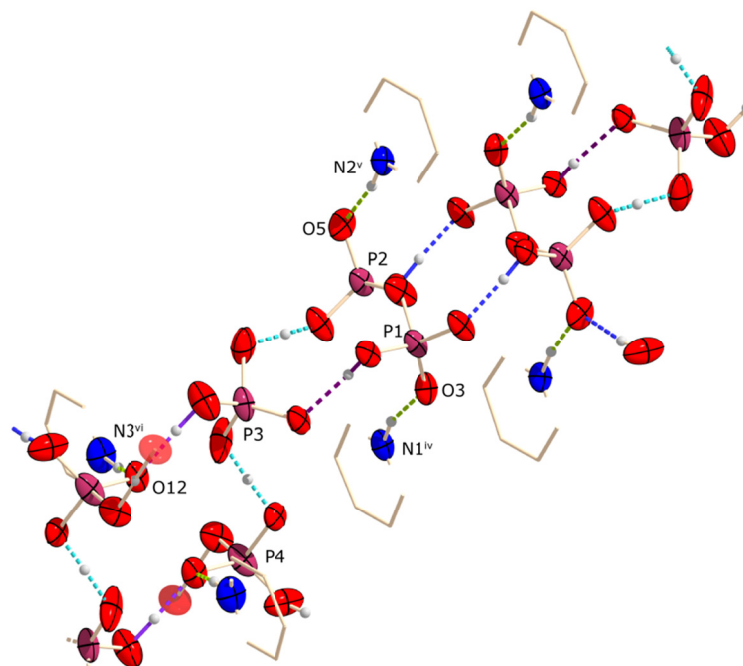


Figure 4. Chains with anion-cation interactions in **1**.

Each chain is linked to the two adjacent ones on each side by very strong O15–H15–O15ⁱ hydrogen bonds (Figure 5), with a X–H and H–Y distance of 1.23(1) Å and an overall X···Y contact of 2.468(5) Å. Also the linearity of O–H–O (angle of 180(1)°) points towards a very strong hydrogen bond.

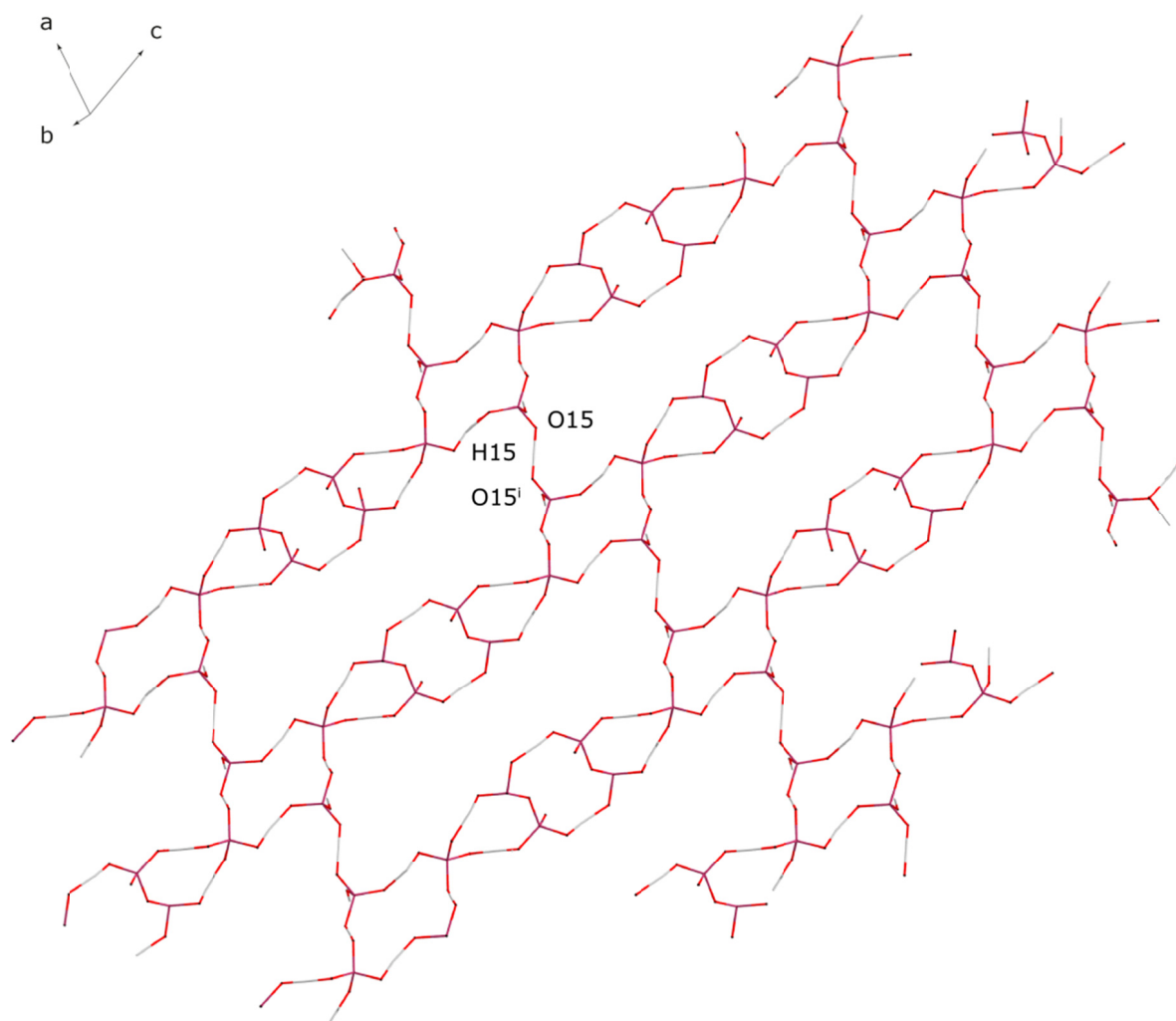


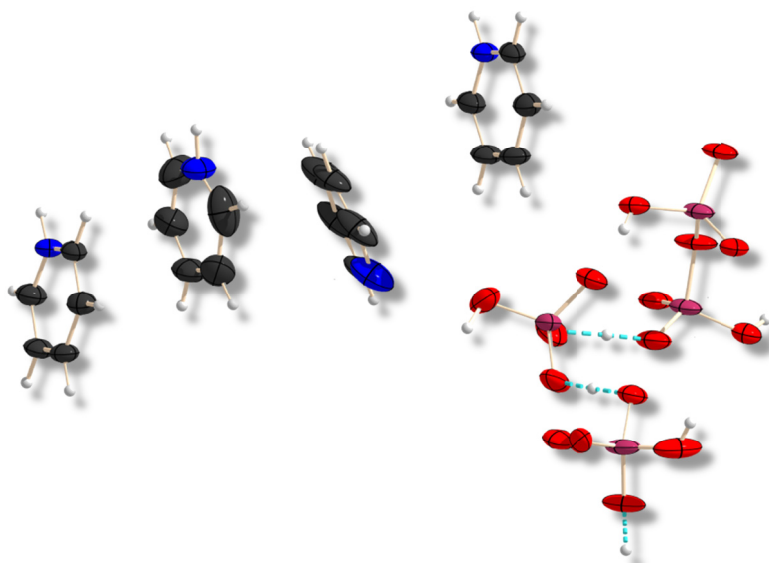
Figure 5. Layer in the crystal structure of **1**. Drawn in wires and sticks model, and pyridinium ions omitted for clarity.

Parallel layers formed this way are connected by $\text{O13-H13}\cdots\text{O5}^{\text{iii}}$ interactions. This connection shows the largest $\text{O}\cdots\text{O}$ distance with a value of $2.558(5)$ Å and an angle of $165(1)^\circ$.

Overall a three-dimensional anionic sub network is formed by three different building units A1–3, connected by weak and strong hydrogen bonds. The rings formed within this network, resolve in channels throughout the three dimensional build up.

Conclusion

The mixed pyridinium phosphate salt $[\text{pyH}]_3[\text{H}(\text{HP}_2\text{O}_7)(\text{H}(\text{HPO}_4))]\cdot 0.5 \text{ py}$ (**1**) was obtained in a small amount from the hydrolysis of the bis(pyridine) adduct of $\text{P}_2\text{S}_4\text{O}$ in pyridine. At first sight this new compound looks rather simple but it shows a complicated and at the same time exciting arrangement in the solid state.



The structure contains both, weak and strong hydrogen bonds and shows clearly how the interplay of these interactions results in a compact, vast and exciting build-up in the crystal. Strong hydrogen bonds are observed between the diphosphate and phosphate anions, as well as between the two phosphate ones, while the pyridinium cations are involved in weaker $\text{N-H}\cdots\text{O}$ bonds. The analysis of such structures contributes to a better understanding of the relation between hydrogen bonds and structure, which is crucial for the engineering of open framework materials.

Experimental Section

General: P_4S_{10} was commercially obtained (Riedel-de Haen) and was purified by extraction with CS_2 before use. Pyridine was used as obtained (Sigma Aldrich). **^{31}P NMR** Chemical shifts are referred to 85% H_3PO_4 as external standard. All spectra were measured, if not mentioned otherwise, at 25 °C. The %-data correspond to the intensities in the ^{31}P NMR spectra with respect to the total intensity. The difference to 100 % belongs to not determinable signals.

X-ray Crystallography. The single-crystal X-ray diffraction data were collected using an Oxford Xcalibur3 diffractometer equipped with a Spellman generator (voltage 50 kV, current 40 mA), Enhance molybdenum K α radiation source ($\lambda = 71.073$ pm), Oxford Cryosystems Cryostream cooling unit, four circle kappa platform and a Sapphire CCD detector. Data collection and reduction were performed with CrysAlisPro.^[10] The structures were solved with SIR97^[11], SIR2004^[12], refined with SHELXL-97^[13], and checked with PLATON^[14], all integrated into the WinGX software suite^[15]. The finalized CIF files were checked with checkCIF.^[16] All non-hydrogen atoms were refined anisotropically. The hydrogen atoms were located in difference Fourier maps and placed with a C–H distance of 0.98 Å for C–H bonds. Intra- and intermolecular contacts were analyzed with DIAMOND (version 3.2i), thermal ellipsoids are drawn at the 50% probability level. Selected crystallographic data and refinement details for the structure determination of compound **1** are summarized in Table 3.

Table 3. Crystallographic and refinement data of **1**.

1			
Formula	C _{17.5} H ₂₇ N _{3.5} P ₄ O ₁₅	$\rho_{\text{calc}}[\text{g}/\text{cm}^{-3}]$	1.609
M [g/mol]	650.31	$\mu [\text{mm}^{-1}]$	0.360
Crystal system	triclinic	$F(000)$	673
Space group	$P-1$	θ range [°]	4.21–25.35
Colour/Habit	colourless block	T [K]	173(2)
Crystal size	0.20x0.25x0.15	data collected	18232
a [Å]	9.086(5)	data unique	4860
b [Å]	10.401(5)	data observed	3781
c [Å]	15.183(5)	R_{int}	0.0452
α [°]	98.746(5)	GOOF	1.033
β [°]	102.519(5)	R_1, wR_2 ($I > 2\sigma I$)	0.0659, 0.1525
γ [°]	101.753(5)	R_1, wR_2 (all data)	0.0858, 0.1714
V [Å ³]	1342.2(11)	larg. diff peak/hole	
Z	2	(e/Å)	0.962/–0.723

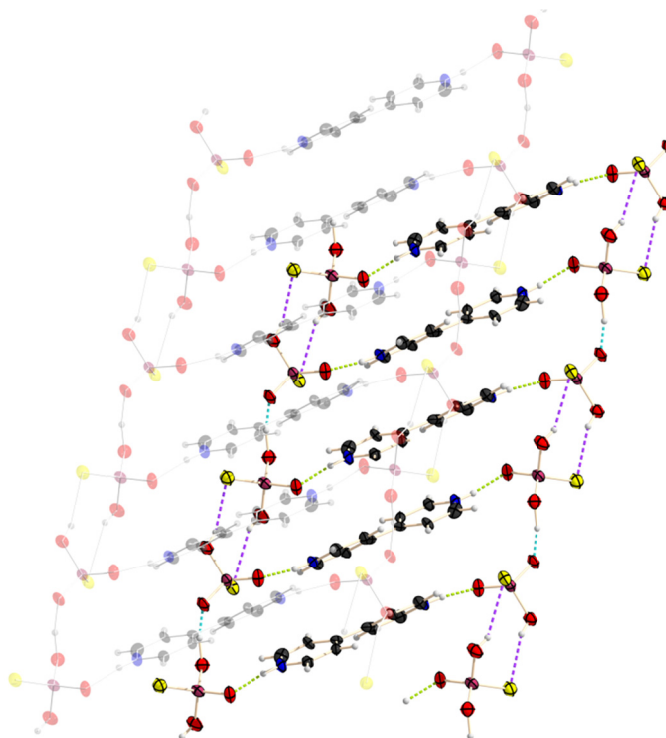
Synthesis of 1: py₂P₂S₄O (2 mmol, 728.8 mg) (Part IV) was suspended in pyridine (30 mL) and water (2 mL) were added. After refluxing the suspension for 2 h the yellow precipitate was removed. After 9 d colourless block shaped crystals of **1** could

be obtained from the orange solution. A yield could not be determined, as only a few crystals were obtained.

³¹P NMR (pyridine, rt): δ [ppm] = 41.9 (s, 58.4%), 1.7 (s, 41.6%).

-
- [1] L. C. Pauling, *The Nature of the Chemical Bond and the Structure of Molecules and Crystals. An Introduction to Modern Structural Chemistry*. 3rd ed, **1960**.
 - [2] H. S. Biswal, P. R. Shirhatti, S. Wategaonkar, *J. Phys. Chem. A* **2010**, *114*, 6944-6955.
 - [3] J. Emsley, *Chem. Soc. Rev.* **1980**, *9*, 91-124.
 - [4] a) S. J. Grabowski, *Annu. Rep. Prog. Chem., Sect. C* **2006**, *102*, 131-165; b) Ammer, C. Nolte, K. Karaghiosoff, S. Thallmair, P. Mayer, R. de Vivie-Riedle, H. Mayr, *Chem. Eur. J.* **2013**, *19*, 14612-14630.
 - [5] G. C. Pimentel, A. L. McClellan, *Annu. Rev. Phys. Chem.* **1971**, *22*, 347-385.
 - [6] S. Dhanuskodi, S. Manivannan, K. Kirschbaum, J. Philip, S. Selladurai, *J. Cryst. Growth* **2006**, *290*, 548-553.
 - [7] D. G. Tuck, *Progr. Inorg. Chem.* **1968**, *9*, 161-194.
 - [8] A. Bondi, *J. Phys. Chem.* **1966**, *70*, 3006-3007.
 - [9] G. R. Desiraju, *Acc. Chem. Res.* **2002**, *35*, 565-573.
 - [10] *CrysAlisPro 1.171.36.21*, Agilent Technologies, **2012**.
 - [11] A. Altomare, G. Cascarano, C. Giacovazzo, A. Guagliardi, A. A. G. Moliterni, M. C. Burla, G. Poidori, M. Camalli, R. Spagne, **1997**, 343.
 - [12] a) M. C. Burla, R. Caliendo, M. Camalli, B. Carrozzini, G. L. Cascarano, L. De Caro, C. Giacovazzo, G. Polidori, R. Spagna, Institute of Crystallography, Bari (Italy), **2004**; b) M. C. Burla, R. Caliendo, M. Camalli, B. Carrozzini, G. L. Cascarano, L. De Caro, C. Giacovazzo, G. Polidori, R. Spagna, *Journal of Applied Crystallography* **2005**, *38*, 381-388.
 - [13] a) G. M. Sheldrick, *SHELXL-97, Program for the Refinement of Crystal Structures*. University of Göttingen, Göttingen (Germany), **1997**; b) G. M. Sheldrick, *Acta Crystallographica, Section A: Foundations of Crystallography* **2008**, *A64*, 112-122.
 - [14] A. L. Spek, *Platon, A Multipurpose Crystallographic Tool*, Utrecht University, Utrecht, The Netherlands, **2012**.
 - [15] L. J. Farrugia, *J. Appl. Crystallogr.* **1999**, *32*, 837-838.
 - [16] <http://journals.iucr.org/services/cif/checkcif.html>

On the Structural Chemistry of the $\text{H}_2\text{PO}_3\text{S}^-$ Anion



*The great difference in the tendency to form hydrogen bonds between oxygen and its heavier homologue sulfur can be used to control dimensionality in hydrogen bonded networks. On the basis of the investigation of the two crystal structures of $(\text{pyH})(\text{H}_2\text{PO}_3\text{S})$ (**1**) and $(4,4'\text{-bipyH})(4,4'\text{-bipyH}_2)\text{H}(\text{HPO}_3\text{S})_2$ (**2**) it is shown, that the partial substitution by sulfur in phosphate anions has a great influence on the build-up in the crystal. Especially in salts containing a phosphate anion and an organic cation like pyridine or bipyridine, this is of great importance regarding their use as intermediates for the formation of open framework materials.*

Introduction

Regarding phosphates many salts are known up to now and have been fully characterized. But in many scientific fields like biochemistry a partial substitution of oxygen by sulfur is favourable. For example nucleotides with monothiophosphates result in chiral entities which is highly welcomed in stoichiometric investigations of nucleotide-enzyme interactions and also for slowing down the reaction rate.^[1]

Only a few salts containing the inorganic H_2PO_4^- and an organic cation have been described so far, but over the past decades their use in organic inorganic hybrid open frameworks has become ever more important. These compounds have been proven to have remarkable properties, depending on their structural build up.

Especially the use of amines as counter ions is in the focus of investigations, due to their structure directing abilities and their density of charge has a main impact on the dimension of the network.^[2] Compounds consisting of an amine as polarizable organic cation and an inorganic anion, which can form strong hydrogen bonds, are widely used as intermediates to metal containing open frameworks, as they show high solubility.^[3] Examples are 4-dimethylaminopyridinium (Figure 1)^[4], piperidinium^[5] and piperazinium^[3] dihydrogenphosphate.

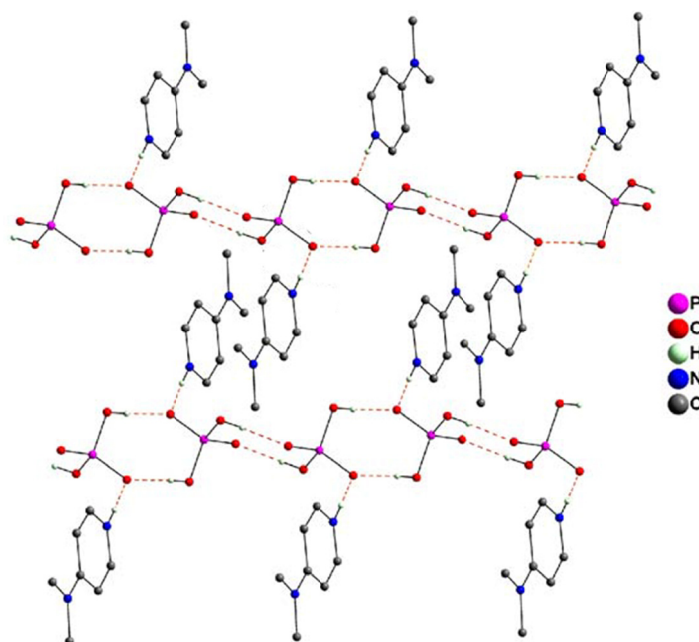


Figure 1. Structure of 4-dimethylaminopyridine dihydrogenphosphate, synthesised by Dhanuskodi *et al.*.

These compounds have the additional advantage of showing no phase transition over a broad temperature range.^[4] The diversity of potential topologies is enormous, as they can be designed based on the nature and number of intra- and intermolecular interactions. The organic cation can act as a hydrogen donor and therefore also influence the structure. It further stabilizes the whole entity and an additional advantage is the lowering of thermal conductivity. Therefore this material is claimed to be a third order non-linear optics, amongst many more possible applications.^[4, 6]

Consequently, the intra- and intermolecular interactions are the fundamental condition for the chemical and physical properties of these salts. Another very important structure directing factor is the π - π interaction, which is an attractive, non-covalent force between two aromatic ring systems. Today this kind of assembly is used in many applications such as stabilizing protein and DNA structures, influencing molecular recognition, self-assembly, host guest systems or the design of organic electronics and many more.^[7]

Masse and Tordjman were able to synthesise the pyridinium dihydrogenphosphate phosphoric acid.^[8] Their aim was to produce a layered structure with the pyridinium ions anchored inside the anionic framework, but claimed that this was not possible, as pyridinium is a single hydrogen donor. They never took into consideration that the substitution of oxygen with sulfur would make the difference. In the following the $\text{H}_2\text{PO}_3\text{S}^-$ anion is discussed and it is shown, that the substitution induces indeed a layered structure. This anion has first been described as its sodium salt in 1847.^[9]

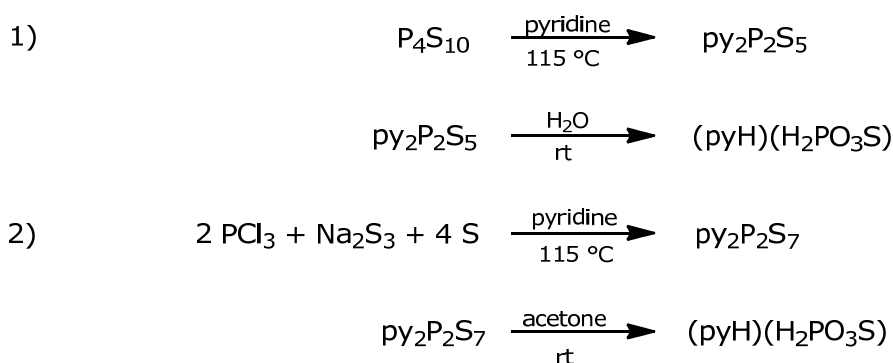
Zierner and Rabis were the first to describe a salt containing this anion and an organic cation, namely the pyridinium ion.^[10] Their work however only includes the synthesis and a brief overview of the basic information on crystal refinement data, but lacks a proper discussion of the structure, especially the role of interactions and the arrangement in the crystal. In the following this void will be filled and the intra- and intermolecular interactions and their impact on the crystal structure of $(\text{C}_5\text{H}_5\text{N})(\text{H}_2\text{PO}_3\text{S})$ are discussed extensively.

Also a new salt is presented. It consists of two $\text{HPO}_3\text{S}^{2-}$ fragments connected by a very strong hydrogen bond^[11], yielding a $\text{H}(\text{HPO}_3\text{S})^{3-}$ entity. The organic counter ions are one single and one twofold protonated 4,4'-bipyridine molecule. This compound shows an even more remarkable build up, as a vast and very complex network is formed.

Results and Discussion

Molecular and Crystal Structure of (pyH)(H₂PO₃S) (**1**)

Compound **1** could be obtained from two different reactions. In reaction 1) P₄S₁₀ is refluxed in pyridine, leading to the formation of the bis(pyridine) stabilized P₂S₅ which is then stirred in water. Reaction 2) proceeds with py₂P₂S₇ as intermediate which has to be suspended and stirred in acetone at room temperature.



Scheme 1. Synthetic routes to **1**.

This salt crystallizes in the monoclinic space group $P2_1/n$ with four asymmetric units in the unit cell. Figure 2 depicts the molecular structure of **1** and selected atom distances and bond angles are listed.

The values of the atom distances and bond angles within the H₂PO₃S[−] entity are in good accordance with those found by Ziemer *et al.*^[10].

As imposed in the introduction the interactions in this molecule are essential for the structural composition of the crystal. The molecules are held together by N–H⋯O and O–H⋯O hydrogen bonds (Table 1), forming chains parallel to the *b* axis and O–H⋯S interaction, connecting the chains, along the *c* axis (Figure 3). This leads to the formation of layers.

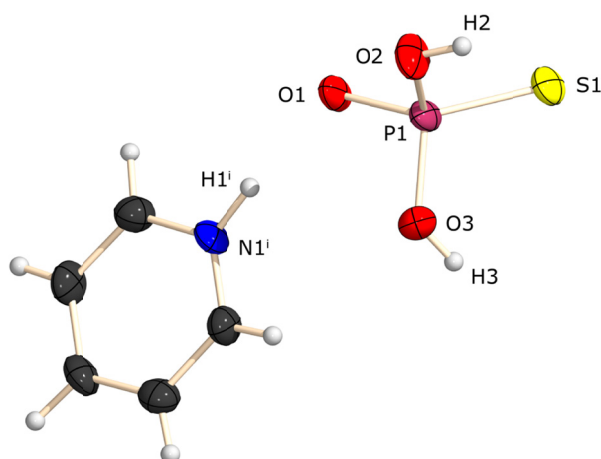


Figure 2. Molecular structure of **1**. Thermal ellipsoids are set at 50% probability level.

Symmetry operation $i = 1-x, 1-y, 1-z$

P1–S1 1.970(1); P1–O1 1.513(3), P1–O2 1.580(2), P1–O3 1.560(2); O1–P1–S1 116.2(2), O2–P1–S1 112.4(2), O3–P1–S1 112.9(2), O1–P1–O2 104.0(2), O1–P1–O3 106.3(2), O2–P1–O3 104.0(2).

Table 1. Intermolecular interaction in **1** (the sum of the van der Waals radii of hydrogen and sulfur atom mounts up to 3.00 Å, hydrogen and oxygen to 2.72 Å).

D–H···A	d(D–H) (Å)	d(H···A) (Å)	d(D···A) (Å)	∠ D–H···A (°)
N1 ⁱ –H1 ⁱ ···O1	0.88(4)	1.78(4)	2.660(4)	174(4)
O3 ⁱⁱ –H3 ⁱⁱ ···O1	1.02(1)	1.58(2)	2.567(3)	169(4)
O2–H2···S1 ⁱⁱⁱ	1.02(2)	2.18(1)	3.132(3)	156(4)

symmetry operations: $i = 1-x, 1-y, 1-z$; $ii = 0.5-x, -0.5+y, 1.5-z$; $iii = 1-x, 1-y, 2-z$.

Along one chain the (pyH)(H₂PO₃S) molecules are inversion related and connected *via* a hydrogen bond between H3 at O3 to the oxygen O1 of the next H₂PO₃S[−] entity. The values for this interaction are in the expected range for this type of bond. The donor acceptor distance is 2.573(3) Å, the angle has a value of 169(4)°.

The counter ions are held together by a hydrogen bond between the H1 atom of the pyridinium and the O1 of the anion. The contact of the hydrogen to the acceptor has a value of 1.78(4) Å, the sum of the van der Waals radii of hydrogen and oxygen is 2.72 Å^[12]. N1ⁱ–H1ⁱ···O1 is with an angle of 174(4)° very close to linearity.

The parallel chains are connected to each other by O–H···S interactions. The donor acceptor distance has a value of 3.132(3) Å which is well within the range below the sum of the S,N van der Waals radii (3.35 Å).^[12] The hydrogen sulfur contact is 2.18(1) Å, the O2–H2···S1ⁱⁱⁱ angle is 156(4)°.

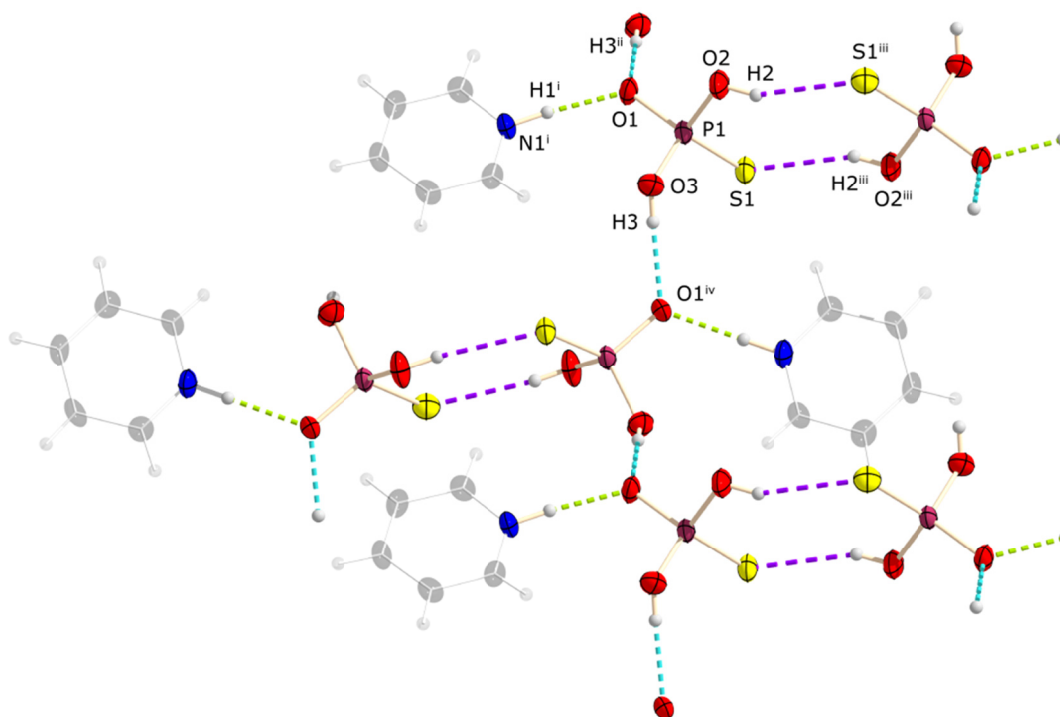


Figure 3. D–H···A Interactions in **1**.

The connection between the chains is further stabilized by antiparallel pi stacking of the aromatic pyridinium molecules (Figure 4). The mean planes of the rings are parallel, with a centroid–centroid distance of 3.366 Å, which is even shorter than 3.510(2) Å as found in the literature.^[13]

So taking all discussed interactions into consideration, the crystal structure of **1** is built up of two dimensional layers parallel to each other. Figure 5 shows two neighbouring layers and the cell edges of the unit cell.

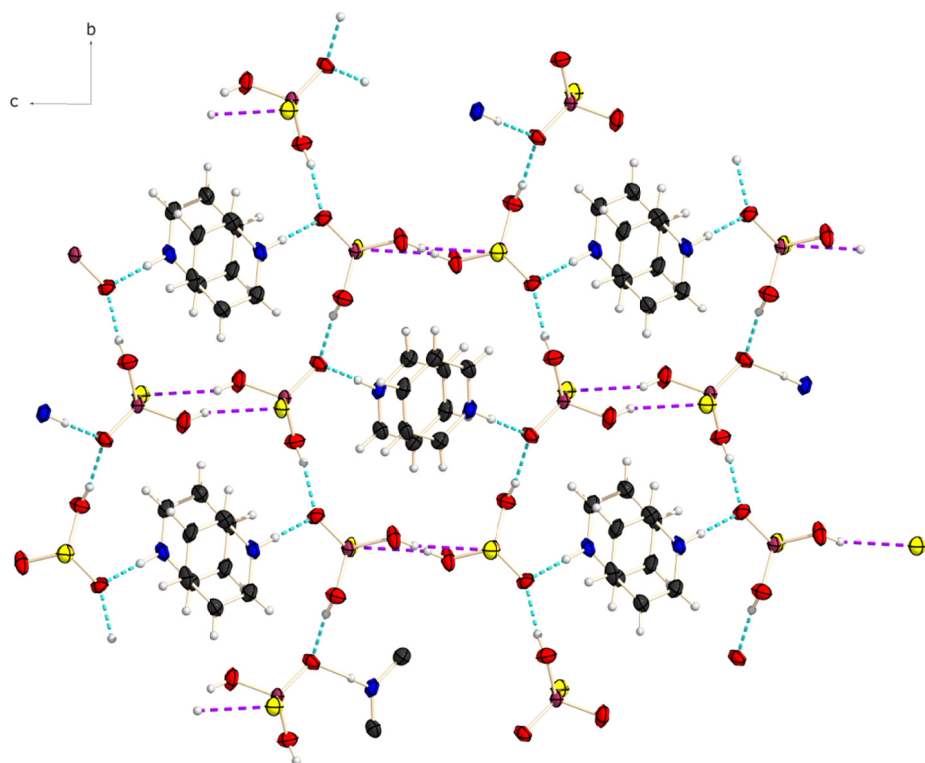


Figure 4. n-n interaction between the pyridine molecules.

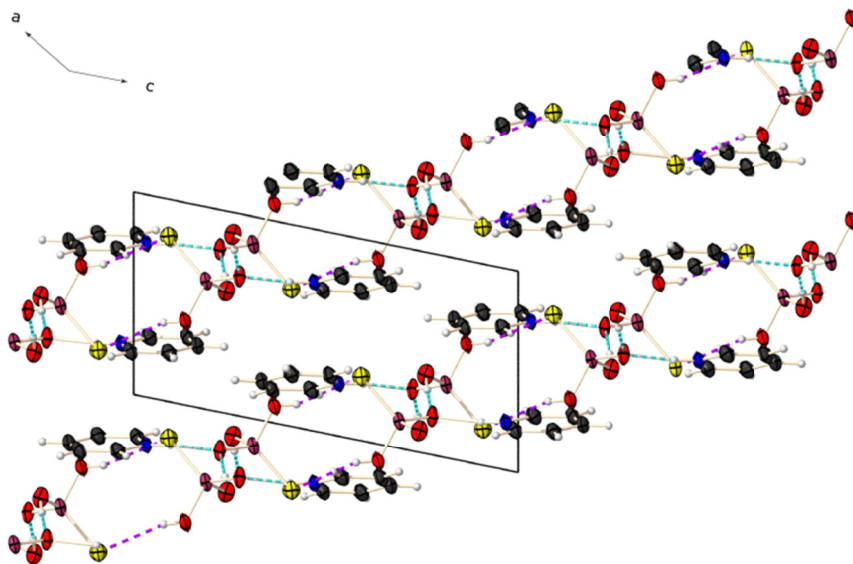


Figure 5. Layered structure of **1** with all intermolecular interactions.

Molecular and Crystal Structure of (4,4'-bipyH)(4,4'-bipyH₂)H(HPO₃S)₂ (**2**)

The second structure discussed in here, is even more interesting than **1**, as it displays much more and divers intra- and intermolecular interactions forming a three dimensional network.

(4,4'-bipyH)(4,4'-bipyH₂)H(HPO₃S)₂ (**2**) could be obtained as yellow block shaped crystals by refluxing P₄S₃ and lithium in pyridine and recrystallization from THF. This salt consists of two organic cations, a single and a twice protonated 4,4'-bipyridine and the inorganic anion H(HPO₃S)₂³⁻.

Compound **2** crystallizes in the triclinic space group *P*–1 with two asymmetric units in the unit cell. Figure 6 shows the molecular structure of **2** and selected atom distances and bond angles are listed.

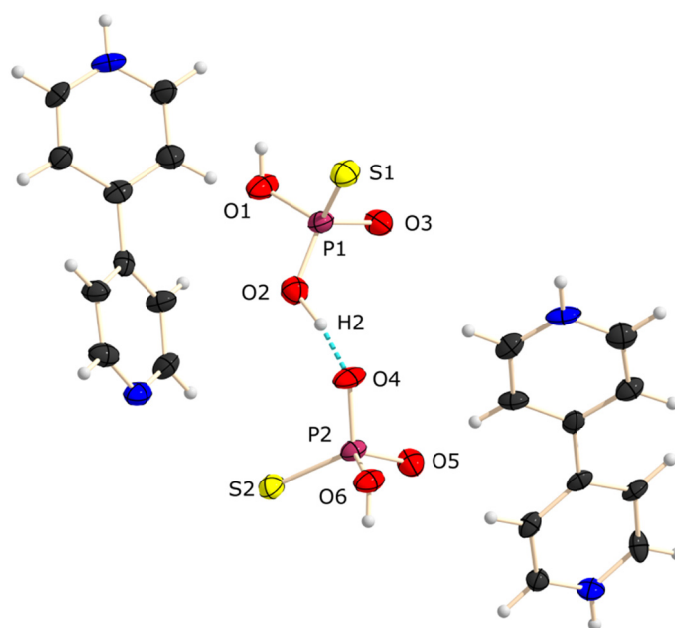


Figure 6. Molecular structure of **2**. Thermal ellipsoids are set at 50% probability level.

P1–S1 1.981(2), P1–O1 1.599(3), P1–O2 1.518(3), P1–O3 1.552(3), O2–H2 1.197(6), P2–S2 1.986(3), P2–O4 1.545(3), P2–O5 1.514(3), P2–O6 1.604(3); S1–P1–O1 110.5(2), S1–P1–O2 116.2(2), O2–P1–S1 112.4(2), O3–P1–S1 112.9(2), O1–P1–O2 104.0(2), O1–P1–O3 106.3(2), O2–P1–O3 104.0(2).

This anion comprises two $\text{HPO}_3\text{S}^{2-}$ entities which are held together by a very strong hydrogen bond (introduced in the previous chapter). The hydrogen (H2) is partially covalently linked to both oxygen atoms (O2 and O4).^[11] With a X–H/H–Y distance of 1.197(6)/1.324(7) Å, X⋯Y of 2.517(5) Å and a X–H–Y angle of 172(6)°. The values for this connection are well within the range described for a strong hydrogen bond.^[14] Table 2 summarizes the main intra- and intermolecular interactions found within **2**. The average atom distances and bond angles around the phosphorus atoms do not differ substantially from those found in **1**.

Table 2. Intra- and intermolecular interaction in **2** (Van der Waals radii [Å]: H: 1.20; C: 1.70; N: 1.55; O: 1.52; S: 1.80)^[12].

X–H–Y	d(X–H) (Å)	d(H–Y) (Å)	d(X⋯Y) (Å)	∠ X–H–Y (°)
O2–H2⋯O4	1.20(1)	1.32(1)	2.517(5)	172(6)
D–H⋯A	d(D–H) (Å)	d(H⋯A) (Å)	d(D ⋯A) (Å)	∠ D–H⋯A (°)
O1–H1⋯S2 ⁱ	0.84(1)	2.59(1)	3.348(5)	150.4(3)
O6–H6⋯S1 ⁱⁱ	0.84(1)	2.39(1)	3.200(5)	159.8(3)
N1–H21⋯N2 ⁱ	0.88(1)	1.77(1)	2.647(8)	173.0(3)
N4–H4⋯O3 ⁱⁱⁱ	0.88(1)	1.73(1)	2.603(7)	171.4(4)
N3–H3⋯O5 ^{iv}	0.88(1)	1.72(1)	2.591(7)	173.2(4)
C11 ^v –H11 ^v ⋯S2	0.95(1)	2.90(1)	3.645(7)	137.0(5)
C10–H10⋯S2	0.95(1)	2.91(1)	3.844(7)	170.4(4)
C3 ^{vi} –H25 ^{vi} ⋯S2	0.95(1)	2.30(1)	3.6745	129.6(3)
C4–H24⋯S1	0.95 (1)	2.80(1)	3.660(6)	150.2(4)
C13 ^{vii} –H13 ^{vii} ⋯O5	0.95(1)	2.50(1)	3.316(8)	144.7(4)
C18 ^{viii} –H18 ^{viii} ⋯O3	0.95(1)	2.46(1)	3.387(7)	164.9(4)

symmetry operations: i = 1–x, 1–y, 1–z; ii = 0.5–x, –0.5+y, 1.5–z; iii = 1–x, 1–y, 2–z; iv = x–1, y, z; v = 1+x, y, z; vi = x, 1+y, z; vii = –1–x, 1–y, z; viii = x, 1+y, z.

Each anion is connected to the next one, which adopts the same orientation, by O–H⋯S contacts. With a H6⋯S1/H1⋯S2 distance of 2.394(3)/2.591(2) Å, every $\text{H}_3\text{P}_2\text{O}_6\text{S}_2^{3-}$ forms four such interactions, leading to infinite parallel chains. The N–H groups N4–H4 and N3–H3 of the bipyH₂ counterions interact with O3 and O5 respectively on either side of the cation which therefore acts as a bridge between two parallel strands. The values of the O–H⋯N interactions are in good accordance with the expected ones (see **1**).

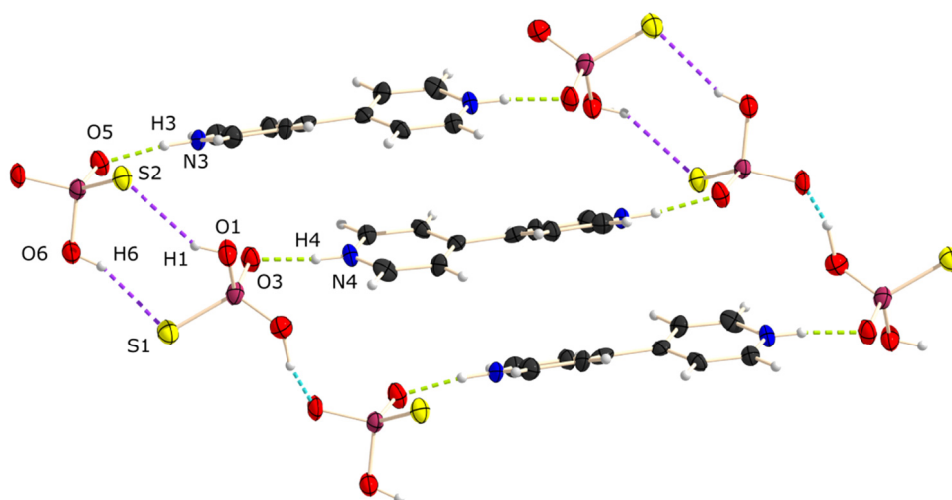


Figure 7. O–H···S linkage between the $\text{H}(\text{HPO}_3\text{S})_2^{3-}$ entities and O–H···N interactions with the bipyH_2 cations in **2**.

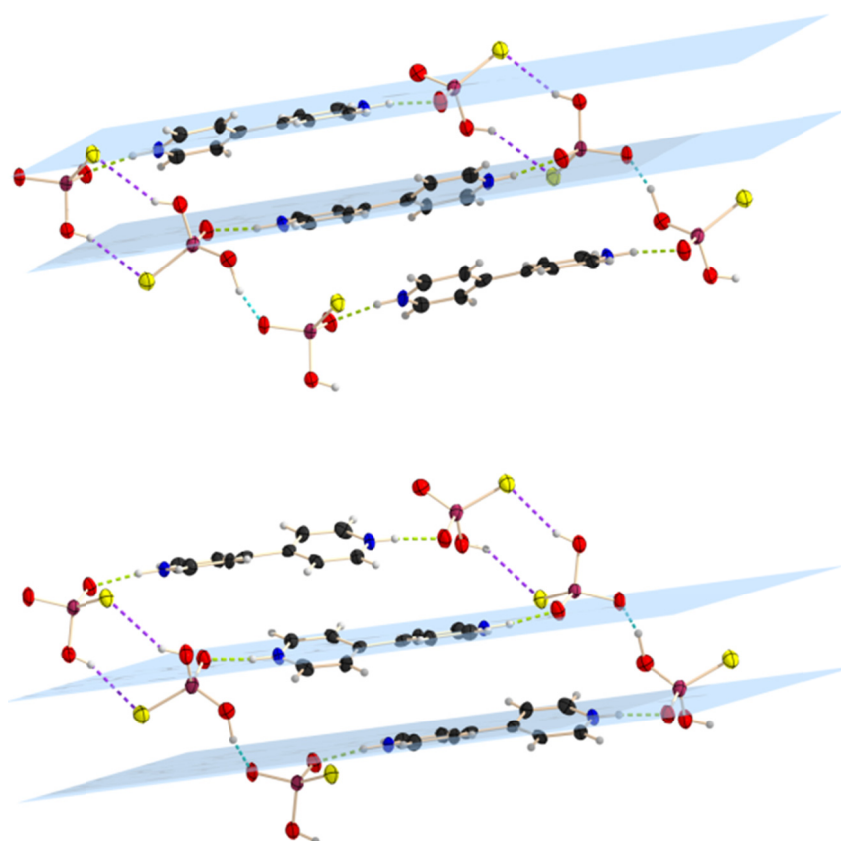


Figure 8. Planes indicating the n–n interaction between adjacent bipyH_2 ions.

The structure is further stabilized by antiparallel pi stacking between the bipyH₂ cations. The two rings of one bipyH₂ are contorted in reference to each other by an angle of 22(2)°. The pyridine rings of adjacent bipyH₂ molecules are parallel to each other with a centroid-centroid distance of the mean plains of 3.354(5) Å and 3.239(5) Å respectively, as shown in Figure 8.

These motives are arranged staggered along the *b* axis and stabilized by electrostatic C–H···O interactions (Figure 9). While the O···H distances are with 2.495(4) and 2.460(4) Å below the sum of their van der Waals radii, the C···O distances (3.316(8) and 3.387(7) Å) are slightly higher. These contacts can therefore be described as very weak electrostatic interactions.

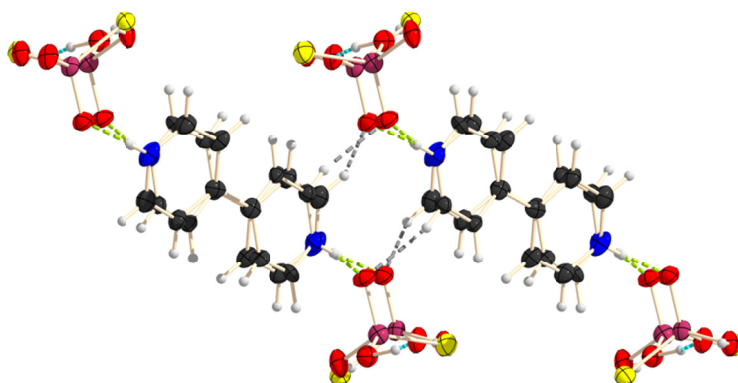


Figure 9. C–H···O interactions between the layers in **2**.

The single protonated bipyridinium molecules interact with each other *via* N–H···N contacts. The values of these interactions are in good accordance with those found in the literature.^[15] The infinite chains formed this way, run parallel to the anionic part and act as spacers between those motives.

In Figure 10 the overall structural build up in the crystal is shown from two different viewing directions. Between the encircled motives further electrostatic interactions can be found.

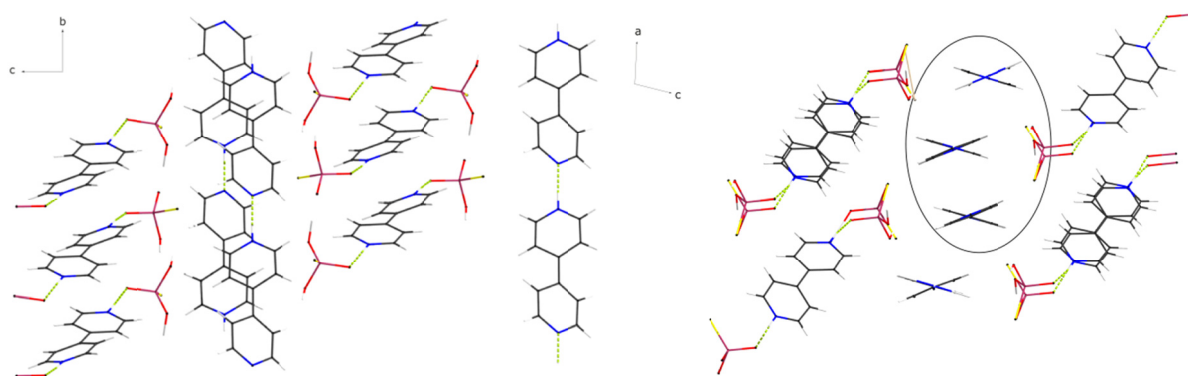
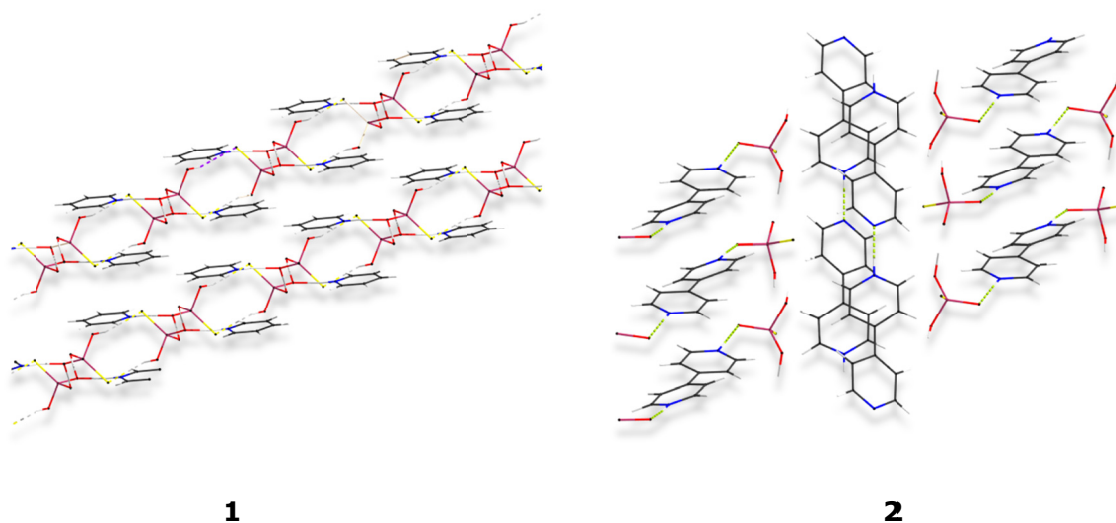


Figure 10. Structural build up in the crystal of **2**.

Conclusion

The great difference in the tendency to form hydrogen bonds between oxygen and its heavier homologue sulfur is responsible for and can be used to control dimensionality of networks in the crystal. This becomes clearly evident when comparing the structural chemistry of the H_2PO_4^- and $\text{H}_2\text{PO}_3\text{S}^-$ anions. The pyridinium salt of $\text{H}_2\text{PO}_3\text{S}^-$ (**1**) was readily obtained from the hydrolysis of $\text{py}_2\text{P}_2\text{S}_5$. The 4,4'-bipyridinium salt of $\text{H}(\text{HPO}_3\text{S})_2^{3-}$ is formed by refluxing P_4S_3 and lithium in pyridine and recrystallization from THF.

In compound **1** one sulfur atom makes the difference between a three-dimensional anionic subnetwork (phosphate anions) and a two-dimensional layered structure. Introduction of a bifunctional base (4,4'-bipy) in **2** provides an additional functionality capable of hydrogen bonding, which causes an increase in dimensionality and results in the formation of a three-dimensional network.



Summarizing, we could gain a first insight into how the interplay between base functionality and sulfur content in the phosphate anion controls the dimension of the network. These new results are of great importance because these compounds can be used as intermediates to new metal containing open frameworks (see PART III – Chapter 1).

Experimental Section

General: Na₂S was obtained from Sigma-Aldrich Inc., used as supplied without further purification and stored under inert gas atmosphere. P₄S₁₀ was commercially obtained (Riedel-de H  en) and was purified by extraction with CS₂ before use. P₄ was commercially obtained from ThermPhos. All solvents were dried using commonly known methods and freshly distilled before use. **³¹P NMR** Chemical shifts are referred to 85% H₃PO₄ as external standard. All spectra were measured, if not mentioned otherwise, at 25 °C. The %-data correspond to the intensities in the ³¹P NMR spectra with respect to the total intensity. The difference to 100 % belongs to not determinable signals. Infrared **IR** spectra were recorded on a PerkinElmer BX FT IR spectrometer equipped with a Smiths DuraSamlIR II diamond ATR unit. Transmittance values are qualitatively described as “very strong” (vs), “strong” (s), “medium” (m), “weak” (w) and “very weak” (vw). **Raman** spectra were recorded on a Bruker RAM II spectrometer equipped with a Nd:YAG laser (200 mW) operating at 1064 nm and a reflection angle of 180 °. The intensities are reported as percentages

of the most intense peak and are given in parentheses. Low resolution mass spectra were recorded on a JEOL MStation JMS-700 with 4-nitrobenzyl alcohol as matrix for FAB measurements. **Elemental analyses** (CHNS) were performed with an Elementar Vario EL. Due to the formation of glassy $(\text{P}_2\text{O}_5)_x(\text{H}_2\text{O})_y\text{C}$ during measurement, the values deviate considerably from the calculated ones. **Melting and decomposition points** were determined by differential scanning calorimetry (Linseis DSC-PT10, calibrated with standard pure indium and zinc). Measurements were performed at a heating rate of $5\text{ }^\circ\text{C min}^{-1}$ in closed aluminum sample pans with a 0.1 mm hole in the lid for gas release to avoid an unsafe increase in pressure under a nitrogen flow of 20 mL min^{-1} with an empty identical aluminum sample pan as a reference. Melting points were checked with a Büchi Melting Point B-540 in open glass capillaries.

X-ray Crystallography. The single-crystal X-ray diffraction data were collected using an Oxford Xcalibur3 diffractometer equipped with a Spellman generator (voltage 50 kV, current 40 mA), Enhance molybdenum K_α radiation source ($\lambda = 71.073\text{ pm}$), Oxford Cryosystems Cryostream cooling unit, four circle kappa platform and a Sapphire CCD detector. Data collection and reduction were performed with CrysAlisPro.^[16] The structures were solved with SIR97^[17], SIR2004^[18], refined with SHELXL-97^[19], and checked with PLATON^[20], all integrated into the WinGX software suite^[21]. The finalized CIF files were checked with checkCIF.^[22] All non-hydrogen atoms were refined anisotropically. The hydrogen atoms were located in difference Fourier maps and placed with a C–H distance of 0.98 \AA for C–H bonds. Intra- and intermolecular contacts were analyzed with DIAMOND (version 3.2i), thermal ellipsoids are drawn at the 50% probability level. Selected crystallographic data and refinement details for the structure determination of compound **1** and **2** are summarized in Table 3.

(pyH)(H₂PO₃S) (**1**)

1) P_4S_{10} (444.5 mg, 1 mmol) was refluxed in pyridine (40 mL) for 2 h. Afterwards the yellow precipitate of $\text{py}_2\text{P}_2\text{S}_5$ was separated from the solution, dried *in vacuo*. The yellow powder was dissolved in H_2O and five drops of conc. HNO_3 were added. Immediately yellow block shaped crystals of **1** could be observed. (yield: 82.8%, 148.3 mg, 0.83 mmol)

$^1\text{P}\{^1\text{H}\}$ NMR (H_2O , rt): δ [ppm] = 57.6 (**1**, 73.8%), 3.5 (s, 26.2%).

Table 3. Crystallographic and refinement data of **1** and **2**.

	1	2
empirical formula	C ₅ H ₈ NPO ₃ S	C ₄₀ H ₄₄ N ₈ O ₁₂ P ₄ S ₄
formula mass	193.16	583.32
<i>T</i> [K]	173(2)	173(2)
crystal size [mm]	0.3× 0.2×0.15	0.1×0.1×0.05
crystal description	yellow block	yellow block
crystal system	monoclinic	triclinic
space group	<i>P</i> 2 ₁ / <i>n</i>	<i>P</i> −1
<i>a</i> [Å]	6.7949(11)	8.477(10)
<i>b</i> [Å]	9.0254(14)	9.609(10)
<i>c</i> [Å]	13.2563(17)	15.887(16)
<i>α</i> [°]		92.192(8)
<i>β</i> [°]	101.499(14)	97.370(9)
<i>γ</i> [°]		115.545(11)
<i>V</i> [Å ³]	796.6(2)	1151.6(10)
<i>Z</i>	4	2
<i>ρ</i> _{calcd.} [g cm ^{−3}]	1.610	1.682
<i>μ</i> [mm ^{−1}]	0.563	0.961
<i>F</i> (000)	400	583
<i>θ</i> range [°]	4.34–25.34	3.87–25.34
index ranges	−8 ≤ <i>h</i> ≤ 8 −10 ≤ <i>k</i> ≤ 10 −15 ≤ <i>l</i> ≤ 15	−10 ≤ <i>h</i> ≤ 10 −11 ≤ <i>k</i> ≤ 11 −19 ≤ <i>l</i> ≤ 19
reflns. collected	7145	10234
reflns. obsd.	872	1847
reflns. unique	1456	4166
<i>R</i> _{int}	0.0614	0.1264
<i>R</i> ₁ , <i>wR</i> ₂ (2σ data)	0.0347, 0.0807	0.0680/0.0894
<i>R</i> ₁ , <i>wR</i> ₂ (all data)	0.0672, 0.0859	0.1783/0.1107
GOOF on <i>F</i> ²	0.881	0.868
larg. diff peak/hole (e/Å)	0.651/−0.247	0.442/−0.386

2) $\text{py}_2\text{P}_2\text{S}_7$ (PART IV – Chapter 1) was suspended in acetone. After one day yellow crystals of **1** were observed in the solution. (yield: 91.4%, 163.7 mg, 0.91 mmol).

$^{31}\text{P}\{^1\text{H}\}$ NMR (acetone, rt): δ [ppm] = 46.1 (**1**, 89.5%), 0.7 (s, 10.5%).

Elemental analysis. Calc. N 7.33, C 31.42, H 3.16, S 16.78; found. N 8.81, C 37.35, H 4.82, S 1.90. **IR** (200 mW, RT): $\tilde{\nu}$ [cm^{-1}] = 3144 (9), 3058 (81), 2956 (12), 2919 (9), 1599 (19), 1576 (22), 1483 (11), 1382 (11), 1217 (24), 1152 (11), 1065 (14), 1032 (92), 1011 (53), 992 (100), 915 (12), 734 (10), 652 (20), 473 (18), 220 (22). **Raman** (200 mW, RT): $\tilde{\nu}$ [cm^{-1}] = 3052 (ww), 3000 (ww), 2367 (ww), 1921 (ww), 1633 (ww), 1596 (w), 1580 (m), 1488 (w), 1482 (w), 1436 (s), 1354 (ww), 1213 (w), 1146 (w), 1067 (m), 1030 (m), 990 (m), 941 (s), 903 (s), 747 (vs), 700 (vs). **Mass** (FAB[−]): m/z = 113 ($[\text{PO}_3\text{SH}_2]^-$), 97 ($[\text{PO}_2\text{SH}_2]^-$), 79 ($[\text{pyridine}]^-$), 46 ($[\text{PO}]^-$).

(4,4'-bipyH)(4,4'-bipyH₂)H(HPO₃S)₂ (**2**)

P_4S_3 (660 mg, 3 mmol) and Li (42 mg, 6 mmol) were refluxed in pyridine (9 mL) for 10 min. The yellow precipitated was separated from the red solution, dried *in vacuo* and suspended in THF. After one day yellow block shaped crystals of **2** were obtained.

$^{31}\text{P}\{^1\text{H}\}$ NMR (THF, rt): δ [ppm] = 82.4 (2.2%), 35.0 (**2**, 96.0%), −7.5 (1.8%).

Elemental analysis. Calc. N 10.40, C 44.61, H 3.74, S 11.91; found. N 14.26, C 58.24, H 5.77, S 4.41. **IR** (200 mW, RT): $\tilde{\nu}$ [cm^{-1}] = 2964 (m), 2878 (w), 2363 (m), 2122 (w), 1998 (ww), 1915 (w), 1638 (w), 1489 (w), 1404 (w), 1356 (ww), 1261 (w), 1215 (m), 1192 (m), 1078 (vs), 1020 (vs), 800 (vs), 681 (s). **Mass** (FAB[−]): m/z = 195 ($[\text{P}_2\text{O}_4\text{S}_2\text{H}_5]^-$), 177 ($[\text{P}_2\text{O}_3\text{S}_2\text{H}_5]^-$), 159 ($[\text{P}_2\text{O}_4\text{SH}_2]^-$), 113 ($[\text{PO}_3\text{SH}_2]^-$), 97 ($[\text{PO}_2\text{SH}_2]^-$), 79 ($[\text{pyridine}]^-$), 46 ($[\text{PO}]^-$).

- [1] a) P. A. Frey, R. D. Sammons, *Science (Washington, DC, United States)* **1985**, 228, 541-545; b) C. Liang, L. C. Allen, *J. Am. Chem. Soc.* **1987**, 109, 6449-6453.
- [2] G. Ferey, *J. Solid State Chem.* **2000**, 152, 37-48.
- [3] S. Neeraj, S. Natarajan, C. N. R. Rao, *Angew. Chem., Int. Ed.* **1999**, 38, 3480-3483.
- [4] S. Dhanuskodi, S. Manivannan, K. Kirschbaum, J. Philip, S. Selladurai, *J. Cryst. Growth* **2006**, 290, 548-553.
- [5] C. B. Aakeroy, P. B. Hitchcock, B. D. Moyle, K. R. Seddon, *J. Chem. Soc., Chem. Commun.* **1989**, 1856-1859.
- [6] a) C. B. Aakeroy, P. B. Hitchcock, B. D. Moyle, K. R. Seddon, *J. Chem. Soc., Chem. Commun.* **1989**, 1856-1859; b) T. Kolev, B. B. Koleva, M. Spiteller, H. Mayer-Figge, W. S. Sheldrick, *Dyes and Pigments* **2008**, 79, 7-13.
- [7] a) J. E. Anthony, *Chem. Rev. (Washington, DC, United States)* **2006**, 106, 5028-5048; b) C. G. Claessens, J. F. Stoddart, *J. Phys. Org. Chem.* **1997**, 10, 254-272; c) E. A. Meyer, R. K. Castellano, F. Diederich, *Angew. Chem., Int. Ed.* **2003**, 42, 1210-1250; d) H.-J. Schneider, *Angew. Chem., Int. Ed.* **2009**, 48, 3924-3977.
- [8] R. Masse, I. Tordjman, *Acta Cryst., Section C* **1990**, C46, 606-609.
- [9] M. A. Wurtz, *Ann. Chim. Phys.* **1847**, 3.
- [10] B. Ziemer, A. Rabis, *Acta Cryst., Section C* **2000**, C56, e94.
- [11] J. Emsley, *Chem. Soc. Rev.* **1980**, 9, 91-124.
- [12] A. Bondi, *J. Phys. Chem.* **1966**, 70, 3006-3007.
- [13] G. Shan, Z. Li, L. Hu, J. Jiang, Z. Liu, *Acta Cryst., Section E* **2013**, 69, o584.
- [14] S. J. Grabowski, *Annual Reports on the Progress of Chemistry, Section C: Physical Chemistry* **2006**, 102, 131-165.
- [15] G. C. Pimentel, A. L. McClellan, *Annu. Rep. Prog. Chem., Sect. C Phys. Chem.* **1971**, 22, 347-385.
- [16] *CrysAlisPro 1.171.36.21, Agilent Technologies*, **2012**.
- [17] A. Altomare, G. Cascarano, C. Giacovazzo, A. Guagliardi, A. A. G. Moliterni, M. C. Burla, G. Polidori, M. Camalli, R. Spagna, **1997**, 343.
- [18] a) M. C. Burla, R. Caliendo, M. Camalli, B. Carrozzini, G. L. Cascarano, L. De Caro, C. Giacovazzo, G. Polidori, R. Spagna, Institute of Crystallography, Bari (Italy), **2004**; b) M. C. Burla, R. Caliendo, M. Camalli, B. Carrozzini, G. L. Cascarano, L. De Caro, C. Giacovazzo, G. Polidori, R. Spagna, *Journal of Applied Crystallography* **2005**, 38, 381-388.
- [19] a) G. M. Sheldrick, *SHELXL-97, Program for the Refinement of Crystal Structures. University of Göttingen, Göttingen (Germany)*, **1997**; b) G. M. Sheldrick, *Acta Crystallographica, Section A: Foundations of Crystallography* **2008**, A64, 112-122.
- [20] A. L. Spek, *Platon, A Multipurpose Crystallographic Tool, Utrecht University, Utrecht, The Netherlands*, **2012**.
- [21] L. J. Farrugia, *J. Appl. Crystallogr.* **1999**, 32, 837-838.
- [22] <http://journals.iucr.org/services/cif/checkcif.html>

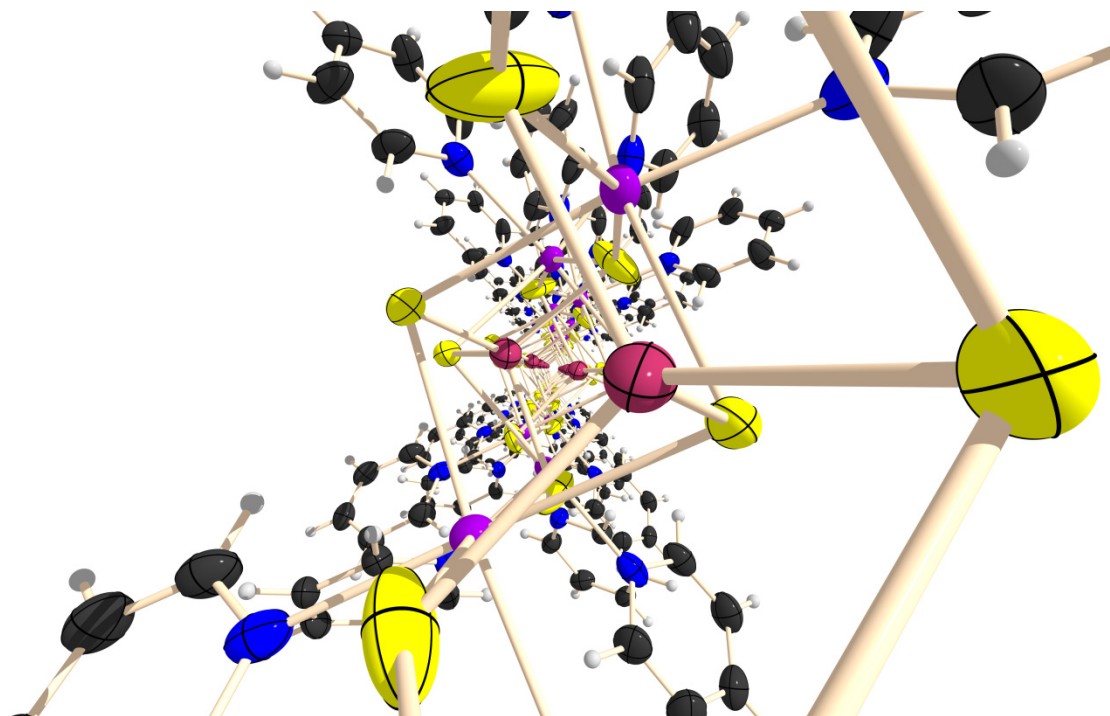
PART III

Pyridine-Stabilized Metal

Complexes of P,S,O Anions

Pyridine Stabilized Mn(II) Thio- and Oxophosphate Complexes

As to be submitted to *Dalton Trans.*



In the field of organic inorganic hybrid open frameworks a great variety of transition metal complexes has been investigated in the past. But the number of compounds containing manganese(II) is still very limited.

*To gain a better insight into this matter in the following three new compounds containing Mn(II) are presented. With the help of the novel compounds $[py_2MnPS_4]_2[pyH]_2 \cdot 4py$ (**1**), $py_4NaMnPS_4$ (**2**) and $py_4Mn(H_2PO_4)_2$ (**3**), the usefulness of thio- and oxophosphates as ligands is investigated.*

Further the importance of the participation of organic cations, especially amines, in the arrangement of the structure shall be enlightened.

Introduction

As already mentioned in PART II – Chapter 4 inorganic open-framework materials become ever more important due to their various applications.^[1] They are widely used in matters of catalysis, ion exchange and intercalation chemistry, but also in photo-physics and the ever growing field of optical devices.^[2]

Organic inorganic hybrid open frameworks are built up based on strong semi ionic connections, while organic ligands in general have the advantage of being able to form various strong and weak intermolecular interactions. Over the past decades the insertion of transition metal atoms into phosphates has gained growing interest, as they increase the possible formation of new conformations and therefore topologies. The use of transition metal coordination complexes in this field of chemistry has the advantage of adding the properties of the d-block elements to the ones of the framework.^[3] The number of manganese containing representatives with open frameworks, however, is still very limited.^[1]

In these compounds amines are widely used as organic component. They fulfil a bifunctional role. Not only are they structure directing but they can also act as organic templating ligands, occupying coordination space at the metal atom.

Especially the linkage *via* H–N or M–N bonds is important for the arrangement in the crystal, therefore the number of those bonds has to be taken into consideration. So the structure and density of the framework can be manipulated by the choice of the organic ligand. This means that the compound can be specially tailored for every different guest molecule.

Since 1989 also chalcogenide containing compounds have gained growing attraction as a new class of cluster forming material.^[4] Combining the advantages of phosphorus, chalcogenides, transition metals in various coordination numbers and amines, in their templating role, the range of possibilities can be further extended.

Our primary goal was to investigate the impact of pyridine as amine, manganese as transition metal and sulfur as substitution for oxygen in the phosphate entity, on the dimension of the network.

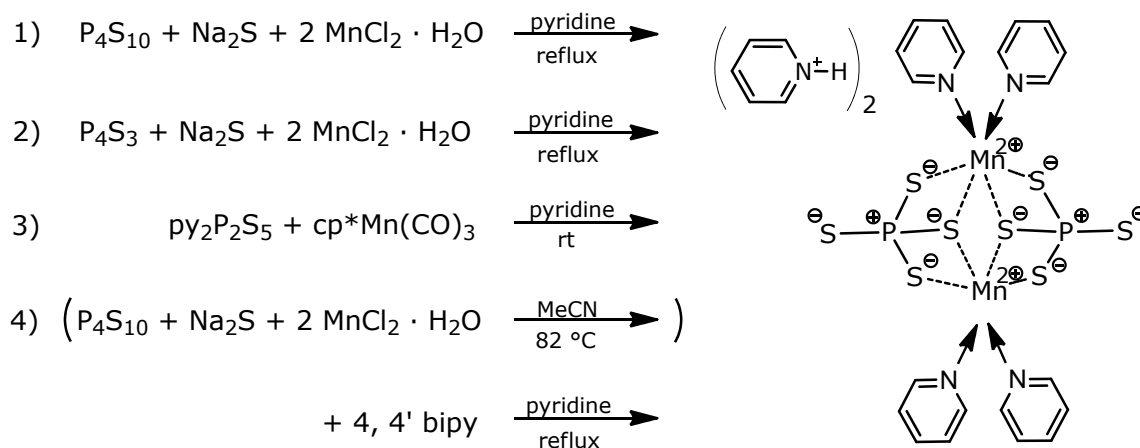
Results and Discussion

Molecular and Crystal Structure of $[\text{py}_2\text{MnPS}_4]_2[\text{pyH}]_2 \cdot 4\text{py}$ (**1**)

The first compound we could isolate fitting all the above mentioned criteria, is $[\text{py}_2\text{MnPS}_4]_2[\text{pyH}]_2 \cdot 4\text{py}$ (**1**).

To the best of our knowledge only one ternary Mn,P,S compound has been described in the literature so far. Yamaguchi *et al.* characterized the MnPS_3 , which, in contrast to our compound adopts a neutral coordination polymeric structure rather than discrete molecules with ionic structure and is generally used as intercalation compound.^[5] But the anionic PS_3^- part in this structure has to be described rather as the hexathiohypodiphosphate, because of the observed P–P atom distance of 2.187(2) Å, which is even shorter than 2.254 Å as described for $\text{Na}_2\text{P}_2\text{S}_6 \cdot 6 \text{H}_2\text{O}$.^[6]

Compound **1** is rather stable, which shows the great diversity of different synthetic routes (Scheme 1).



Scheme 1. Synthetic routes to **1**.

In reaction 1–3 the educts were refluxed in pyridine and dark yellow block shaped crystals of **1** could be obtained from the solution after removing the precipitate. In reaction 4 acetonitrile was used as solvent. After refluxing, the precipitate was removed and 4,4'-bipyridine, dissolved in pyridine, was added. It was only after the addition of the nitrogen containing aromatic base, that **1** was formed. This leads to the

conclusion that the coordination product of manganese(II) and PS_4^{3-} can only be obtained by stabilization *via* complexation with pyridine.

Compound **1** crystallizes in the monoclinic space group $P2_1/c$ with two formula units in the unit cell. Figure 1 shows the molecular structure of **1** without the pyridinium cations, additionally selected bond lengths and angles are listed.

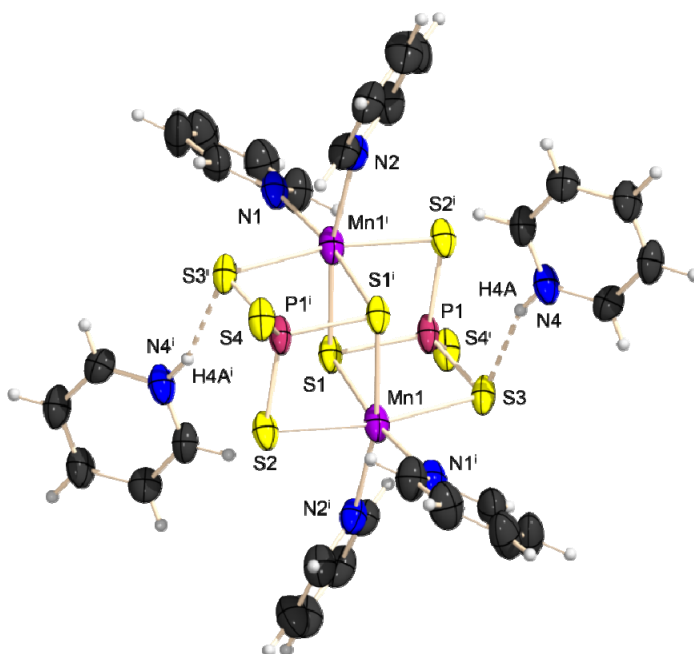


Figure 1. Molecular structure of **1** drawn without the solvent pyridine molecules. Ellipsoids are drawn at the 50% probability level. Symmetry operation: $i = -x, -y, -z$. Selected bond lengths [\AA] and angles [$^\circ$] for **1**: Mn1–N1 2.277(4), Mn1–N2 2.280(4), Mn1–S1 2.570(1), Mn1–S1ⁱ 2.646(1), Mn1–S2 2.584(1), Mn1–S3 2.582(1), P1–S1 2.075(2), P1–S2 2.043(2), P1–S3ⁱ 2.071(2), P1–S4 1.993(2);

N1–Mn1–N2 94.19(14); N2–Mn1–S1ⁱ 87.72(10), N1–Mn1–S1 92.02(10), N1–Mn1–S2 93.74(10), N1–Mn1–S3 92.52(10), N2–Mn1–S2 91.75(10), N2–Mn1–S3 95.19(10), S2–Mn1–S1ⁱ 78.46(4), S3–Mn1–S1 93.91(4), S3–Mn1–S2 170.29(5), N1–Mn1–S1ⁱ 170.61(10), N2–Mn1–S1 168.74(10), S3–Mn1–S1 78.14(4), S2–Mn1–S1 95.39(4), S1–Mn1–S1ⁱ 87.67(4), Mn1–S1–Mn1 92.33(4).

The crystal contains discrete $(\text{py}_2\text{MnPS}_4)_2^{2-}$ molecules, with the manganese being distorted octahedrally surrounded. The angles around the central metal atom range between 78.14(4) and 94.19(14) $^\circ$. The bonding partners are four sulfur atoms and two pyridine molecules (Figure 2).

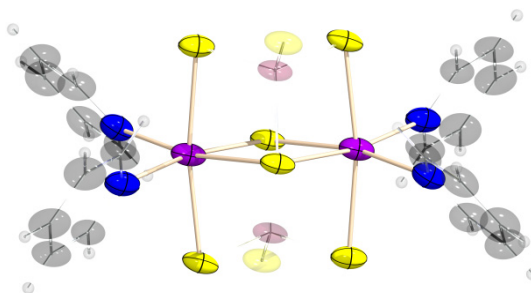


Figure 2. Octahedral surrounding of manganese.

The distances of the manganese to the nitrogen atoms of the pyridine molecules are with 2.277(4) and 2.280(4) Å in the same range as those found in $[\text{Mnpy}_4(\text{NO}_3)_2] \cdot 2 \text{ py}$ (2.245(9), 2.303(6) Å)^[7] the N–Mn–N angles, however, differ slightly with 94.2(2)° compared to 90°, which can be explained by the different conformations.

The planar four membered ring of Mn_2S_2 forms the core of the anionic part. In the above mentioned compound MnPS_3 ^[5] (**I**, Figure 3), the manganese atoms are surrounded distorted octahedrally by eight sulfur atoms with values of the S–Mn–S angles between 85.5(1) and 96.4(1)°. With the angles within the ring being 92.3(1) and 97.7(1)° in **1** this structural element is closer to a square base compared to 95.5(1) and 84.5(1)° as found in **I**. The Mn–S bonds are with an average value of 2.608(1) Å, only slightly shorter than 2.622(1) Å in **I**, whereas the Mn–Mn distance is with 3.777(1) Å in **1** larger compared to 3.524(2) Å (**I**).

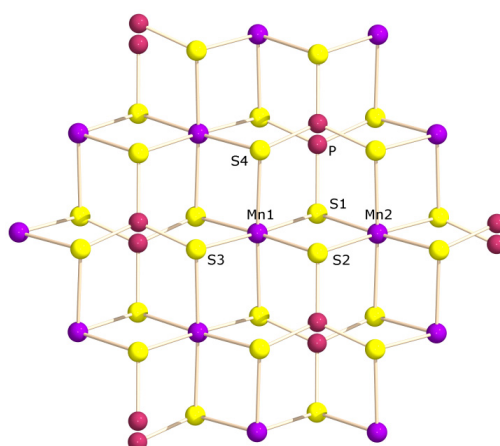


Figure 3. Molecular structure of MnPS_3 (**I**). Selected bond lengths [Å] and angles [°]: Mn–S1/S2 2.622, Mn–S3 2.619, P–S 2.031; Mn–S1/S2–Mn 84.5(1) Mn–S3–P 103.4(1), S1–Mn–S2 95.5(1), S1–Mn–S4 92.6(1), S2–Mn1–S3 85.8(1).^[5]

In the tetrathiodiphosphate entity one sulfur participates in a coordination to both manganese atoms. It is therefore threefold coordinated, building a bridge between the two cations, with a P–S distance of 2.075(2) Å. Two further sulfur atoms coordinate to one manganese each. Their distance to the manganese(II) is 2.583(1) Å in average. These values deviate just slightly from the Mn–S bond lengths found within the ring (av. 2.608(1) Å). Also all three S atoms, which engage in the coordination to the Mn(II) atoms show nearly the same distance to the phosphorus with (P1–S1 2.075(2) Å, P1–S2 2.043(2) Å, P1–S3 2.071(2) Å) This leads to the conclusion, that the number of coordinative bonds to the manganese atom does not have an influence on the P–S bond length. The fourth P–S bond has a value of 1.993(2) Å, which is shortened compared to the 2.013(4) Å as found in the salt K_2AuPS_4 .^[8] This indicates a slightly higher ionic character for this bond. The coordination leads to a slight deviation from a regular tetrahedron of the PS_4^{3-} but the S–P–S angles lie in the expected range compared to the potassium salt.

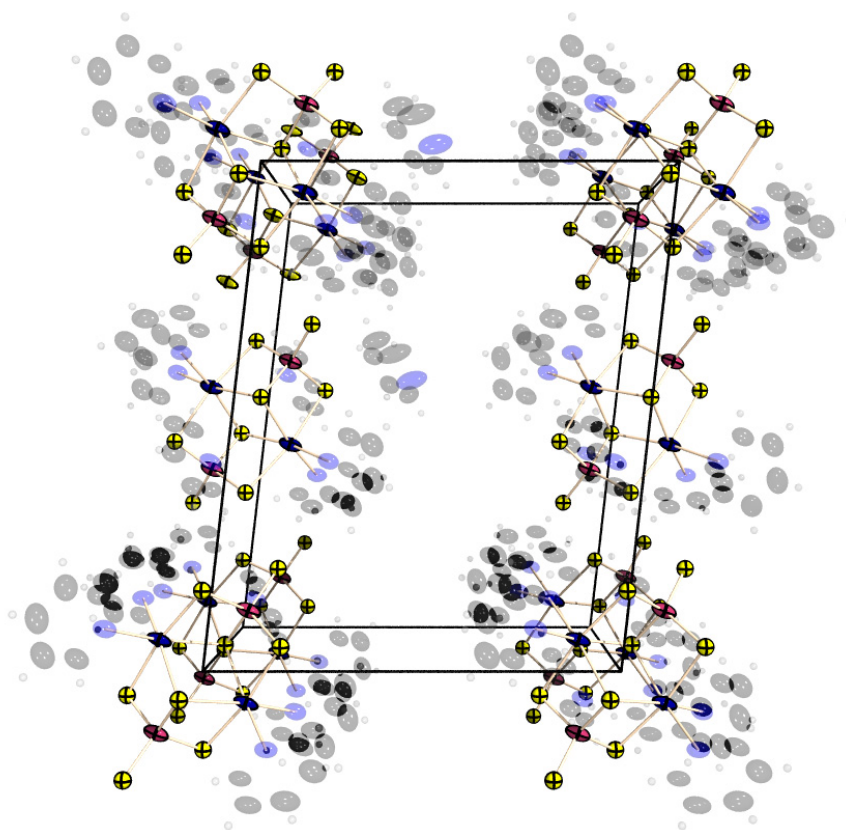


Figure 4. Unit cell of **1** with view along the *c* axis. Ellipsoids are drawn at the 50% probability level. Coordinative pyridine molecules are drawn translucent and free pyridine molecules omitted for clarity.

The pyridinium cations interact electrostatically with the anionic part of **1** (Figure 1) with D–H \cdots A being N4–H4A \cdots S3. The value $d(\text{D} \cdots \text{A})$ of 3.255(4) Å is below the sum of the van der Waals radii of sulfur and nitrogen (3.35 Å^[14]). Additional values are: $d(\text{D}–\text{H}) = 0.860(4)$ Å, $d(\text{H} \cdots \text{A}) = 2.431$ Å, $\angle \text{D}–\text{H} \cdots \text{A}$ 160.6(3)°. The Mn₂(PS₄)₂ entity is overall surrounded by four pyridine molecules acting as ligands at the manganese(II) atoms and two pyridinium cations. This leads to a shielding of the anionic part from the outside.

The outward neutral monomeric moieties of **1** arrange staggered along the *c* axis with four additionally pyridine molecules *per* entity filling the free space between them (Figure 4).

Molecular and Crystal Structure of py₄NaMnPS₄ (**2**)

Originally sulfur was used, because it is softer than oxygen and therefore can coordinate to more than one metal atom (see **1**). Using KMnO₄ instead of MnCl₂ · 2 H₂O, with the intent to partially substitute sulfur with oxygen, yields the coordination polymeric structure py₄NaMnPS₄ (**2**). So the pyridinium was substituted as cation by sodium, which leads to the formation of a coordination polymer, due to its high coordination sphere. It can be reasoned that KMnO₄ prohibits the pyridinium cation to coordinate to the PS₄^{3–}, so the sodium can occupy this place. As Na⁺ has a higher coordination sphere it can increase the dimension of the structure from isolated clusters to one dimensional chains.

Yellow block shaped crystals of **2** could be obtained from refluxing P₄S₁₀, Na₂S and KMnO₄ in pyridine. It crystallizes in the orthorhombic space group *Pbca* with 8 formula units in the unit cell. Figure 5 shows the molecular structure of **2** without the pyridinium cations, additionally selected atom distances and bond angles are listed.

The asymmetric unit contains two metal atoms (M = Na/Mn). The positions are statistically distributed occupied by a sodium and a manganese atom. So this compound is overall neutral in contrast to the ionic molecule in **1**. Thus **2** polymerizes along the *b* axis, prohibited in the other two directions by the pyridine molecules coordinated to the metal centre.

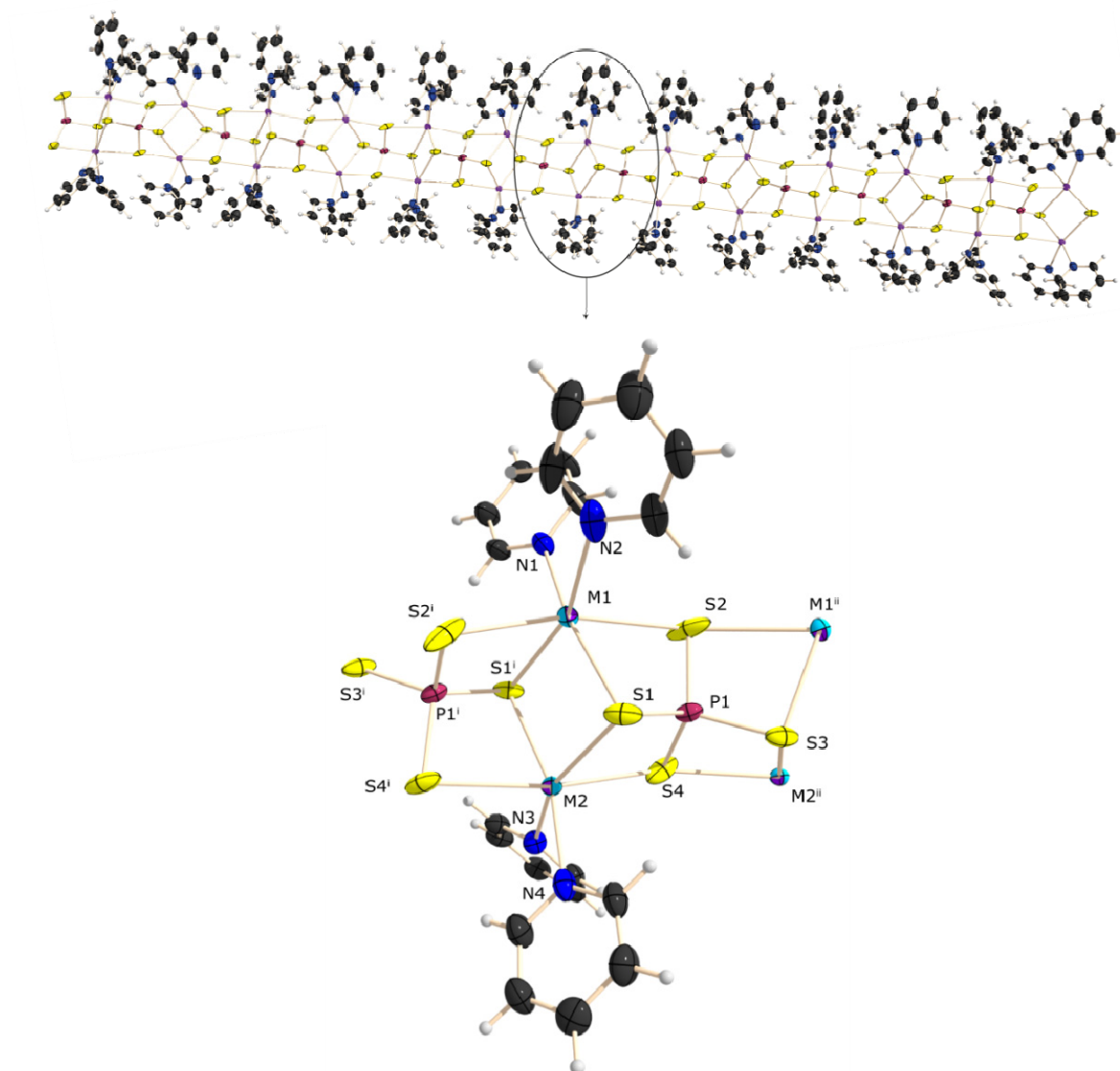


Figure 5. Molecular structure of **2** (M = Na/Mn). Ellipsoids are drawn at the 50% probability level. Symmetry operation: i = 1.5–x, –0.5+y, z, ii = 1.5–x, 0.5+y, z. Selected atom distances [Å] and bond angles (torsion)angles [°] for **2**: M1–N1 2.434(3), M1–N2 2.445(4), M2–N3 2.397(3), M2–N4 2.405(3), M1–S1 2.815(2), M1–S2 2.792(2), M2–S1 2.804(2), M2–S4 2.755(2), P1–S1 2.040(2), P1–S2 2.051(2), P1–S3 2.043(2), P1–S4 2.049(2); M1–S1–M2 85.2(2), N1–M1–N2 82.7(2), N1–M1–S1 169.2(1), N2–M1–S1 99.2(2), N1–M1–S2 101.5(2), N2–M1–S2 91.2(1), S1–M1–S2 89.1(1), S1–M1–S1ⁱ 93.8(2), S2–M1–S2ⁱ 161.2(2), S1ⁱ–M1–S2 106.5(2), N3–M2–S1 158.4(2), N4–M2–S1 92.7(1), N3–M2–S4 85.5(2), N4–M2–S4 101.9(2), N3–M2–N4 87.3(2), S1–M2–S1ⁱ 92.7(2), S4–M2–S4 164.8(2), S1–M2–S4 73.3(2), S1ⁱ–M2–S4 111.6(2), M1–S2–M1ⁱⁱ 151.7(2), M2–S4–M2ⁱⁱ 160.7(2), M1ⁱⁱ–S3–M2ⁱⁱ 88.4(2); S1–M1–S1ⁱ–M2 0.4(1).

The structures of **1** and **2** are very similar. Both contain two metal atoms coordinated by two pyridine rings each, connected by a bridging sulfur atom of two PS_4^{3-} ions on both sides and further bonded to two sulfur atoms of these entities. M is distorted octahedrally surrounded by the ligands with angles between $82.7(2)$ and $101.5(2)^\circ$.

Because of the polymerisation the asymmetric units twist slightly in relation to each other because of the sterical hindrance of the pyridine rings (Figure 6). Therefore the N–M–N bond angles in **2** (av. $85.0(2)^\circ$) are smaller compared to the ones in **1** (av. $94.2(2)^\circ$). The two pyridine molecules are avoiding each other, as reflected by elongated M–N distance compared to **1** ($2.421(4)$ Å and $2.279(4)$ Å, respectively). Furthermore the N–M–M–N torsion angles have different values. Those are $32.6(2)^\circ$ for $\text{N1-M1-M1}^i\text{-N2}^i$, $29.8(2)^\circ$ for $\text{N2-M1-M1}^i\text{-N1}^i$, $16.7(2)^\circ$ for $\text{N3-M2-M2}^i\text{-N4}^i$ and $17.8(2)^\circ$ for $\text{N4-M2-M2}^i\text{-N3}^i$.

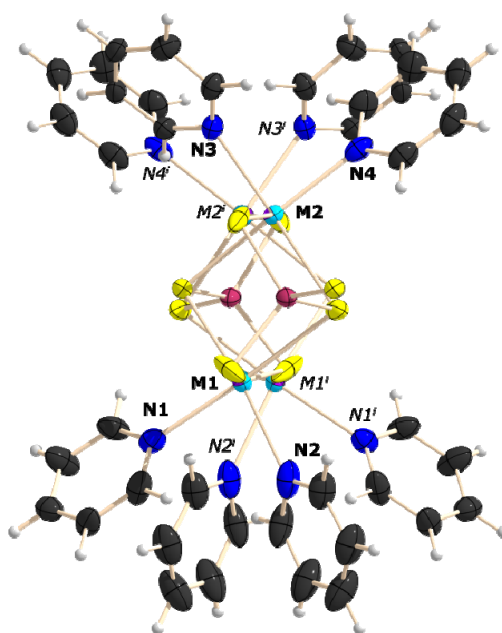


Figure 6. Arrangement of the pyridine ligands in **2**.

Due to the higher ionic character of the Na–S interaction compared to the Mn–S bond, the overall metal–sulfur distance is elongated by an average $0.184(2)$ Å. The angles in the planar four membered M_2S_2 ring differ only by about 2° in both compounds, thus the M–M distance is with $3.802(2)$ Å only slightly longer than $3.777(1)$ Å found in **1**.

Figure 7 shows the unit cell of **2** with view along the chains along the *b* axis. It can be observed, that each chain is shielded from the other by the coordinating pyridine rings.

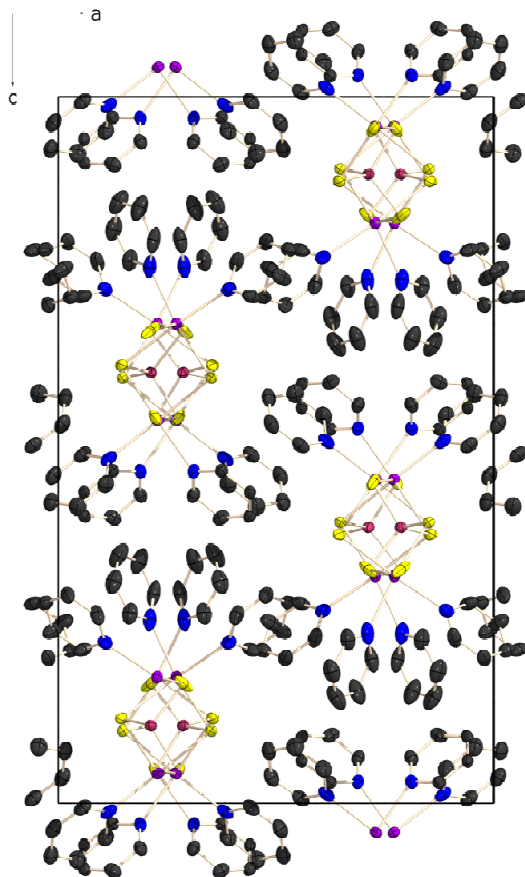


Figure 7. Unit cell of **2**. Ellipsoids are drawn at the 50% probability level. Hydrogen atoms are omitted for clarity.

Molecular and Crystal Structure of $\text{py}_4\text{Mn}(\text{H}_2\text{PO}_4)_2$ (**3**)

The next step was to substitute Na_2S with H_2O to yield a substitution of sulfur with oxygen. Dissolving the precipitate of the reaction of P_4S_{10} and KMnO_4 in pyridine, yields colourless block shaped crystals of $\text{py}_4\text{Mn}(\text{H}_2\text{PO}_4)_2$ (**3**).

This compound crystallizes in the tetragonal space group $P-42_1/c$ with four formula units in the unit cell. Figure 8 shows the molecular structure of **3** and gives selected atom distances and bond angles.

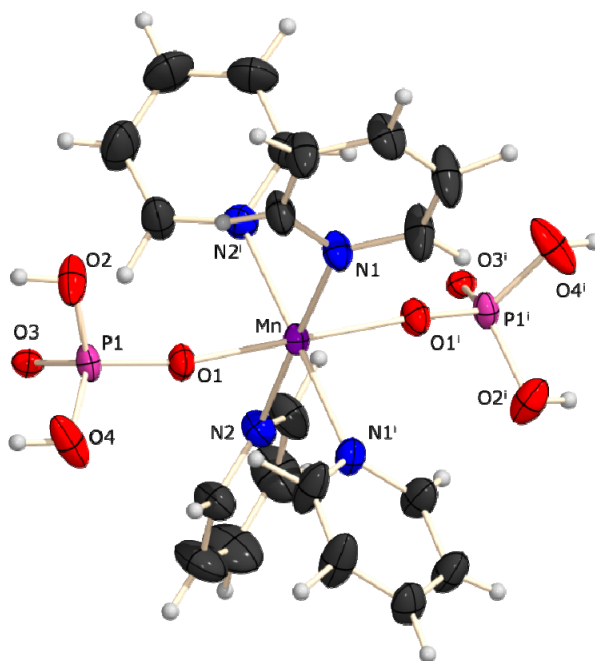


Figure 8. Molecular structure of **3**. Ellipsoids are drawn at the 50% probability level. Symmetry operation: $i = 1-x, -y, z$. Selected atom distances [Å] and bond angles [°]: Mn–N1 2.311(2), Mn–N2 2.314(2), Mn–O1 2.075(2), P1–O1 1.491(2), P1–O2 1.580(3), P1–O3 1.517(2), P1–O4 1.561(2); N1–Mn–N2 88.8(1); N1–Mn–N1i 90.6(1), N2–Mn–N2i 91.8(1), N1–Mn–O1 90.2(1), N1i–Mn–O1 87.6(1), N2–Mn–O1 90.8(1), N2i–Mn–O1 91.3(1).

The central manganese atom is octahedrally surrounded by two H_2PO_4^- anions and four pyridine rings. The octahedron deviates from regularity only very slightly, which confirms the range of the angles around the Mn(II) between 87.6(1) and 91.8(1)°.

Only one other compound consisting of manganese(II) and dihydrogenphosphate has been found in the literature. In 2006 Tang *et al.* were able to synthesise a similar structure starting from MnCO_3 , H_2O , H_3PO_4 and 2,2'-bipyridine.^[10] The structure of $[(\text{bipy})\text{Mn}(\text{H}_2\text{PO}_4)_2]$ (bipy = 2,2'-bipyridine) (**II**) is shown in Figure 9.

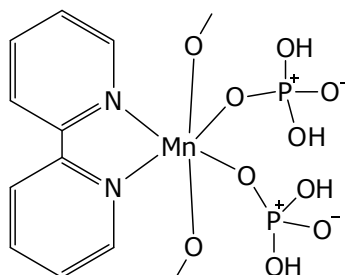


Figure 9. Structure of $(\text{bipy})\text{Mn}(\text{H}_2\text{PO}_4)_2$ (**II**), synthesized by Tang *et al.*.

It is built up by edge-sharing Mn(II) octahedra. In each case two asymmetric units share one edge and are connected to the next *via* one corner. Attention should be paid to the fact that **II** disposes four H_2PO_4^- entities and one 2,2'-bipyridine acting as chelating ligand, while **3** consists of four pyridine and two H_2PO_4^- ligands. Because of the compulsory bond angle of $73.4(1)^\circ$ of the bipyridine skeleton the other angles of the octahedron at the central atom differ quite strongly from 90° . They are in the range of $75.6(2)$ and $99.6(1)^\circ$.

The Mn–N bond lengths in **3** are with $2.311(2)$ and $2.314(2)$ Å in **3** longer compared to $2.239(2)$ and $2.247(3)$ Å in **II**, while the Mn–O distances ($2.075(2)$ Å) are shortened compared to $2.144(2)$ and $2.157(2)$ Å.

The H_2PO_4^- entity in $\text{py}_4\text{Mn}(\text{H}_2\text{PO}_4)_2$ deviates with $105.9(2)$ to $109.4(1)^\circ$ only slightly from a regular tetrahedron, while the similar angles in **II** diverse strongly between $102.4(2)$ and $113.7(2)^\circ$. This may be caused by the Mn(II) octahedron being partially connected over edges.

Because of each bipyridine being 180° rotated to the previous one in **II** the H_2PO_4^- entities are sterically hindered from interacting with one another, which leads to the formation of chains. In **3** the four pyridine molecules coordinate to the manganese in a plane with the two H_2PO_4^- entities on either side of that plane. This situation gives the oxygen atoms the opportunity to form hydrogen bonds and therefore to arrange in layers. The hydrogen H1 is with a bond length of $0.85(3)$ Å connected to the O2 and interacts with the terminal O3 atom of the next moiety ($d(\text{H}\cdots\text{A})=1.72(4)$ Å). The distance of the donor to the acceptor has a value of $2.565(3)$ Å, with a O2–H11 \cdots O3 angles of $170(4)^\circ$.

Figure 10a shows an excerpt of a layer, with the hydrogen bonds presented in dashed light blue lines. Ever four motives accumulate in such a manner forming channels throughout the layer (Figure 10b). Figure 10c shows the unit cell with view from the top of the layers.

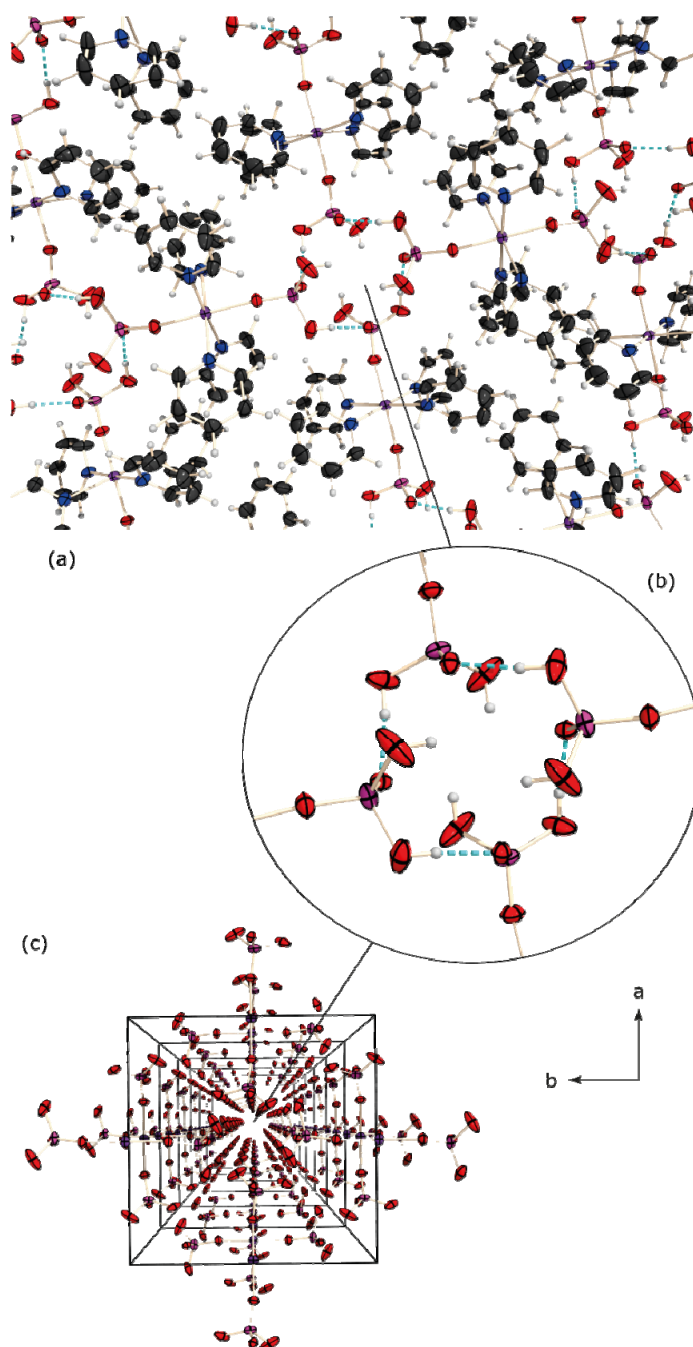


Figure 10. Section of the layered structure of **3** (a, b) and unit cell (c). View along the *c* axis. Ellipsoids are drawn at the 50% probability level. In (c) pyridine molecules are omitted for clarity.

The pyridine molecules arrange regularly on both sides of a layer. This shields the phosphate layers electrostatically against each other, so that no interaction between the levels can take place (Figure 11).

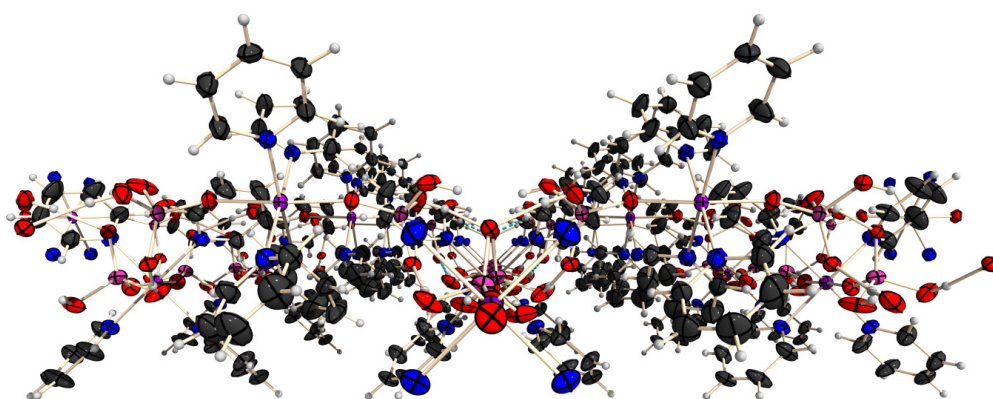


Figure 11. Molecular structure of **2** with view along the *b* axis.

Figure 12 shows the view along the layers and the arrangement in the unit cell.

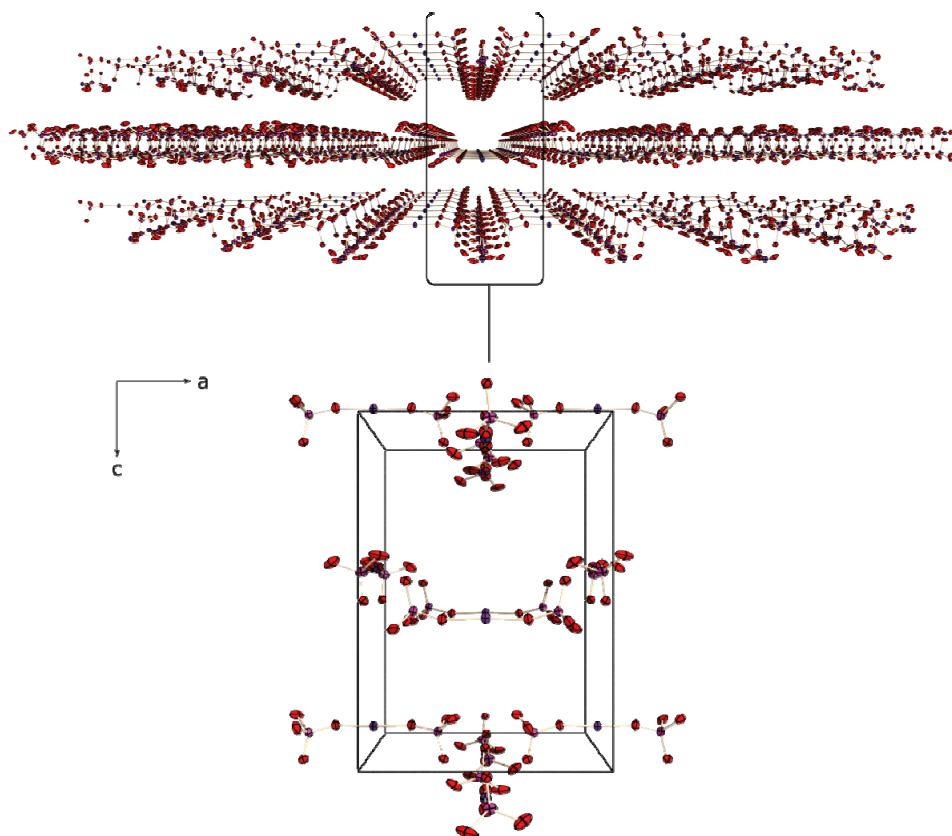
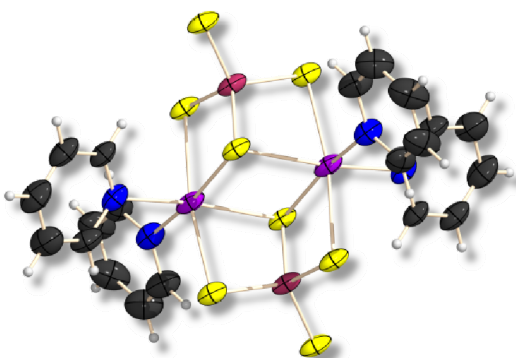


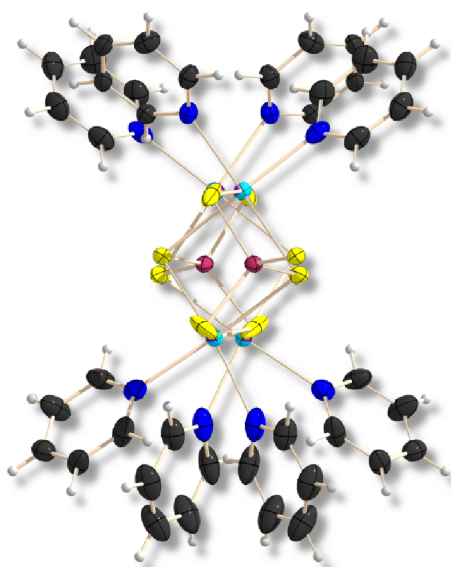
Figure 12. View along the layers (upper picture) and unit cell with view along the *b* axis (lower picture). Ellipsoids are drawn at the 50% probability level. Pyridine molecules are omitted for clarity.

Conclusion

Manganese(II) in combination with polydentate anions is often used to yield coordination polymers. The tetrathiophosphate anion PS_4^{3-} provides four soft coordination sites and is a good candidate for the combination with a low valent transition metal. In the course of our investigations to introduce PS_4^{3-} as a building block in coordination polymers prepared from solution, a first Mn(II) tetrathiophosphate complex $[\text{py}_2\text{MnPS}_4]_2[\text{pyH}]_2 \cdot 4 \text{ py}$ (**1**) was obtained.

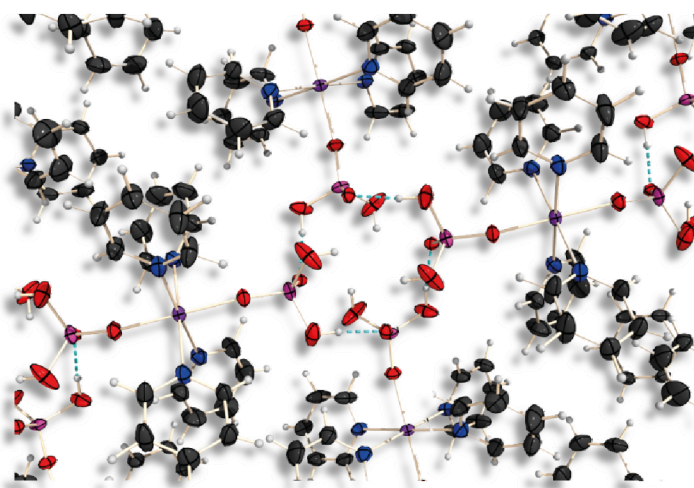


Compound **1** has a high tendency of formation as it is obtained from several different reactions. In this complex manganese, tetrathiophosphate and pyridine together form isolated monomeric entities. The formal substitution of the organic cation pyH^+ with a monovalent metal cation like Na^+ leads to the formation of a one dimensional coordination polymer $\text{py}_4\text{NaMnPS}_4$ (**2**). This is caused by the higher coordination sphere at the sodium cation.



Complex **2** is obtained when P_4S_{10} , Na_2S and $KMnO_4$ are refluxed in pyridine. The chains, formed by the manganese and sodium cations and the PS_4^{3-} anions are shielded by coordinated pyridine molecules, thus preventing the polymer from higher dimensionality.

Using oxo- instead of a thiophosphate leads to a layered arrangement in the crystal. This can be achieved by the formation of hydrogen bonds, as shows the structural arrangement in $py_4Mn(H_2PO_4)_2$ (**3**).



Experimental Section

General conditions. All reactions were carried out under inert gas atmosphere using Argon (Messer Griesheim, purity 4.6 in 50 L steel cylinder) and working with Schlenk techniques. The glass vessels used were stored in a 130 °C drying oven. Before filling they were flame dried *in vacuo* at 10^{-3} mbar. Elemental sulfur was used as obtained (Acros Organics). P_4S_{10} was commercially obtained (Riedel-de H  en) and purified by extraction with CS_2 before use. All other chemicals were used as obtained (Sigma Aldrich). The solvents were dried with commonly known methods and freshly distilled before use. **NMR Spectroscopy.** NMR spectra were recorded using a Jeol EX 400 Eclipse instrument operating at 161.997 MHz (^{31}P). Chemical shifts are referred to 85% H_3PO_4 as external standard. If not mentioned otherwise, all spectra were

measured at 25 °C. The % data correspond to the intensities in the ^{31}P NMR spectra with respect to the total intensity. The difference to 100% belongs to not assignable signals. **Mass Spectrometry.** The mass spectrometry was performed with a MStation JMS 700 (Jeol). Measurements were carried out using the ionisationmethode DEI+/EI+. This method involves the problem of exposing the compounds to air, while embedding them into the matrix (p-nitroalcohol). **IR Spectroscopy.** The spectra were recorded using a PerkinElmer Spektrum one FT-IR instrument (KBr); Perkin-Elmer Spectrum BXII FT-IR instrument equipped with a Diamant-ATR Dura Sampler at 25 °C (neat). Raman spectra were recorded on a Bruker RAMII Raman instrument ($\lambda = 1064\text{ nm}$, 200 mW, 25 °C) equipped with D418-T Detector at 200 mW at 25 °C. **Melting and decomposition points** were determined by differential scanning calorimetry (Linseis DSC-PT10, calibrated with standard pure indium and zinc). Measurements were performed at a heating rate of 5 °C min^{-1} in closed aluminum sample pans with a 0.1 mm hole in the lid for gas release to avoid an unsafe increase in pressure under a nitrogen flow of 20 mL min^{-1} with an empty identical aluminum sample pan as a reference. Melting points were checked with a Büchi Melting Point B-540 in open glass capillaries.

X-ray Crystallography. The single-crystal X-ray diffraction data were collected using an Oxford Xcalibur3 diffractometer equipped with a Spellman generator (voltage 50 kV, current 40 mA), Enhance molybdenum K_{α} radiation source ($\lambda = 71.073\text{ pm}$), Oxford Cryosystems Cryostream cooling unit, four circle kappa platform and a Sapphire CCD detector. Data collection and reduction were performed with CrysAlisPro.^[16] The structures were solved with SIR97^[17], SIR2004^[18], refined with SHELXL-97^[19], and checked with PLATON^[20], all integrated into the WinGX software suite^[21]. The finalized CIF files were checked with checkCIF.^[22] All non-hydrogen atoms were refined anisotropically. The hydrogen atoms were located in difference Fourier maps and placed with a C-H distance of 0.98 Å for C-H bonds. Intra- and intermolecular contacts were analysed with DIAMOND (version 3.2i), thermal ellipsoids are drawn at the 50% probability level. Selected crystallographic data and refinement details for the structure determination of compounds **1–3** are summarized in Table 1. These data can be obtained free of charge from The Cambridge Crystallographic Data Centre via www.ccdc.cam.ac.uk/data_request/cif.

Table 1. Crystallographic and refinement data

	$[\text{py}_2\text{MnPS}_4]_2 [\text{pyH}]_2 \cdot 4 \text{ py}$	$\text{py}_4\text{NaMnPS}_4$	$\text{py}_4\text{Mn}(\text{H}_2\text{PO}_4)_2$
formula	$\text{C}_{50}\text{H}_{52}\text{N}_{10}\text{Mn}_2\text{P}_2\text{S}_8$	$\text{C}_{20}\text{H}_{20}\text{N}_4 \text{NaMnPS}_4$	$\text{C}_{20}\text{H}_{24}\text{N}_4\text{MnP}_2\text{O}_8$
M [g/mol]	1221.32	546.59	565.31
crystal system	monoclinic	orthorombic	tetragonal
space group	$P2_1/c$	$Pbca$	$P-42_1/c$
colour/habit	orange block	yellow block	colourless block
crystal size	0.25x0.25x0.05	0.25x0.25x0.15	0.4x0.35x0.3
a [Å]	14.734(3)	16.7522(7)	12.26570(10)
b [Å]	10.8245(9)	10.8304(5)	12.26570(10)
c [Å]	18.064(2)	27.2171(11)	17.3552(3)
α [°]	90	90	90
β [°]	96.527(16)	90	90
γ [°]	90	90	90
V [Å ³]	2862.3(7)	4938.1(3)	2611.04(5)
Z	2	8	4
ρ_{calc} [g/cm ⁻³]	1.417	1.470	1.438
μ [mm ⁻¹]	0.833	0.869	0.678
$F(000)$	1260	2240	1164
θ range [°]	4.13–24.99	4.17–25.35	4.40–28.26
T [K]	173(2)	173(2)	173(2)
data collected	25210	43637	30383
data unique	4983	4399	3226
data observed	3256	3839	3007
R (int)	0.0919	0.0551	0.0309
GOOF	1.000	1.054	0.992
R_1, wR_2 ($I > 2\sigma I_0$)	0.0564, 0.1367	0.0482, 0.0842	0.0289, 0.0720
R_1, wR_2 (all data)	0.0988, 0.1591	0.0573, 0.0882	0.0327, 0.0756
larg. diff	0.634	0.572	0.460
peak/hole (e/Å)	−0.417	−0.775	−0.286

Syntheses

[py₂MnPS₄]₂[pyH]₂ · 4py (1): P₄S₁₀ (542.3 mg, 1.2 mmol), Na₂S (95.0 mg, 1.2 mmol) and MnCl₂ · 2 H₂O (395.0 mg, 2.4 mmol) were dissolved in pyridine (12 mL) and refluxed for 1 h. After one day the yellow precipitate is removed from the colourless solution by filtration. After another day orange block shaped crystals of **1** could be observed together with colourless crystals of MnCl₂ · 4 py. An exact yield could not be determined, as both products could not be separated.

³¹P{¹H} NMR (pyridine): δ [ppm] = 150.5 (s, 6.8%, br), 112.4 (s, 40.3%, br), 59.8 (s, 53.0%). **Elemental analysis** calc. N 9.29, C 39.82, H 3.56, S 28.35; found. N 6.99, C 29.86, H 3.16, S 13.26. **Raman** (200 mW, rt): ν [cm⁻¹] = 3229 (10), 3156 (7), 3071 (50), 3021 (7), 3003 (8), 2969 (12), 2942 (8), 2930 (7), 2878 (8), 2543 (14), 1770 (8), 1666 (8), 1630 (8), 1607 (29), 1573 (9), 1412 (12), 1229 (8), 1192 (25), 1182 (12), 1152 (9), 1009 (100), 474 (81, PS₄³⁻), 426 (6), 387 (11), 305 (10), 268 (9), 222 (75), 196 (6), 154 (58). **IR** (200 mW, rt): ν [cm⁻¹] = 3060 (ww) 3038 (ww) 3001 (ww) 2961 (ww) 1634 (ww) 1600(w) 1573 (ww) 1535 (ww), 1489 (w), 1445 (s), 1364 (ww), 1260 (w), 1220(w), 1096 (w), 1080 (m), 1038 (s), 1077 (s), 880 (s), 801 (w), 754 (vs), 692 (vs), 677 (s). **Mass spectrometry** *m/z* (ESI-) *m/z* = 741 ([py₄Mn₂P₂S₈]⁻), 428 ([Mn₂P₂S₈]⁻), 406 ([H₁₀Mn₂P₂S₇]⁻), 303 ([H₂Mn₂PS₅]⁻), 283 ([H₆MnPS₆]⁻), 219 ([H₇MnPS₄]⁻). **DSC** (5 °C/min): T_{dec} = 196.1 °C.

py₄NaMnPS₄ (2): One equivalent of P₄S₁₀ (444.5 mg, 1.0 mmol), Na₂S (77.0 mg, 1.0 mmol) and two equivalents KMnO₄ (316.0 mg, 2.0 mmol) were dissolved in pyridine (10 mL) and refluxed for 1 h. 0.6 mL of the brownish solution were filled into an NMR tube for analytical reasons. After one week yellow block shaped crystals of **2** were observed in the NMR tube.

³¹P{¹H} NMR (pyridine, rt): δ [ppm] = 174.7 (s, br, 80.1%), 104.4 (s, 13.3%).

py₄Mn(H₂PO₄)₂ (3): A suspension of P₄S₁₀ (2716.0 mg, 6.1 mmol) in pyridine (40 mL) was refluxed for 1 h. The yellow precipitate was dissolved in water (30 mL) and again refluxed for 1h. KMnO₄ was added and the suspension was stirred. Colorless block shaped crystals of **3** were obtained from the solution after 7 d.

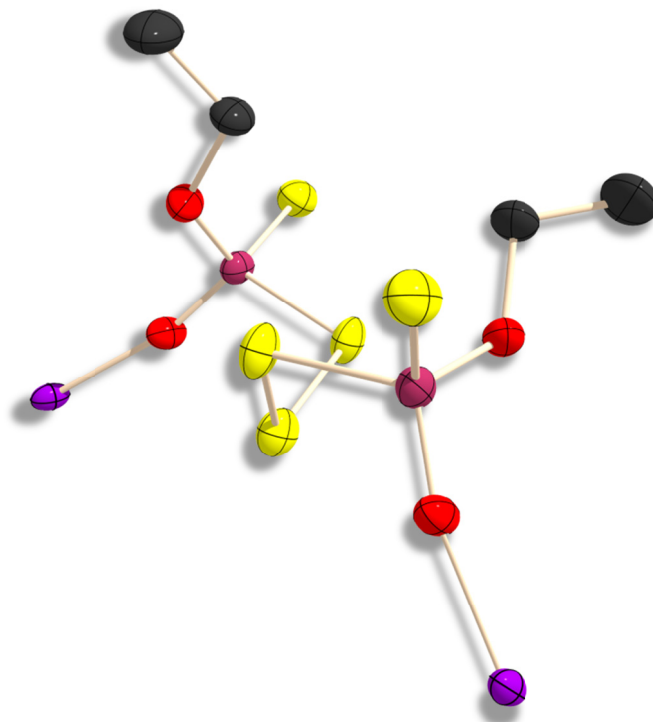
$^{31}\text{P}\{^1\text{H}\}$ NMR (pyridine, rt): no resonances detected. **IR** (200 mW, rt): ν [cm^{-1}] = 3371 (br, w), 1641 (ww), 1611 (ww), 1588 (s), 1581 (m), 1573 (w), 1484 (w), 1356 (ww), 1215 (w), 1148 (m), 1068 (m), 1031 (s), 997 (s), 990 (m), 959 (m), 748 (vs), 700 (vs). **Mass spectrometry** m/z (FAB+) = 539 ($[\text{py}_4\text{MnP}_2\text{O}_5\text{H}_{10}]^-$), 461 ($[\text{py}_4\text{MnPO}_4]^-$), 307 ($[\text{py}_2\text{MnPO}_4]^-$), 233 ($[\text{H}_4\text{MnP}_2\text{O}_7]^-$), 154 ($[\text{H}_4\text{MnPO}_4]^-$), 80 ($[\text{H}_2\text{PO}_4]^-$). **DSC** (5 $^\circ\text{C}/\text{min}$): $T_{\text{dec}} = 223.7$ $^\circ\text{C}$.

-
- [1] Loewig, *Grundriss der Organischen Chemie* **1852**, 383-386.
- [2] R. B. E. Krause, *Ber. Dt. Chem. Ges.* **1919**, 173.
- [3] C. Löw, *Dissertation* Dortmund **2002**.
- [4] S. S. Kostina, T. Singh, W. J. Leigh, *Organometallics* **2012**, 31, 3755-3767.
- [5] J. E. Anderson, S. M. Sawtelle, J. S. Thompson, S. A. K. Nguyen, J. Calabrese, *Inorg. Chem.* **1992**, 31, 2778-2785.
- [6] K. Karaghiosoff, M. Schuster, *Phosphorus, Sulfur Silicon Relat. Elem.* **2001**, 168-169, 117-122.
- [7] E. Gokcinar, K. Karaghiosoff, T. M. Klapoetke, C. Evangelisti, C. Rotter, *Phosphorus, Sulfur Silicon Relat. Elem.* **2010**, 185, 2527-2534.
- [8] A. Dimitrov, I. Hartwich, B. Ziemer, D. Heidemann, M. Meisel, *Z. Anorg. Allg. Chem.* **2005**, 631, 2439-2444.
- [9] a) S. Natarajan, M. P. Attfield, A. K. Cheetham, *Angew. Chem., Int. Ed. Engl.* **1997**, 36, 978-980; b) S. Natarajan, A. K. Cheetham, *Chemical Commun.* **1997**, 1089-1090; c) S. Natarajan, A. K. Cheetham, *J. Solid State Chem.* **1997**, 134, 207-210.
- [10] P. B. Hitchcock, M. F. Lappert, B. J. Samways, E. L. Weinberg, *Journal of the Chemical Society, Chem. Commun.* **1983**, 0, 1492-1494.
- [11] S. Banerjee, C. D. Malliakas, M. G. Kanatzidis, *Inorg. Chem.* **2012**, 51, 11562-11573.
- [12] A. F. Holleman, E. Wiberg, N. Wiberg, *Lehrbuch der anorganischen Chemie*, Walter de Gruyter Verlag, Berlin, **2007**.
- [13] F. H. Allen, O. Kennard, D. G. Watson, L. Brammer, A. G. Orpen, R. Taylor, *J. Chem. Soc., Perkins Trans 2* **1987**, S1-S19.
- [14] A. Bondi, *J. Phys. Chem.* **1966**, 70, 3006-3007.
- [15] A. K. Cheetham, G. Ferey, T. Loiseau, *Angew. Chem., Int. Ed.* **1999**, 38, 3268-3292.
- [16] *CrysAlisPro 1.171.36.21*, Agilent Technologies, **2012**.
- [17] A. Altomare, G. Cascarano, C. Giacovazzo, A. Guagliardi, A. A. G. Moliterni, M. C. Burla, G. Poidori, M. Camalli, R. Spagna, **1997**, 343.
- [18] a) M. C. Burla, R. Caliandro, M. Camalli, B. Carrozzini, G. L. Cascarano, L. De Caro, C. Giacovazzo, G. Polidori, R. Spagna, Institute of Crystallography, Bari (Italy), **2004**; b) M. C.

- Burla, R. Caliandro, M. Camalli, B. Carrozzini, G. L. Cascarano, L. De Caro, C. Giacovazzo, G. Polidori, R. Spagna, *Journal of Applied Crystallography* **2005**, 38, 381-388.
- [19] a) G. M. Sheldrick, *SHELXL-97, Program for the Refinement of Crystal Structures*. University of Göttingen, Göttingen (Germany), **1997**; b) G. M. Sheldrick, *Acta Crystallographica, Section A: Foundations of Crystallography* **2008**, A64, 112-122.
- [20] A. L. Spek, *Platon, A Multipurpose Crystallographic Tool*, Utrecht University, Utrecht, The Netherlands, **2012**.
- [21] L. J. Farrugia, *J. Appl. Crystallogr.* **1999**, 32, 837-838.
- [22] <http://journals.iucr.org/services/cif/checkcif.html>

$\text{py}_4\text{Mn}[(\text{EtO}(\text{S})\text{P}(\text{O})\text{S})_2\text{S}] \cdot \text{py}$ **A New Coordination Polymer**

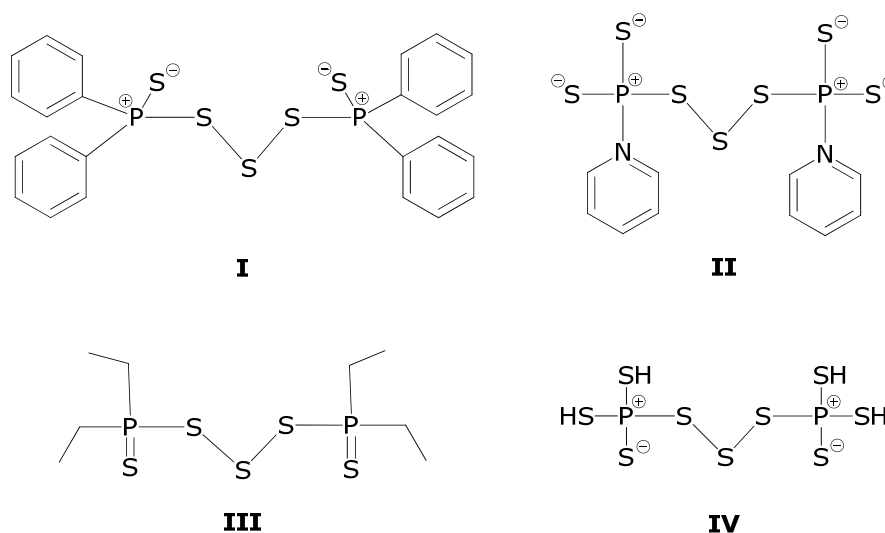
As to be submitted to *Chem. Commun.*



A novel one-dimensional manganese(II) O-ethyl phosphorodithioate, templated by pyridine, has been prepared by reacting phosphorus pentasulfide with sodiumsulfide and KMnO_4 in pyridine and subsequent addition of ethanol. The structure of $\text{py}_4\text{Mn}[(\text{EtO}(\text{S})\text{P}(\text{O})\text{S})_2\text{S}] \cdot \text{py}$ (**1**) could be determined using single crystal X-ray diffraction.

Introduction

The family of compounds, containing polysulfide linkages between phosphorus atoms, shows a remarkable diversity. But to the best of our knowledge only four acyclic compounds containing an S_3 bridge have been described in the literature so far (Scheme 1).

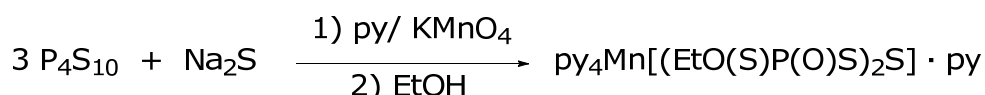


Scheme 1. Diposphorus compounds with polysulfidic linkage (I^[1], II^[2], III^[3], IV^[4])

In recent times it has been reported on the ability of transition metals to induce polymerization in at least one dimension, so chains, layers or even three dimensional networks can be formed.^[5] In many cases additionally amines are included into the structure as they show a rather great templating potential. In the following it is reported on a new compound containing a trisulfide bridge, manganese(II) and pyridine in the role of the structure directing amine.

Results and Discussion

The compound py₄Mn[(EtO(S)P(O)S)₂S] (**1**) was prepared by stirring a suspension of P₄S₁₀, Na₂S and KMnO₄ in pyridine and subsequent dissolving of the precipitate in ethanol (Scheme 1). Compound **1** was isolated as colourless block shaped crystals, which are quite air and water stable and melt at 233.4 °C.



Scheme 1. Synthesis of py₄Mn[(EtO(S)P(O)S)₂S] · py(**1**)

The structure of **1** was determined using single-crystal X-ray diffraction. It crystallizes in the monoclinic space group C2/c with four formula units in the unit cell. Figure 1 shows the molecular structure of **1** and selected atom distances and bond angles are listed.

Compound **1** consists of [(EtO(S)P(O)S)₂S]²⁻ dianions with one phosphorus atom being surrounded by an ethoxy group, an oxygen and two sulfur atoms. Two phosphorus atoms are connected by an S₃ bridge. The dianions are connected *via* Mn(II) atoms with oxygen in the bridging position. Each manganese atom is coordinated by four pyridine molecules, which play a structure directing role and at the same time satisfy the coordination sphere at the manganese atom by acting as ligands. This leads to the formation of one dimensional coordination polymers.

Taking a look at the bonding situation at the phosphorus atom, a comparison of selected atom distances and bond angles with those described for compounds **I–III** can be found in Table 1. The distance of the phosphorus to the one-coordinated sulfur atom (S1) is with a value of 1.952(1) Å closer to a P–S double than a single bond (1.922(14) Å^[6] and 2.11 Å^[7] respectively). The bond between the twofold coordinated sulfur (S2) and the phosphorus atom has a length of 2.118(2) Å, which shows rather pure single bond character. The value for the S2–S3 distance, with S3 occupying the bridging position between two sulfur atoms, is 2.064(1) Å. It therefore lies in the range given for polysulfide chains (2.051(22) Å^[6]) and is only slightly enlarged compared to the values found in **I–III**.

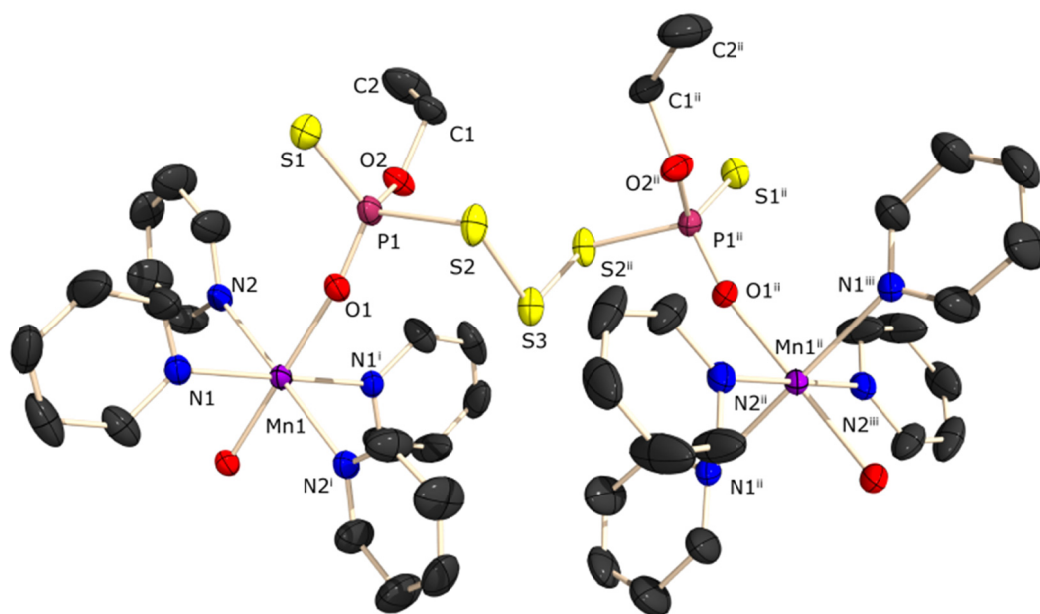


Figure 1. Molecular structure of **1** in the crystal. Thermal ellipsoids are shown at 50% probability level. Hydrogen atoms are omitted for clarity. Symmetry operation: $i = x, -y, 0.5+z$. Selected atom distances and bond angles: Mn1–O1 2.143(2), Mn1–N1 2.307(2), Mn1–N2 2.301(2), P1–O1 1.497(3), P1–O2 1.594(2), P1–S1 1.952(3), P1–S2 2.118(3), S2–S3 2.064(3); O1–Mn1–O1ⁱ 180.0, O1–Mn1–N1 90.3(1), O1–Mn1–N2 89.7(2), N2–Mn1–N1ⁱ 92.6(2), N2–Mn1–N1 87.4(2), N2–Mn1–N2ⁱ 180.0, O1–P1–O2 104.3(3), O1–P1–S1 120.0(2), O2–P1–S1 113.4(1), O1–P1–S2 109.4(1), O2–P1–S2 104.7(1), S1–P1–S2 104.1(1), S3–S2–P1 102.9(1), P1–O1–Mn1 166.8(2), S2–S3–S2ⁱ 106.6(1).

The P1–O2 bond length, with O2 being the oxygen atom of the ethoxy group, is with 1.594(2) Å very similar to the value measured in [pyH]₂[P₂S₆(OEt)₂] (1.606(2) Å)^[8] and does not deviate substantially from the calculated one (1.621(7) Å)^[6].

The P–S–S–S torsion angle of 87.9(1)° lies in the same range of magnitude as the corresponding torsion angles described in the literature.^[1–3]

Comparing the data in Table 1 it becomes evident, that the formula of the coordination polymer and the insertion of the huge manganese atom have little influence on the structural parameters in the anionic part of this compound.

The manganese atom is octahedrally surrounded by two oxygen atoms and four pyridine rings. The polyhedron deviates only very slightly from regularity, which confirms the range of the angles around the manganese atom being between 89.7(2)°

and 90.3(1)°. The Mn–N and Mn–O distances are with average values of 2.304 Å and 2.143 Å in the same range as those found in py₄Mn(NO₃)₂ · 2py (Mn–N 2.274(9) Å and Mn–O 2.133(7) Å respectively).^[9]

Table 1. Comparison of atom distances and angles of **1**

	1	I ^[1]	II ^[2]	III ^[3]
atom distances [Å]				
P1–S1	1.952(1)	1.933(2)	1.930(1)	1.941(2)
P1–S2	2.118(1)	2.123(2)	2.125(2)	2.114(3)
S2–S3	2.064(1)	2.043(2)	2.053(2)	2.056(3)
P1–O2	1.594(2)			
angles [°]				
S1–P1–S2	104.1(1)	114.1(1)		103.7(2)
S2–P1–O2	104.7(1)			
S2–S3–S2 ⁱⁱ	106.6(1)	106.8(1)	107.6(1)	107.0(1)
S3–S2–P1	102.9(1)	100.0(1)	105.4(1)	106.5(2)
P1–S2–S3–S2 ⁱⁱ	87.9(1)	87.4(2)	85	89.2(2)

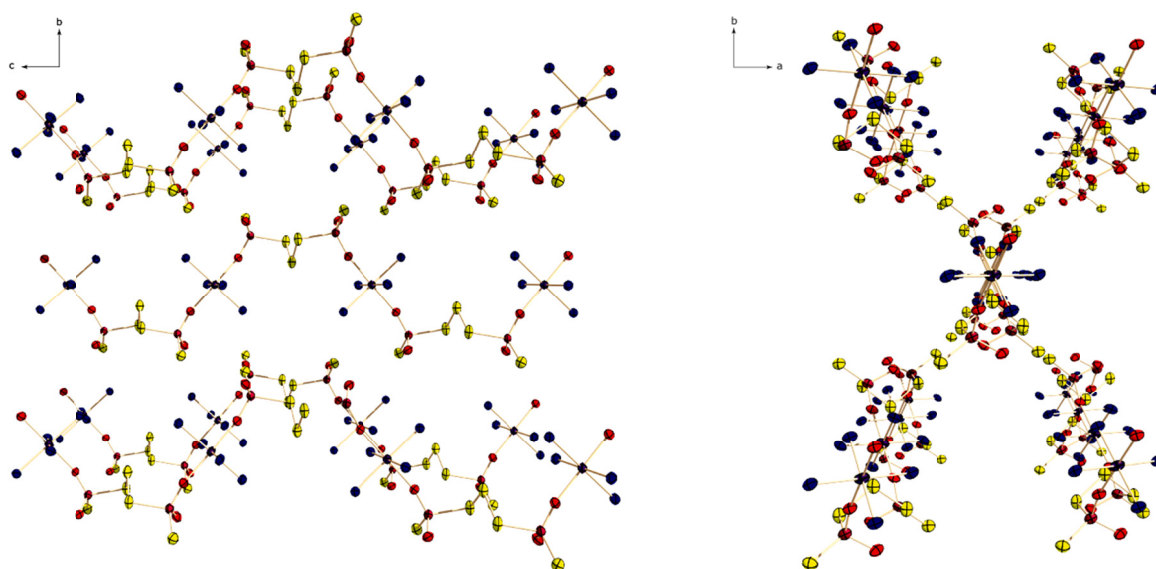


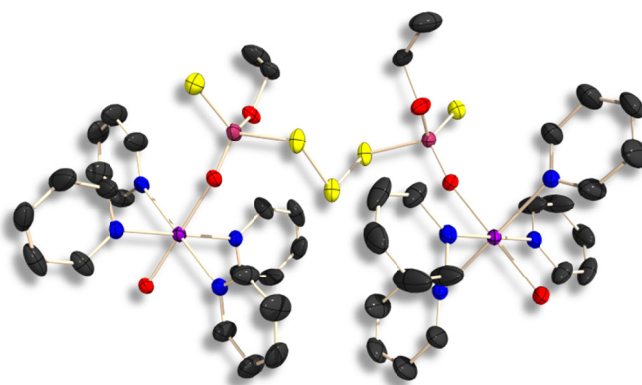
Figure 2. Unit cell of **1** with two different viewing directions. Thermal ellipsoids are shown at 50% probability level. Carbon and hydrogen atoms are omitted for clarity.

The py₄Mn entities are located *gauche* in reference to the anionic part, with a Mn–P–P–Mn torsion angle of 58.1(1)°. Thus corrugated infinite one dimensional chains are

built, which run parallel to the *c* axis and are arranged in a staggered conformation along the *b* axis (Figure 2).

Conclusions

The new one-dimensional coordination polymer $\text{py}_4\text{Mn}[(\text{EtO}(\text{S})\text{P}(\text{O})\text{S})_2\text{S}] \cdot \text{py}$ (**1**) was obtained from the reaction of P_4S_{10} with Na_2S and KMnO_4 in pyridine and subsequent ethanolysis. It contains the first thiodiphosphate anion with a trisulfide bridge between the two phosphorus atoms, as part of the complex.



The formation of the one-dimensional polymer **1** underlines the importance of the structure directing role of the pyridine and the versatile ligand properties of mixed oxo/thiophosphate anions.

Experimental Section

General. All chemical reagents and solvents were obtained from Sigma-Aldrich Inc. or Acros Organics (analytical grade) and were used as supplied without further purification. **NMR Spectroscopy.** NMR spectra were recorded using a Jeol EX 400 Eclipse instrument operating at 161.997 MHz (^{31}P). Chemical shifts are referred to 85% H_3PO_4 as external standard. If not mentioned otherwise, all spectra were measured at 25 °C. The % data correspond to the intensities in the ^{31}P NMR spectra with respect to the total intensity. The difference to 100% belongs to not determinable signals. **Mass Spectrometry.** The mass spectrometry was performed with a MStation JMS 700 (Jeol). Measurements were carried out using the ionisation method

DEI+/EI+. This method involves the problem of exposing the compounds to air, while embedding them into the matrix (p-nitroalcohol). **IR Spectroscopy.** The spectra were recorded using a PerkinElmer Spektrum one FT-IR instrument (KBr); Perkin-Elmer Spectrum BXII FT-IR instrument equipped with a Diamant-ATR Dura Sampler at 25 °C (neat). Raman spectra were recorded on a Bruker RAMII Raman instrument ($\lambda = 1064 \text{ nm}$, 200 mW, 25 °C) equipped with D418-T Detector at 200 mW at 25 °C. **Melting and decomposition points** were determined by differential scanning calorimetry (Linseis DSC-PT10, calibrated with standard pure indium and zinc). Measurements were performed at a heating rate of $5 \text{ }^\circ\text{C min}^{-1}$ in closed aluminum sample pans with a 0.1 mm hole in the lid for gas release to avoid an unsafe increase in pressure under a nitrogen flow of 20 mL min^{-1} with an empty identical aluminum sample pan as a reference. Melting points were checked with a Büchi Melting Point B-540 in open glass capillaries.

X-ray Crystallography. The single-crystal X-ray diffraction data were collected using an Oxford Xcalibur3 diffractometer equipped with a Spellman generator (voltage 50 kV, current 40 mA), Enhance molybdenum K_α radiation source ($\lambda = 71.073 \text{ pm}$), Oxford Cryosystems Cryostream cooling unit, four circle kappa platform and a Sapphire CCD detector. Data collection and reduction were performed with CrysAlisPro.^[10] The structures were solved with SIR97^[11], SIR2004^[12], refined with SHELXL-97^[13], and checked with PLATON^[14], all integrated into the WinGX software suite^[15]. The finalized CIF files were checked with checkCIF.^[16] All non-hydrogen atoms were refined anisotropically. The hydrogen atoms were located in difference Fourier maps and placed with a C-H distance of 0.98 \AA for C-H bonds. Intra- and intermolecular contacts were analysed with DIAMOND (version 3.2i), thermal ellipsoids are drawn at the 50% probability level. Selected crystallographic data and refinement details for the structure determination of compound **1** are summarized in Table 2. CCDC 966118 contains the supplementary crystallographic data for compounds **1**. These data can be obtained free of charge from The Cambridge Crystallographic Data Centre via www.ccdc.cam.ac.uk/data_request/cif.

$\text{py}_4\text{Mn}[(\text{EtO}(\text{S})\text{P}(\text{O})\text{S})_2\text{S}] \cdot \text{py}$ (1**):** P_4S_{10} (284.9 mg, 0.641 mmol) and Na_2S (15.0 mg, 0.192 mmol) and KMnO_4 (50.6 mg, 0.320 mmol) were suspended in pyridine (5 mL) and stirred for 24 h at ambient temperature, yielding an orange reaction mixture and a white precipitate. The precipitate was separated from the solution, dried *in vacuo* and dissolved in EtOH (5 mL). After 7 d colourless crystals of **1** could be obtained from the yellow solution.

^{31}P { ^1H } NMR (Pyridine, rt): δ [ppm] = 173.2 (s, 41.7%, PS_3^-), 129.3 (s, 4.0%, $\text{P}_2\text{S}_7^{2-}$), 120.2 (s, 5.6%, $\text{P}_2\text{S}_8^{2-}$ (twist)), 104.3 (s, 40.8%, $\text{py}_2\text{P}_2\text{S}_5$), 97.8 (s, 5.6%, $\text{py}_2\text{P}_2\text{S}_4\text{O}$), 56.3 (s, 1.3%, $\text{P}_2\text{S}_8^{2-}$ (chair)). **Raman** (300 mW, rt): ν [cm^{-1}] = 3070 (32), 2924 (12), 2889 (8), 1600 (18), 1574 (16), 1455 (7), 1228 (14), 1216 (8), 1149 (7), 1040 (20), 1009 (88), 991 (17), 653 (24), 635 (47), 510 (12), 474 (73), 439 (12), 371 (10), 248 (12), 220 (100). **IR** (200 mW, rt): ν [cm^{-1}] = 3373.6 (br, vw), 3066.0 (vw), 2977.1 (vw), 2935.2 (vw), 2890.0 (vw), 1954.8 (vw), 1872.9 (vw), 1633.6 (vw), 1598.1 (m), 1574.2 (vw), 1486.0 (vw), 1441.9 (m), 1384.6 (vw), 1253.2 (vw), 1232.7 (vw), 1218.1 (vw), 1135.0 (s), 1097.2 (w), 1065.3 (m), 1036.4 (s), 1005.9 (m), 942.5 (m), 879.7 (w), 769.2 (m), 750.2 (s), 699.9 (vs). **Mass spectrometry** m/z (FAB $^-$) 712.5 ($[\text{Mn}(\text{NC}_5\text{H}_5)_4[(\text{EtO}(\text{S})\text{P}(\text{O})\text{S})_2\text{S}]^-]$), 376.3 ($[\text{Mn}(\text{NC}_5\text{H}_5)]^-$), 185.3 ($[(\text{EtOP}(\text{O})\text{S})_2\text{S}]^-$), 153.2 ($[(\text{EtOP}(\text{O})\text{S})_2]^-$), 111.1 ($[\text{PS}_2\text{O}]^-$), 95.1 ($[\text{PS}_2]^-$), 32.1 ($[\text{S}]^-$). **DSC** (5 $^\circ\text{C}/\text{min}$): $T_{\text{dec}} = 233.4^\circ\text{C}$

Table 2. Details for X-ray data collection and structure refinement for **1**.

1			
empirical formula	$\text{C}_{29}\text{H}_{35}\text{MnN}_5\text{O}_4\text{P}_2\text{S}_5$	$F(000)$	1644
formula mass	794.80	θ range [$^\circ$]	4.37 – 25.25
T [K]	173(2)	index ranges	$-14 \leq h \leq 14$
crystal size [mm]	0.2 x 0.1 x 0.1		$-21 \leq k \leq 21$
crystal description	colourless needles		$-22 \leq l \leq 22$
crystal system	monoclinic	reflns. collected	24960
space group	$C2/c$	reflns. obsd.	2678
a [\AA]	11.771(4)	reflns. unique	3305
b [\AA]	17.505(5)	R_{int}	0.0481
c [\AA]	18.520 (5)	R_1, wR_2 (2σ data)	0.0387, 0.0871
β [$^\circ$]	104.17 (3)	R_1, wR_2 (all data)	0.0523, 0.0952
V [\AA^3]	3700.1(2)	GOOF on F^2	0.976
Z	4	larg. diff peak	0.758/−0.365
$\rho_{\text{calcd.}}$ [g cm^{-3}]	1.427	hole ($\text{e}/\text{\AA}$)	
μ [mm^{-1}]	0.766		

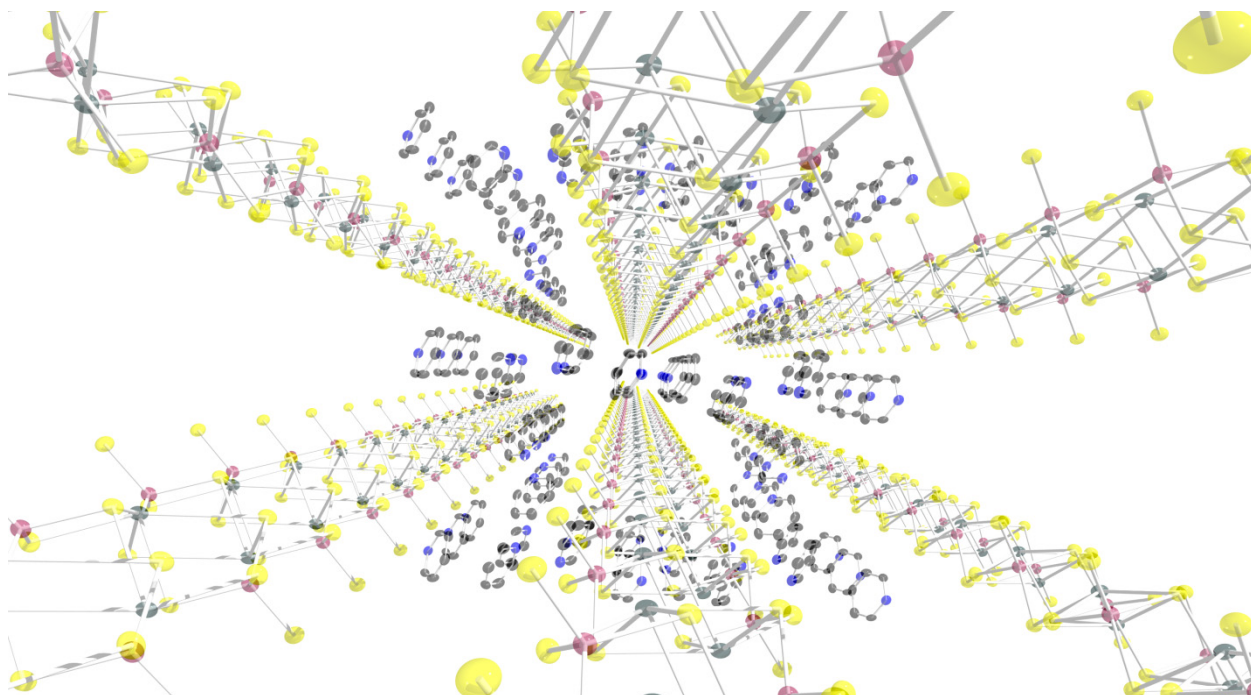
Acknowledgement

Financial support by the Department of Chemistry, Ludwig Maximilian University, is gratefully acknowledged. We thank Prof. T. M. Klapötke, Department of Chemistry, Ludwig Maximilian University, for the generous allocation of diffractometer time and for his continuous support.

-
- [1] M. Kulcsar, A. Silvestru, M. Vonas, *Acta Crystallogr., Sect. E: Struct. Rep. Online* **2008**, 64, o1683-o1684.
 - [2] C. Rotter, C. Evangelisti, S. Schoenberger, T. M. Klapötke, K. Karaghiosoff, *Chem. Commun. (Cambridge, U. K.)* **2010**, 46, 5024-5025.
 - [3] A. C. Gallacher, A. A. Pinkerton, *Acta Crystallogr., Sect. C* **1992**, C48, 701-703.
 - [4] a) J.-M. Babo, L. Jouffret, J. Lin, E. M. Villa, T. E. Albrecht-Schmitt, *Inorg. Chem.* **2013**, 52, 7747-7751; b) T. Roedl, R. Weihrich, J. Wack, J. Senker, A. Pfitzner, *Angew. Chem., Int. Ed.* **2011**, 50, 10996-11000, S10996/10991-S10996/10995.
 - [5] A. K. Cheetham, G. Férey, T. Loiseau, *Angew. Chem. Int. Ed.* **1999**, 38, 3268-3292.
 - [6] F. H. Allen, O. Kennard, D. G. Watson, L. Brammer, A. G. Orpen, R. Taylor, *J. Chem. Soc., Perkin Trans. 2* **1987**, S1-S19.
 - [7] A. F. Holleman, E. Wiberg, N. Wiberg, *Lehrbuch der anorganischen Chemie*, Walter de Gruyter Verlag, Berlin, **2007**.
 - [8] S. Schoenberger, S. Kroenauer, K. Karaghiosoff, submitted to *Z. Anorg. Allg. Chem.*
 - [9] D. V. Soldatov, J. Lipkowski, *J. Struct. Chem.* **1998**, 39, 238-243.
 - [10] *CrysAlisPro 1.171.36.21*, Agilent Technologies, **2012**.
 - [11] A. Altomare, G. Cascarano, C. Giacovazzo, A. Guagliardi, A. A. G. Moliterni, M. C. Burla, G. Poidori, M. Camalli, R. Spagne, **1997**, 343.
 - [12] a) M. C. Burla, R. Caliendo, M. Camalli, B. Carrozzini, G. L. Cascarano, L. De Caro, C. Giacovazzo, G. Polidori, R. Spagna, Institute of Crystallography, Bari (Italy), **2004**; b) M. C. Burla, R. Caliendo, M. Camalli, B. Carrozzini, G. L. Cascarano, L. De Caro, C. Giacovazzo, G. Polidori, R. Spagna, *Journal of Applied Crystallography* **2005**, 38, 381-388.
 - [13] a) G. M. Sheldrick, *SHELXL-97, Program for the Refinement of Crystal Structures*. University of Göttingen, Göttingen (Germany), **1997**; b) G. M. Sheldrick, *Acta Crystallographica, Section A: Foundations of Crystallography* **2008**, A64, 112-122.
 - [14] A. L. Spek, *Platon, A Multipurpose Crystallographic Tool*, Utrecht University, Utrecht, The Netherlands, **2012**.
 - [15] L. J. Farrugia, *J. Appl. Crystallogr.* **1999**, 32, 837-838.
 - [16] <http://journals.iucr.org/services/cif/checkcif.html>

On the Synthesis and Structural Characterization of Pyridine-Stabilised Tin(II) Thiophosphates

As to be submitted to *Eur. J. Inorg. Chem.*



By reacting P_4S_{10} with Na_2S and $SnCl_2$ in pyridine as solvent, the products $py_2Sn(pyPS_3)_2 \cdot 0.5 py$ (**1**) and $[SnPS_4][py_2H] \cdot py$ (**2**) could be obtained.

In compound **1** two pyridine stabilized PS_3^- anions connected to a tin(II) atom which is further stabilized by two pyridine molecules resulting in a monomeric stannylene. This compound is the first to contain the $pyPS_3^-$ anion as a ligand and is a very rare example for a monomeric stannylene with Sn–S bonds. Compound **2** is a coordination polymer. The heteropolyanion consisting of $[SnPS_4^-]_x$, forms one dimensional chains, separated by free pyridine molecules and with $[py_2H]^+$ as counterion. The question, which arises from the simultaneous formation of a neutral monomeric and a charged polymeric structure in one reaction solution is, which role the ligand plays in the formation of mono- and polymeric tin(II) compounds.

Introduction

Stannylenes are organotin(II) derivatives of the form SnR_2 . The first representative of this class of compounds was proposed to be Et_2Sn by Löwig *et al.* in 1852.^[1] It was synthesised by reacting ethyl iodide on a tin alloy. In 1920 Krause *et al.* mentioned the Ph_2Sn .^[2] The existence of both these products however could not be verified.

Because of the tin(II) being low valent and highly reactive such compounds may exist monomeric in solution but in the solid state they appear polymerized, whereas the degree of oligomerisation depends on the organic ligand.^[3]

With increasing quantum number the preference of M(II) over M(IV) in group 14 elements gets significantly stronger. To explain this observation one has to have a deeper look into the quantum chemical properties of this group. Carbenes adopt a singlet or triplet ground state conditioned by the ligand. Due to the increasing energy difference between the two possible states, the heavier stannylenes prefer the singlet ground state. Here the lone pair is relatively inert due to its high s character. So the high reactivity of tin(II) can be explained with a vacant p orbital and an overall valence electron number of six.

Heavier group 14 elements are likely to favour $(ns)^2(np)^2$ configuration, which means they lack the ability form hybrid orbitals. So it has to be understood, that in order to obtain monomeric Sn(II) compounds thermodynamic and/or kinetic stabilization of the vacant p orbital is necessary.^[4]

Lappert and co-workers were the first to be able to isolate a monomeric stannylene by using the sterically demanding ligand $\text{CH}(\text{SiMe}_3)_2$.

The second possibility to receive monomeric SnR_2 molecules in the solid state besides the use bulky ligands is the insertion of donor stabilizing ligands such as cyclobutadienyl derivatives or nitrogen containing compounds. Also chalcogen and pnictogen containing ligands have been found to be of great use.

Over the last few years now a remarkable progress in the field of bivalent SnR_2 species has taken place.

But still the search goes on. Especially for new examples of compounds which are monomeric in the solid state. These stannylenes can be used as precursors for the synthesis of organometallic complexes as well as heterocycles or even new coordination polymers which are rather attractive with regard to the ever growing

demand for open framework materials. Some representatives of the stannylenes have been found to show catalytic activity or are of pharmaceutical relevance.^[5]

Furthermore we were able to present new findings gained about the trithiometaphosphate ion. The PS_3^- can be regarded as higher homologue of the nitrate ion. But because of the unfavourable bonding situation at the phosphorus atom, in the solid state it exists only coordinated by a base. First syntheses of various salts of these adducts have already been reported by our group (see PART I – Chapter 2) and we could also contribute to its investigation with results of quantum chemical calculation on the structure and bonding situation within this molecule.^[6, 7] Dimitrov *et al.* were able to describe the crystal structures of salts of the pyridine adduct.^[8] Experimental investigations concerning this anion showed that the phosphorus atom is a rather poor electrophile, which shows the rather weak coordination to the base. So the logical next step was to analyse the nucleophilic character by attacking the sulfur atom. And we were indeed able to synthesise the compound $\text{py}_2\text{Sn}(\text{pyPS}_3)_2 \cdot 0.5 \text{ py}$ (**1**), which, to the best of our knowledge, is the first to actually contain the pyPS_3^- entity.

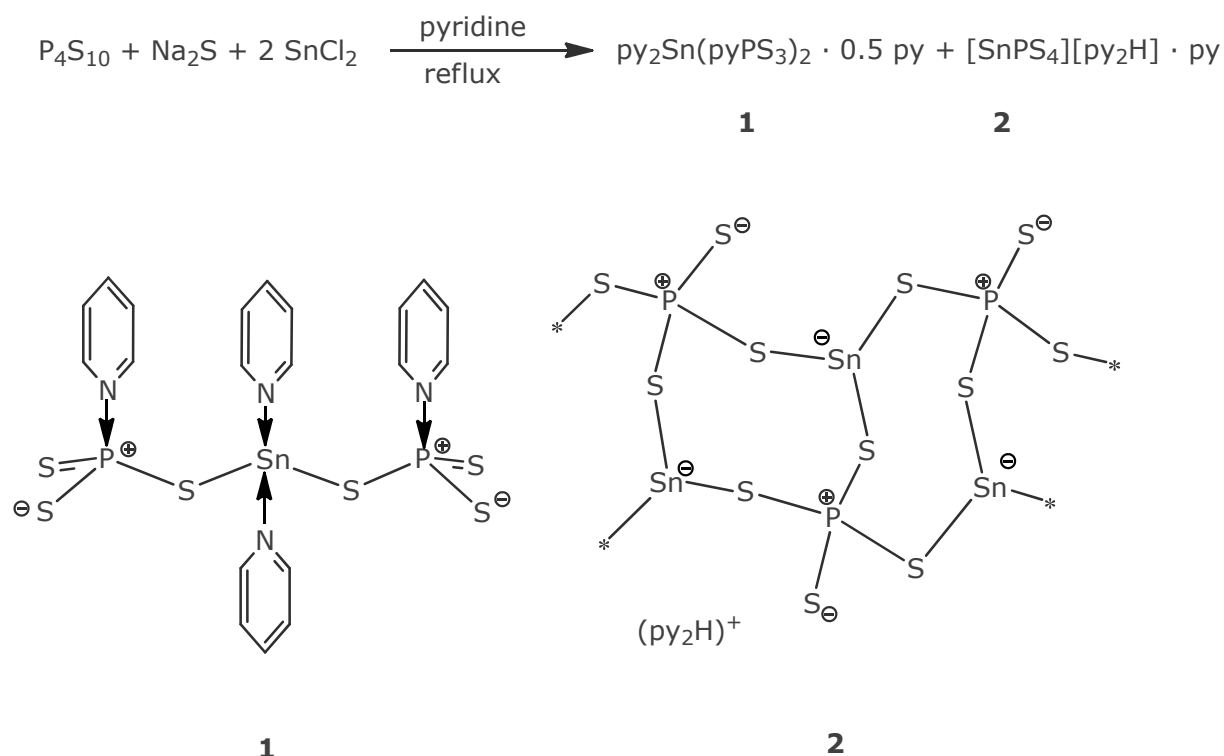
Besides this rather stunning molecule a new salt could be obtained from the same reaction mixture, the $[\text{SnPS}_4][\text{py}_2\text{H}] \cdot \text{py}$ (**2**). Sn(II) phosphates have been proposed to be unusually stable, making them attractive for the use in inorganic open frameworks. Such materials have already been described with organic counterions as structure directing elements.^[9] The tin(II) is threefold coordinated by oxygen bridging to the phosphorus atoms, displaying eight-membered rings, which form channels. Also a quaternary divalent compounds ASnPS_4 (A = K, Rb, Cs) have been described recently, forming rather exciting layered structures.^[10]

These results give a good insight into the role, the choice of ligand plays in the formation of mono- and polymeric tin(II) compounds.

In the following a reaction mixture containing both species (**1** and **2**) shall be discussed.

Results and Discussion

By refluxing P_4S_{10} with Na_2S and $SnCl_2$ (1:1:2) in pyridine, two different sorts of crystals could be isolated (Scheme 1). They were characterized as $py_2Sn(pyPS_3)_2 \cdot py$ (**1**) and $[SnPS_4][py_2H] \cdot py$ (**2**) using single crystal X-ray diffraction.



Scheme 1. Synthesis of **1** and **2**.

Molecular and Crystal Structure of $py_2Sn(pyPS_3)_2 \cdot 0.5 py$ (**1**)

Compound **1** was isolated as yellow block shaped crystals. This structure crystallizes in the monoclinic space group $P2_1/n$ with four formula unit in the unit cell. The asymmetric unit consists of two crystallographically independent molecules of **1**. The molecular structure, as well as selected atom distances and bond angles are given in Figure 1.

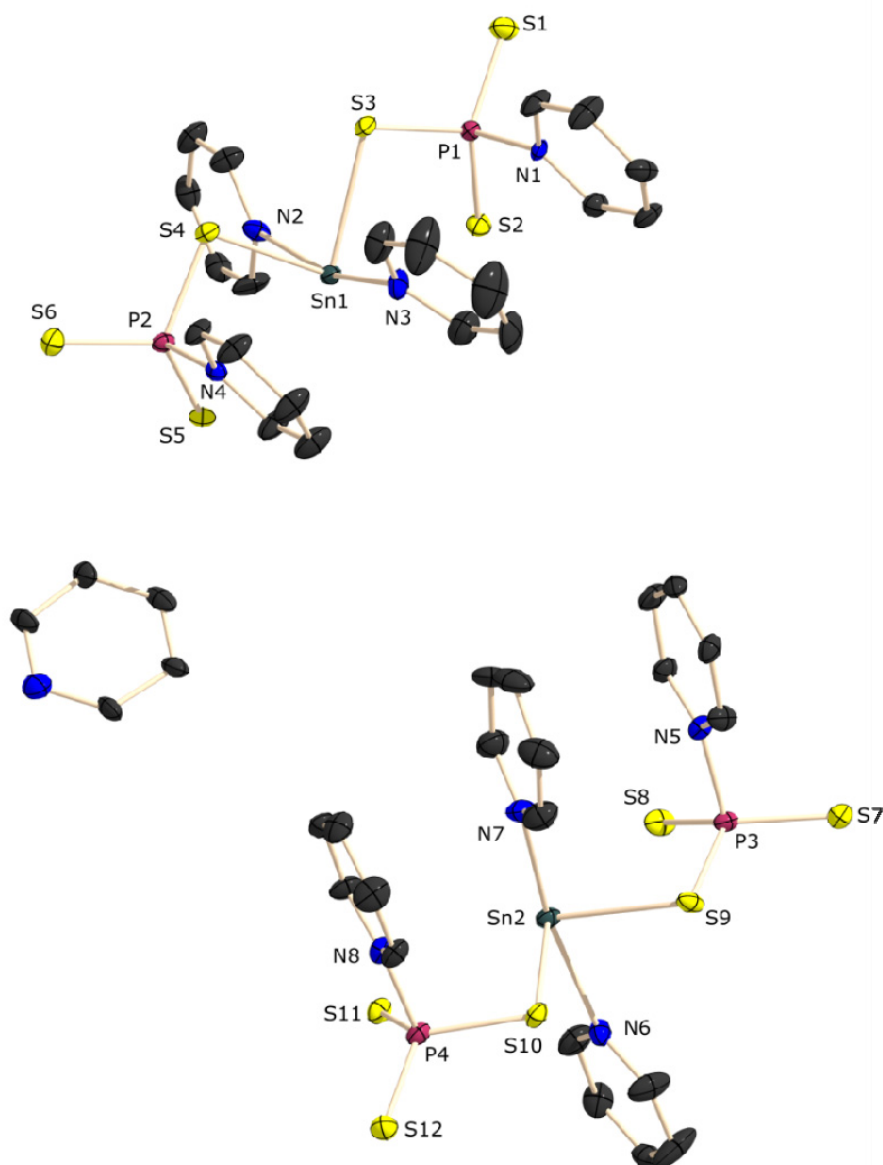


Figure 1. Molecular structure of **1**. Ellipsoids are drawn at the 50% probability level. Hydrogen atoms are omitted for clarity. Selected atom distances [Å] and bond angles [°] for **1**: Sn1–S3/Sn2–S9 2.627(3)/ 2.625(3), Sn1–S4/ Sn2–S10 2.632(3)/ 2.637(3), Sn1–N2/ Sn2–N6 2.501(8)/2.487(8), Sn1–N3/ Sn2–N7 2.501(8)/ 2.632(10), P1–S1/P1–S2 1.957(4)/ 1.982(4), P1–S3/P2–S4 2.048(4)/ 2.050(4), P2–S5/P2–S6 1.969(4)/ 2.050(4), P1–N1/P2–N4 1.881(8)/ 1.895(8);

S3–Sn1–S4 81.2(1) S3–Sn1–N2 85.6(2), S4–Sn1–N2 86.5(2), S3–Sn1–N3 81.3(2), S4–Sn1–N3 83.9(2), N2–Sn1–N3 164.8(3), Sn1–S3–P1 95.93(12), Sn1–S4–P2 96.19(12), S1–P1–S3 113.08(17), S1–P1–N1 103.5(3), S1–P1–S2 120.42(17), S2–P1–N1 104.6(3), S3–P1–N1 100.8(3), S2–P1–S3 111.6(2).

One molecule of **1** contains one tin(II) atom which is bonded to two pyridine stabilized PS_3^- entities and coordinated by two pyridine rings. One additional solvent pyridine molecule is also incorporated in the crystal structure.

This structure can be regarded as stannylene because the tin is bonded to one sulfur atom of each PS_3^- entity so it has two covalent bonds and a free electron pair. The hence created electronic gap is filled by coordination of two pyridine molecules.

For this compound a trigonal bipyramidal like structure (Figure 2a) is expected. The S–Sn–S angle of $81.2(1)^\circ$ hint towards pure p character of the S–Sn bonds with the third p orbital being involved in the Sn–N interaction and the lone pair at Sn having s character. As can be seen in Figure 2b one additional sulfur atom of each PS_3^- unit coordinates to the tin. So the covalent bonded sulfur atoms shift closer together resulting in the S–Sn–S angle deviating from 90° .

Because of the additional occupation of space in the horizontal plane by the two further sulfur atoms the free electron pair has to shift out of the plane causing a slightly bent N–Sn–N angle of $164.8(1)^\circ$ (Figure 2c).

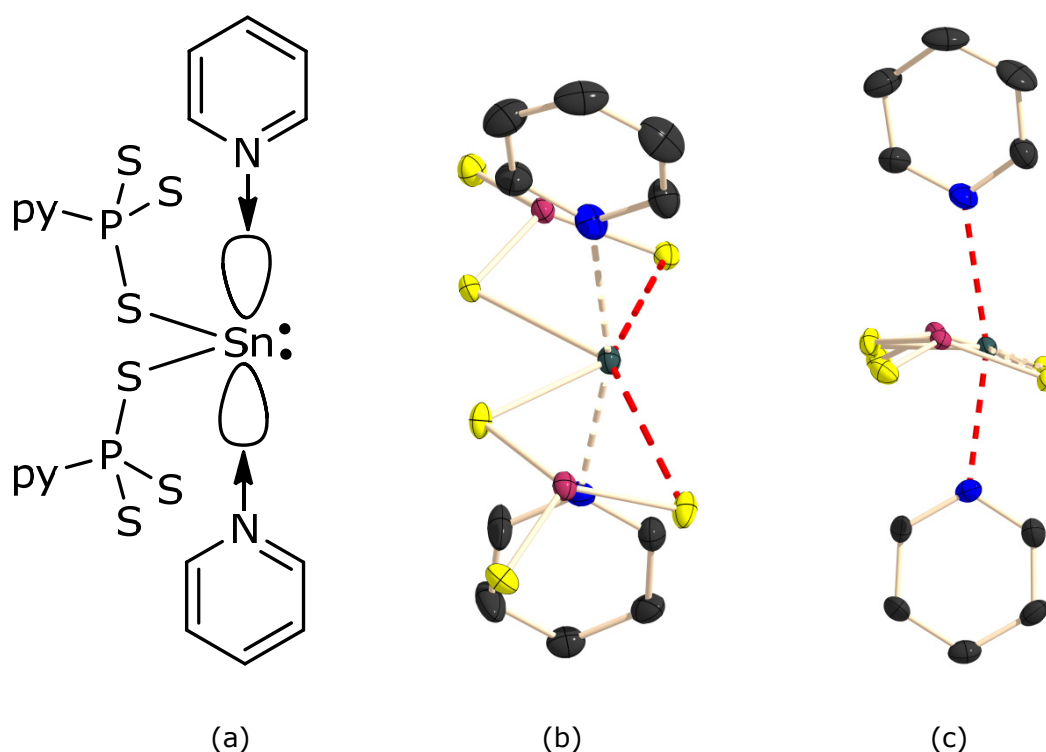


Figure 2. Bonding situation around the tin(II) atom.

Another question that has to be discussed is, how the pyPS_3^- entity is influence by the altered bonding situation. In Table 1, all necessary atom distances and bond angles of compound **1**, the pyridinium salt synthesised by our group and the one of Dimitrov *et al.* are listed.

Table 1. Comparison of atom distances and bond angles in the pyPS_3^- entity of **1**, by Karaghiosoff (**Ia**) and Dimitrov (**Ib**).

	$\text{py}_2\text{Sn}(\text{pyPS}_3)_2 \cdot \text{py}$ (1)	$(\text{pyH})(\text{pyPS}_3)^{[\text{a}]}$	$(\text{pyH})(\text{pyPS}_3)^{[\text{b}]}$
bond lengths [Å]			
P1–S1/P2–S6	1.957(4)/ 1.956(4)	1.989(1)	1.980(2)
P1–S2/P2–S5	1.982(4)/ 1.969(4)	1.985(1)	1.986(2)
P1–S3/P2–S4	2.048(4)/ 2.050(4)	1.979(1)	2.004(1)
P1–N1/P2–N4	1.881(8)/ 1.895(8)	1.920(1)	1.906(2)
bond angles [°]			
S1–P1–S3	113.1(2)	117.2(1)	113.8(2)
S1–P1–S2	120.4(2)	114.6(1)	116.7(1)
S2–P1–S3	111.6(2)	115.8(1)	116.4(1)
Σ S–P–S	345.1	347.6	346.9
S1–P1–N1	103.5(3)	100.2(1)	
S2–P1–N1	104.6(3)	102.4(1)	
S3–P1–N1	100.8(3)	103.1(1)	

[a] see PART I – Chapter 2 [b] Dimitrov *et al.*

The bond lengths in the pyPS_3^- unit in this compound differ from the free molecule. For **Ia** and **Ib** average P–S values of 1.984(1) and 1.990(2) Å are described, while the connection to the tin leads to deviated values (1.957(4), 1.982(4) and 2.048(4) Å). The bond between P1 and S3 is elongated with 2.048(4) Å compared to 1.979(1) Å and 2.004(1) Å, as expected with the sulfur being twofold covalently bonded. The smaller P1–S1 distance derives from the P–S double bond not being able to rotate freely anymore and also due to the electron withdrawing effect of the S3–Sn1 bond

Comparing the S–P–S bond angles of **1** with the values found in the free pyPS_3^- (**Ia**, **Ib**), the altered bonding situation in **1** causes a smaller angle between the phosphorus and the two twofold coordinated sulfur atoms with 111.6(1)° compared to 115.8(1)° and 116.4(1)°. Remarkably the sum of the S–P–S angles is with 345.1° rather coherent with the one we (347.6°) and Dimitrov (346.9°) observed, so the coordination to the tin has obviously no influence in this situation. This means that the

smaller S2–P1–S3 angle leaves more space causing an extremely enlarged S1–P1–S3 angle with 120.4(2)° in comparison to 116.7(1)° and 114.6(1)°.

Two other compounds containing a tin(II), being covalently bonded to two sulfur atoms, are described in the literature (Figure 3). In the bis(ethy-1-cysteinato)tin(II)^[5] (**II**), with HCEE being L-cysteine ethyl ester, the tin is surrounded by two sulfur and two nitrogen atoms, while Sn(SAr), (Ar = C₆H₄, Bu^t, -2,4,6)^[11] (**III**) can be regarded as a real stannylene, with the tin being only covalently bonded to two sulfur atoms.

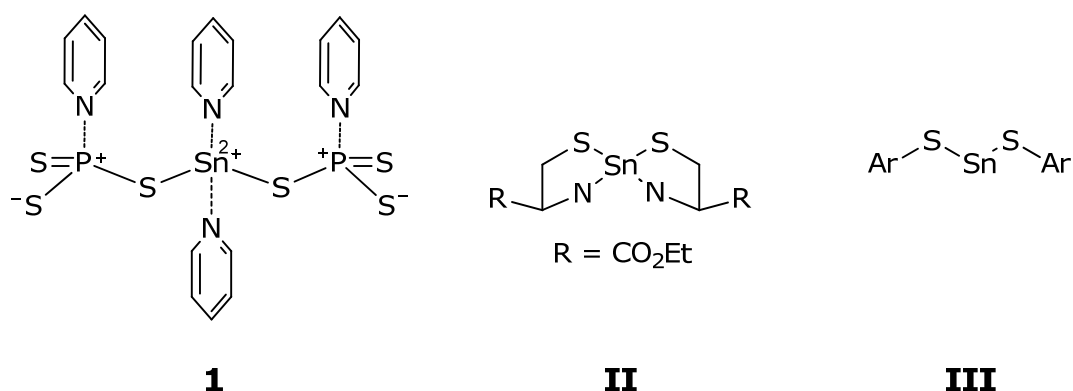


Figure 3. Comparison of **1**, bis(ethy-1-cysteinato)tin(II), and Sn(SAr).

Table 2. Comparison of selected atom distances and bond angles in **1**, bis(ethy-1-cysteinato)tin(II), and Sn(SAr).

	py ₂ Sn(pyPS ₃) ₂ · py (1)	Sn(CEE) ₂	[Sn(SAr) ₂] ₃
Sn–S [Å]	2.630(3)	2.520(1)	2.435(1)
Sn–N [Å]	2.570(8)	2.475(4)	
S–Sn–S [°]	81.2(1)	100.9(4)	85.4(1)
N–Sn–N [°]	164.8(3)	146.3(1)	

Due to the chelating nature of the ligand in compound **II** the N–Sn–N bond angle is more acute with 146.3°. The consequence is a rather poor overlap of the p orbitals, which leads to a greater covalent character of the Sn–S bond, resulting in a shortened distance between these atoms (2.520(1) Å compared to 2.630(3) Å in **1**) and an enlarged S–Sn–S angle. As **1** does not have to comply to chelating effects, the N–Sn–N angle is closer to linearity with 164.8°.

In contrast to the situation found in **II**, the tin atom in **III** is solely surrounded by two sulfur atoms and therefore a real stannylene. The S–Sn–S angle of **1** is in the same range as the one found in **III** (81.2° and 85.4° respectively). This indicates for **1** to be a sp^3 hybrid. Consequently **1** can be regarded as pyridine stabilized stannylene.

Molecular and crystal structure of $[\text{SnPS}_4][\text{py}_2\text{H}] \cdot \text{py}$ (**2**)

Colourless block shaped crystals of **2** could be isolated and characterized *via* single crystal X-ray diffraction. The compound crystallizes in the triclinic space group $P\bar{1}$ with two asymmetric units in the unit cell. The molecular structure and selected atom distances and bond angles are given in Figure 4.

The structure of compound **2** consists of the P,S,Sn-heteropolyanion $[(\text{PS}_4\text{Sn})^-]_x$ with $[\text{py}_2\text{H}]^+$ as counterion and contains one further pyridine molecule per formula unit. In the crystal tetrathiophosphate units (PS_4) are linked by tin atoms. Every tin(II) is coordinated by three phosphorus atoms, bridged over sulfur atoms, so that every PS_4^{3-} unit coordinates with three of its sulfur to three different tin atoms, while the fourth sulfur atoms remains single coordinate. This terminal atom interacts with the cations. This arrangement results in the formation of corrugated double chains parallel to the *a* axis, consisting of strongly twisted $\text{P}_2\text{S}_4\text{Sn}_2$ eight-membered rings (Figure 5).

Very recently, Kanatzidis and co-workers reported on similar structures. They were able to synthesize ASnPS_4 ($A = \text{K}, \text{Rb}, \text{and Cs}$), which are rare examples of quaternary divalent tin thiophosphates.^[10] These compounds are prepared by chalcophosphate flux technique at high temperature. In contrast to **2**, they build up a layered structure because of the higher coordination sphere of the alkali metal cation. They report further on the glass formation properties and the semiconducting abilities of these compounds. As the potassium and rubidium representatives are isostructural, in the following compound **2** is compared with KSnPS_4 (**IV**).

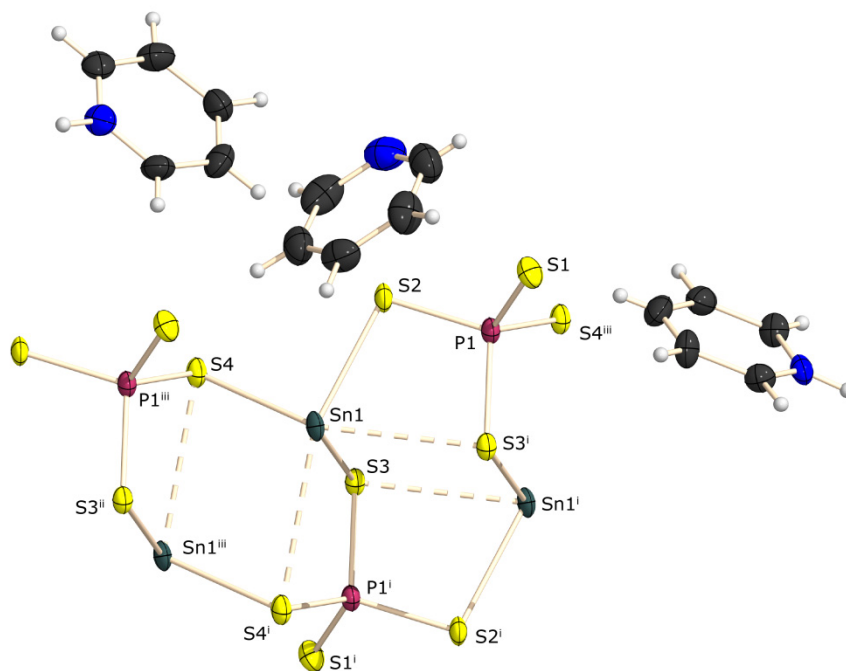


Figure 4. Molecular structure of **2**. Ellipsoids are drawn at the 50% probability level. Symmetry operations: i = 1–x, 1–y, 2–z; ii = 2–x, 1–y, 2–z; iii = 1+x, y, z. Selected atom distances [Å] and bond angles [°]: P1–S1 1.991(3), P1–S2 2.053(4), P1–S3ⁱ 2.094(3), P1–S4ⁱⁱⁱ 2.058(3), Sn1–S2 2.616(3), Sn1–S3 3.073(3), Sn1–S4 2.700(3);

S1–P1–S2 112.8(2), S1–P1–S3ⁱ 110.0(2), S1–P1–S4 111.6(2), S2–P1–S3 107.5(2), S2–P1–S4ⁱⁱⁱ 107.6(2), S3ⁱ–P1–S4ⁱⁱⁱ 107.0(2), Sn1–S2–P1 97.1(2), Sn1–S3–P1 83.5(1), S2–Sn1–S3 90.9(1), S2–Sn1–S4 86.8(1), S3–Sn1–S4 83.7(6).

The coordination of the phosphorus atom in **2** deviates only slightly from a tetrahedral conformation (S–P–S angles between 107.5(2)° and 112.8(2)°). P–S distances to the bridging sulfur atoms are with values between 2.053(4) Å and 2.094(3) Å closer to P–S single^[12] than double bonds^[13]. The P–S distance to the single coordinate sulfur atom is shorter with 1.991(3) Å compared to 2.054(2) Å (**IV**). This is conditioned by the different cations. While sulfur is not able to form strong hydrogen bonds because of its rather dispersive nature, the P–S distance is shorter compared to the strongly ionic character of the S–K interaction which leads to an electron withdrawing effect and thus an elongated P–S bond length.

The tin atoms form covalent bonds to three sulfur atoms of three different PS₄ units resulting in the formation of SnS₃ pyramids, with the lone pair of the tin(II) completing a tetrahedral surrounding. The average Sn–S bond lengths are in very good accordance with 2.773(3) Å (**2**) and 2.775(1) Å (**IV**) but the discrepancy

between the values in **2** is rather high. All three Sn–S distances are different with values of 2.616(3) Å, Sn1–S3 3.073(3) Å and Sn1–S4 2.700(3) Å.

The bond angles at the tin atom are close to 90°, in the range of 83.7(6)° – 90.9(1)°. At the bridging sulfur atoms S2 and S3 the P–S–Sn bond angles are about 100° (99.1(2)° and 97.0(1)°), while the corresponding angle at S4 is almost 90°.

Remarkable about the structure of this heteropolyanion is the presence of quite strong intra- and interannular Sn–S interactions within the eight-membered rings consisting of Sn₂P₂S₄ entities (Figure 5). These interactions are shorter than the sum of the van der Waals radii of sulfur and tin (3.90 Å^[14]). With distances of 3.074(2) Å between Sn1 and S3 and 3.296(2) Å between Sn1 and S4, these interactions are obviously responsible for the strong bending of the eight-membered rings. Further, considerably weaker Sn–S interactions of 3.622(2) Å and 3.688(2) Å to S1 and S3, respectively, are observed.

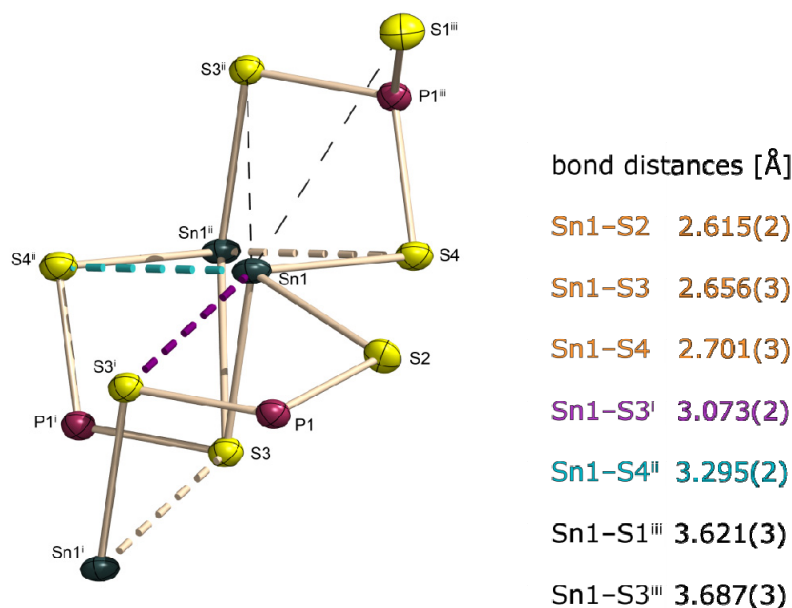


Figure 5. Bonding situation in **2**.

As already mentioned in the beginning, tin(II) phosphates are becoming ever more important in the field of open framework materials, as the tin shows a threefold coordination in these kinds of compounds. Mostly they are prepared with organic templating molecules.^[15] It is reported on three-dimensional systems consisting of alternating PO₄ and SnO₃ entities, forming channels of eight- or even twelve-membered rings.^[9a, 9b] Taking a closer look at the overall structural build-up of **2** in

the crystal, the eight-membered rings consisting of $\text{Sn}_2\text{P}_2\text{S}_4$ form channels perpendicular to the direction of propagation of the one-dimensional chains (Figure 6).

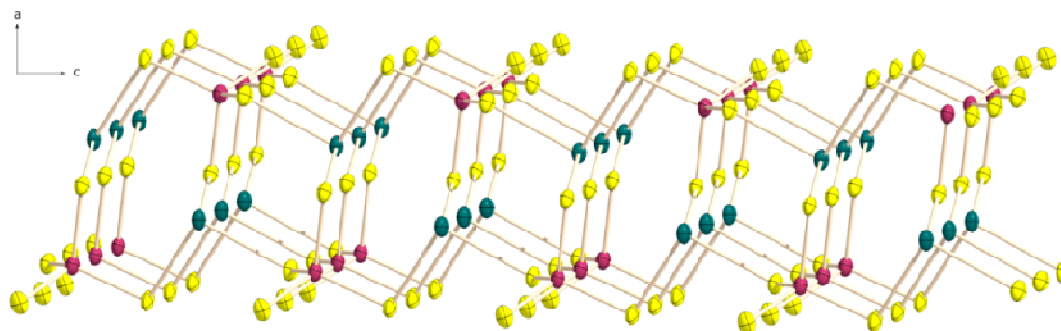


Figure 6. Bonding situation in **2**.

Hereby the organic cations and solvent molecules act as spacers between those chains, as can be seen in Figure 7, showing the unit cell with view along the chains.

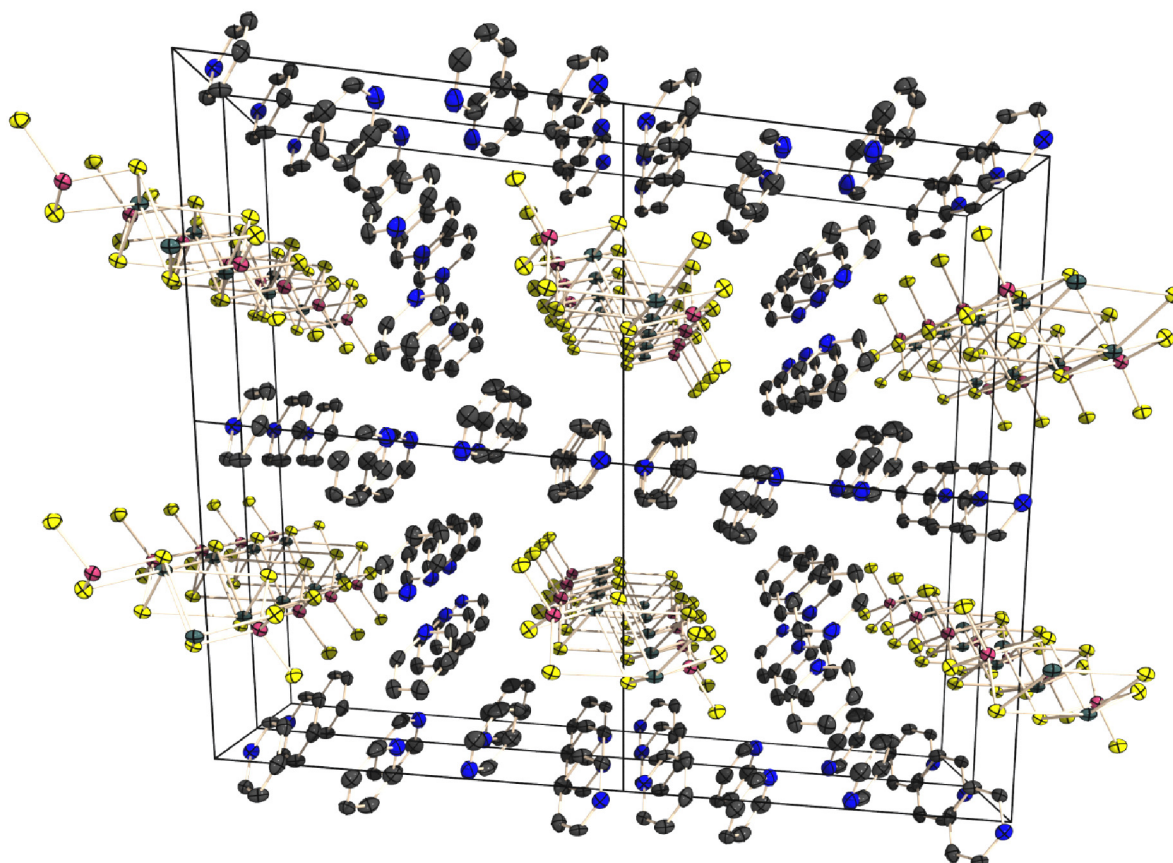
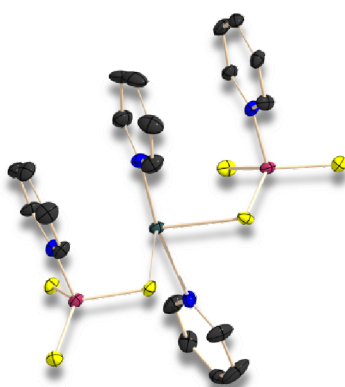


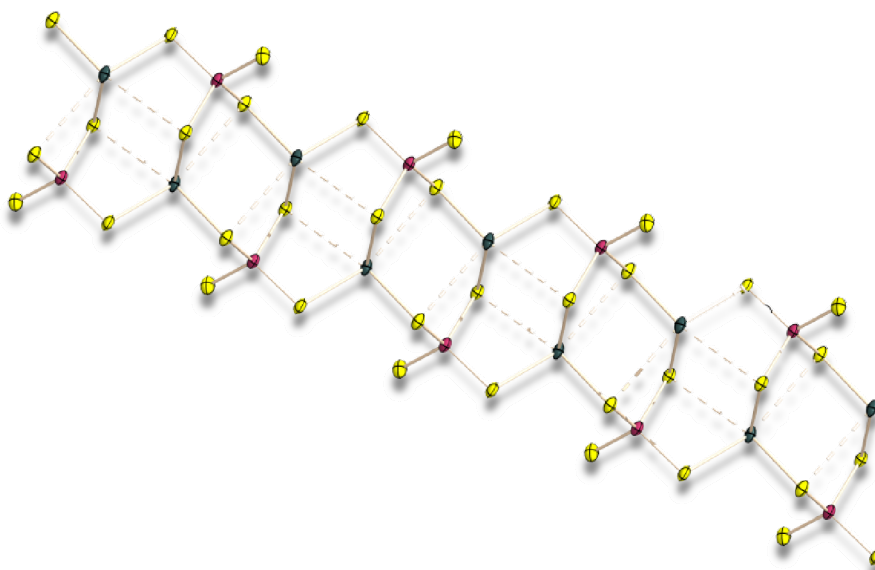
Figure 7. Olsch view of the unit cell of **2** with view along c axis, hydrogen atoms omitted for clarity.

Conclusion

The trithiometaphosphate anion, PS_3^- , stabilized as its pyridine adduct, as well as the tetrathiophosphate anion PS_4^{3-} are found to be good ligands for soft Lewis centres, like Sn(II). This is demonstrated by the synthesis and structural characterization of the neutral stannylene $\text{py}_2\text{Sn}(\text{pyPS}_3)_2 \cdot 0.5 \text{ py}$ (**1**) and of the heteropolyanion $[\text{SnPS}_4][\text{py}_2\text{H}] \cdot \text{py}$ (**2**). Compound **1** is the first example of the pyridine adduct of the trithiometaphosphate anion as a ligand towards metals and one of the very few thiosubstituted stannylenes.



The Sn(II) tetrathiophosphate **2** contains the remarkable chain-like $[\text{SnPS}_4^-]_n$ heteropolyanion and complements the contribution of M. G. Kanatzidis on Sn(II) thiophosphates adding an organic cation containing compound to this family. The striking build-up in the crystal of **2** implies further use as inorganic organic hybrid open framework material.



Experimental Section

Table 3. Details for X-ray data collection and structure refinement for **1** and **2**.

	1	2
CCDC	940974	940973
empirical formula	C ₄₅ H ₄₅ N ₉ Sn ₂ P ₄ S ₁₂	C ₁₅ H ₁₆ N ₃ SnPS ₄
formula mass	1457.88	515.20
<i>T</i> [K]	173(2)	173(2)
crystal size [mm]	0.3 × 0.2 × 0.15	0.1 × 0.1 × 0.05
crystal description	yellow block	yellow block
crystal system	monoclinic	triclinic
space group	<i>P</i> 2 ₁ / <i>n</i>	<i>P</i> –1
<i>a</i> [Å]	20.158(1)	6.471(1)
<i>b</i> [Å]	14.772(1)	11.553(2)
<i>c</i> [Å]	20.162(1)	13.831(1)
<i>α</i> [°]		83.021(13)
<i>β</i> [°]	93.952(2)	83.879(12)
<i>γ</i> [°]		76.679(12)
<i>V</i> [Å ³]	5989(2)	995.4(2)
<i>Z</i>	4	1
<i>ρ</i> _{calcd.} [g cm ^{−3}]	1.617	1.721
<i>μ</i> [mm ^{−1}]	1.400	1.786
<i>F</i> (000)	2920	511
<i>θ</i> range [°]	4.15–25.00	4.17–32.36
index ranges	−23 ≤ <i>h</i> ≤ 23 −17 ≤ <i>k</i> ≤ 17 −23 ≤ <i>l</i> ≤ 23	−7 ≤ <i>h</i> ≤ 7 −13 ≤ <i>k</i> ≤ 13 −16 ≤ <i>l</i> ≤ 16
reflns. collected	23812	9192
reflns. obsd.	9746	2665
reflns. unique	10489	3500
<i>R</i> _{int}	0.0320	0.0929
<i>R</i> ₁ , <i>wR</i> ₂ (2σ data)	0.0778, 0.1877	0.0586, 0.1380
<i>R</i> ₁ , <i>wR</i> ₂ (all data)	0.0814, 0.1885	0.0858, 0.1498
GOOF on <i>F</i> ²	1.354	1.060
larg. diff peak/hole (e/Å)	1.810/−1.855	2.382/−1.291

General conditions. All reactions were carried out under inert gas atmosphere using Argon (Messer Griesheim, purity 4.6 in 50 L steel cylinder) and working with Schlenk techniques. The glass vessels used were stored in a 130 °C drying oven. Before filling they were flame dried *in vacuo* at 10^{-3} mbar. SnCl_2 was used as obtained (Acros Organics). P_4S_{10} was commercially obtained (Riedel-de H  en) and purified by extraction with CS_2 before use. The solvents were dried with commonly known methods and freshly distilled before use. **NMR Spectroscopy.** NMR spectra were recorded using a Jeol EX 400 Eclipse instrument operating at 161.997 MHz (^{31}P). Chemical shifts are referred to 85% H_3PO_4 as external standard. If not mentioned otherwise, all spectra were measured at 25 °C. The % data correspond to the intensities in the ^{31}P NMR spectra with respect to the total intensity. The difference to 100% belongs to not assignable signals. **Mass Spectrometry.** The mass spectrometry was performed with a MStation JMS 700 (Jeol). Measurements were carried out using the ionisationmethode DEI+/EI+. This method involves the problem of exposing the compounds to air, while embedding them into the matrix (p-nitroalcohol). **IR Spectroscopy.** The spectra were recorded using a PerkinElmer Spektrum one FT-IR instrument (KBr); Perkin-Elmer Spectrum BXII FT-IR instrument equipped with a Diamant-ATR Dura Sampler at 25 °C (neat). Raman spectra were recorded on a Bruker RAMII Raman instrument ($\lambda = 1064$ nm, 200 mW, 25 °C) equipped with D418-T Detector at 200 mW at 25 °C. **Melting and decomposition points** were determined by differential scanning calorimetry (Linseis DSC-PT10, calibrated with standard pure indium and zinc). Measurements were performed at a heating rate of 5 °C min^{-1} in closed aluminum sample pans with a 0.1 mm hole in the lid for gas release to avoid an unsafe increase in pressure under a nitrogen flow of 20 mL min^{-1} with an empty identical aluminum sample pan as a reference. Melting points were checked with a B  chi Melting Point B-540 in open glass capillaries.

X-ray Crystallography. The single-crystal X-ray diffraction data were collected using an Oxford Xcalibur3 diffractometer equipped with a Spellman generator (voltage 50 kV, current 40 mA), Enhance molybdenum K_α radiation source ($\lambda = 71.073$ pm), Oxford Cryosystems Cryostream cooling unit, four circle kappa platform and a Sapphire CCD detector. Data collection and reduction were performed with CrysAlisPro.^[16] The structures were solved with SIR97^[17], SIR2004^[18], refined with SHELXL-97^[19], and checked with PLATON^[20], all integrated into the WinGX software suite^[21]. The finalized CIF files were checked with checkCIF.^[22] All non-hydrogen atoms were refined anisotropically. The hydrogen atoms were located in difference Fourier maps and placed with a C-H distance of 0.98    for C-H bonds. Intra- and intermolecular contacts were analysed with DIAMOND (version 3.2i), thermal ellipsoids

are drawn at the 50% probability level. Selected crystallographic data and refinement details for the structure determination of compounds **1** and **2** are summarized in Table 3. CCDC 940974, 940973 contains the supplementary crystallographic data for compounds **1** and **2**. These data can be obtained free of charge from The Cambridge Crystallographic Data Centre *via* www.ccdc.cam.ac.uk/data_request/cif.

Synthesis: P_4S_{10} (685 mg, 1.54 mmol), Na_2S (120 mg, 1.54 mmol) and $SnCl_2$ (584 mg, 3.08 mmol) were dissolved in pyridine (20 mL) and stirred at room temperature for 1 d. Afterwards the yellow suspension was refluxed for 1 h. Yellow blockshaped crystals of $py_2Sn(pyPS_3)_2 \cdot py$ and colorless needles of $[SnPS_4][pyH_2] \cdot py$ precipitated from the orange reaction solution.

$^{31}P\{^1H\}$ NMR (pyridine, rt): δ [ppm] = 146.2 (s, 61.8%), 104.4 (s, 18.6%), 98.8 (s, 7.4%), 37.8 (m, 6.9%). **$^{119}Sn\{^1H\}$ NMR** (pyridine, rt): δ [ppm] = no ^{119}Sn NMR resonances could be observed. **Elemental Analysis:** calc. N 6.81, C 30.36, H 2.55, S 23.08; found. N 4.85, C 30.97, H 2.30, S 21.73. **Raman** (200 mW, rt): ν [cm^{-1}] = 3072 (65), 1627 (20), 1607 (36), 1569 (16), 1192 (31), 1181 (27), 1155 (13), 1015 (100), 640 (15), 609 (14), 474 (90), 415 (25), 340 (28), 307 (28), 268 (33), 210 (33). **IR** (200 mW, rt): ν [cm^{-1}] = 3053 (ww), 1629 (s), 1607 (w), 1593 (w), 1516 (m), 1475 (w), 1451 (ww), 1330 (s), 1258 (s), 1207 (s), 1193 (m), 1181 (s), 1155 (s), 1091 (vs), 1056 (w), 1044 (w), 1013 (w), 914 (vs), 764 (m), 749 (w), 713 (s), 683 (ww), 652 (ww), 643 (ww), 622 (w), 596 (ww), 469 (ww), 409 (vs). **Mass spectrometry** m/z (DEI+) 18 (4), 31 ($[P]^+$), 32 ($[S]^+$), 79 ($[C_5H_5N]^+$), 65($[S_2]^+$), 95 ($[PS_2]^+$), 127 ($[PS_3]^+$), 158 ($[PS_4]^+$), 173 ($[C_5H_5NPS_2]^+$), 283 ($[SnPS_4]^+$). (ESI–) 279 ($[SnPS_4]^-$), 478 ($[SnPS_3]^-$), 743 ($[SnP_2S_{10}]^-$), 883 ($[SnP_3S_{12}]^-$), 957 ($[H_2SnP_3S_{14}]^-$), 1116 ($[H_4Sn_4P_4S_{16}]^-$), 1191 ($[HSnP_3S_{12}]^-$), 1273 ($[Sn_4P_5S_{20}]^-$), 1906 ($[Sn_7P_7S_{35}]^-$). **m.p.:** 146–152 °C

Acknowledgement

Financial support by the Department of Chemistry, Ludwig Maximilian University, is gratefully acknowledged. We thank Prof. T. M. Klapötke, Department of Chemistry, Ludwig Maximilian University, for the generous allocation of diffractometer time and for his continuous support.

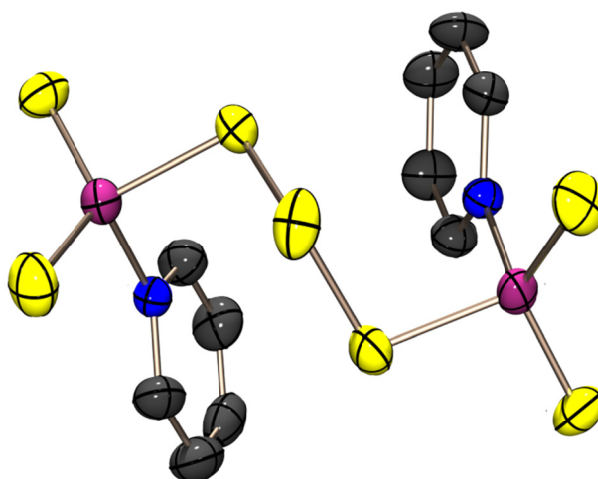
- [1] Loewig, *Grundriss der Organischen Chemie* **1852**, 383-386.
- [2] R. B. E. Krause, *Ber. Dt. Chem. Ges.* **1919**, 173.
- [3] C. Löw, *Dissertation* Dortmund **2002**.
- [4] S. S. Kostina, T. Singh, W. J. Leigh, *Organometallics* **2012**, 31, 3755-3767.
- [5] J. E. Anderson, S. M. Sawtelle, J. S. Thompson, S. A. K. Nguyen, J. Calabrese, *Inorg. Chem.* **1992**, 31, 2778-2785.
- [6] K. Karaghiosoff, M. Schuster, *Phosphorus, Sulfur Silicon Relat. Elem.* **2001**, 168-169, 117-122.
- [7] E. Gokcinar, K. Karaghiosoff, T. M. Klapoetke, C. Evangelisti, C. Rotter, *Phosphorus, Sulfur Silicon Relat. Elem.* **2010**, 185, 2527-2534.
- [8] A. Dimitrov, I. Hartwich, B. Ziemer, D. Heidemann, M. Meisel, *Z. Anorg. Allg. Chem.* **2005**, 631, 2439-2444.
- [9] a) S. Natarajan, M. P. Attfield, A. K. Cheetham, *Angew. Chem., Int. Ed. Engl.* **1997**, 36, 978-980; b) S. Natarajan, A. K. Cheetham, *Chem. Commun.* **1997**, 1089-1090; c) S. Natarajan, A. K. Cheetham, *J. Solid State Chem.* **1997**, 134, 207-210.
- [10] S. Banerjee, C. D. Malliakas, M. G. Kanatzidis, *Inorg. Chem.* **2012**, 51, 11562-11573.
- [11] P. B. Hitchcock, M. F. Lappert, B. J. Samways, E. L. Weinberg, *J. Chem. Soc., Chem. Commun.* **1983**, 0, 1492-1494.
- [12] A. F. Holleman, E. Wiberg, N. Wiberg, *Lehrbuch der anorganischen Chemie*, Walter de Gruyter Verlag, Berlin, **2007**.
- [13] F. H. Allen, O. Kennard, D. G. Watson, L. Brammer, A. G. Orpen, R. Taylor, *J. Chem. Soc., Perkins Trans. 2* **1987**, S1-S19.
- [14] A. Bondi, *J. Phys. Chem.* **1966**, 70, 3006-3007.
- [15] A. K. Cheetham, G. Ferey, T. Loiseau, *Angew. Chem., Int. Ed.* **1999**, 38, 3268-3292.
- [16] *CrysAlisPro 1.171.36.21*, Agilent Technologies, **2012**.
- [17] A. Altomare, G. Cascarano, C. Giacovazzo, A. Guagliardi, A. A. G. Moliterni, M. C. Burla, G. Polidori, M. Camalli, R. Spagna, **1997**, 343.
- [18] a) M. C. Burla, R. Caliandro, M. Camalli, B. Carrozzini, G. L. Cascarano, L. De Caro, C. Giacovazzo, G. Polidori, R. Spagna, Institute of Crystallography, Bari (Italy), **2004**; b) M. C. Burla, R. Caliandro, M. Camalli, B. Carrozzini, G. L. Cascarano, L. De Caro, C. Giacovazzo, G. Polidori, R. Spagna, *Journal of Applied Crystallography* **2005**, 38, 381-388.
- [19] a) G. M. Sheldrick, *SHELXL-97, Program for the Refinement of Crystal Structures*. University of Göttingen, Göttingen (Germany), **1997**; b) G. M. Sheldrick, *Acta Crystallographica, Section A: Foundations of Crystallography* **2008**, A64, 112-122.
- [20] A. L. Spek, *Platon, A Multipurpose Crystallographic Tool*, Utrecht University, Utrecht, The Netherlands, **2012**.
- [21] L. J. Farrugia, *J. Appl. Crystallogr.* **1999**, 32, 837-838.
- [22] <http://journals.iucr.org/services/cif/checkcif.html>

PART IV

Acyclic Phosphorus Sulfides

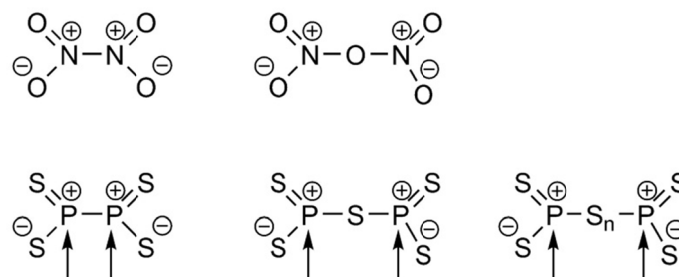
py₂P₂S₇: A Bis(pyridine)adduct Stabilized Phosphorus Sulfide

As published in *Chem. Comm.* **2010**.



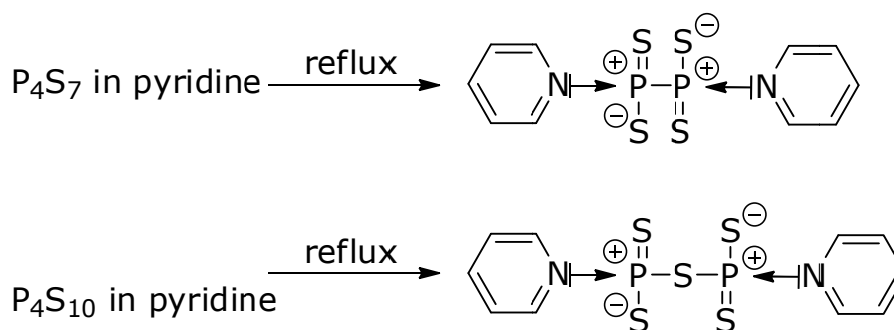
The new phosphorus sulfide P₂S₇, stabilized as the bis(pyridinium) adduct was obtained from the reaction of P₄S₁₀ and sulfur in pyridine, and could be isolated in form of colourless blockshaped crystals which were characterized using single crystal X-ray diffraction. Coordination of pyridine is weak (d(P–N) = 187 pm) which is supported also by quantum chemical calculations.

Binary neutral phosphorus sulfides have been known for a long time and belong to the basics of inorganic chemistry, described in every chemistry textbook.^[1] Acyclic phosphorus sulfides (comparable to nitrogen oxides) would imply unusually coordinated and bonded phosphorus atoms (Scheme 1).



Scheme 1. Binary neutral acyclic N,O and P,S compounds.

In contrast to the well-known dinitrogen tetraoxide N_2O_4 and dinitrogenpentaoxide N_2O_5 , the corresponding phosphorus sulfides P_2S_4 and P_2S_5 are not stable, due to the presence of $\sigma^3\lambda^5$ phosphorus atoms. Formally the dimers P_4S_8 and P_4S_{10} in which phosphorus avoids this unfavorable bonding situation, are known and represent stable molecules. The “monomers” however can be stabilized by adduct formation with a base (Scheme 2). The concept of stabilizing reactive species by adduct formation with nitrogen compounds has been used in several cases.^[2]

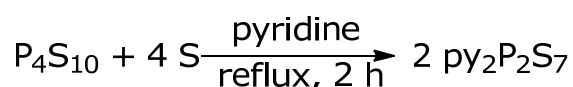


Scheme 2. Literature known bis(py)adduct stabilized phosphorus sulphides.

Neels and co-workers tried to answer the question, to which of the above mentioned compounds the observed ^{31}P NMR shift can be assigned.^[3] For the formation of the $\text{py}_2\text{P}_2\text{S}_4$ was synthesized by Wolf *via* refluxing P_4S_7 in pyridine. No analytical data is given in the literature for this compound.^[3] $\text{py}_2\text{P}_2\text{S}_5$ was first described by Fluck *et al.* and characterized using ^{31}P NMR spectroscopy ($\delta^{31}\text{P}$ 105.5 ppm).^[4] Meisel *et al.* also investigated $\text{py}_2\text{P}_2\text{S}_5$ ^{31}P NMR spectroscopically in the solid state ($\delta^{31}\text{P}$ (crystalline

py₂P₂S₇) 70±20; δ³¹P (glassy py₂P₂S₇) 103±10).^[5] One might think of py₂P₂S₅ being the first member of a series py₂P₂S₄(S)_x (x = 1), due to the tendency of sulfur to form chains.

So we modified the reported syntheses and used P₄S₁₀ and elemental sulfur as educts (Scheme 3). On refluxing the educts in pyridine for 2 h py₂P₂S₇ could be isolated in form of colourless blockshaped crystals which were characterized using single crystal X-ray diffraction.



Scheme 3. Synthesis of py₂P₂S₇.

py₂P₂S₇ crystallizes in the monoclinic space group *P*2₁/*c* (Figure 1 and 2).^[6]

Each phosphorus atom is distorted tetrahedrally coordinated by three sulfur atoms a pyridine molecule. The P–S distances are within the range expected for P–S single bonds (211 pm) and P=S double bonds (191 pm).^[1] The P–N distances with 186.9(3) pm (P1–N1) and 186.4(3) pm (P2–N2) are significantly longer than P–N single bonds (176 pm) described in literature.^[1] The S–S bond in the S₃ bridge corresponds with 204.2(2) pm (S4–S5) and 206.3(2) pm (S3–S4) very well to the S–S bond distance found in elemental sulfur.^[1] The S–P–S bond angles have values between 125° and 103°. The angle between the three sulfur atoms S3–S4–S5 is 107° thus forming a helix. The corresponding torsion angles P1–S3–S4–S5 (S3–S4–S5–P2) have values of 84.9(1)° (90.9(1)°). The sum of all S–P–S angles for each central phosphorus atom is 344° thus indicating only a slight deviation from planarity for the central phosphorus atoms. This suggests that py₂P₂S₇ might be viewed as the new acyclic phosphorus sulfides P₂S₇, which is stabilized by weak coordination of pyridine to the σ³λ⁵ phosphorus atoms.

The corresponding torsion angles P1–S3–S4–S5 (S3–S4–S5–P2) have values of 84.9(1)° (90.9(1)°) and are therefore in the same range like found in bis(diaryl/dialkylphosphoryl)trisulfides.^[7,8]

In order to further investigate this point, quantum DFT calculations at the MPW1PW91 level of theory using an augmented polarized double-zeta basis set (aug-cc-pVDZ) were performed. Interestingly the calculated values for the bond angles of the hypothetical compound P₂S₇ correspond very well to the determined values using single crystal X-ray diffraction. In contrast, the calculated values for py₂P₂S₇ result in

longer distances. This suggests that coordination of pyridine is indeed weak and does not affect the bond lengths within the molecule.

Table 1 Calculated and experimentally observed distances [pm] and bond angles [°] of $\text{py}_2\text{P}_2\text{S}_7$ (average values).

Distances			
	observed $\text{py}_2\text{P}_2\text{S}_7$	calculated $\text{py}_2\text{P}_2\text{S}_7$	calculated P_2S_7
P-N	187	196	-
P-S _{oc}	193	196	192
P-S _{tc}	212	217	213
S-S	205	208	207
Angles			
	observed $\text{py}_2\text{P}_2\text{S}_7$	calculated $\text{py}_2\text{P}_2\text{S}_7$	calculated P_2S_7
S _{oc} -P-S _{oc}	126	128	134
S _{oc} -P-S _{tc}	103/114	103/115	107/118
S3-S4-S5	107	105	106
Torsion Angles			
	observed $\text{py}_2\text{P}_2\text{S}_7$	calculated $\text{py}_2\text{P}_2\text{S}_7$	calculated P_2S_7
P1-S3-S4-S5	85	96	85
S3-S4-S5-P2	91	96	85

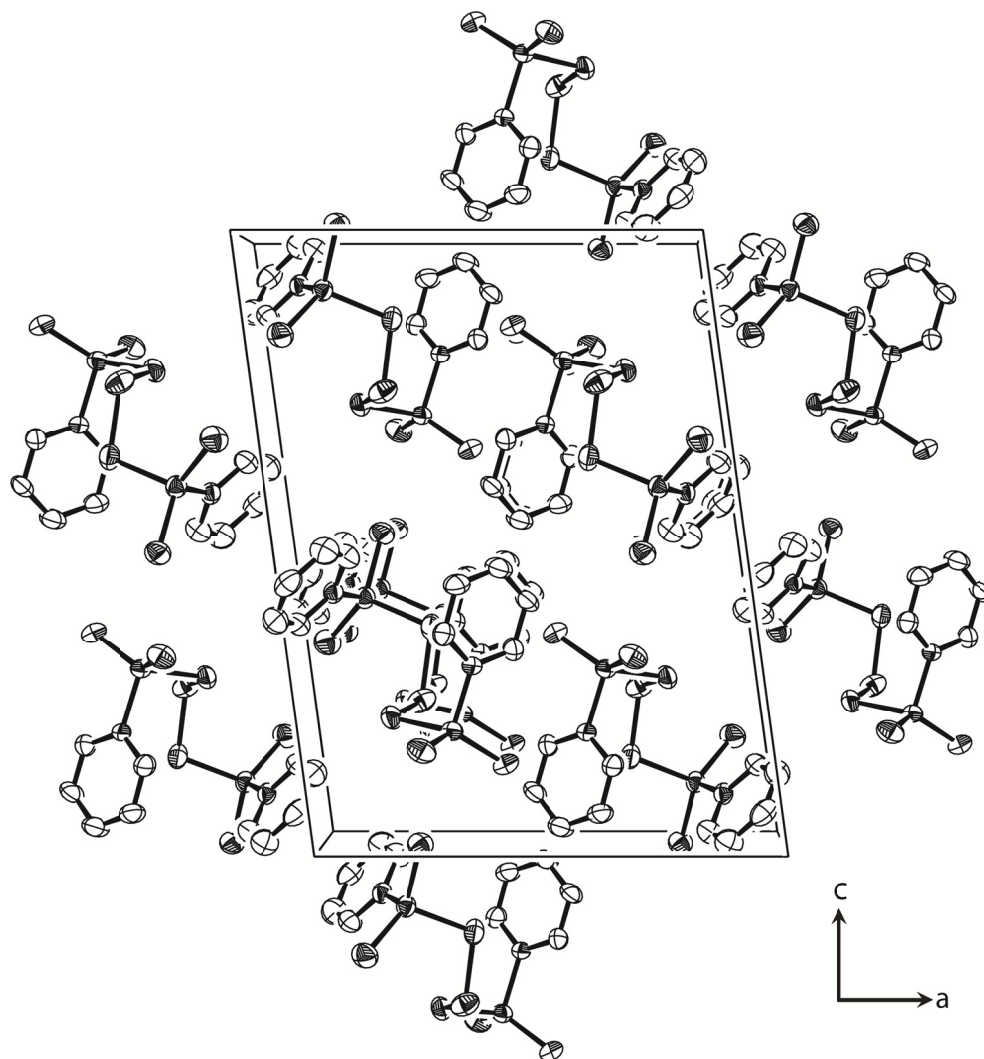


Fig. 1 Crystal structure of py₂P₂S₇. View of the unit cell along *b* axis. Ellipsoids are drawn at the 50% probability level. Hydrogen atoms are omitted for clarity.

In the ³¹P NMR spectrum of py₂P₂S₇ a singlet at 82.2 ppm is observed. To support the assignment of the ³¹P NMR chemical shift of py₂P₂S₇ quantum chemical calculations at the MPW1PW91 level of theory using an augmented polarized double-zeta basis set (aug-cc-pVDZ) for phosphorus were performed. The calculated ³¹P NMR chemical shift of 84.2 ppm corresponds very well to the experimentally observed value of 82.2 ppm.

As suggested by the structural parameters and by the quantum chemical calculations, py₂P₂S₇ can be viewed as the new acyclic phosphorus sulfide P₂S₇, stabilized by phosphorus coordination by pyridine molecules.

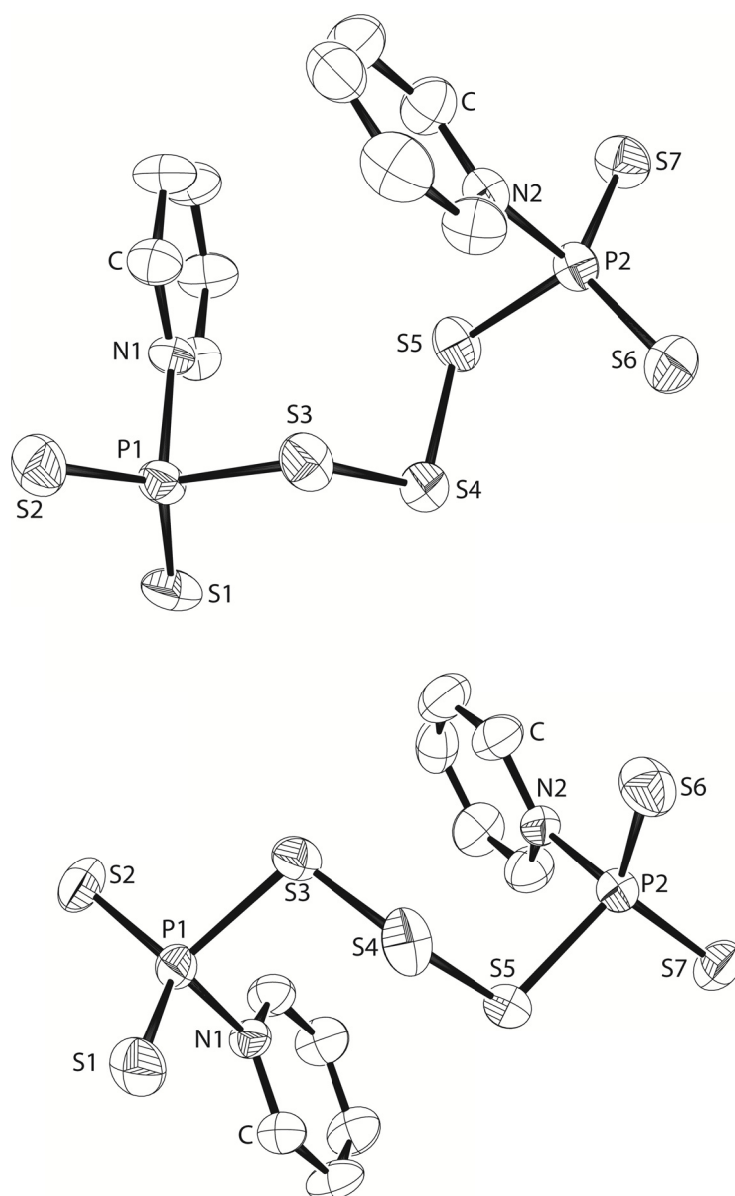


Fig 2 Molecular structure of $\text{py}_2\text{P}_2\text{S}_7$. Thermal ellipsoids are set at 50% probability level. Hydrogen atoms are omitted for clarity. Selected bond lengths [pm] and angles [°]: P1–S1 192.0(1), P1–S2 193.9(1), P1–S3 212.5(1), P1–N1 186.9(1), P2–S6 192.4(1), P2–S7 193.9(1), P2–S5 211.2(1), P2–N2 186.5(1), S3–S4 206.3(1), S4–S5 204.2(1); S1–P1–S2 125.7(1), S6–P2–S7 125.5(1), S3–S4–S5 107.1(1), S1–P1–S3 113.8(1), S6–P2–S5 114.5(1), S2–P1–S3 103.4(1), S7–P2–S5 103.1(1).

Notes and References

^a Department of Chemistry, Ludwig-Maximilian University of Munich, Butenandtstr. 5-13 (D), D-81377 Munich, Germany.

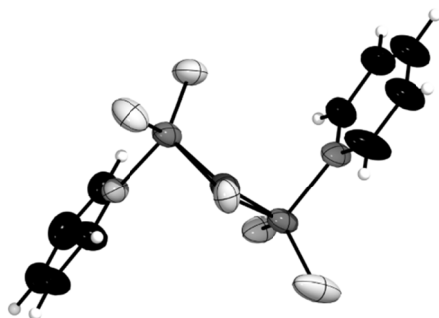
Financial support by the Department of Chemistry, University of Munich, is gratefully acknowledged.

† Electronic Supplementary Information (ESI) available: Crystallographic data and experimental details of py₂P₂S₇. See DOI: 10.1039/b000000x/

-
- [1] A. F. Holleman, E. Wiberg, N. Wiberg, *Lehrbuch der anorganischen Chemie*, 102nd ed.; Walter de Gruyter Verlag, Berlin, **2007**.
 - [2] for example: a) W. S. Sheldrick *J. Chem. Soc., Dalton Trans.* **1974**, 1402, b) T. Averbuch-Pouchot, M. Meisel *Acta Crystallogr.* **1989**, C45, 1937, c) M. Meisel, P. Lönnecke, A.-R. Grimmer, D. Wulff-Molder *Angew. Chem., Int. Ed. Engl.* **1997**, 36(17), 1869, d) G. Bouhadir, R. W. Reed, R. Réau, G. Bertrand *Heteroatom Chem.* **1995**, 6(4), 371, e) N. Burford, P. Losier, A. D. Phillips, P. J. Ragona, T. S. Cameron *Inorg. Chem.* **2003**, 42(4), 1087, f) J. J. Weigand, N. Burford, A. Decken, A. Schulz *Eur. J. Inorg. Chem.* **2007**, 4868.
 - [3] G. U. Wolf Patentnummer DD245878, **1987**.
 - [4] E. Fluck, H. Binder *Z. Anorg. Allg. Chem.* **1967**, 354(3-4), 114-129.
 - [5] M. Meisel, H. Grunze *Z. Anorg. Allg. Chem.* **1968**, 360, 277-283.
 - [6] CCDC 762680 contains the supplementary crystallographic data for this paper. These data can be obtained free of charge via www.ccdc.cam.ac.uk/data_request/cif, or by emailing data_request@ccdc.cam.ac.uk, or by contacting The Cambridge Crystallographic Data Centre, 12, Union Road, Cambridge CB2 1EZ, UK; fax: +44 1223 336033.
 - [7] A. C. Gallacher, A. A. Pinkerton *Acta Crystallogr., Sect. C* **1992**, C48, 701-703.
 - [8] M. Kulcsar, A. Silvestru, M. Vonas *Acta Crystallogr., Sect. E* **2008**, E64, o1683-o1684.

New Acyclic Neutral Phosphorus Sulfides and Sulfide Oxides

As published in *Z. Anorg. Allg. Chem.* **2013**.



A great number of binary neutral phosphorus sulfides has been discovered and investigated. However all stable representatives of this family of compounds adopt a polycyclic structure in contrast to their lighter homologues, the nitrogen oxides. Acyclic representatives can be stabilized by adduct formation with a nitrogen base. The bis(pyridine) adduct $\text{py}_2\text{P}_2\text{S}_5$ of the unstable acyclic phosphorus sulfide P_2S_5 is readily obtained stirring P_4S_{10} in pyridine at ambient temperature. X-ray diffraction studies on single crystals of $\text{py}_2\text{P}_2\text{S}_5 \cdot 0.5 \text{ py}$ (**1b**) show for the P_2S_5 framework a N_2O_5 like structure. The long P–N distances of 1.86 Å indicate only weak coordination of the pyridine molecules to phosphorus.

Single crystal X-ray diffraction studies on $\text{py}_2\text{P}_2\text{S}_{4.34}\text{O}_{0.66}$ (**2**) reveal the presence of $\text{py}_2\text{P}_2\text{S}_4\text{O}$ (**3**) together with $\text{py}_2\text{P}_2\text{S}_5$ in the crystal. Compound **3** contains the mixed phosphorus oxide sulfide molecule $\text{P}_2\text{S}_4\text{O}$ stabilized as bis(pyridine) adduct. It is readily obtained from pyP_2S_5 by oxidation with KMnO_4 in pyridine. The oxygen atom occupies the bridging position between the two phosphorus atoms. Quantum chemical calculations at the MPW1PW91 level of theory as well as DTA/TG thermal analyses confirm the weak coordination of the pyridine molecules in $\text{py}_2\text{P}_2\text{S}_5$, $\text{py}_2\text{P}_2\text{S}_4\text{O}$ and $\text{py}_2\text{P}_2\text{S}_7$ to phosphorus.

Introduction

Binary neutral phosphorus sulfides have been known for a long time. It was Berzelius, who in 1843 was the first to investigate the behaviour of sulfur towards phosphorus and synthesized the first representative of this class of compounds, the 'P₂S₅'.^[1] This molecule was later discovered to be the dimer P₄S₁₀. Since then many more phosphorus sulfides P₄S_x (x = 3–10) have been discovered.^[2] It is striking that all these neutral compounds adopt a polycyclic structure. This occurs due to the problem of an unfavourable $\sigma^3\lambda^5$ bonding situation at the phosphorus atom in acyclic representatives. In order to stabilize the $\sigma^3\lambda^5$ -phosphorus in such a molecule the missing fourth coordination partner might be provided by adduct formation, for example by coordination of a base like pyridine.

In fact 1967 Fluck and Binder were able to describe such a compound.^[3] In the course of their investigations on perthiophosphonic acid anhydrides they discovered, that on heating P₄S₁₀ in pyridine the bis(pyridine) adduct of the monomeric unit P₂S₅ is formed. This system has been used as sulfur removing agent in organic chemistry before. Fluck *et al.* described the synthesis of the bis(pyridine) adduct of P₂S₅ and reported its ³¹P NMR chemical shift.

Meisel and co-workers used this compound as educt to synthesize new betaines containing pyridine and one phosphorus atom.^[4] In 1982 Wolf and Meisel attempted to synthesise the structurally analogue adduct py₂P₂O₅.^[5] They proposed this molecule to be generated by refluxing P₄O₁₀ in pyridine but could not identify the product of this reaction by any means. In our group this experiment was repeated several times; however we were also not able to verify the existence of this molecule.

Shortly after this publication Wolf patented the compounds py₂P₂S₅ and py₂P₂S₄, which he claimed to have synthesized by refluxing P₄S₇ in pyridine.^[6] Also in this case, however, no proper characterization of the products was given.

In 2009 our group presented the crystal structures of py₂P₂S₅ and py₂P₂S₇ together with a full characterization of these compounds.^[7] The py₂P₂S₇ was synthesized by refluxing stoichiometric amounts of P₄S₁₀ and elemental sulfur in pyridine. Two years later the Swedish group of Prof Bergman also published the crystal structure of py₂P₂S₅ and discussed its use as thionating agent.^[8]

In the following an improved synthesis and the new structure of py₂P₂S₅ · 0.5 py are presented. Quantum chemical calculations at the MPW1PW91 level of theory using a

polarized double-zeta Basis Set (aug-cc-pVDZ) have been accomplished to verify the ^{31}P NMR spectroscopic properties and to enlighten the possible existence of a pyridine free acyclic phosphorus sulfide P_2S_5 . Also the question whether analogous mixed phosphorus sulfide oxide molecules can be stabilized by pyridine coordination will be discussed.

Results and Discussion

The pyridine Adduct $\text{py}_2\text{P}_2\text{S}_5$ (**1a**)

In course of our investigations of $\text{py}_2\text{P}_2\text{S}_5$ (**1a**) we found, that for its synthesis refluxing P_4S_{10} in pyridine is not necessary; the yield of **1a** can be improved by just stirring the starting material in pyridine at ambient temperature for a short period of time. Refluxing only causes the formation of larger amounts of $\text{py}_2\text{P}_2\text{S}_4\text{O}$ (**3**) as byproduct. This is shown in Figure 1, where the ^{31}P NMR spectra of the respective reaction solutions are compared. We observed the ^{31}P NMR shift of $\text{py}_2\text{P}_2\text{S}_5$ at 104.4 ppm and the one for $\text{py}_2\text{P}_2\text{S}_4\text{O}$ at 98.5 ppm.

In the literature only one compound has been reported, containing a 1,3,5,4-thiadiazaphosphinine ring, which has been characterized in terms of single crystal X-ray diffraction. Woollins *et al.* described the formation of the *P*-ferrocenyl substituted 2,6-bis(dimethylamino)-1,3,5,4-thiadiazaphosphorine-4-sulfide (**5**) in good yield together with small amounts of the thiocyanate (**6**) from the reaction of the corresponding ferrocenyl perthiophosphonic acid anhydride (**4**) with an excess of dimethyl cyanamide.^[6]

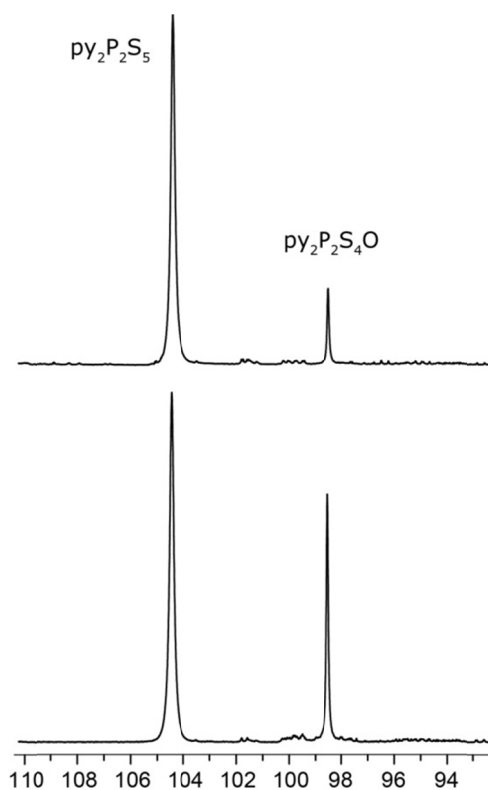


Figure 1. $^{31}\text{P}\{^1\text{H}\}$ NMR [ppm] spectrum of a solution of P_4S_{10} in pyridine before (top) and after (bottom) refluxing for 1 h at 120 °C.

Molecular Structure of $\text{py}_2\text{P}_2\text{S}_5 \cdot 0.5 \text{ py}$ (**1b**)

Colorless blockshaped single crystals of $\text{py}_2\text{P}_2\text{S}_5 \cdot 0.5 \text{ py}$ (**1b**) were isolated after refluxing a pyridine solution of $\text{py}_2\text{P}_2\text{S}_5$ and investigated by X-ray diffraction. Compound **1b** crystallizes in the triclinic space group $P\bar{1}$, with one molecule of $\text{py}_2\text{P}_2\text{S}_5$ and half a molecule of pyridine in the asymmetric unit. Figure 2 shows the molecular structure of **1b** together with selected atom distances and bond angles.

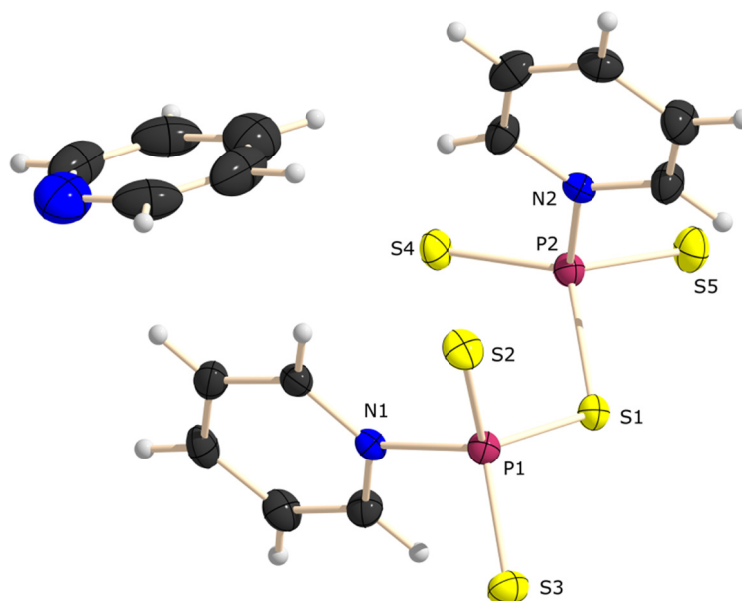


Figure 2. Molecular structure of **1b**. Thermal ellipsoids are set at 50% probability level. Selected atom distances [Å] and bond angles [°]: P1–S1/P2–S1 2.107(2)/2.121(2), P1–S2/P1–S3 1.931(2)/1.947(2), P2–S4/P2–S5 1.933(2)/1.945(2), P1–N1/P2–N2 1.863(2)/1.855(2); S1–P1–S2/S1–P2–S4 116.2(1)/114.7(1), S1–P1–S3/S1–P2–S5 103.6(1)/102.0(1), S2–P1–S3/S4–P2–S5 122.63(4)/124.5(1), P1–S1–P2 111.8(1).

The distance of the phosphorus atoms to the single coordinated sulfur atoms is with an average value of 1.939(1) Å within the range expected for a P–S double bond (1.922(14) Å).^[9] The distance between the phosphorus atoms and the bridging sulfur atom is averagely 2.114(1) Å, which is in good accordance with the one expected for a single bond (2.11 Å^[2a]). The P–N distances are with an average value of 1.859 Å around 0.2 Å longer than expected for a P–N single bond (1.652(24) Å)^[9], which indicates only weak coordination of the pyridine molecule to phosphorus. Similar strongly elongated P–N distances have been reported for the solvent free $\text{py}_2\text{P}_2\text{S}_5$ (1.862(6) Å and 1.865(3) Å)^[7], $\text{py}_2\text{P}_2\text{S}_7$ (1.869(3) Å and 1.865(3) Å)^[7], and also for the pyridine adduct of the PS_3^- anion (190.6(2) Å),^[10] in which a similar bonding situation is found.

The phosphorus atoms are surrounded distorted tetrahedrally by three sulfur atoms and one pyridine molecule. The largest values for S–P–S angles are found between the phosphorus and the two single coordinated sulfur atoms with 123.6°. The angles involving the bridging sulfur atom are smaller with values around 102.8°. The P1–S1–P2 angle has a value of 111.9°. Although only a slight distortion of the tetrahedral environment around the phosphorus atom might be expected, the sum of the S–P–S angles indicates with a value of 341.8° a strong deviation towards a planar PS_3

arrangement. A similar situation is found for solvent free $\text{py}_2\text{P}_2\text{S}_5^{[7]}$, $\text{py}_2\text{P}_2\text{S}_7^{[7]}$ and for the pyridine adduct of the PS_3^- $^{[10]}$ anion with values of 341° , 344° and 347° , respectively. This provides further evidence for an only weak coordination of the pyridine to the phosphorus.

Crystal Structure of $\text{py}_2\text{P}_2\text{S}_{4.34}\text{O}_{0.66}$ (**2**)

Crystals of $\text{py}_2\text{P}_2\text{S}_{4.34}\text{O}_{0.66}$ suitable for X-ray diffraction were obtained from the reaction of P_4S_3 with elemental sulfur in pyridine. The structure was solved in the monoclinic space group $P2_1/c$.

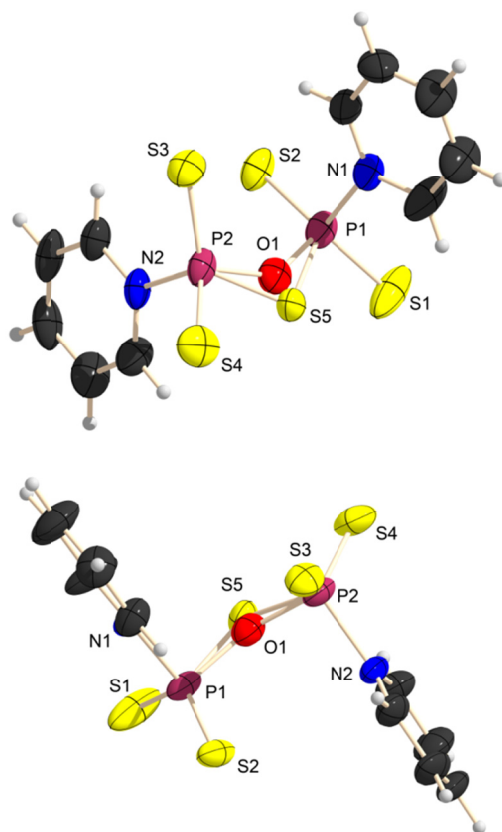


Figure 3. Molecular structure of **2** (two different viewing directions). Thermal ellipsoids are set at 50% probability level. Selected atom distances [\AA] and bond angles [$^\circ$]: P1–S1/P1–S2 1.928(2)/1.925(2), P1–S5/P2–S5 1.968(9)/2.013(9), P1–O1/P2–O1 1.687(11)/1.695(11), P1–N1/P2–N2 1.852(4)/1.854(4); S1–P1–S2/S3–P2–S4 123.0(1)/123.7(1), S1–P1–S5/S4–P2–S5 92.5(3)/93.2(3), S2–P1–S5/S3–P2–S5 125.2(3)/124.1(3), S1–P1–O1/S4–P2–O1 109.7(5)/109.9(5), S2–P1–O1/S3–P2–O1 110.0(5)/110.7(4).

The crystal contains both, the compound $\text{py}_2\text{P}_2\text{S}_5$ and the related oxygen derivative $\text{py}_2\text{P}_2\text{S}_4\text{O}$, with the oxygen atom in the bridging position. The two molecules occupy the same positions in the crystal except for the bridging O1 and S5 between the two phosphorus atoms, which results in a disorder in this position. Figure 3 shows the molecular structure and contains selected atom distances and bond angles.

The phosphorus atoms are again surrounded distorted tetrahedrally by two single coordinated sulfur atoms, one molecule of pyridine and the bridging sulfur or oxygen atom, completing the tetrahedron. The oxygen can be found with 66%, while the sulfur is occupying the bridging position with 34%. Because of the different P–O and P–S distances and the deviation in the angles at the bridging chalcogen atoms, the positions of the two atoms could be identified and the atoms refined anisotropically. The distances between the phosphorus and the single coordinated sulfur atoms differ with a value of $1.930(2) \text{ \AA}$ only slightly from the distance expected for a P–S double bond ($1.922(14) \text{ \AA}^{[9]}$). The P–O1 ($1.691(11) \text{ \AA}$) and P–S5 ($1.991(9) \text{ \AA}$) distances lie in the expected ranges for single bonds ($1.621(7) \text{ \AA}^{[9]}$; $2.11 \text{ \AA}^{[2a]}$). Due to the disorder in the crystal all values are afflicted with higher standard uncertainties.

The nitrogen atom of the pyridine molecule has a distance of $1.853(4) \text{ \AA}$ to the phosphorus atom, which is elongated compared to the expected $1.652(24) \text{ \AA}^{[9]}$ for a P–N single bond. So this indicates again only a weak coordination of the pyridine molecules to the phosphorus. This is further supported by the sum of the S–P–S(O) angles of $341.0(5)^\circ$ and $344.3(4)^\circ$ respectively, which again show a deviation towards a planar surrounding of phosphorus by the chalcogen atoms.

Table 1. Details for X-ray data collection and structure refinement for compounds **1b** and **2**.

	py ₂ P ₂ S ₅ · 0.5 py (1b)	py ₂ P ₂ S _{4,34} O _{0,66} (2)
CCDC	937614	940974
formula	C _{12.5} H _{12.5} N _{2.5} P ₂ S ₅	C ₁₀ H ₁₀ N ₂ P ₂ S _{4.25} O _{0.75}
M [g/mol]	419.99	368.40
color, habit	colorless block	colorless block
cryst. system	triclinic	monoclinic
space group	<i>P</i> –1	<i>P</i> 2 ₁ / <i>c</i> (No. 53)
<i>a</i> [Å]	8.976(2)	14.564(1)
<i>b</i> [Å]	9.203(2)	11.061(1)
<i>c</i> [Å]	12.672(2)	9.884(1)
α [°]	102.547(5)	90
β [°]	90.241(4)	92.890(7)
γ [°]	118.501(6)	90
<i>V</i> [Å ³]	890.870(10)	1590.2(2)
<i>Z</i>	2	4
ρ_{calc} [g/cm ³]	1.566	1.539
μ [mm ^{–1}]	0.826	0.346
θ range [°]	4.44–28.28	4.20–25.00
data collected	10688	17380
data	4381	2786
parameters	203	172
<i>R</i> _{int}	0.0329	0.0748
<i>R</i> ₁ [<i>I</i> > 2 σ]	0.0370	0.0660
<i>wR</i> ₂ [<i>I</i> > 2 σ]	0.0830	0.1961
<i>R</i> ₁ [all data]	0.0537	0.1097
<i>wR</i> ₂ [all data]	0.0933	0.1961
GOOF on <i>F</i> ²	1.001	1.017
larg. diff peak/hole (e/Å)	0.917/–0.464	0.557/–0.493

The Pyridine Adduct $\text{py}_2\text{P}_2\text{S}_4\text{O}$ (**3**)

The bis(pyridine) adduct $\text{py}_2\text{P}_2\text{S}_4\text{O}$ (**3**) ($n = 1$) is the first member of a series of pyridine stabilized mixed phosphorus sulfide oxides $\text{P}_2\text{S}_{5-n}\text{O}_n$ ($n = 1-4$), which fill the gap between $\text{py}_2\text{P}_2\text{S}_5$ and the still unknown adduct $\text{py}_2\text{P}_2\text{O}_5$. Compound **3** can be obtained by stirring **1a** and KMnO_4 in pyridine for two days at ambient temperature. It is identified by the ^{31}P NMR signal at 98.5 ppm (Figure 4), which fits the one predicted by quantum chemical calculations (see below).

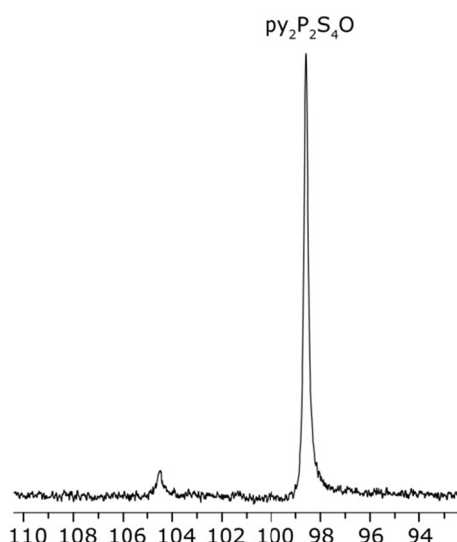


Figure 4. $^{31}\text{P}\{^1\text{H}\}$ NMR spectrum of **3** in pyridine.

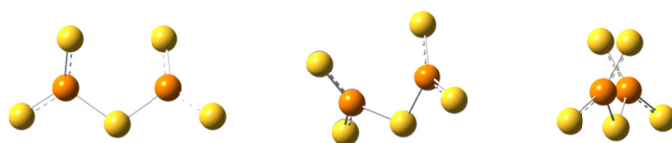
Quantum Chemical Calculations

The compounds $\text{py}_2\text{P}_2\text{S}_5$ and $\text{py}_2\text{P}_2\text{S}_7$ can be viewed as loose pyridine adducts of the acyclic phosphorus sulfides P_2S_5 and P_2S_7 ; so it is interesting to investigate how the coordination of pyridine influences the atom distances and the structures of the free P_2S_5 and P_2S_7 molecules. In order to give an answer to this question quantum chemical calculations at the MPW1PW91 level of theory using a polarized triple-zeta basis set (aug-cc-pVTZ) for $\text{py}_2\text{P}_2\text{S}_5$ and a polarized double-zeta basis set (aug-cc-pVDZ) for the free P_2S_5 were carried out. Furthermore energy values for both molecules were determined on the level of CBS-4M and the ^{31}P NMR data for $\text{py}_2\text{P}_2\text{S}_5$ and $\text{py}_2\text{P}_2\text{S}_4\text{O}$ were calculated.

Table 2. Calculated and experimentally observed distances [\AA] and bond angles [$^\circ$] of **1** (average values).

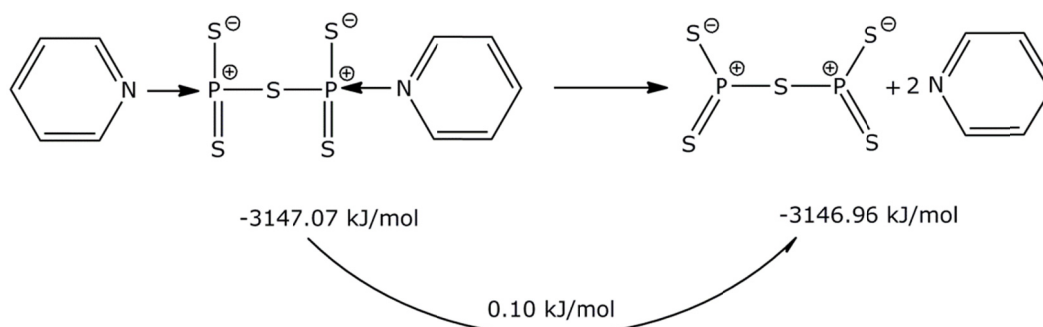
	py ₂ P ₂ S ₅ (obs.)	P ₂ S ₅ (calc.)	py ₂ P ₂ S ₅ (calc.)
Distances [\AA]			
P–N	1.86	–	1.86
P–S _{sc}	1.93	1.92	1.94
P–S _{tc}	2.12	2.13	2.12
S–S			
Angles [$^\circ$]			
S _{sc} –P–S _{sc}	123	134	128
S _{sc} –P–S _{tc}	104/115	107/118	103/115
S _{tc} –S _{tc} –S _{tc}			
P–S _{tc} –P	112	113	112

sc = single coordinated; tc = twofold coordinated

**Figure 5.** Optimized structure of P₂S₅ (three different orientations).

The optimized structure of the P₂S₅ molecule is shown in Figure 5. The calculated atom distances and bond angles within the py₂P₂S₅ molecule correspond very well to those observed for **1b** in the crystal (Table 2). Remarkably the calculated atom distances and bond angles for the pyridine free sulfide P₂S₅ also do not differ much from the calculated and experimentally determined values for py₂P₂S₅. Obviously adduct formation has little influence on the bonding situation within the P₂S₅ framework. Coordination of pyridine affects mainly the geometry around the phosphorus atom causing a slight deviation from planarity for the PS₃ moiety.

Furthermore quantum chemical calculations on the level of CBM-4M were carried out to compare the enthalpy values of **1** and the pyridine free compound P₂S₅ (Scheme 1).



Scheme 1. Dissociation of $\text{py}_2\text{P}_2\text{S}_5$ in P_2S_5 and pyridine.

The difference in the enthalpies resulting from the calculations is 0.10 kJ/mol. Thus the composition according to the reaction in Scheme 1 is slightly endothermic. This small difference of enthalpy fits well to the experimentally determined strongly elongated P–N distance in the bis(pyridine) adduct **1b**. Both suggest that the P–N bonds in **1** should be cleaved easily at higher temperatures generating free P_2S_5 , which should be stable in the gas phase.

$\text{py}_2\text{P}_2\text{S}_7$. A similar situation is found for the bis(pyridine) adduct of P_2S_7 . The results of a quantum chemical study of the bonding situation in this compound compared to free P_2S_7 (Figure 6) have been discussed in detail.^[7b]

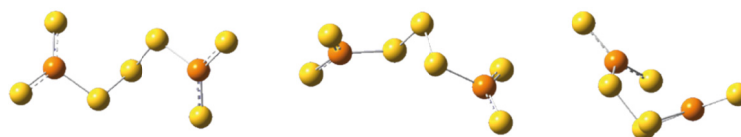
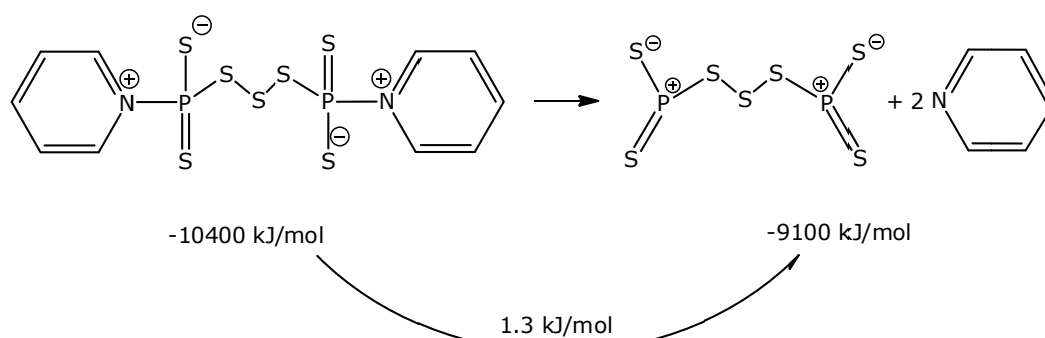


Figure 6. Optimized structure of P_2S_7 (three different orientations).



Scheme 2. Dissociation of $\text{py}_2\text{P}_2\text{S}_7$ in P_2S_7 and pyridine.

For the dissociation of $\text{py}_2\text{P}_2\text{S}_7$ in free P_2S_7 and pyridine (Scheme 2) an enthalpy difference of 1.3 kJ/mol was calculated. This result suggests that in this case it might also be possible to promote the dissociation thermally as depicted in the scheme above and thus to generate free acyclic P_2S_7 in the gas phase.

NMR spectroscopy. In order to estimate the ^{31}P NMR chemical shift of $[(\text{py})\text{PS}_2]_2\text{S}$ (**1**) and $[(\text{py})\text{PS}_2]_2\text{O}$ (**3**), the isotropic magnetic shieldings were computed using the GIAO (Gauge-Independent Atomic Orbital) method implemented in G03.^[11,12] The structures were optimized in C_2 symmetry (Figure 7) and the frequencies calculated ($NIMAG = 0$) at MPW1PW91/aug-cc-pVDZ level of theory. Subsequently, the NMR shielding tensors were calculated at the same level of theory using the GIAO method.^[11,12] Table 3 summarizes the computed isotropic magnetic shieldings and relative ^{31}P NMR chemical shifts (ppm) referenced to H_3PO_4 .

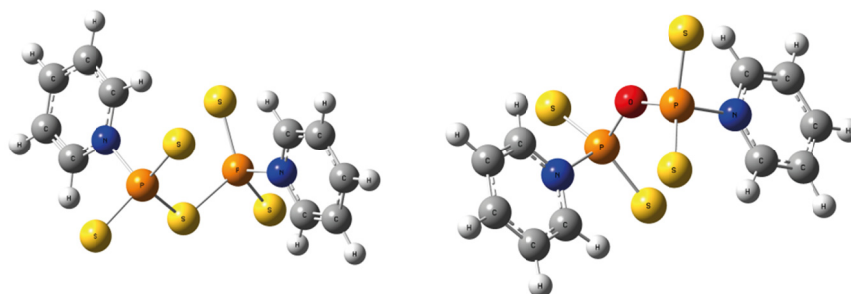


Figure 7. Computed C_2 structures of $[(\text{py})\text{PS}_2]_2\text{S}$ (left) and $[(\text{py})\text{PS}_2]_2\text{O}$ (right) at MPW1PW91/aug-cc-pVDZ level of theory.

The calculated ^{31}P NMR chemical shifts for $\text{py}_2\text{P}_2\text{S}_5$ and the oxygen derivative $\text{py}_2\text{P}_2\text{S}_4\text{O}$ compare well to the experimentally observed values. Introduction of oxygen in the bridging position in place of sulfur causes only a small shift of $\delta^{31}\text{P}$ to higher field.

Table 3. Computed isotropic magnetic shieldings (GIAO method^[11,12], MPW1PW91/aug-cc-pVDZ) and relative ³¹P chemical shifts (ppm) referenced to H₃PO₄.

compound	py ₂ P ₂ S ₅	py ₂ P ₂ S ₄ O	H ₃ PO ₄
- <i>E</i> / a.u.	3170.462064	2847.464794	644.135802
<i>NIMAG</i>	0	0	0
<i>p.g.</i>	C ₂	C ₂	C ₃
δ ³¹ P / ppm, calcd. isotr. shielding	249.9	260.8	364.3
δ ³¹ P / ppm, calcd. (ref. to H ₃ PO ₄)	114.3	103.5	0.0
δ ³¹ P / ppm, exptl., (ref. to H ₃ PO ₄)	104.4	98.5	0.0

Thermal Analyses

In order to gain further insight into the thermal stability of the pyridine adducts **1a**, **1b**, **2** and py₂P₂S₇ and investigate the possibility of generating the pyridine free phosphorus sulfides and sulfide oxides DTA/TG thermal analyses were performed. For this purpose the compounds were heated up to 400 °C in steps of 5 °C/min. In the thermograms (Figures 8–11) the dashed curve shows the weight signal while the black one represents the heat flow signal, which indicates changes in the energy at a certain temperature.

The thermal analysis of the bis(pyridine) adduct of P₂S₅ **1a** is shown in Figure 8. The endothermic heat flow signal at 168 °C derives from the two pyridine molecules leaving the solid, while the sharp peak at 261 °C quotes the melting point of the resulting P,S material. The melting point of P₄S₁₀ is reported to be 288 °C^[13] and thus differs by 27 °C from that observed for the P,S material obtained. The resulting material almost immediately starts to decompose releasing volatile products.

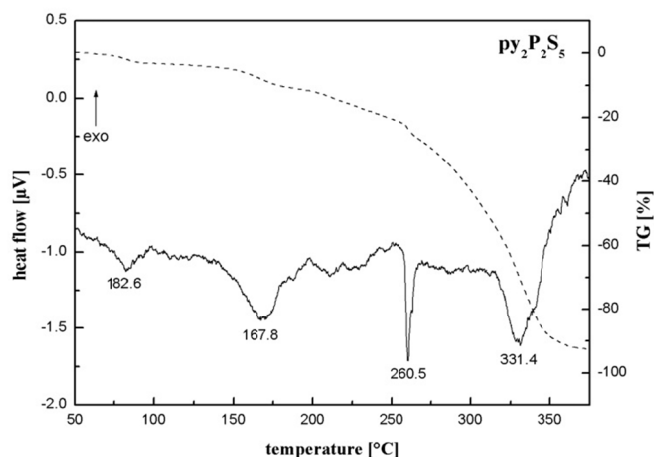


Figure 8. Thermogram of $\text{py}_2\text{P}_2\text{S}_5$ (**1a**).

The thermal behaviour of the bis(pyridine) adduct of P_2S_5 **1b** is particularly interesting as it contains an additional free pyridine molecule in the crystal. Its thermogram is depicted in Figure 9. The first endothermic heat flow signal can be assigned to the free pyridine being released. This temperature is in accordance to the melting point of $\text{py}_2\text{P}_2\text{S}_5 \cdot 0.5 \text{ py}$ **1b** (115 °C). The other three signals correspond very well to those observed for the adduct $\text{py}_2\text{P}_2\text{S}_5$ **1a**.

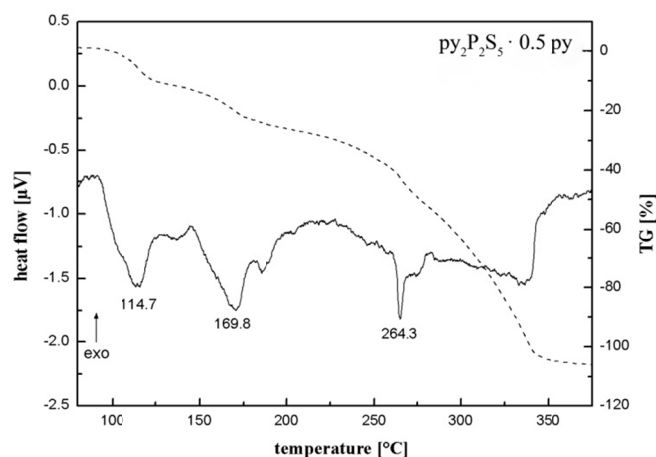


Figure 9. Thermogram of $\text{py}_2\text{P}_2\text{S}_5 \cdot 0.5 \text{ py}$ (**1b**).

The thermogram of $\text{py}_2\text{P}_2\text{S}_{4.34}\text{O}_{0.66}$ **2**, which in fact contains $\text{py}_2\text{P}_2\text{S}_5$ **1** and $\text{py}_2\text{P}_2\text{S}_4\text{O}$ **3**, shows a slightly different behaviour. The two pyridine molecules leave the solid already at 148 °C. The resulting material, which in addition to phosphorus and sulfur

now contains also oxygen, undergoes a further transformation at 226 °C and melts at 300 °C, followed by decomposition and release of volatile products.

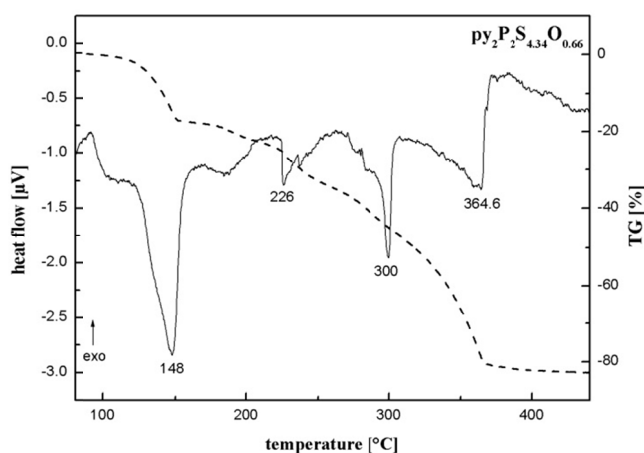


Figure 10. Thermogram of $\text{py}_2\text{P}_2\text{S}_{4.34}\text{O}_{0.66}$ (**2**).

In the case of the bis(pyridine) adduct of P_2S_7 (**4**), the thermogram of which is shown in Figure 10, only two endothermic transformation can be observed. The first one occurs at 161.6 °C and is assigned to the loss of pyridine. Thus a material of the composition P_2S_7 remains. At a temperature of 242.4 °C it melts and begins to decompose releasing volatile products. Decomposition is complete at 298 °C.

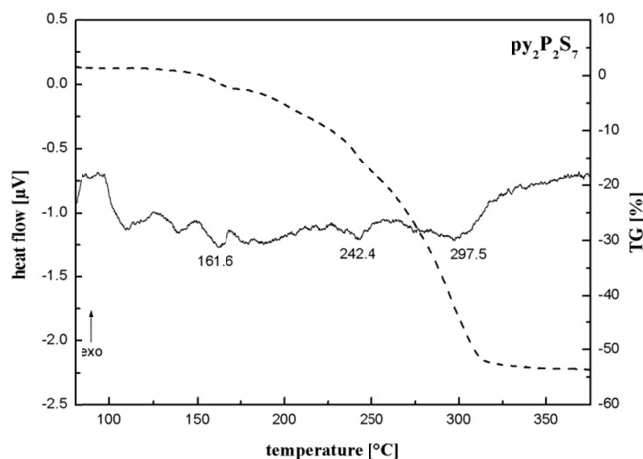
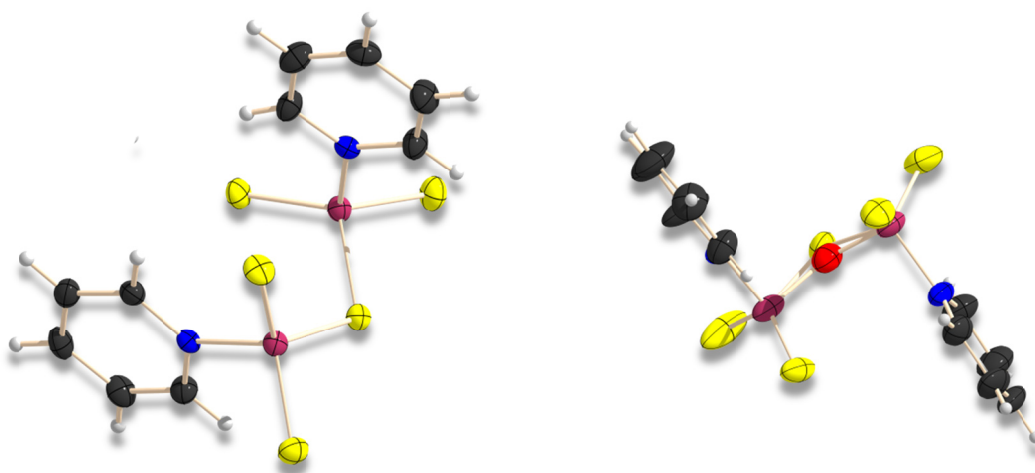


Figure 11. Thermogram of $\text{py}_2\text{P}_2\text{S}_7$ (**4**).

The results of the thermal analysis of the adducts **1–4** show, that all adducts release pyridine at temperatures between 140 °C and 170 °C before melting, thus confirming the relatively weak coordination of pyridine to phosphorus.

Conclusion

The bis(pyridine) adduct of the acyclic binary phosphorus sulfide P_2S_5 is readily obtained by stirring P_4S_{10} in pyridine at ambient temperature. Single crystal X-ray diffraction studies on $py_2P_2S_5 \cdot 0.5\ py$ (**1**) confirm stabilization of the P_2S_5 framework by weak coordination of the pyridine molecules to phosphorus. X-ray diffraction studies on $py_2P_2S_{4.34}O_{0.66}$ (**2**) provide first evidence for the existence of $py_2P_2S_4O$, a bis(pyridine)adduct of the mixed phosphorus sulfide oxide P_2S_4O with oxygen bridging the two phosphorus atoms. These results point to a general concept of stabilizing reactive phosphorus species containing $\sigma^2\lambda^5$ phosphorus atoms by weak coordination of a nitrogen base to phosphorus. It should be possible to extend this concept to other small molecules with three coordinated phosphorus(V) atoms. Thermogravimetric investigations on $py_2P_2S_5$, $py_2P_2S_{4.34}O_{0.66}$ and $py_2P_2S_7$ confirm the weak coordination of pyridine to phosphorus and indicate, that these adducts might be of interest as precursors for the generation of gaseous acyclic phosphorus sulfides and sulfide oxides.



Experimental Section

General conditions. All reactions were carried out under inert gas atmosphere using Argon (Messer Griesheim, purity 4.6 in 50 L steel cylinder) and working with Schlenk techniques. The glass vessels used were stored in a 130 °C drying oven. Before filling they were flame dried *in vacuo* at 10^{-3} mbar. Elemental sulfur was used

as received (Acros Organics). P_4S_{10} and P_4S_3 were commercially obtained (Riedel-de H  en). The pyridine used was dried with commonly known methods and freshly distilled before use.

X-ray Crystallography. The single-crystal X-ray diffraction data were collected using an Oxford Xcalibur3 diffractometer equipped with a Spellman generator (voltage 50 kV, current 40 mA), Enhance molybdenum K_α radiation source ($\lambda = 71.073$ pm), Oxford Cryosystems Cryostream cooling unit, four circle kappa platform and a Sapphire CCD detector. Data collection and reduction were performed with CrysAlisPro.^[14] The structures were solved with SIR97^[15], refined with SHELXL-97^[16], and checked with PLATON^[17], all integrated into the WinGX software suite^[18]. The finalized CIF files were checked with checkCIF.^[19] Intra- and intermolecular contacts were analyzed with DIAMOND (version 3.2i), plots are shown with thermal ellipsoids at the 50% probability level. Details for data collection and structure refinement are summarized in Table 1. CCDC 937614 (**1b**) and 940974 (**2**) contain the supplementary crystallographic data for this paper. These data can be obtained free of charge from The Cambridge Crystallographic Data Centre via www.ccdc.cam.ac.uk/data_request/cif.

NMR Spectroscopy. NMR spectra were recorded using a Jeol EX 400 Eclipse instrument operating at 161.997 MHz (^{31}P). Chemical shifts are referred to 85% H_3PO_4 as external standard. All spectra were measured, if not mentioned otherwise, at 25 °C. **DTA/TG.** Thermal analytic measurements were carried out with a Thermoanalyzer TG-DTA-92 (Setaram) under inert gas atmosphere (He). The compound was heated in a corundum melting pot up to a temperature of 750 °C in steps of 5 °C/min. **Mass Spectrometry.** Mass spectra were obtained with a MStation JMS 700 (Jeol) using the ionisation method DEI+/EI+. **IR Spectroscopy.** The spectra were recorded using a PerkinElmer Spektrum one FT-IR instrument (KBr pellets) equipped with a Diamant-ATR Dura Sampler at 25 °C (neat). Raman spectra were recorded on a Bruker RAMII Raman instrument ($\lambda = 1064$ nm, 200 mW, 25 °C) equipped with D418-T Detector at 200 mW at 25 °C.

py₂P₂S₅ (1a**).** P_4S_{10} (889.2 mg, 2 mmol) was stirred in pyridine (40 mL) for 1 h. Colourless needles of **1a** crystallized overnight they were separated by filtration and dried *in vacuo*. (Yield: 1415.4 mg, 93%).

$^{31}P\{^1H\}$ NMR (pyridine): δ [ppm] = 104.2 (s). **Elemental analysis** (py₂P₂S₅): calcd. C 31.57, N 7.36, H 2.65, P 16.28, S 42.14; found C 32.92, N 7.69, H 3.30, S 31.78. **Mass** (EI+) m/z = 379.8 ($[C_{10}H_{10}N_2P_2S_5]^+$), 347.8 ($[M-S]^+$), 299.9 ($[M-py]^+$),

221.9 ([M-py₂]⁺), 191.9 ([M-py₂S]⁺), 160.0 ([M-py₂S₂]⁺), 128.0 ([PS₃]⁺), 96.0 ([PS₂]⁺), 63.0 ([PS]⁺). **Raman** (200 mW, rt): ν [cm⁻¹] = 3066 (31), 1609 (36), 1567 (29), 2000 (43), 1014 (100), 468 (50), 448 (37). **IR** (200 mW, rt): ν [cm⁻¹] = 1087 (s), 3060 (m), 1633 (vw), 1606 (m), 1532 (vw), 1484 (vw), 1471 (vw), 1452 (vs), 1330 (vw), 1262 (vw), 1194 (w), 1154 (vw), 1093 (vw), 1053 (m), 1044 (s), 1011 (m), 762 (m), 734 (vs), 673 (vs), 655 (w), 642 (w), 575 (vs), 461 (w), 454 (w), 423 (w).

py₂P₂S₅ · 0.5 py (1b). 380.5 mg (1 mmol) of **1a** was dissolved in refluxing pyridine (40 mL) for 2 h. The yellow reaction mixture turned orange when cooling down to ambient temperature and the formation of a colourless crystalline precipitate consisting of py₂P₂S₅ could be observed. The needles were separated and dried *in vacuo* (Yield: 363.1 mg, 83%).

³¹P{¹H} NMR (pyridine): δ [ppm] = 104.3 (s). **Elemental analysis** ((py₂P₂S₅)₂ · py): calcd. C 35.76, N 8.35, H 3.00, P 14.77, S 38.12; found C 32.92, N 7.74, H 2.86, S 40.76. **Mass** (EI+) m/z = 379.8 ([C₁₀H₁₀N₂P₂S₅]⁺), 347.9 ([M-S]⁺), 299.9 ([M-py]⁺), 221.9 ([M-py₂]⁺), 191.9 ([M-py₂S]⁺), 160.0 ([M-py₂S₂]⁺), 128.0 ([PS₃]⁺), 63.0 ([PS]⁺). **Raman** (200 mW, rt): ν [cm⁻¹] = 3068 (63), 1610 (23), 1565 (5), 1202 (25), 1012 (100), 465 (37), 448 (14), 417 (30). **IR** (200 mW, rt): ν [cm⁻¹] = 3094 (w), 3044 (w), 1610 (m), 1577 (vw), 1476 (vw), 1452 (vs), 1431 (m), 1342 (vw), 1262 (vw), 1199 (vw), 1156 (vw), 1091 (ww), 1057 (m), 1045 (s), 1014 (m), 843 (vw), 763 (vw), 748 (w), 739 (s), 720 (vs), 668 (vs), 642 (vw), 565 (vs), 468 (vw), 457 (s), 421 (w).

py₂P₂S_{4.34}O_{0.66} (2). 220.1 mg P₄S₃ (1 mmol) were refluxed and dissolved in 10 mL of pyridine in the presence of traces of water. Afterwards 192.4 mg sulfur (0.75 mmol) were added to the yellow reaction mixture and refluxed for 1 h at a temperature of 120 °C. Colorless crystals of py₂P₂S_{4.34}O_{0.66} were obtained while cooling the solution to ambient temperature. The precipitate was separated from the solution and dried *in vacuo* (Yield: 299.4 mg, 43%).

³¹P{¹H} NMR (pyridine): δ [ppm] = 104.3 (s). **Elemental analysis** (py₂P₂S_{4.34}O_{0.66}): calcd. C 32.49, N 7.58, H 2.73, S 37.57; found C 32.60, N 8.48, H 3.61, S 33.74. **Mass** (DEI+) m/z = 379.8 (M_S = [C₁₀H₁₀N₂P₂S₅]⁺), 363.6 (M_O = [C₁₀H₁₀N₂P₂S₄O]⁺), 347.9 ([M_S-S]⁺), 299.9 ([M_S-py]⁺), 284.7 ([M_O-py]⁺), 252.8 ([M_O-pyS]⁺), 221.9 ([M-py₂]⁺), 188.8 ([M_O-pyPS₂]⁺), 128.0 ([PS₃]⁺), 63.0

([PS]⁺). **Raman** (200 mW, rt): ν [cm⁻¹] = 3068 (25), 1604 (46), 1182 (53), 1031 (55), 1015 (100), 472 (84). **IR** (200 mW, rt): ν [cm⁻¹] = 3009 (w), 2510 (w), 2124 (w), 1629 (w), 1602 (m), 1596 (w), 1517 (m), 1484 (m), 1476 (s), 1447 (s), 1390 (w), 1323 (w), 1252 (w), 1187 (m), 4481 (m), 1159 (m), 1129 (m), 1051 (m), 1023 (w), 1041 (m), 1014 (m), 998 (m), 896 (br, vs), 767 (m), 743 (s), 731 (m), 718 (m), 675 (vs).

py₂P₂S₄O (4): To 41.7 mg (0.264 mmol) KMnO₄ a solution of 46.8 mg **1** in pyridine (5 mL) was added and stirred for 48 h at room temperature. The precipitate was filtrated and the solvent was removed from the yellow solution *in vacuo* (Yield: 44 mg, 98%).

³¹P{¹H} NMR (pyridine): δ [ppm] = 98.0 (s). **Elemental analysis** (py₂P₂S₄O): calcd. C 32.96, N 7.69, H 2.77, S 35.20; found C 37.42, N 8.71, H 3.48, S 28.24. **Mass** (EI+) m/z = 363.9 ([C₁₀H₁₀N₂P₂S₄O]⁺), 331.9 ([M-S]⁺), 284.7 ([M-py]⁺), 252.9 ([M-pyS]⁺), 205.0 ([M-py₂]⁺), 190.0 ([M-pyS₂]⁺), 173.0 ([M-pyPS₂O]⁺), 128.0 ([PS₃]⁺), 63.0 ([PS]⁺). **Raman** (200 mW, rt): ν [cm⁻¹] = 3062 (49), 1615 (48), 1016 (100), 470 (60), 385 (52). **IR** (200 mW, rt): ν [cm⁻¹] = 3056 (vw), 2397 (w), 1631 (w), 1593 (w), 1532 (w), 1484 (m), 1444 (w), 1385 (vw), 1248 (w), 1211 (w), 1151 (w), 1051 (w), 1033 (vw), 1021 (vw), 998 (w), 868 (br, vs), 743 (s), 680 (vs), 666 (s).

Acknowledgement

Financial support by the Department of Chemistry, University of Munich, is gratefully acknowledged. Stefanie Schedlbauer is thanked for her help with the syntheses.

- [1] J. Berzelius, *Liebigs Ann. Chem.* **1843**, 46, 129.
- [2] a) E. W. A. Holleman, N. Wiberg, *Lehrbuch der anorganischen Chemie*, Walter de Gruyter Verlag, Berlin, **2007**; b) R. Blachnik, A. Hoppe, *Z. Anorg. Allg. Chem.* **1979**, 457, 91; c) R. Blachnik, U. Peukert, A. Czediwoda, *Z. Anorg. Allg. Chem.* **1995**, 621, 1637; d) M. E. Jason, T. Ngo, S. Rahman, *Inorg. Chem.* **1997**, 36, 2633; e) H. Nowotnick, R. Blachnik, *Z. Anorg. Allg. Chem.* **1999**, 625, 1966; f) H. Nowotnick, R. Blachnik, *Z. Anorg. Allg. Chem.* **2000**, 626, 611; g) R. Thamm, G. Heckmann, E. Fluck, *Phosphorus, Sulfur, Silicon Relat. Elem.* **1981**, 11, 273-278; h) T. Roedl, A. Pfitzner, *Z. Anorg. Allg. Chem.* **2011**, 637, 1507.

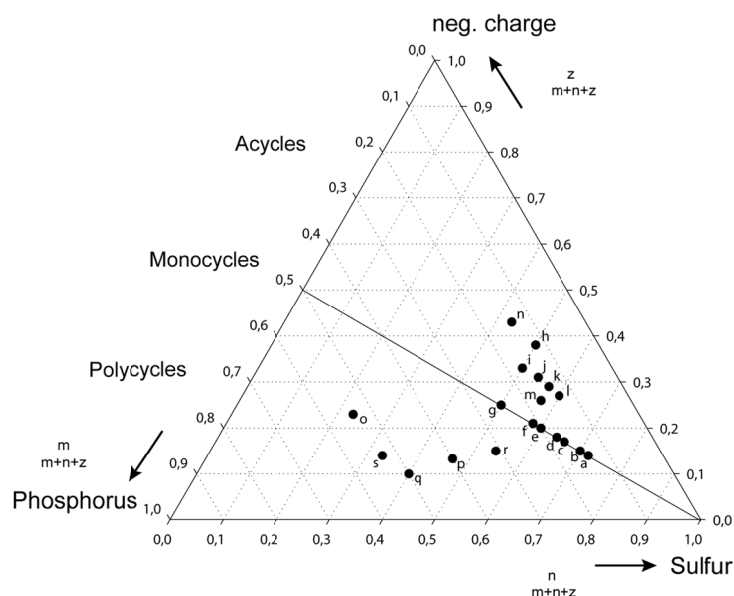
- [3] E. Fluck, H. Binder, *Z. Anorg. Allg. Chem.* **1967**, 354, 113.
- [4] M. Meisel, H. Grunze, *Z. Anorg. Allg. Chem.* **1968**, 360, 277.
- [5] G. U. Wolf, M. Meisel, *Z. Chem.* **1982**, 22, 54.
- [6] G. U. Wolf, *DD 245878*, DDR, **1986**.
- [7] a) C. Rotter, *Dissertation*, LMU Munich **2008**; b) C. Rotter, C. Evangelisti, S. Schoenberger, T. M. Klapötke, K. Karaghiosoff, *Chem. Comm.* **2010**, 46, 5024.
- [8] J. Bergman, B. Pettersson, V. Hasimbegovic, P. H. Svensson, *J. Org. Chem.* **2011**, 76, 1546.
- [9] F. H. Allen, O. Kennard, D. G. Watson, L. Brammer, A. G. Orpen, R. Taylor, *J. Chem. Soc., Perkin Trans. 2 (1972-1999)* **1987**, S1–S19.
- [10] A. Dimitrov, I. Hartwich, B. Ziemer, D. Heidemann, M. Meisel, *Z. Anorg. Allg. Chem.* **2005**, 631, 2439.
- [11] Gaussian 03, Revision C.02, M. J. Frisch, G. W. Trucks, H. B. Schlegel, G. E. Scuseria, M. A. Robb, J. R. Cheeseman, J. A. Montgomery, Jr., T. Vreven, K. N. Kudin, J. C. Burant, J. M. Millam, S. S. Iyengar, J. Tomasi, V. Barone, B. Mennucci, M. Cossi, G. Scalmani, N. Rega, G. A. Petersson, H. Nakatsuji, M. Hada, M. Ehara, K. Toyota, R. Fukuda, J. Hasegawa, M. Ishida, T. Nakajima, Y. Honda, O. Kitao, H. Nakai, M. Klene, X. Li, J. E. Knox, H. P. Hratchian, J. B. Cross, C. Adamo, J. Jaramillo, R. Gomperts, R. E. Stratmann, O. Yazyev, A. J. Austin, R. Cammi, C. Pomelli, J. W. Ochterski, P. Y. Ayala, K. Morokuma, G. A. Voth, P. Salvador, J. J. Dannenberg, V. G. Zakrzewski, S. Dapprich, A. D. Daniels, M. C. Strain, O. Farkas, D. K. Malick, A. D. Rabuck, K. Raghavachari, J. B. Foresman, J. V. Ortiz, Q. Cui, A. G. Baboul, S. Clifford, J. Cioslowski, B. B. Stefanov, G. Liu, A. Liashenko, P. Piskorz, I. Komaromi, R. L. Martin, D. J. Fox, T. Keith, M. A. Al-Laham, C. Y. Peng, A. Nanayakkara, M. Challacombe, P. M. W. Gill, B. Johnson, W. Chen, M. W. Wong, C. Gonzalez, and J. A. Pople, Gaussian, Inc., Pittsburgh PA, **2003**.
- [12] a) R. Ditchfield, *Mol. Phys.* **1974**, 789; b) R. J. L. M. Dodds, A. Sadlej, *J. Mol. Phys.* **1980**, 1419; c) R. McWeeny, *Phys. Rev.* **1962**, 1028; d) K. Wolinski, J. F. Hinton, P. Pulay, *J. Am. Chem. Soc.* **1990**, 112, 8251.
- [13] M. C. Demarcq, *J. Mater. Sci. Lett.* **1992**, 11, 758.
- [14] *CrysAlisPro 1.171.36.21*, Agilent Technologies, **2012**.
- [15] A. Altomare, G. Cascarano, C. Giacovazzo, A. Guagliardi, A. G. G. Moliterni, M. C. Burla, G. Polidori, M. Camalli, R. Spagna, *SIR97, Package for Crystal Structure Solution*, University of Bari (Italy), **1997**.
- [16] G. M. Sheldrick, *SHELXL-97, Program for the Refinement of Crystal Structures*. University of Göttingen, Germany, **1997**.
- [17] A. L. Spek, *Platon, A Multipurpose Crystallographic Tool*, Utrecht University, Utrecht, The Netherlands, **2012**.

PART V

^{31}P NMR Investigation of Polyphosphides

Motivation

The motivation to investigate polyphosphides is the synthesis of new phosphorus rich binary phosphorus-chalcogen anions. The following scheme is exemplary for the status quo in this chemistry.



Scheme 1. Phosphorus-chalcogen anions.^[1]

The thiophosphates which are already known are pointed out as black dots. Obviously there is only a small amount of black colour and the dots are not spread across the whole triangular but gathered in the right corner. These are thiophosphates with a great amount of sulfur and therefore sparsely charged.

This leaves a great area which is blank and thus undiscovered. In order to gain an insight into this region it was tried to access it by reacting polyphosphides with elemental sulfur or in general chalcogens.

So the first goal was to synthesise distinct polyphosphides in solution, which has been a rather complex problem during previous investigations.

Alkaliphosphides should be synthesised starting from white phosphorus under mild conditions and at low temperature, the optimum would be room temperature. So maybe the number of different polyphosphides in one reaction mixture could be

reduced for example by using different solvents, different forms of the educts and activation of the alkali metals beforehand.

^{31}P NMR is used to identify the products and to check their purity.

At last a new way should be found to synthesise new P-Ch compounds, starting from the obtained products and elemental chalcogenes.

Introduction

An overview of polyphosphides to be obtained in reaction solution is given in Figure 1.

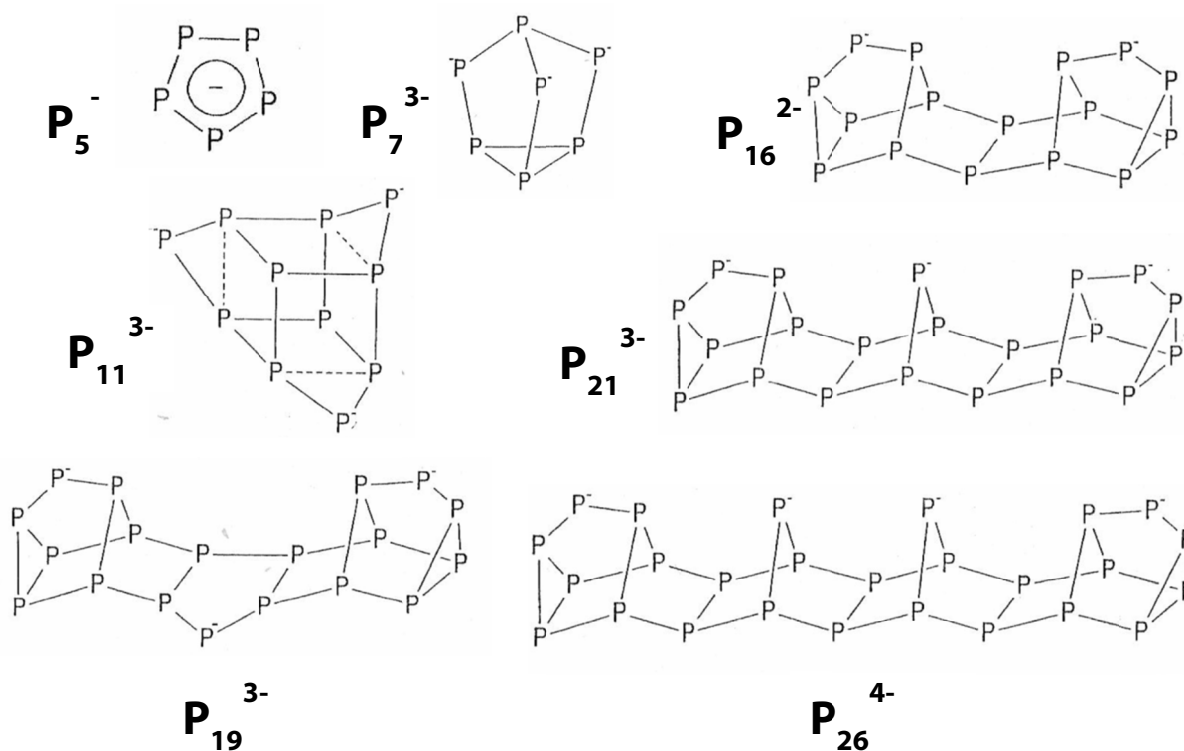


Figure 1. Examples of different polyphosphides.^[2]

Polyphosphorus Hydrides – Historical Notes

In 1877, a compound with the formal composition "PhP", the first cyclophosphane was described by Köhler and Michealis.^[3] The compound was identified as cyclopentaphosphane (PPh)₅ in the year 1969.^[4] Since then, an unexpected variety of mono- and polycyclophosphanes have been discovered.^[4,5] All compounds having a skeleton of phosphorus atoms can be regarded as derivatives of phosphorus hydrides P_nH_n (phosphanes) and are of great interest for a better understanding of nucleophilic cleavage of white phosphorus.^[6]

Especially *Marianne Baudler* engaged herself in this field of chemistry, focussing on compounds inheriting P–P bonds. Her big goal was to synthesize polycyclic P_n^{m-} anions *via* reaction of white phosphorus with LiPH₂ in THF or monoglyme.^[2]

Already in 1979 she reported on the synthesis and characterization of Li₃P₇. She used ³¹P NMR spectroscopy to analyze the fluxional nature of the P₇³⁻ cluster in THF which is explained in the next passage.^[7]

Three years later, in 1982, the polyphosphide P₁₆²⁻ was obtained *via* nucleophilic cleavage of white phosphorus with lithium dihydrogenphosphide.^[8]

Also the group of *von Schnering* prepared the same anion P₁₆²⁻ but this time *via* reaction of Na₃P₇ with (Ph₄P)Cl.^[9]

In 1987 *Baudler* investigated the reaction of the alkalimetal sodium and white phosphorus in THF and observed the anion P₅⁻.^[10]

The reaction of white phosphorus with lithium dihydrogenphosphide or sodium results in the formation of the polycyclic anions P₂₁⁴⁻ and P₂₆⁴⁻.^[11]

The major problem of the polyphosphide chemistry is, that always a great number of different polyphosphides together is obtained from one reaction in solution. All metal phosphides and polyphosphides are formed from the elements regardless of the stoichiometric ratio.^[12] For example, *Baudler* received a mixture of Li₃P₁₉, Li₂P₁₆, Li₃P₂₁, Li₄P₂₆, Li₂HP₇, LiH₂P₇ and Li₂H₂P₇ *via* the nucleophilic cleavage of P₄ with LiPH₂ in THF or 1,2-dimethoxyethane and with the reaction of red phosphorus and KPH₃ in hot DMF a mixture of PH₃, KP₅ and K₂HP₇ was formed.^[13] Until now no method has been found to circumvent these problems.

Recently, Korber *et al.* analysed the crystal structures of P_4^{2-} and P_5^- in liquid NH_3 and proposed a new view on aromaticity of these two anions.^[14]

Chemical Properties of Polyphosphides

Phosphorus is likely to build up anions which can be regarded as Zintl ions. These are metallic or metalloid main group elements, which form electronically precise polyanions, which are negatively charged homoatomic clusters.

Phosphorus builds up many aromatic and nonaromatic, mono- and polycyclic cage-like anions. They are homologue to the polysulfides and are generated *via* nucleophilic cleavage of white phosphorus. It is a quasi step wise breakup of the element structure which means that they can be regarded as frozen-in redox steps between the element and its electron-saturated formal anion.^[12]

Most of the polyphosphides are only present in the solid state. This occurs due to the fact that they are not stable as they are not saturated. A steady decomposition and creation of different polyphosphides takes place in the solution. In order to stabilize themselves they form intermolecular interaction to build up polymeric polyphosphides with a great molecular size and this makes them insoluble.^[2,15]

That the P–P bond is indeed rather weak shows the valence isomerisation of the P_7^{3-} ion which undergoes a steady rearrangement *via* migration of electron pairs. (Figure 2)

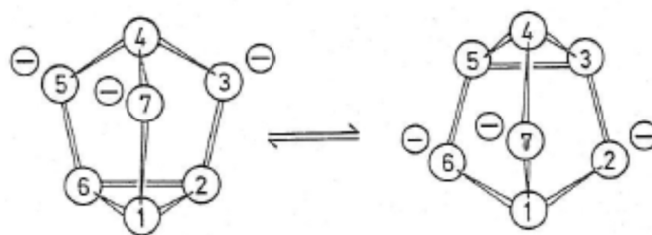


Figure 2. Valence isomerisation of P_7^{3-} .^[16]

This incident is fast and reversible and is called degenerate Cope rearrangement. That means that every rearrangement can shift every atom from one position to another and also from a twofold to a threefold bonded position and *vice versa*.^[16]

Figure 3, shows the ^{31}P NMR spectra of the P_7^{3-} ion at different temperatures.

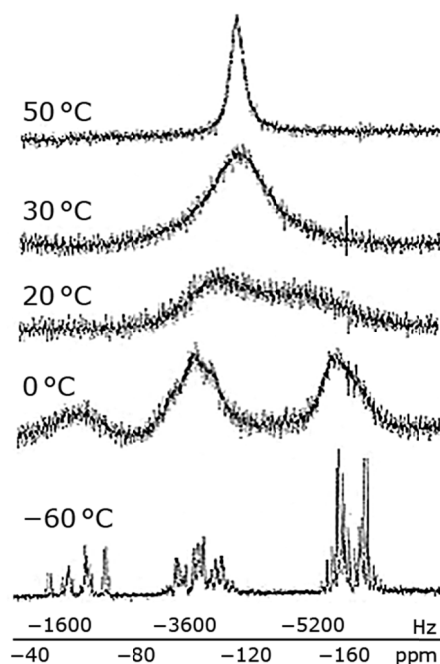


Figure 3. ^{31}P NMR spectra of Li_3P_7 in THF.^[7]

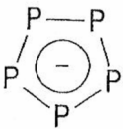
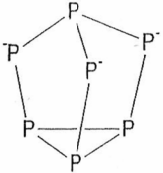
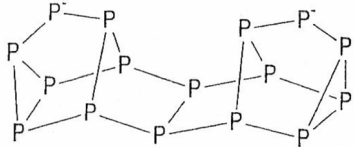
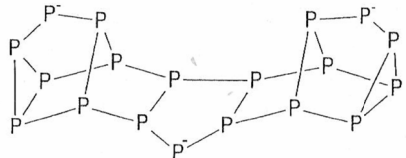
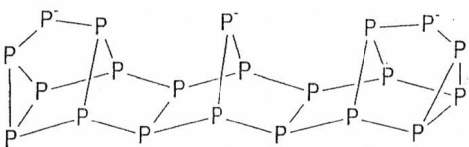
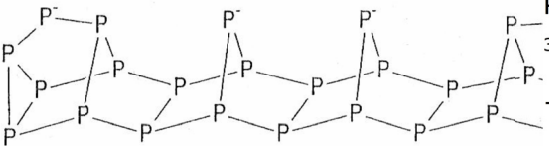
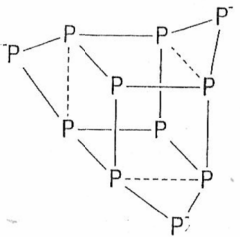
At low temperature (in this case $-60\text{ }^\circ\text{C}$) the rearrangement is too slow to be detected on the NMR timescale. Here the spectrum shows distinct signals, while at room temperature only one broad signal can be observed as all P-atoms are equal.

This means that there is an equilibrium between different polyphosphides in the solution and no distinct polyphosphide is present.^[17]

Results and Discussion

In Table 1 all necessary ^{31}P NMR resonances are listed.

Table 1. ^{31}P NMR data of important polyphosphides.

Number	Structure	Compound and corresponding NMR data
(1)		P_5^- ^{31}P { ^1H } NMR: δ [ppm] = +470.8
(2)		P_7^{3-} ^{31}P { ^1H } NMR: δ [ppm] = -57, -103, -162 at -60°C ^{31}P { ^1H } NMR: δ [ppm] = -120.0 at rt
(3)		P_{16}^{2-} ^{31}P { ^1H } NMR: δ [ppm] = +60, +38, +6, -34, -134, -172
(4)		P_{19}^{3-} ^{31}P { ^1H } NMR: δ [ppm] = +49, +6, -55, -74, -95, -170, -192
(5)		P_{21}^{3-} ^{31}P { ^1H } NMR: δ [ppm] = +72, +61, -15, -108, -118, -146, -169
(6)		P_{26}^{4-} ^{31}P { ^1H } NMR: δ [ppm] = +84, +54, +30, -15, -88, -128, -135, -169
(7)		P_{11}^{3-} ^{31}P { ^1H } NMR: δ [ppm] = +174.5/+167.9, -102.3, -209.4

Reaction of P_4 with Sodium

The first synthetic route tried starts from P_4 and Na in THF. Instead of just mixing the compounds like it was done by former groups, the sodium was first dissolved in THF and naphthalene was added in order to activate the alkali metal. To the green solution white phosphorus was added. After one day of stirring a redish precipitate could be gained, which was analysed via ^{31}P NMR spectroscopy.

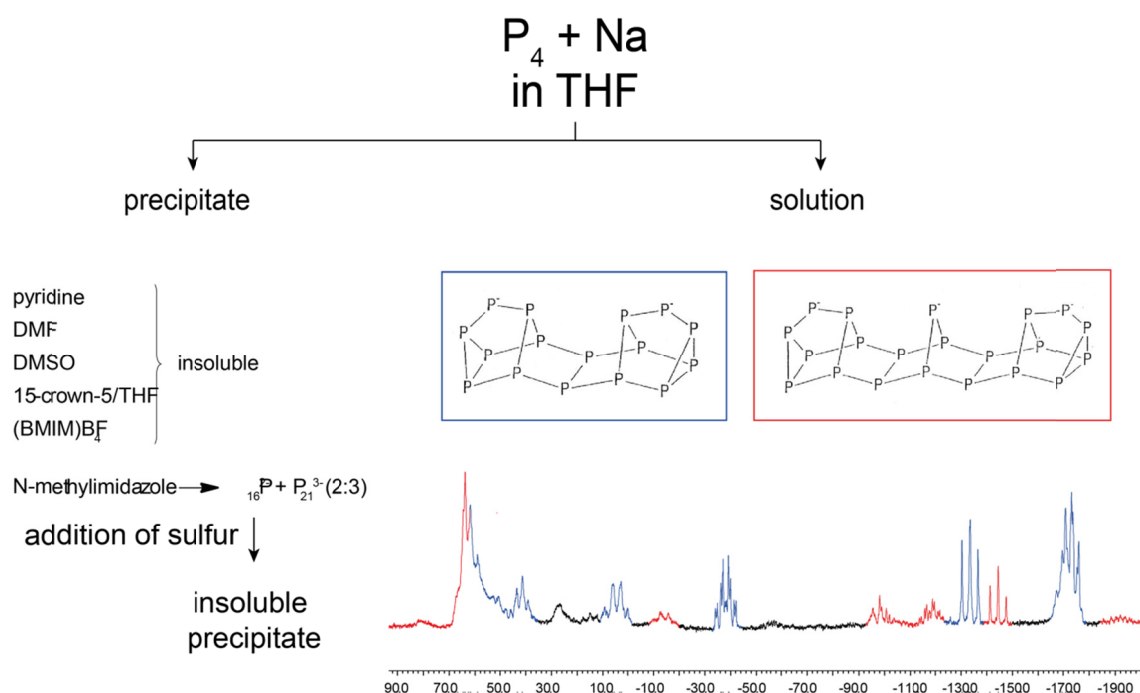


Figure 4. Reaction of P_4 and sodium in THF (part 1).

The spectrum in Figure 4, the spectrum that only P_{16}^{2-} and P_{21}^{3-} are present in the solution of the precipitate dissolved in *N*-MeIm. Unfortunately the addition of elemental sulfur only led to an insoluble precipitate.

The next step was to show how much the steady rearrangement influences the composition of the solution.

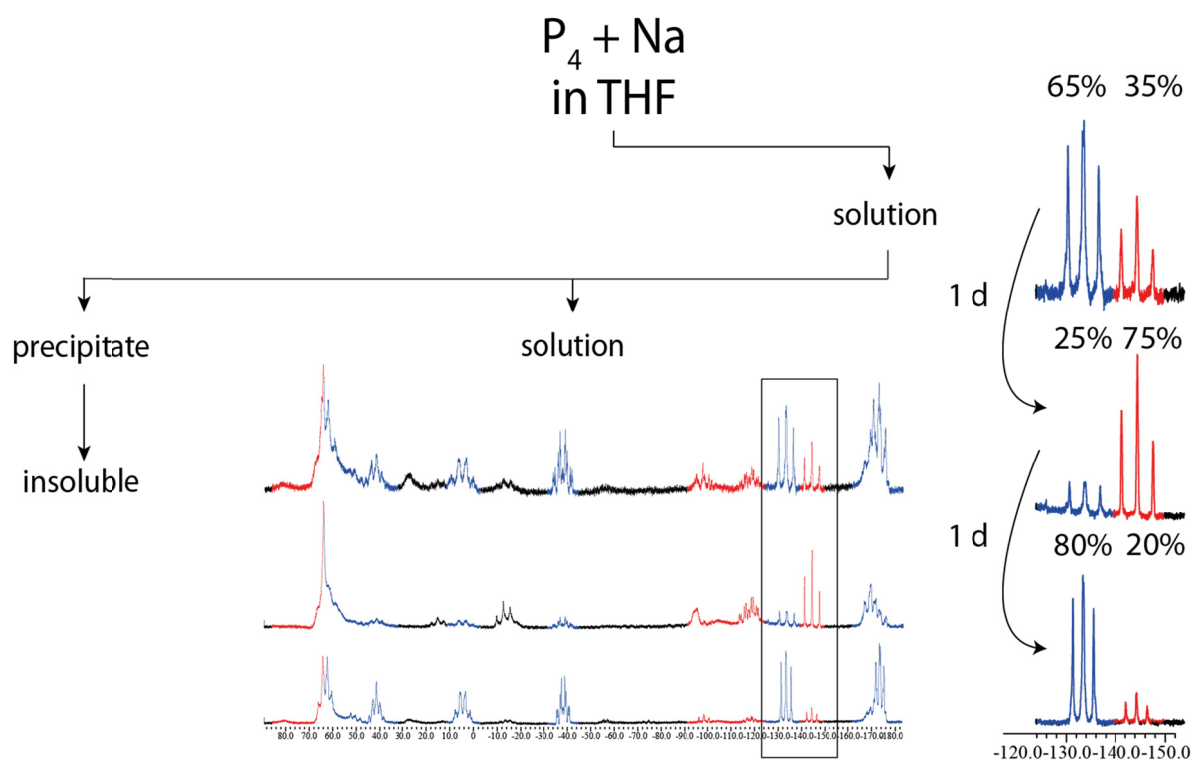


Figure 5. Reaction of P_4 with sodium in THF (part 2).

The spectra of Figure 5 were taken one day after the other. For a proper comparison the two triplets with a chemical shift between 130–150 ppm are chosen because they originate from the two bridging atoms in the P_{16}^{2-} and P_{21}^{3-} . As can be seen there is no precise ration but a great fluctuation takes place. Apart from that movement the products are rather pure as hardly any by-products can be observed in the NMR spectra.

After gaining this inside into the composition of the products in solution elemental sulfur was added. The received precipitate is another time insoluble. But the NMR analysis of the solution shows that a reaction between the sulfur and the polyphosphides must have taken place, which can be seen in Figure 6 where the above shows the solution before and the second one the solution after the addition.

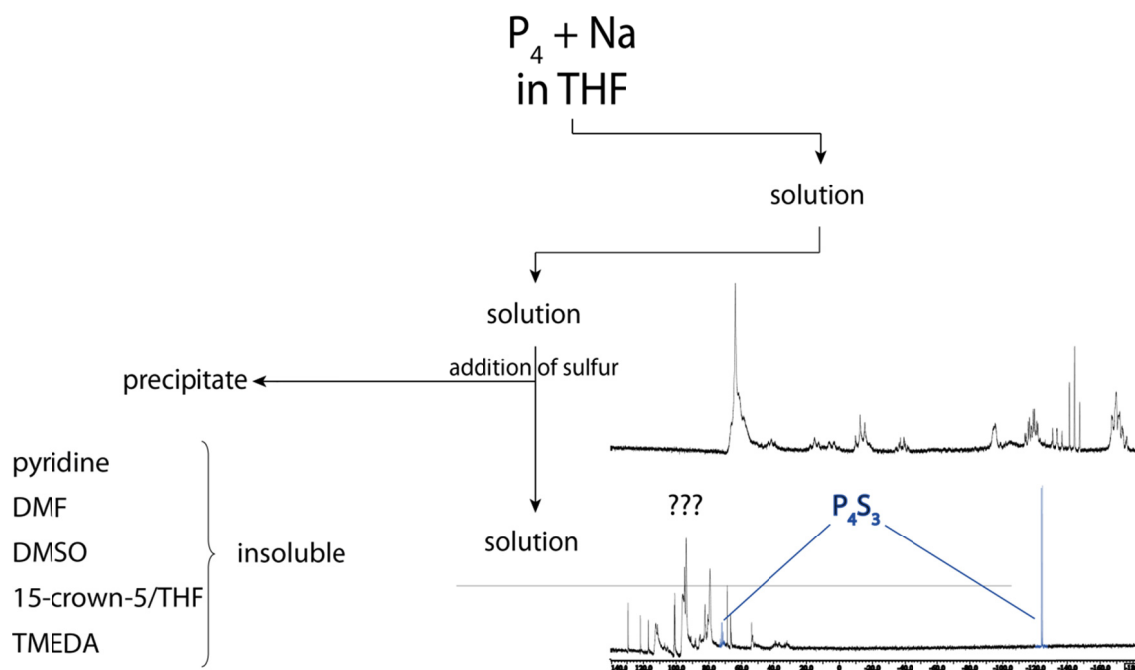


Figure 6. Reaction of P_4 with sodium in THF (part 3).

Unfortunately, the products were still not clearly identified apart from P_4S_3 .

Reaction of P_4 with lithium

White phosphorus was reacted with lithium. The outcome of these reactions was independent of the stoichiometric amounts of the educts (range $P_4:Li$ between 7:12 and 0.125 – $\frac{7}{8}$).

Different solvents do not influence the educt diversity as well but the amount of the received products, as can be seen in Table 2.

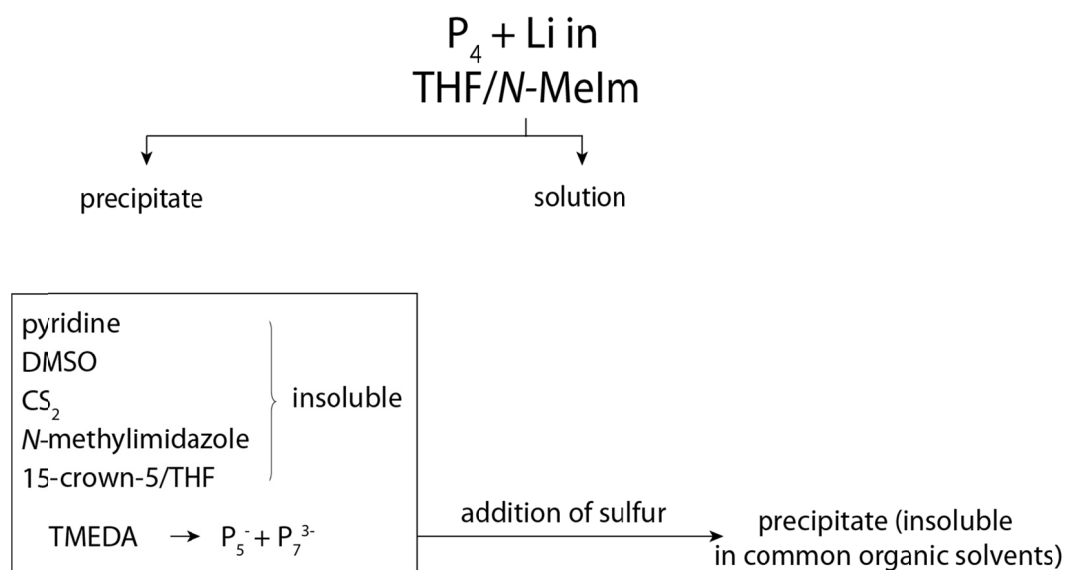
Further attention was drawn to the form of lithium used (Table 3). Here the best outcome could be received by using lithium with an oxide layer. It was suspended in THF and naphthalene was added. P_4 was dissolved in *N*-MeIm and both solutions were mixed.

Table 2. Reaction of P_4 with lithium in different solvents.

Experiment	Solvent	Ratio [P_4 :Li]	Products
1	N-MeIm	7:12	42% P_{16}^{2-} / 18% P_{21}^{3-}
2			1) 86% P_7^{3-}
3	THF/N-MeIm	1:8	2) 65% P_7^{3-} / 23% P_5^-
4			3) 62% P_7^{3-} / 29% P_5^-
5	pyridine	1:8	71% P_7^{3-}
6	acetonitrile	1:8	--
7		1:8	--
8			

Table 3. Reaction of P_4 with different types of lithium in THF/N-MeIm.

lithium	ratio [P_4 :Li]	products
granules without oxide layer	7:12	42% P_{16}^{2-} / 18% P_{21}^{3-}
granules with oxide layer	1:8	8% P_5^- / 63% P_{16}^{2-} / 25% P_{21}^{3-}
powder with oxide layer	1:8	1) 1.5% P_5^- / 25% P_{16}^{2-} / 38% P_{21}^{3-} 2) 71% P_7^{3-} / 7% P_5^- 3) 86% P_7^{3-} 4) 65% P_7^{3-} / 23% P_5^- 5) 62% P_7^{3-} / 29% P_5^-

**Figure 7.** Reaction of white phosphorus with lithium (granules with an oxide layer) in THF/N-MeIm (part 1).

The brownish precipitate was rather insoluble. Only in TMEDA a small amount of P_5^- and P_7^{3-} could be observed. The following addition of sulfur only led to another insoluble precipitate.

The NMR spectrum of the solution revealed that P_7^{3-} was present with 86%. An excess of sulfur was added and a solution containing thiophosphates with a great amount of sulfur was gained. These thiophosphates are already known and are therefore not of further interest.

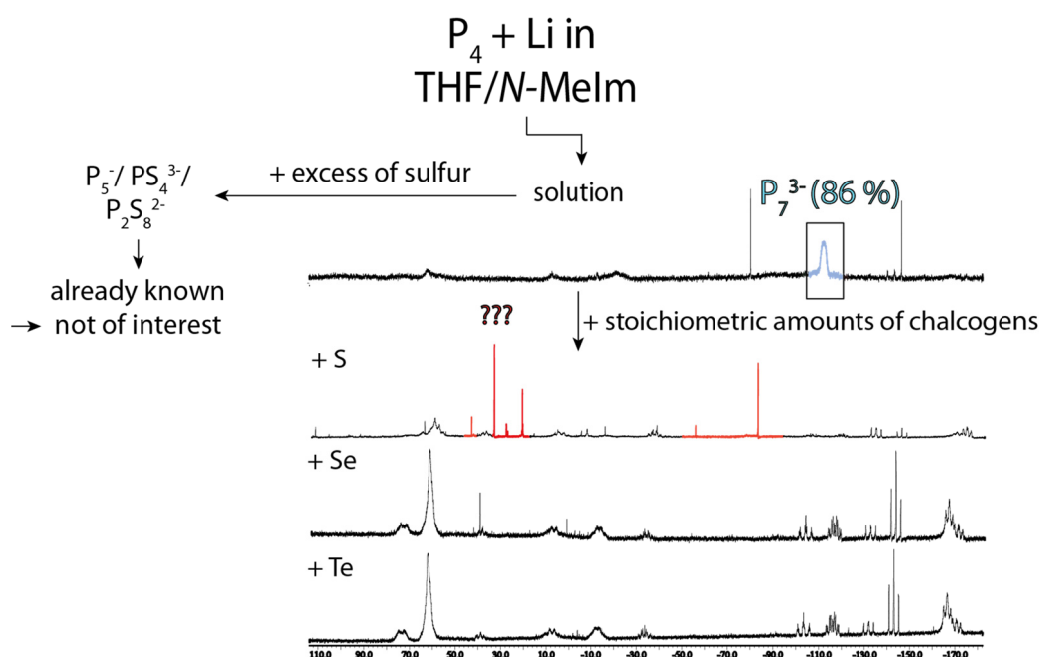


Figure 8. Reaction of polyphosphides with stoichiometric amounts of chalcogens.

The addition of different stoichiometric amounts of chalcogens lead to the formation of the larger polyphosphides P_{16}^{2-} and P_{21}^{3-} (Table 4). Only with sulfur a small amount of another product which could not be identified has been produced.

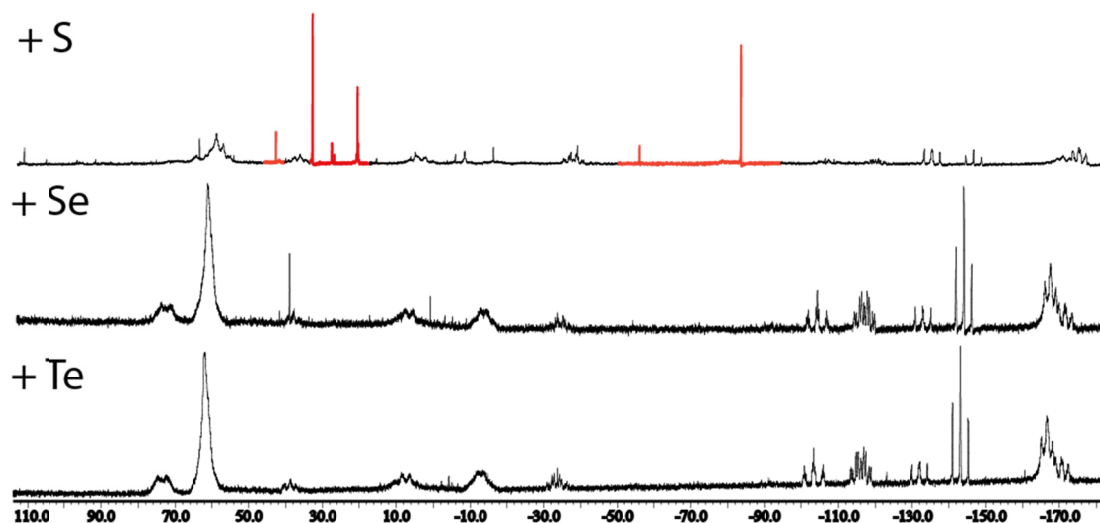
Table 4. Reaction of polyphosphides with different chalcogens.

Experiment	Chalcogen	Ratio [P_4 :chalcogen]
9	S	1:1,4
10	Se	1:1,5
11	Te	1:0,9

Conclusion

The formation of polyphosphides from the reaction of white phosphorus with alkali metals in basic media was investigated with the aim to use the polyphosphides for reactions with heavier chalcogens (S and Se). Phosphorus-rich binary P,S and P,Se anions should become accessible by this route.

But the situation turned out to be quite complicated. The results indicate clearly, that the activation of the alkali metal with naphthalene beforehand has a great influence on the product diversity in the solution. In addition the polyphosphides formed from P_4 and alkali metals in pyridine or *N*-methylimidazole were almost independent of the stoichiometric ratio of the educts under the conditions applied. In all cases a mixture of different polyphosphides, predominantly P_{16}^{2-} , P_{21}^{3-} and P_7^{3-} was obtained. ^{31}P NMR spectroscopic investigations of these mixtures over a longer period of time indicated an equilibrium among these polyphosphides. Over time insoluble polyphosphides formed. Oxidation of P_7^{3-} with S, Se and Te resulted in the formation of the larger polyphosphides P_{16}^{2-} and P_{21}^{3-} .



Experimental Section

General. All reactions were carried out under inert gas atmosphere using Schlenk techniques.

Argon was used as inert gas received from Messer Griesheim. All glasses vessel were stored in a 120 °C drying oven and were flame dried three times *in vacuo* at 10^{-3} mbar before use.

White phosphorus was peeled under water, washed with dry THF and TMS-Cl and dried *in vacuo*. Sodium was peeled under pentane, washed with THF and dried *in vacuo*. Sulfur, selenium, tellurium and lithium were used as received. Pyridine and *N*-MeIm were stored under argon atmosphere and were dried over molecular sieve. Li_2S was stored under nitrogen atmosphere in a glovebox.

NMR Spectroscopy. NMR spectra were recorded using a Jeol EX 400 Eclipse instrument operating at 161.997 MHz (^{31}P). Chemical shifts are referred to 85% H_3PO_4 as external standard. If not mentioned otherwise, all spectra were measured at 25 °C. The % data correspond to the intensities in the ^{31}P NMR spectra with respect to the total intensity. The difference to 100% belongs to not determinable signals.

Reaction of P_4 with Sodium

White phosphorus (193.4 mg, 1.56 mmol), sodium (14.4 mg, 0.624 mmol) and naphthalene (288.0 mg, 2.25 mmol) were suspended in THF (60 mL) and stirred over night at ambient temperature. The brownish precipitate was removed from the red reaction solution and dissolved in different solvents (Table 5).

From the solution, three NMR spectra were measured in three days in a row.

1. day: ^{31}P $\{^1\text{H}\}$ NMR (THF, rt): δ [ppm] = **3** (65%), **5** (35%).

2. day: ^{31}P $\{^1\text{H}\}$ NMR (THF, rt): δ [ppm] = **3** (25%), **5** (75%).

3. day: ^{31}P $\{^1\text{H}\}$ NMR (THF, rt): δ [ppm] = **3** (80%), **5** (20%).

To the remaining solution an sulfur (12.5 mg, 0.4 mmol) was added. The red precipitate was insoluble in the solvents from Table 5 and the solution contained only not assignable signals in the ^{31}P NMR along with P_4S_3 .

$^{31}\text{P}\{^1\text{H}\}$ NMR (THF, rt): δ [ppm] = 109 (m, 35%), 93.1 (m, 23%), 80.1 (m, 22%), 68.9 (s P_4S_3 , 2%), -124.0 (d, P_4S_3 , 9%).

Table 5. Suspension of the brown precipitate in different solvents ("-" refers to no phosphorus signal in the $^{31}\text{P}\{^1\text{H}\}$ NMR)

Solvent	Observation	Result: $^{31}\text{P}\{^1\text{H}\}$ NMR (solvent, rt): δ [ppm]
THF/15-crown-5	no reaction	-
dimethylformamide	brown solution, red precipitate	-
<i>N</i> -Methylimidazole	brown solution, brown precipitate	3 (34%), 5 (66%) (only small amounts)
dimethylsulfoxide	no reaction	-
BMIMBF ₄ (ionic liquid)	no reaction	-
pyridine	solution turns yellow	-

Reaction of P_4 with Lithium

Introductory experiments:

In Table 2, the reactions of white phosphorus (170.0 mg, 1.4 mmol) with lithium in different solvents are listed.

In Table 3, the reactions of white phosphorus (200.0 mg, 1.6 mmol) with different forms of lithium are listed.

Synthesis:

White phosphorus (170.0 mg, 1.4 mmol) was suspended in THF (18 mL). In another glass vessel, lithium powder with an oxide layer (76.2 mg, 11.0 mmol) was suspended in *N*-MeIm (26 mL). This solution was added to the one containing white phosphorus. Immediately the solution turned brown. After stirring for five days lithium was not dissolved completely and was removed by filtration.

2 mL of the solution were transferred into another glass vessel for crystallization and 6 mL diethyl ether was diffused slowly into the solution.

The residual solution was divided into three parts and elemental sulfur, selenium and tellurium were added, respectively.

^{31}P { ^1H } NMR (THF/*N*-MeIm, rt): δ [ppm] = -143.1 (s, 5.8%); -131.5 (s, 11.4%); (**1**) (1.5%); (**3**) (25.4%); (**5**) (37.9%).

To the solution was then added in different vessels:

a) an excess of sulfur:

^{31}P { ^1H } NMR (THF/*N*-MeIm, RT): δ [ppm] = 36.3 (s, 38.3%, $\text{P}_2\text{S}_6^{2-}$); 55.5 (s, 6.8%); 86.4 (s, 5.9%); 92.6 (s, 8.1%); 214.1 (s br, 4.0%, PS_5^-).

b) sulfur (ratio $\text{P}_4\text{:S}$ 1:1.4):

^{31}P { ^1H } NMR (THF/*N*-MeIm, RT): δ [ppm] = -2.2 (s, 12.3); 24.1 (s, 7.9%); 36.4 (s, 12.4%); (**1**) (25.5%); (**3**) (19.9%); (**5**) (12.9%).

c) selenium (ratio $\text{P}_4\text{:Se}$ 1:1.5):

^{31}P { ^1H } NMR (THF/*N*-MeIm, RT): δ [ppm] = -79.6 (s, 33.5%); (**1**) (29.7%); (**3**) (12.8%); (**5**) (16.9%).

d) tellurium (ratio $\text{P}_4\text{:Te}$ 1:0.9):

^{31}P { ^1H } NMR (THF/*N*-MeIm, RT): δ [ppm] = (**1**) (40.1%); (**3**) (22.2%); (**5**) (29.1%).

-
- [1] M. Schuster, *Dissertation*, Munich, **1999**.
 - [2] M. Baudler, K. Glinka, *Chem. Rev.* **1993**, 93, 1623 – 1667.
 - [3] H. Köhler, A. Michealis, *Ber. Dtsch. Chem. Ges.* **1877**, 10, 816 – 818.
 - [4] I. Haiduc, *The Chemistry of Inorganic Ring Systems*, Wiley-Interscience, London, **1970**, Part I, p 93.
 - [5] L. Maier, G. M. Kosolapoff, Eds.; Wiley-Interscience, London, **1972**, Vol. 1, p. 298.
 - [6] M. Baudler, D. Düster, J. Germeshausen, *Z. Anorg. Allg. Chem.* **1986**, 534, 19 – 26.
 - [7] M. Baudler, H. Ternberger, W. Faber, J. Hahn, *Z. Naturforsch.*, **1979**, 34b, 1690 – 1697.
 - [8] a) M. Baudler, O. Exner, *Chem. Ber.* **1983**, 116, 1268 – 1270. b) M. Baudler, R. Heumüller, J. Hahn, *Z. Anorg. Allg. Chem.* **1985**, 529, 7 – 14.
 - [9] H.-G. von Schnering, V. Manriquez, W. Höhle, *Angew. Chem. Int. Ed. Engl.* **1981**, 20, 594.
 - [10] M. Baudler, D. Düster, D. Ouzounis, *Z. Anorg. Allg. Chem.* **1987**, 544, 87.

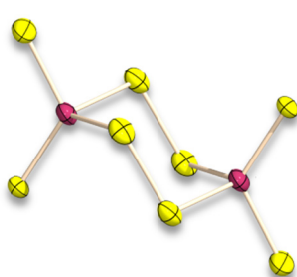
- [11] a) M. Baudler, D. Düster, K. Langerbeins, J. Germeshausen, *Angew. Chem.* **1984**, 96, 309 – 310. b) M. Baudler, R. Heumüller, D. Düster, J. Germeshausen, J. Hahn, *Z. Anorg. Allg. Chem.* **1984**, 518, 7 – 13.
- [12] H.-G. von Schnering, W. Höhle, *Chem. Rev.* **1988**, 88, 243 – 273.
- [13] M. Baudler, T. Etzbach, *Chem. Ber.* **1991**, 124, 1159 – 1160
- [14] N. Korber, F. Kraus, *Chem. Eur. J.* **2005**, 11, 5945 – 5959.
- [15] H.-G. von Schnering, *Angew. Chem. Int. Ed. Engl.* **1981**, 20, 33 – 51.
- [16] M. Baudler, J. Hahn, *Z. Naturforsch.* **1990**, 45b, 1279 – 1281.

Summary

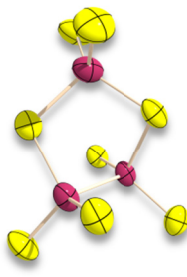
PART I – Anionic Phosphorus Sulfur Compounds

New Salts of Exciting Thiophosphates

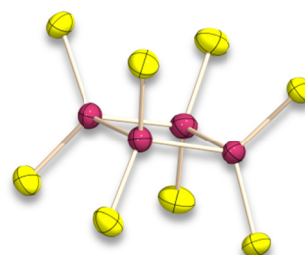
Three new ionic compounds ($[2,6\text{-Me}_2\text{C}_5\text{H}_6\text{N}]_2[\text{P}_2\text{S}_8]$ (**1**), $[\text{pyH}]_3[\text{P}_3\text{S}_8] \cdot 2.5 \text{ py}$ (**2**) and $[\text{pyH}]_4[\text{P}_4\text{S}_8] \cdot \text{py}$ (**3**)) of the cyclic, eight sulfur atoms containing anions $\text{P}_n\text{S}_8^{n-}$ ($n = 2\text{--}4$) have been prepared and their structures elucidated by single crystal X-ray diffraction.



1



2



3

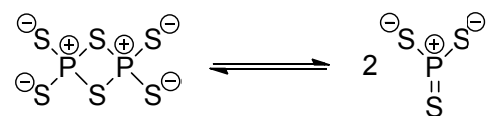
In the series of anions of the form $\text{P}_n\text{S}_8^{n-}$ ($n = 2\text{--}4$) a clear trend towards a decrease in ring size is observed with the increase of the phosphorus content.

PS_3^- - The Mystery has been Cleared Up

PS_3^- forms spontaneously and is stable as the monomer in solution.

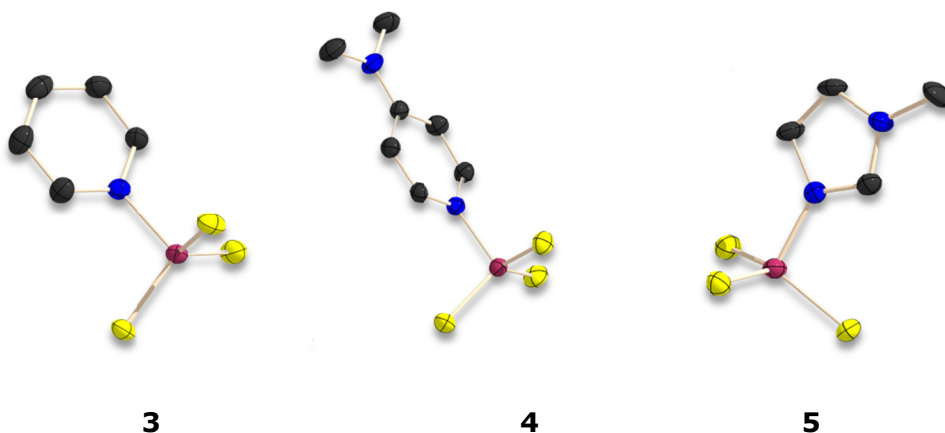
The thiophosphate anion $\text{P}_2\text{S}_6^{2-}$, formally the dimer of the PS_3^- , is an ideal precursor for the monomeric form. Salts with organic cations (Ph_4P^+ , $n\text{Bu}_4\text{N}^+$) were readily obtained from the reaction of P_4S_3 with Na_2S_2 and elemental sulfur in the presence of the bromide salts of the cations. In contrast to metal salts of this anion, (like $\text{K}_2\text{P}_2\text{S}_6$ or $\text{Na}_2\text{P}_2\text{S}_6$), are rather soluble in common polar organic solvents like pyridine,

acetonitrile or propionitrile. In solution the $\text{P}_2\text{S}_6^{2-}$ anion spontaneously dissociates and forms an equilibrium with the monomeric trithiometaphosphate



The presence of this equilibrium is proved by a ^{31}P , ^{31}P EXSY 2D-experiment without any doubt. The ^{31}P NMR chemical shift of the PS_3^- anion ($\delta^{31}\text{P} = 297.5$ ppm) is in accordance with the calculated value and also with the observed values of dithioxophosphoranes.

The spontaneous formation of the PS_3^- anion is nearly as remarkable as the low electrophilicity, which is quite unexpected for a $\sigma^3\lambda^5$ phosphorus atom. With strong nitrogen bases like pyridine (**3**), *p*-dimethylaminopyridine (Steglich's base) (**4**) and *N*-methylimidazole (**5**) only weak adducts are formed. This is clearly demonstrated by variable temperature ^{31}P NMR spectroscopy in solution and by strongly elongated P–N distances within the adducts in the solid state.

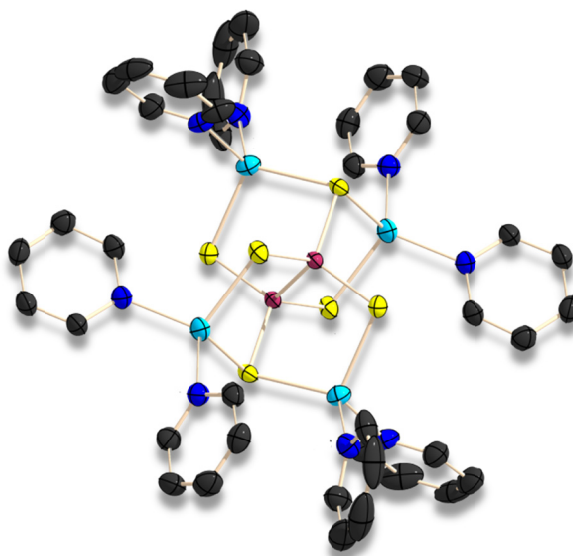


In contrast to statements in the literature, our results show that hydrogen bonding between the sulfur atoms and the cations is not required to stabilize the adducts in the solid state.

With these experimental results it becomes evident that the trithiometaphosphate anion exists as a stable species in solution. The adducts of PS_3^- provide a convenient source of this anion and open the door to a systematic investigation of its reactivity.

A New $\text{Li}_4\text{P}_2\text{S}_6$ Cage: the $[\text{py}_2\text{Li}]_4[\text{P}_2\text{S}_6] \cdot 2 \text{ py}$

The new lithium hexathiohypodiphosphate $[\text{py}_2\text{Li}]_4[\text{P}_2\text{S}_6] \cdot 2 \text{ py}$ was prepared in excellent yield (99%) starting from P_4S_3 , Li_2S and elemental sulfur in pyridine. The reaction proceeds at room temperature.

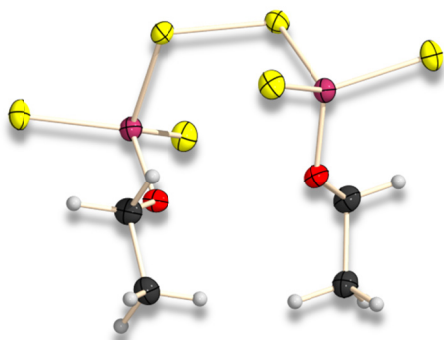


The Li^+ ions coordinate to the staggered $\text{P}_2\text{S}_6^{4-}$ anion to form a novel $\text{Li}_4\text{P}_2\text{S}_6$ polycycle, formally consisting of two heteronorboranes. Compared to solvent free $\text{Li}_4\text{P}_2\text{S}_6$ with LiS_6 octahedra in $[\text{py}_2\text{Li}]_4[\text{P}_2\text{S}_6] \cdot 2 \text{ py}$ the lithium adopts its preferred tetrahedral coordination, with two pyridine molecules completing its coordination sphere. Remarkable is the water stability of the $\text{P}_2\text{S}_6^{4-}$ anion which is an important property for the possible use of its salts in practical applications.

PART II – Structures of Unusual Phosphate Derivatives

A Disulfide Bridged Thiodiphosphate

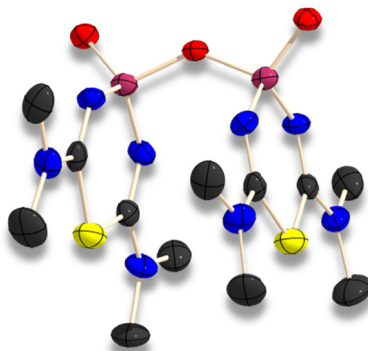
The synthesis of the new anion $\text{P}_2\text{S}_6(\text{OEt})_2^{2-}$ and its isolation as the bis(pyridinium) salt provides a route to a new thiodiphosphate anion with a high sulfur content. The anion is a rare example of a compound with a disulfide bridge between the two phosphorus atoms.



Its molecular structure in the crystal shows a dihedral PSSP angle of $87.3(1)^\circ$. In the crystal electrostatic $\text{N-H}\cdots\text{S}$ and $\text{C-H}\cdots\text{S}$ interactions result in the formation of a complicated three-dimensional network. The new anion $\text{P}_2\text{S}_6(\text{OEt})_2^{2-}$ is anticipated to display an interesting coordination chemistry.

Unexpected Chemistry with P_4S_{10}

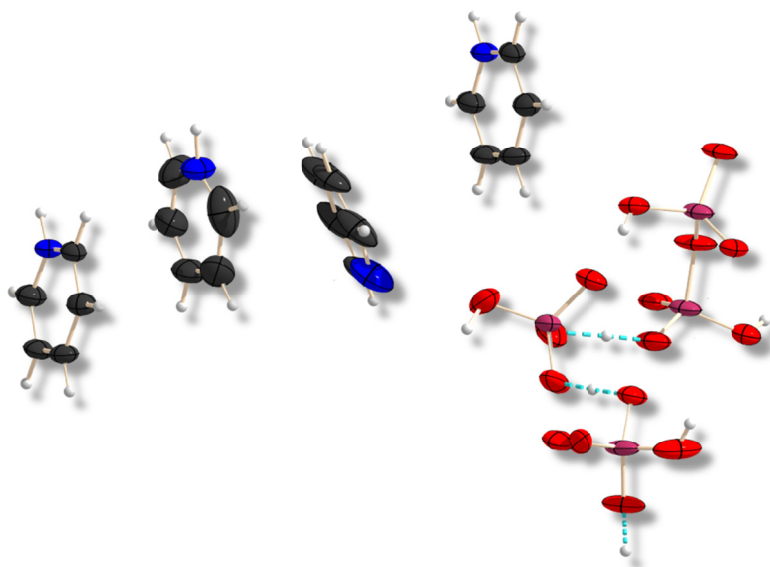
The formation of 4,4'-oxybis(2,6-bis(dimethylamino)-4H-1,3,5,4-thiadiazaphosphinine 4-oxide) in the course of the reaction of P_4S_{10} and dimethyl cyanamide shows the variable reactivity of P_4S_{10} depending on the nitrogen base employed.



This compound is the second representative with a 1,3,5,4-thiadiazaphosphinine ring, which could be characterized using single crystal X-ray diffraction.

Strong Hydrogen Bonds Determine the Structure

The mixed pyridinium phosphate salt $[\text{pyH}]_3[\text{H}(\text{HP}_2\text{O}_7)(\text{H}(\text{HPO}_4))]\cdot 0.5 \text{ py}$ (**1**) was obtained in a small amount from the hydrolysis of the bis(pyridine) adduct of $\text{P}_2\text{S}_4\text{O}$ in pyridine. At first sight this new compound looks rather simple but it shows a complicated and at the same time exciting arrangement in the solid state.



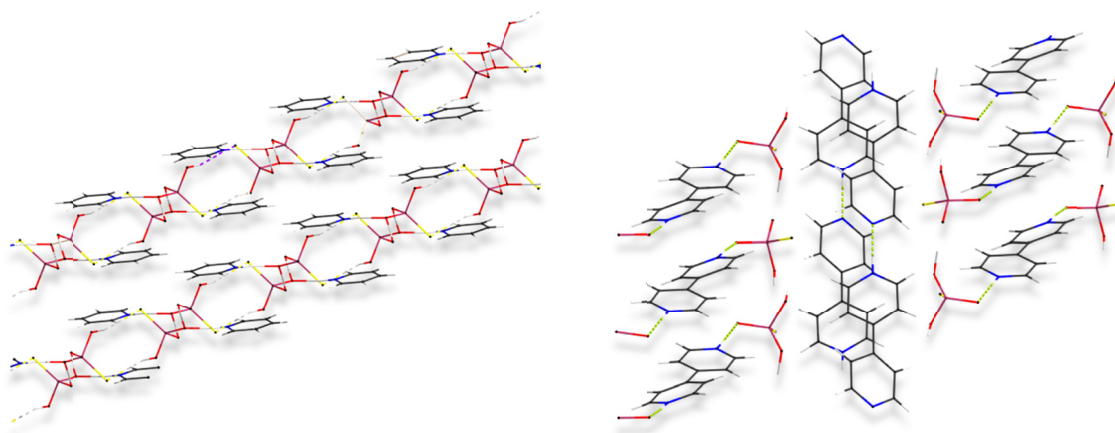
The structure contains both, weak and strong hydrogen bonds and shows clearly how the interplay of these interactions results in a compact, vast and exciting build-up in the crystal. Strong hydrogen bonds are observed between the diphosphate and phosphate anions, as well as between the two phosphate ones.

Hydrogen Bonds and Structure Dimensionality

The great difference in the tendency to form hydrogen bonds between oxygen and its heavier homologue sulfur is responsible for and can be used to control dimensionality of networks in the crystal.

In the pyridinium salt of $\text{H}_2\text{PO}_3\text{S}^-$ one sulfur atom makes the difference between a three-dimensional anionic subnetwork (phosphate anions) and a two-dimensional layered structure. Introduction of a bifunctional base in the 4,4'-bipyridinium salt of $\text{H}(\text{HPO}_3\text{S})_2^{3-}$ provides an additional functionality capable of hydrogen bonding, which

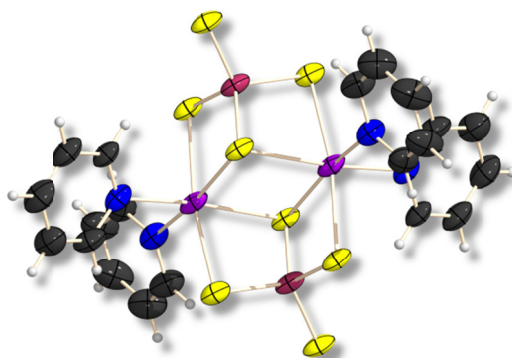
causes an increase in dimensionality and results in the formation again of a three-dimensional network.



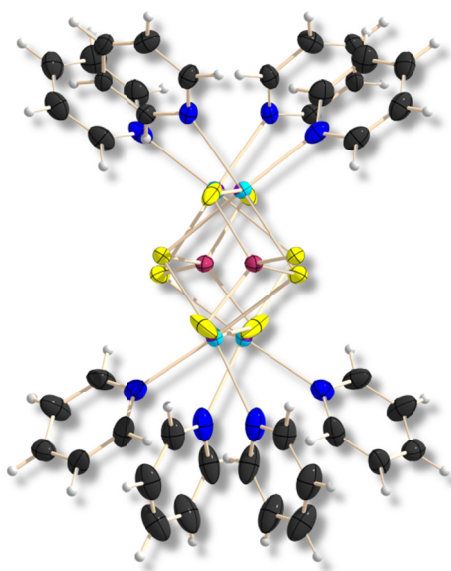
PART III – Pyridine Stabilized Metal Complexes of P,S,O Anions

Mn(II) Thio- and Oxophosphate Complexes

In the course of our investigations to introduce PS_4^{3-} as a building block in coordination polymers prepared from solution, a first Mn(II) tetrathiophosphate complex $[\text{py}_2\text{MnPS}_4]_2[\text{pyH}]_2 \cdot 4\text{py}$ was obtained.

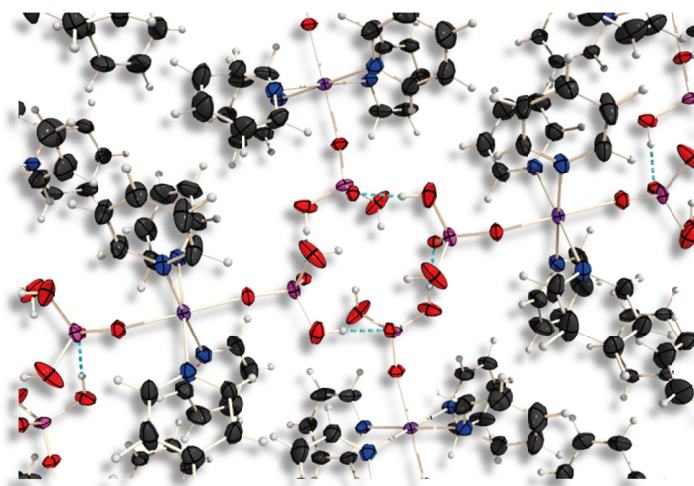


The formal substitution of the organic cation pyH^+ with a monovalent metal cation like Na^+ leads to the formation of a one dimensional coordination polymer $\text{py}_4\text{NaMnPS}_4$. This is caused by the higher coordination sphere at the sodium cation.



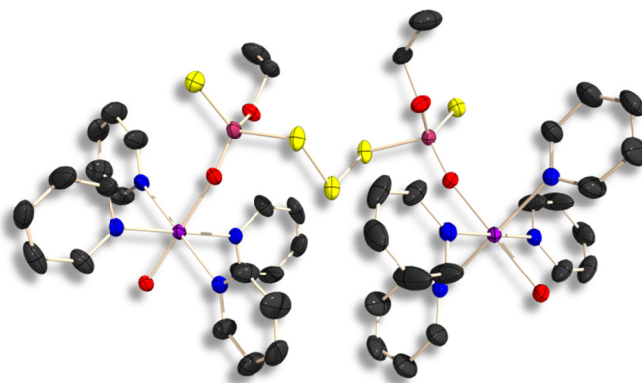
The compound $\text{py}_4\text{NaMnPS}_4$ is obtained when P_4S_{10} , Na_2S and KMnO_4 are refluxed in pyridine. The chains, formed by the manganese and sodium cations and the PS_4^{3-} anions are shielded by coordinated pyridine molecules, thus preventing the polymer from higher dimensionality.

Using oxo- instead of a thiophosphate leads to a layered arrangement in the crystal. This can be achieved by the formation of hydrogen bonds, as shows the structural arrangement in $\text{py}_4\text{Mn}(\text{H}_2\text{PO}_4)_2$.



A New One-Dimensional Coordination Polymer

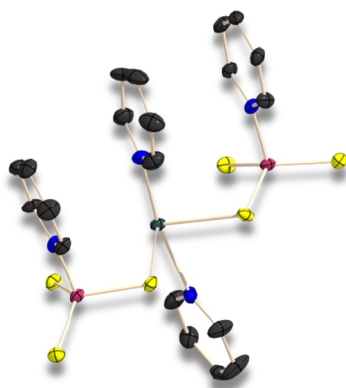
The new one-dimensional coordination polymer $\text{py}_4\text{Mn}[(\text{EtO}(\text{S})\text{P}(\text{O})\text{S})_2\text{S}] \cdot \text{py}$ was obtained from the reaction of P_4S_{10} with Na_2S and KMnO_4 in pyridine and subsequent ethanolysis. It contains the first thiodiphosphate anion with a trisulfide bridge between the two phosphorus atoms, as part of the complex.



The formation of the one-dimensional polymer $\text{py}_4\text{Mn}[(\text{EtO}(\text{S})\text{P}(\text{O})\text{S})_2\text{S}] \cdot \text{py}$ underlines the importance of the structure directing role of the pyridine and the versatile ligand properties of mixed oxo/thiophosphate anions.

From a Monomeric Stannylene and a Chain-like Sn,P,S-heteropolyanion

The trithiometaphosphate anion, PS_3^- , stabilized as its pyridine adduct, as well as the tetrathiophosphate anion PS_4^{3-} are found to be good ligands for soft Lewis centres, like $\text{Sn}(\text{II})$. This is demonstrated by the synthesis and structural characterization of the neutral stannylene $\text{py}_2\text{Sn}(\text{pyPS}_3)_2 \cdot \text{py}$ and of the heteropolyanion $[\text{SnPS}_4][\text{py}_2\text{H}] \cdot \text{py}$. $\text{py}_2\text{Sn}(\text{pyPS}_3)_2 \cdot 0.5 \text{ py}$ is the first example of the pyridine adduct of the trithiometaphosphate anion as a ligand towards metals and one of the very view thiosubstituted stannylenes.

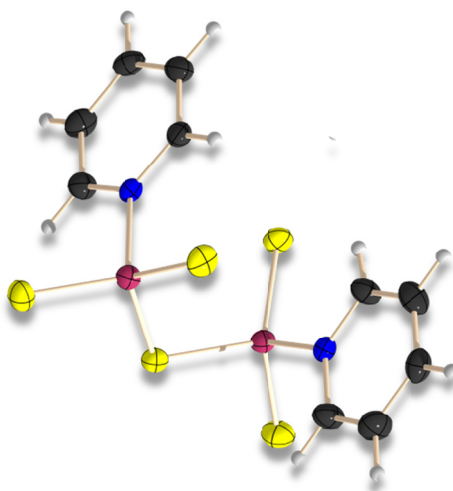


The compound $[\text{SnPS}_4][\text{py}_2\text{H}] \cdot \text{py}$ contains the remarkable chain-like heteropolyanion $[\text{SnPS}_4^-]_n$. The striking build-up in the crystal implies further use as inorganic organic hybrid open framework material.

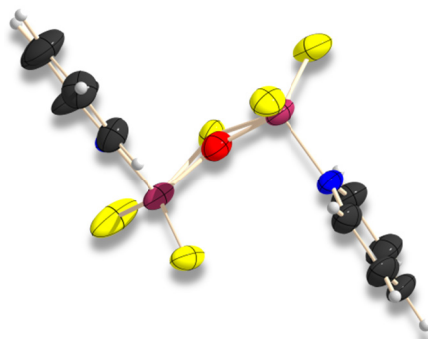
PART IV – Acyclic Phosphorus Sulfides

Stabilized Acyclic Phosphorus Sulfides (Berzelius was right after all)

The bis(pyridine) adduct of the acyclic binary phosphorus sulfide P_2S_5 is readily obtained by stirring P_4S_{10} in pyridine at ambient temperature. Single crystal X-ray diffraction studies on $\text{py}_2\text{P}_2\text{S}_5 \cdot 0.5 \text{ py}$ confirm stabilization of the P_2S_5 framework by weak coordination of the pyridine molecules to phosphorus.

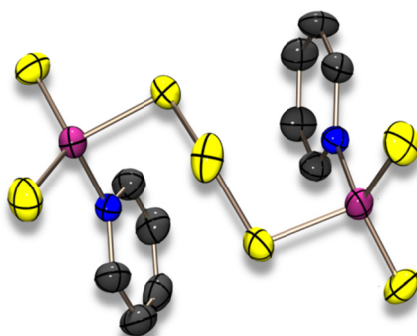


X-ray diffraction studies on $\text{py}_2\text{P}_2\text{S}_{4.34}\text{O}_{0.66}$ provide first evidence for the existence of $\text{py}_2\text{P}_2\text{S}_4\text{O}$, a bis(pyridine)adduct of the mixed phosphorus sulfide oxide $\text{P}_2\text{S}_4\text{O}$ with oxygen bridging the two phosphorus atoms.



These results point to a general concept of stabilizing reactive phosphorus species containing $\sigma^2\lambda^5$ phosphorus atoms by weak coordination of a nitrogen base to phosphorus. It should be possible to extend this concept to other small molecules with three coordinated phosphorus(V) atoms. Thermogravimetric investigations on $\text{py}_2\text{P}_2\text{S}_5$, $\text{py}_2\text{P}_2\text{S}_{4.34}\text{O}_{0.66}$ and $\text{py}_2\text{P}_2\text{S}_7$ confirm the weak coordination of pyridine to phosphorus and indicate, that these adducts might be of interest as precursors for the generation of gaseous acyclic phosphorus sulfides and sulfide oxides.

The new phosphorus sulfide P_2S_7 , stabilized as the bis(pyridinium) adduct was obtained from the reaction of P_4S_{10} and sulfur in pyridine, and could be isolated in form of colourless blockshaped crystals which were characterized using single crystal X-ray diffraction.



That the coordination of pyridine is indeed weak ($d(\text{P-N}) = 187 \text{ pm}$) is supported by quantum chemical calculations.

Polyphosphides – Still a Challenge

The formation of polyphosphides from the reaction of white phosphorus with alkali metals in basic media was investigated with the aim to use the polyphosphides for reactions with heavier chalcogens (S and Se). Phosphorus-rich binary P₄S and P₄Se anions should become accessible by this route.

But the situation turned out to be quite complicated. The results indicate clearly, that the activation of the alkali metal with naphthalene beforehand has a great influence on the product diversity in the solution. In addition the polyphosphides formed from P₄ and alkali metals in pyridine or *N*-methylimidazole were almost independent of the stoichiometric ratio of the educts under the conditions applied. In all cases a mixture of different polyphosphides, predominantly P₁₆²⁻, P₂₁³⁻ and P₇³⁻ was obtained. ³¹P NMR spectroscopic investigations of these mixtures over a longer period of time indicated an equilibrium among these polyphosphides. Over time insoluble polyphosphides formed. Oxidation of P₇³⁻ with S, Se and Te resulted in the formation of the larger polyphosphides P₁₆²⁻ and P₂₁³⁻.

